ABSTRACT

Title of Dissertation: CELL CHANGES DURING AUTOPHAGIC CELL DEATH OF LARVAL SALIVARY GLANDS DURING *DROSOPHILA MELANOGASTER* METAMORPHOSIS.

Damali Nzinga Martin, Doctor of Philosophy, 2004

Dissertation directed by: Dr. Eric H. Baehrecke
Center for Biosystems Research
University of Maryland Biotechnology Institute
University of Maryland, College Park, MD

Dr. Stephen Mount
Department of Cell Biology and Molecular Genetics
University of Maryland, College Park, MD

Autophagic cell death has been implicated in human diseases such as neurodegeneration and cancer. In order to obtain a clearer picture of the mechanisms that regulate autophagic cell death, I have been studying the cell changes that occur during this process using *Drosophila melanogaster* larval salivary glands as a model. During *Drosophila* metamorphosis, larval salivary gland histolysis is triggered by a pulse of the steroid hormone 20-hydroxyecdysone (ecdysone) that occurs twelve hours after puparium formation. Ecdysone directly causes the activation of the early genes *E93*, *BR-C* and *E74A*, with *ßFTZ-F1* serving as a competence factor for their induction. In turn, these transcription regulators activate a set of late genes *rpr*, *hid*, *dronc*, *drice* and *ark* that have a more direct role in the cellular changes that occur during salivary gland cell death.

While dying salivary glands use typical apoptotic machinery, the morphology of their cells resembles autophagic cell death. The morphological changes seen during salivary gland autophagic cell death are a result of active caspase cleavage of structural proteins such as nuclear Lamin, α-Tubulin and α-Spectrin. However, some changes that occur during cell death are caspase-independent, indicating that other proteins are important for histolysis of these glands.

Proteome analyses identified 5,313 proteins that are present before and during salivary gland cell death. These proteins are involved in numerous processes such as autophagy, the ubiquitin mediated proteolysis, cell organization, cell growth regulation and cell cycle regulation. Further analyses of these proteins may illustrate their importance during salivary gland autophagic cell death. Forward genetic screening was also used to identify mutations in genes that affect salivary gland cell death. One such gene *ctp* encodes a light chain of a dynein motor, and animals with mutations in *ctp* have salivary glands that fail to die.

CELL CHANGES DURING AUTOPHAGIC CELL DEATH OF LARVAL SALIVARY GLANDS DURING *DROSOPHILA MELANOGASTER* METAMORPHOSIS

by

Damali Nzinga Martin

Dissertation submitted to the Faculty of the Graduate School of the
University of Maryland, College Park in partial fulfillment
of the requirements for the degree of
Doctor of Philosophy
2004

Advisory Committee:

Professor Eric H. Baehrecke, Co-Chair/Advisor
Professor Stephen Mount, Co-Chair
Professor Louisa Wu
Professor Margaret De Cuevas
Professor Wenxia Song
Professor Leslie Pick

Dedication

To all of my family especially my parents Emil C. George and Joan P. George, my brothers, Carlton and Bediako, my sisters, Patsy, Soyini and Niambi and my husband, Julien V. Martin.

Acknowledgements

I would like to thank my advisor, Dr. Eric H. Baehrecke for all of his guidance and advice throughout my years of graduate school. His support for me was incredible and I would always be grateful for everything that he has done for me. I would also like to thank Dr. Stephen Mount for all of his guidance and advice and serving as co-chair on my committee. I would like to thank the remaining committee members: Dr. Margaret DeCuevas for all of her help, especially for materials needed to carry out my research and her guidance and advice on confocal microscopy, Dr. Louisa Wu for her knowledge and suggestions during laboratory meetings, Dr. Leslie Pick for agreeing to be my Dean's representative and also for sharing antibodies with me and Dr. Wenxia Song for her suggestions and comments during committee meetings. I would also like to thank the Chairman and Director of my department, Dr. Ibrahim Ades and Dr. Todd Cooke and the Center for Biosystems Research and its Director, Dr. Donald Nuss.

I would always be grateful to laboratory members who made the lab a great place to work. Special thanks go to Dr. Cheng-Yu Lee, who demonstrated through words and actions what it took to be a successful graduate student. I will be forever indebted to him for all of his advice and his friendship. Also thanks for Dr. Claudio Simon – it was a pleasure and fun to collaborate with him on projects in the lab. I will also like to thank Jamie Cranford for her friendship and making the lab a fun and lively place to work and to Stamatis Kantartzis for all of his help with my project. I would also like to thank the remaining present and former lab members for all of their help and friendship – Ajjai Alva, Deborah Berry, Sudeshna Dutta, Vanaja Jaligam, Marieko Kobayashi, Alya Raphael, Kent York, Emily Clough, Paula Yellon, Bridget Cooksey, Alvaro Godinez.

I would like to thank collaborators in other labs, Dr. Cheng Lee, Dr. Jenny Chen, and Brian Balgley for their help with the proteome analyses. Also thanks to many others that sent antibodies and fly stocks to me– D. Branton, L. Cooley, P. Fisher, N. Franc, M. Fuller, C. Goodman, B. Hay, E. Knust, S. Kumar, P. Meier, G. Rubin, P. Salvaterra, R. Steward and the Bloomington *Drosophila* stock center. Thanks also to Tim Maguel for training me with TEM techniques.

Last but not least, I would also like to thank my family and friends for all of their support and understanding. Thanks to my parents, Emil C. George and Joan P. George for instilling in me the importance of hard work. Thanks to my husband, Julien V. Martin, for all of his patience and support throughout it all.

TABLE OF CONTENTS

List of Tables

List of Figures

List of Appendices

List of Abbreviations

ATG - Autophagy gene

APF - After puparium formation

BH - Bcl-2 homology domain

BIR - Baculovirus IAP repeat

Cact - Cactus

Cha - Choline acetyltransferase

CNS - Central Nervous System

Crb - Crumbs

DInR - *Drosophila* Insulin receptor

DISC - Death-inducing signaling complex

Dlg - Discs Large

Hiw - Highwire

IAP - Inhibitor of Apoptosis

Kel - Kelch

LC7 - Light Chain 7

LC8 - Light Chain 8

MS - Mass Spectrometry

PNS - Peripheral nervous system

TOR - Target of rapamycin

TUNEL - Terminal deoxynucleotidyl transferase mediated dUPT-biotin nick end labeling

Qua – Quail

Chapter 1

Introduction.

1.1 Abstract.

Programmed cell death plays an important role in maintaining homeostasis during development of higher eukaryotes and defects in this process are associated with human diseases such as cancer and neurodegeneration. Two prominent forms of programmed cell death occur during animal development- apoptosis and autophagic cell death. The mechanisms that regulate apoptosis are conserved in animals including worms, fruit flies and mammals. While much is known about apoptosis, far less is known about autophagic cell death.

1.2 Developmental programmed cell death

Programmed cell death occurs in all animals, and serves to maintain homeostasis during development and adulthood. Morphological studies enable the distinction between physiological and pathological cell death that occurs due to trauma and ischemia, which is referred to as necrosis (Lockshin and Zakeri 1991). Cells that undergo necrotic death lose their membrane integrity, leading to swelling and lysis of the cell and inflammation of the surrounding tissue (Jacobson et al., 1997). By contrast, programmed cell death involves the loss of cells by physiologically and genetically regulated mechanisms. The removal of these cells prevents leaking of the dying cell contents, and hence prevents damage to neighboring cells and tissues (Baehrecke, 2002).

Programmed cell death plays an important role during animal development and adult life by eliminating unwanted cells and controlling cell numbers (Jacobson et al., 1997).

During animal development, cells and tissues that are useful for earlier events and are no longer needed are removed by programmed cell death. For example, during metamorphosis of the fruit fly *Drosophila melanogaster*, the larval salivary glands are removed by programmed cell death following the stage when this tissue is used for secretion of polypeptide glue for pupal adhesion to surfaces (Jiang et al., 1997). Similarly, the process of tail resorption in *Xenopus* tadpoles involves the loss of muscle fibers by programmed cell death (Das et al., 2002). During the development of both the vertebrate and invertebrate nervous systems, neurons and glia are produced in excess, and the cells that fail to receive a survival signal are removed by programmed cell death (Oppenheim et al., 1990; Bergmann et al., 2002). Regulated programmed cell death is also used in the process of digit formation (Saunders, 1966) and lumen formation such as the preamniotic cavity which is formed by elimination of ectodermal cells in the core of developing mouse embryos (Coucouvanis and Martin, 1995). Programmed cell death is also involved in the removal of abnormal cells that could potentially be harmful to the developing animal such as negative selection of mammalian thymocytes. Thymocytes that recognize self-antigens in mice are destroyed and therefore prevent autoimmune disorders (MacDonald and Lees, 1990; Kappler et al., 1987; Jenkinson et al., 1989). Ultimately, programmed cell death plays a very important role in preventing human diseases. When programmed cell death is derailed by inappropriate activation, it contributes to the pathogenesis and diseases such as autoimmunity, cancer, restenosis, ischemia, heart failure and neurodegeneration (Thompson, 1995).

1.3 Types of programmed cell death.

Studies of developing vertebrate embryos resulted in the description of three classes of programmed or physiological cell death based on the role of the lysosome (Clarke, 1990; Schweichel and Merker, 1973; Baehrecke, 2002) (Figure 1). Non-lysosomal cell death is least common, and is characterized by swelling of cavities with membrane borders, followed by degeneration of the cell without the involvement of lysosomes. The other two types of regulated cell killing, apoptosis and autophagic programmed cell death, commonly occur in developing animals (Figure 1).

Apoptotic cells exhibit specific morphological changes including condensation and margination of chromatin, fragmentation of the cell with retention of organelle structure, and the blebbing and formation of apoptotic bodies (Kerr et al., 1972). Biochemical changes that occur during apoptosis include DNA fragmentation (Wyllie, 1980) and the exposure of the phospholipid phosphatidylserine on the outer leaflet of the plasma membrane (Fadok et al., 1992). Apoptosis usually occurs when isolated cells die, and these corpses are eaten by phagocytes. The engulfment of apoptotic cells leads to the formation of an acidic compartment within the phagocyte, which fuses with the lysosome where it is destroyed (Clarke, 1990; Schweichel and Merker, 1973). Even though most forms of apoptosis appear to be dependent on active caspase proteases such as caspase-3, some cells are able to die in a caspase-independent manner. Chromatin condensation is less compacted in these cells than in caspase-dependent apoptosis (Leist and Jaattela, 2001).

Autophagic programmed cell death is often observed when entire tissues or groups of cells die (Clarke, 1990). During this process cytoplasmic proteins and organelles are

sequestered in double-membrane structures called autophagic vacuoles (Baehrecke, 2003; Klionsky and Emr, 2000). The origin of these vacuoles is not clear, but evidence suggests that they are derived from the endoplasmic reticulum in mammals (Dunn, 1990). Based on observations made by transmission electron microscopy, Schweichel and Merker (1973) concluded that the Golgi apparatus exhibits a high amount of diphosphatase activity which is related to the generation of primary lysosomes during autophagic programmed cell death. The membrane surrounding individual lysosomes breaks down and fragmentation of the cytoplasm and cell membranes occurs. Condensation of the nucleus can occur, but is not as striking as in apoptotic cells. In some cases, phagocytes remove remnants of cells during cell death, but this occurs late during autophagic cell degradation.

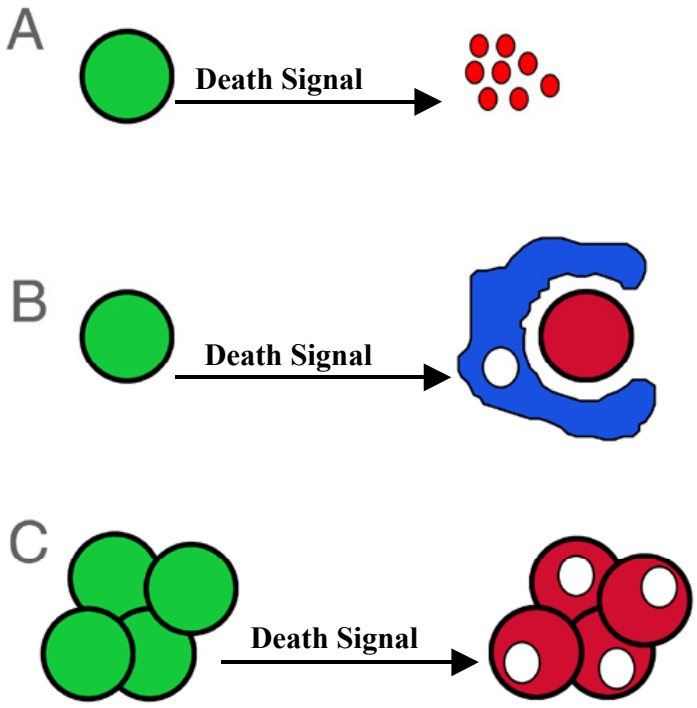

Figure 1. Three types of programmed cell death. (A) Non-lysosomal cell death involves the degradation of the cell without the use of the lysosome. (B) Apoptosis involves the engulfment of an isolated dying cell (red) by a phagocyte (blue). The dying cell is then degraded within the lysosome of the phagocyte (white circle). (C) Autophagic cell death occurs when groups of cells or tissues undergo synchronous cell death (red), and internalize their organelles and cytoplasmic components into double-membrane autophagic vacuoles (white circles in each cell).

1.4 Apoptosis genes.

Genetic studies of programmed cell death in the nematode *Caenorhabditis elegans* led to the identification of genes involved in the execution of cell death and the removal of apoptotic cells. Three of these genes, *ced-3*, *ced-4* and *ced-9*, compose the core cell death machinery (Ellis et al., 1991; Table 1). Loss-of-function alleles of *ced-3* and *ced-4* lead to the survival of cells that would normally undergo developmental programmed cell death. Loss of function alleles of *ced-9* lead to sterility or lethality of the animal, and this is due to the ectopic death of cells that usually live (Hengartner et al., 1992).

Genome sequence analyses indicate that the core machinery of the apoptotic pathway that was identified in *C. elegans* is conserved in organisms such as *Drosophila* and mammals (Aravind et al., 2001; Table 1). *ced-3* encodes a protein that is similar to a family of cysteine proteases known as Caspases (Yuan et al., 1993; Alnemri et al., 1996). There are seven Caspases in Drosophila: Dronc, Dredd/Dcp-2, Dream/Strica, Dcp-1, Drice, Decay and Daydream/Damm (Chen et al., 1998; Dorstyn et al., 1999; Doumanis et al., 2001; Fraser and Evan, 1997; Harvey et al., 2001; Song et al., 1997). In mammals, 14 Caspases have been identified and seven of these participate in cell death including Caspases -2, -3, -6, -7, -8, -9, and -10 (Cain et al, 2002). The other mammalian Caspases appear to function in inflammation.

The Caspases can be divided into the initiator Caspases and executioner Caspases based on their sequence. Initiator Caspases have long pro-domains, and are capable of autoactivation and activation of the executioner Caspases. Executioner Caspases have shorter pro-domains and are thought to play a more direct role in the cleavage of cell substrates, and this substrate cleavage is thought to be responsible for the morphological

changes of apoptotic cells (Green and Kroemer, 1998; Alnemri et al., 1996). The fly Caspases *Dronc, Dredd* and *Dream/Strica* contain long pro-domains and are homologous to the mammalian initiator Caspases -2, -8, -9 and -10. *Dcp-1, Drice, Decay* and *Daydream/Damm* are fly homologs of the mammalian executioner Caspases -3, -6 and -7.

CED-4 is the functional homolog of mammalian *Apaf-1* and *Drosophila Ark/Dark/Hac-1/dApaf-1* (Zhou et al., 1999; Rodriguez et al., 1999). Unlike CED-4, *Apaf-1* and *Ark/Dark/Hac-1/dApaf-1* possess a WD repeat domain in the carboxyl-terminus. This domain interacts with cytochrome c which leads to the activation of initiator pro-caspases in the presence of dATP (Li et al., 1997; Zou et al., 1997).

CED-9 is homologous to a large group of proteins known as the Bcl-2 family. This family of proteins encodes BH domains, and includes both pro-apoptotic molecules such as Bax, Bak, Bad, Bid, Bim and PUMA (BH-3 only members) and anti-apoptotic molecules such as Bcl-2 and Bcl-XL that contain BH-1, 2, 3 and 4 domains (Adams and Cory, 1998). The *Drosophila* genome also possesses orthologs of the CED-9/Bcl-2 family, but only two members of this family exist in flies named *Drob1/debcl/dborg-1* and *dborg-2/buffy* (Brachmann et al., 2000; Colussi et al., 2000; Igaki et al., 2000).

Table 1. The core apoptosis genes are conserved in diverse organisms

C.elegans	*Drosophila*	Mammals
ced-3	*Dronc, Dredd, Dream Dcp-1, Drice, Decay, Daydream/Damm*	*Caspases 1-14*
ced-4	*Ark/Dark/Hac-1/dApaf-1*	*Apaf-1*
ced-9	*Drob-1/debcl/dborg-1, dborg-2/buffy*	*Al, Diva, Bax, Bak, Bok, Bik, Bad, Bid, Hrk, Bim, Bnip, Bcl-2, Bcl-x, Bcl-w, Mcl-1*

1.5 Apoptosome formation and its regulation.

The recognition of the enzymatic complex containing Caspases such as CED-3/Caspase-3, and the caspase cofactor CED-4/Apaf-1, led to the identification of the apoptosome (Hengartner, 2000; Shi, 2002). Caspases are activated through their interaction with Apaf-1 and cytochrome c in the presence of dATP (Li et al., 1997; Zou et al., 1997) (Figure 2). Although substantial in vitro biochemical evidence indicates that cytochrome c is critical for Caspase activity, the in vivo requirement for cytochrome c remains a controversial subject. This is partly because in vivo experiments are difficult to perform as cytochrome c is also involved in mitochondrial oxidative phosphorylation. It is not clear how cytochrome c is able to cross the outer membrane of the mitochondria, but it has been proposed that Bcl-2 family members facilitate this process either by the formation of channels or by destruction or rupture of the outer membrane of the mitochondrion (Reed, 1997; Gross et al., 1999; Shimizu et al., 1999; Loeffler and Kroemer, 2000). Studies of cytochrome c in flies indicate that most cell death occurs in the absence of cytochrome c function although it does appear to be required for caspase-dependent sperm maturation (Arama et al., 2003; Huh et al; 2004). Initiator Caspases can become active through their recruitment in proteins complexes such as the Caspase 9 apoptosome or to cell surface death receptors such as the FAS or TNF receptor complexes. Ligands such as CD95/Fas/APO-1, TRAIL, and TNF can induce trimerization of their receptors, which leads to the formation of the death inducing signaling complex (DISC) (Cain et al, 2002; Sprick and Walczak, 2004). Caspases, such as Caspase 8 are recruited by the receptor by the adapter proteins FADD or TRADD and

this induces Caspase cleavage and activation (Cain et al, 2002; Sprick and Walczak, 2004).

Caspases are maintained in an inactive state through their physical interaction with IAPs (Wu et al., 2003). IAPs encode two BIR (baculovirus IAP repeat) domains and a ring finger domain. Eight IAPs exist in mammals and two IAPs exist in flies. The eight mammalian IAPs contain BIR domains in their N-termini that mediate binding to caspases along with a carboxyl-terminal RING domain which contains E3 ubiquination activity which can participate in the degradation of bound Caspases (Yang et al., 2000; Clem et al., 2001; Huang et al., 2000; Suzuki et al., 2001). IAPs directly bind to and inhibit Caspase-9, Caspase-3 and Caspase-7 activation (Fesik and Shi, 2001; Shi, 2001).

A genetic screen to identify mutations that prevent apoptosis during *Drosophila* embryonic development led to the discovery of the H99 deletion (White et al., 1994). The H99 region contains the *reaper* (*rpr*), *head involution defective* (*hid*), *grim* and *sickle* genes (Christich et al., 2002; Srinivasula et al., 2002; Wing et al., 2002; Chen et al., 1996; Grether et al., 1995; White et al., 1994). *rpr*, *hid*, *grim* and *sickle* encode novel proteins that display limited sequence homology with the mammalian proteins Omi/Htra2 and Smac/Diablo in their first 14 amino acids (Wu et al., 2000; Wu et al., 2001) and no similar proteins have been identified in *C. elegans*. Smac/Diablo and Omi/Htra2 are believed to be located in the intermembrane space of mitochondria and are released to the cytosol upon induction of apoptosis (Hedge et al., 2002; Suzuki et al., 2001; van Loo et al., 2002; Martins et al., 2002; Verhagen et al., 2002).

The N-terminal sequences of Rpr, Grim, Hid and Sickle interact with the *Drosophila* inhibitor of apoptosis Diap1 (Hay et al., 1995; Srinivasula et al; 2002), and this

interaction is similar to the physical relationship between Omi/Htra2 and Smac/Diablo with the mammalian inhibitor of apoptosis gene XIAP (Wu et al., 2000; Wu et al., 2001). The interaction of IAPs with Caspases is altered by Rpr, Hid, Grim and Sickle in flies and Smac/Diablo and Omi/Htra in mammals, and this result in Caspase activation and cell death (Goyal et al., 2000; Wang et al., 1999; Wu et al; 2000, Wu et al; 2001; Wang et al., 1999; Goyal et al., 2000; Martins et al., 2002) (Figure 2).

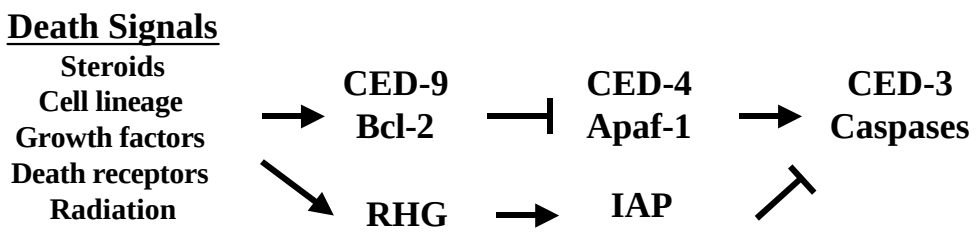

Figure 2. The apoptotic pathway is conserved in worms, flies and mammals. CED-9 (Bcl-2) prevents activation of CED-3 (Caspases) by binding to CED-4(Apaf-1). Upon receipt of a death signal, CED-9 releases CED-4 and CED-3 is activated. In flies, RHG domain of the cell death genes interact with IAP, allowing Caspases to become activated.

1.6 Autophagy genes.

Autophagy has been best studied in yeast as a mechanism to recycle cytoplasmic proteins for amino acids and enable cell survival under starvation conditions. Genetic screens were performed in *Saccharomyces cerevisiae* to identify genes that are required to either form autophagic vacuoles or to target a specific protein to the lysosome under nutrient deprivation conditions (Thumm et al., 1994; Tsukada and Ohsumi, 1993; Harding et al; 1996). This led to the identification of 23 autophagy (Atg) genes. These genes play a role in either the induction of autophagy, formation and size of the autophagic vacuole, or autophagic vacuole docking and fusion with the lysosome (Figure 3). Under nutrient deprivation conditions, a double-membrane vacuole surrounds the cells organelles and cytoplasmic components, and then this vacuole docks and fuses to the lysosome where the inner membrane containing the contents are released for degradation.

The induction of autophagic vacuoles depends on the TOR signaling complex that utilizes the Atg1 Kinase (Klionsky and Emr, 2000). Many of the Atg genes function in two ubiquitin-like conjugation systems to regulate the formation and size of the autophagic vacuoles (Ohsumi, 2001). During this process, cytoplasmic proteins and organelles are targeted to the forming autophagic vacuole by mechanisms that are not clear. The formation of the double-membrane autophagic vacuole involves the yeast ubiquitin-like systems where ATG12 and ATG8 function to recruit a small group of proteins to the isolation membrane of the autophagic vacuole. ATG7 acts as an E1-like protein by physically interacting with ATG12 and ATG8 in an ATP dependent manner. ATG7 then transfers ATG12 to the E2-like protein ATG10. ATG12 is then associated

with ATG5 and ATG16 and this complex is associated with the isolation membrane that is used to form the autophagic vacuole. ATG8 is transferred from ATG7 to the E2-like ATG3 protein, and ATG8 is then covalently bound to the lipid phosphatidylethanolamine that is then inserted directly into the isolation membrane of autophagic vacuoles (Ichimura et al., 2000). The process of autophagic vacuole docking and fusion with the lysosome involves proteins such as Rabs and Snares (Laage and Ungermann, 2001).

Some of the yeast Atg genes are conserved in higher eukaryotes such as worms, *Drosophila*, and mammals (Baehrecke, 2002; Baehrecke 2003). These conserved genes include *TOR*, *Atg1*, *Atg2*, *Atg4*, *Atg5*, *Atg6*, *Atg7*, *Atg8*, *Atg10*, *Atg12* and *Cvt18*. Like yeast, higher animals utilize an autophagy system to degrade proteins during nutrient deprivation (Melendez et al., 2003). Although autophagic vacuoles occur in dying cells, it has not been clear if autophagy is required for programmed cell death.

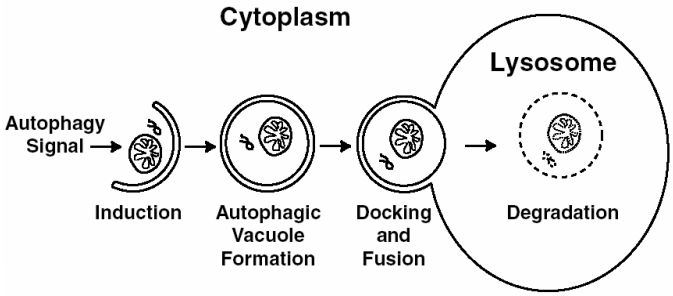

Induction	Formation	Docking & Fusion
Tor	Atg4	Snares
Atg1	Atg5	Rab7
	Atg6	
	Atg7	
	Atg8	
	Atg9	
	Atg10	
	Atg12	
	Atg16	

Figure 3. Atg genes are involved in the induction, formation and docking of autophagic vacuoles during yeast nutrient starvation. Induction leads to the formation of a double-membrane vacuole that surrounds the cells organelles and cytoplasmic components. The outer membrane of the vacuole then docks to and fuses with a lysosome and releases the inner membrane with the cell components for degradation. Genes that are conserved between yeast and mammals that function at distinct steps during autophagy are listed. Figure adapted from Klionsky and Emr (2000) and Baehrecke (2003).

1.7 Genetic regulation of autophagic programmed cell death.

Steroid-regulated larval salivary destruction during *Drosophila* metamorphosis is one of the best characterized systems where autophagic programmed cell death occurs. Ten to twelve hours after puparium formation, a pulse of the steroid 20-hydroxyecdysone (ecdysone) induces the histolysis of the larval salivary glands (Figure 4). Ecdysone is bound by its heterodimeric nuclear receptor encoded by the ecdysone receptor (*EcR*) and ultraspiracle (*usp*) genes, and directly induces the transcription of the early genes *E93*, *BR-C* and *E74* (Burtis et al., 1990; DiBello et al., 1991; Seagraves and Hogness, 1990). Ecdysone receptor induction of these genes depends on the function of the nuclear receptor *βFTZ-F1* that serves as a competence factor (Broadus et al., 1999; Woodard et al., 1994). The early genes *E93*, *BR-C* and *E74* encode transcription regulators that repress their own activities and activate a set of late genes, which function more directly in controlling biological responses to the hormone (Crossgrove et al., 1996; Urness and Thummel, 1995). Transcription of the apoptosis regulators *rpr*, *hid*, *dronc*, *ark* and *croquemort* (*crq*) increases immediately prior to salivary gland cell death, and depends on the function of *E93*, *BR-C*, and *E74A* (Jiang et al., 1997; Lee et al., 2000; Lee et al., 2002; Jiang et al., 2000).

While salivary gland cells use apoptotic genes for destruction, their morphology resembles autophagic programmed cell death. At the start of cell death, salivary gland cells have large vacuoles that fragment one hour later. Two hours after the start of cell death, the cytoplasm of salivary gland cells contain a large number of vacuoles, some of which contain organelles such as mitochondria (Lee and Baehrecke, 2001). Mutations in *E93* block vacuole changes in dying cells and also perturb induction of some Atg genes

(Lee et al., 2001; Lee et al., 2003). While it is unclear if Atg genes are required for programmed cell death of salivary glands, recent studies have shown that six Atg genes are induced after the start of autophagic programmed cell death of these cells (Lee et al., 2003; Gorski et al, 2003).

Several cancer cell lines undergo autophagic programmed cell death when exposed to different death signals. When three dimensional cultures of the human mammary epithelial cell line MCF-10A are exposed to tumor necrosis factor-related apoptosis-inducing ligand TRAIL during lumen formation, induction of cell death with autophagic vacuoles occurs (Debnath et al., 2002). Like salivary glands, these dying cells also appear to use caspases. Inhibition of TRAIL signaling prevented the formation of autophagic vacuoles that normally accompanies the formation of the lumen (Mills et al., 2004). Significantly, recent studies of mouse and human cells indicate that Atg genes are required to activate an alternative cell death pathway in a caspase-independent manner (Yu et al., 2004). Induction of cell death in the presence of the broad spectrum caspase inhibitor zVAD induced the formation of autophagic vacuoles that contained cytoplasmic components in mouse L929 fibroblast cells, RAW 264.7 macrophages, and human U937 monocytoid cells. Reducing the expression of the autophagy genes Atg7 and Beclin-1 prevented the formation of autophagic vacuoles and death of these cell lines (Yu et al., 2004).

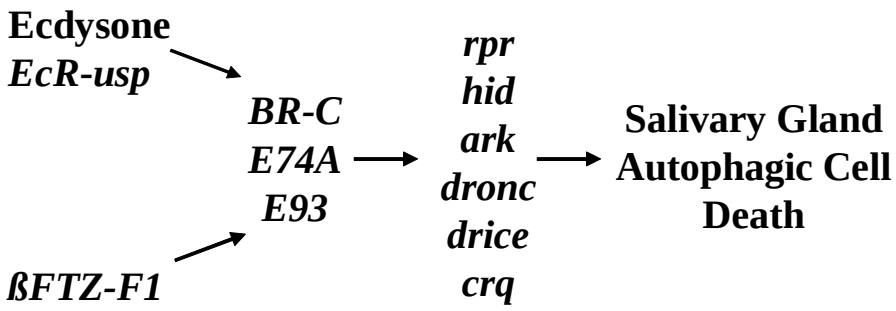

Figure 4. Steroid regulation of autophagic programmed cell death of salivary glands during *Drosophila* metamorphosis. Ecdysone acts through its heterodimer receptor EcR and Usp and the competence factor *βFTZ-F1* to regulate transcription of the ecdysone regulated genes *E93*, *BR-C* and *E74A*. These genes in turn activate a subset of late apoptotic genes *rpr*, *hid*, *ark*, *dronc*, *drice* and *crq* which play a more direct role in salivary gland autophagic cell death.

1.8 Conclusion.

Programmed cell death is an important part of eukaryotic development. Even though much is known about this process, many significant questions remain unanswered about the mechanisms that mediate different forms of cell death. Since the morphologies of cells undergoing apoptotic and autophagic programmed cell death are so different, it was suggested that the mechanisms controlling them are distinct (Schwartz et al., 1993). However, recent studies have shown that cells undergoing these two types of cell death utilize several of the same genes to execute their demise. For example, during *Drosophila* development, the cell death genes *rpr* and *hid* and the caspases *dronc* and *drice* are transcriptionally upregulated in cells undergoing apoptosis during embryonic development as well as during salivary gland cell death (Chen et al., 1996; Grether et al., 1995; White et al., 1994; Lee et al., 2000; Lee and Baehrecke, 2001). Although much is known about the mechanism of apoptosis, little is understood about the cell changes that occur during autophagic programmed cell death. Here I focus on understanding what cellular changes occur during autophagic cell death, and what groups of proteins may function in this understudied process. The combined strength of *Drosophila* genetics and the wealth of knowledge of the steroid signaling hierarchy make the salivary gland a good model for in vivo studies of cellular changes during autophagic cell death.

Chapter 2

Caspases function in autophagic programmed cell death in *Drosophila*.

2.1 Abstract.

Self-digestion of cytoplasmic components is the hallmark of autophagic programmed cell death. This auto-degradation appears to be distinct from what occurs in apoptotic cells that are engulfed and digested by phagocytes. While much is known about the apoptosis, far less is known about the mechanisms that regulate autophagic cell death. Here we show that autophagic cell death is regulated by steroid activation of caspases in *Drosophila* salivary glands. Salivary glands exhibit some morphological changes that are similar to apoptotic cells, including the fragmentation of cytoplasm, but do not appear to use phagocytes in their degradation. Changes in the levels and localization of filamentous Actin, α -Tubulin, α -Spectrin, and nuclear Lamins precede salivary gland destruction, and coincide with increased levels of active Caspase-3 and a cleaved form of nuclear Lamin. Mutations in the steroid-regulated genes *ßFTZ-F1*, *E93*, *BR-C* and *E74A* that prevent salivary gland cell death possess altered levels and localization of filamentous Actin, α -Tubulin, α -Spectrin, nuclear Lamins, and active Caspase-3. Inhibition of caspases by expression of either the caspase inhibitor p35 or a dominant negative form of the initiator caspase Dronc is sufficient to inhibit salivary gland cell death, and prevent changes in nuclear Lamins and α -Tubulin but not reorganization of filamentous Actin. These studies suggest that aspects of the cytoskeleton may be required for changes in dying salivary glands. Furthermore, caspases are not only used during apoptosis, but also function in the regulation of autophagic cell death.

2.2 Introduction.

Programmed cell death plays an important role in the maintenance of animal homeostasis by eliminating unwanted cells and tissues, sculpting developing structures, controlling cell numbers, and removing abnormal cells (Jacobson et al., 1997). Apoptosis and autophagic cell death are the two most prominent morphological forms of cell death that occur during development of animals (Clarke, 1990; Schweichel and Merker, 1973). Apoptotic cells exhibit specific morphological and biochemical changes including the condensation and margination of chromatin, DNA fragmentation, blebbing, formation of apoptotic bodies, and exposure of the lipid phosphatidylserine on the outer leaflet of the plasma membrane (Fadok et al., 1992; Kerr et al., 1972; Wyllie, 1980). While far less is known about autophagic cell death, DNA fragmentation occurs, and autophagic vacuoles form that are used for destruction of cytoplasm (Lee and Baehrecke, 2001; Schweichel and Merker, 1973). Apoptosis and autophagic cell death differ in several ways, and the clearest distinction appears to be the mechanisms that are used for degradation of the dying cell. During apoptosis, the dying cell is engulfed by and degraded in the lysosome of a phagocyte. In contrast, cells undergoing autophagic cell death internalize cytoplasmic components, including organelles, into vacuoles that are targeted to the lysosome of the dying cell for degradation. Until recently, it was believed that apoptosis and autophagic cell death were controlled by different mechanisms. Studies of Drosophila salivary gland cell destruction indicate, however, that some of the genes that function during apoptosis including caspases also function in autophagic cell death (Lee and Baehrecke, 2001).

Steroids are important regulators of programmed cell death in animals

(Baehrecke, 2000; Distelhorst, 2002; Evans-Storm and Cidlowski, 1995). During *Drosophila* development, the steroid 20-hydroxyecdysone (ecdysone) triggers cell death of many larval tissues including the larval salivary glands (Jiang et al., 1997). Elevation of the ecdysone titer 12 hours after puparium formation triggers autophagic cell death in the salivary gland, and this tissue is completely destroyed by 16 hours after puparium formation (Jiang et al., 1997). Ecdysone is bound by its heterodimeric receptor that is encoded by *EcR* and *usp*, and acts in combination with the competence factor *ßFTZ-F1* to regulate transcription of the primary response genes *E93*, *BR-C* and *E74* (Broadus et al., 1999; Woodard et al., 1994). Salivary glands fail to die in animals with mutations in *ßFTZ-F1*, *E93*, *BR-C* and *E74A*, and exhibit altered transcription of the secondary response cell death genes *rpr*, *hid*, *ark*, *dronc*, and *drice* during autophagic cell death (Broadus et al., 1999; Jiang et al., 2000; Lee et al., 2003; Lee et al., 2002b; Lee et al., 2000; Restifo and White, 1992).

The *Drosophila* genome contains the cell death genes that have been conserved between nematodes and humans (Aravind et al., 2001; Vernooy et al., 2000). While the *Drosophila* cell death genes *rpr*, *hid*, *grim* and *sickle* appear novel (Chen et al., 1996; Christich et al., 2002; Grether et al., 1995; Srinivasula et al., 2002; White et al., 1994; Wing et al., 2002), they contain limited but significant N-terminal sequence identity with the mammalian proteins Omi/Htra2 and Smac/Diablo (Wu et al., 2000; Wu et al., 2001). These conserved N-terminal sequences interact with the *Drosophila* inhibitor of apoptosis DIAP1 (Hay et al., 1995), and this interaction is similar to the interaction of Omi/Htra2 and Smac/Diablo with mammalian IAPs (Wu et al., 2000; Wu et al., 2001). The interaction of Rpr, Hid, Grim and Sickle with DIAP1 relieves inhibition of caspase

proteases that then cleave substrates (Goyal et al., 2000; Wang et al., 1999). Seven caspases have been identified in Drosophila including Dronc, Dredd, Dream/Strica, Decay, Daydream/Damm, Drice, and Dcp-1 (Chen et al., 1998; Dorstyn et al., 1999a; Dorstyn et al., 1999b; Doumanis et al., 2001; Fraser and Evan, 1997; Harvey et al., 2001; Song et al., 1997). Dronc, Dredd, and Dream/Strica are initiator caspases that can be activated in the presence of the homologue of mammalian Apaf-1 Ark/Dark/DApaf1/Hac-1 (Kanuka et al., 1999; Rodriguez et al., 2002; Rodriguez et al., 1999; Zhou et al., 1999). Once active, the initiator Caspases activate the effector or executioner Caspases including Decay, Daydream/Damm, Drice, and Dcp-1 that in turn cleave cell substrates during programmed cell death.

Dying salivary gland cells contain autophagic vacuoles, but also appear to use apoptosis genes including caspases. Expression of the caspase inhibitor p35 blocks salivary gland cell death and DNA fragmentation (Jiang et al., 1997). Furthermore, the apoptosis genes *rpr*, *hid*, *ark*, *dronc*, and *drice* are induced just before autophagic cell death (Dorstyn et al., 1999a; Jiang et al., 1997; Jiang et al., 2000; Lee et al., 2003; Lee et al., 2002b; Lee et al., 2000). These data suggest similarities between autophagic cell death and apoptosis, but little is known about how salivary gland cells are degraded. Salivary glands appear to have the lysosomal machinery that is required to degrade their own organelles, yet it is not clear if they require the assistance of phagocytes.

Although salivary gland cells also appear to use genes that are considered part of the core apoptotic machinery including caspases, the morphology of these cells and cells undergoing apoptosis are distinct. While caspase function is required for DNA fragmentation in dying salivary glands (Lee and Baehrecke, 2001), it is not known if

these proteases cleave similar substrates in cells that die by apoptotic and autophagic cell death.

Here we show that salivary gland destruction exhibits some similarities to apoptosis including blebbing and fragmentation of cells. Changes in the levels of proteins including nuclear Lamins and α -Tubulin are regulated by caspase cleavage of these substrates. In contrast, filamentous Actin appears to reorganize in a caspase-independent manner prior to degradation. Animals with mutations in *ßFTZ-F1*, *E93*, *BR-C* and *E74A* possess altered levels of active Caspase, and altered levels of structural proteins during salivary gland autophagy. Expression of either the caspase inhibitor p35 or a dominant negative form of the initiator caspase Dronc is sufficient to prevent changes in nuclear Lamins and α -Tubulin, but not filamentous Actin. Combined, these studies indicate that Caspases and cytoskeleton reorganization are needed to drive the process of salivary gland autophagic cell death.

2.3 Results.

Dying salivary gland cells exhibit some characteristics of apoptosis.

Dying salivary gland cells contain autophagic vacuoles suggesting that these cells are capable of degrading themselves (Lee and Baehrecke, 2001). It is not clear, however, what happens to these cells in the late stages of destruction. To address this issue, wild-type Canton S animals were aged either 12, 14, 14.5 or 15 hours after puparium formation, embedded in paraffin, sectioned and stained (Figure 5). Salivary glands have large vacuoles and intact nuclei 12 hours after puparium formation (Figure 5A, n = 10 animals/stage). By 14 hours after puparium formation, vacuoles are smaller in size and

nuclei appear to have separated from the cytoplasm (Figure 5B, n = 12 animals/stage). This separation is more apparent by 14.5 hours, and is accompanied by blebbing and separation of cytoplasmic fragments (Figure 5C and D, n = 12animals/stage). At 15 hours after puparium formation, cellular debris is scattered throughout the area where salivary glands were located (Figure 5E, n = 10 animals/stage).

To determine the nature of the cellular debris as salivary glands are destroyed, the TUNEL assay was used to distinguish nuclei containing fragmented DNA from possible cytoplasmic fragments (Figure 6). TUNEL-positive nuclei begin to separate from the cytoplasm 14 hours after puparium formation (Figure 6A, n = 13 animals/stage). At 15 and 16 hours after puparium formation, TUNEL-positive nuclei and TUNEL-negative structures that are presumably fragments of cytoplasm are present (Figure 6B and C, n = 22 animals/stage). Differentially-stained cells also appear when most of the salivary gland degradation has occurred, but it is unclear if these cells are phagocytes based on this resolution. Transmission electron microscopy (TEM) analyses of salivary glands isolated 14.5 hours after puparium formation revealed the separation of nuclei from the cytoplasm (Figure 6D, n = 15 animals/stage). Furthermore, membranous structures resembling smooth endoplasmic reticulum are present in the balls of cellular debris indicating that these are spheres of cytoplasm (Figure 6E, n = 15 animals/stage). Although differentially-stained cells were observed at very late stages of salivary gland degradation (Figures 6B,C), no obvious phagocytes containing cell fragments were observed using TEM.

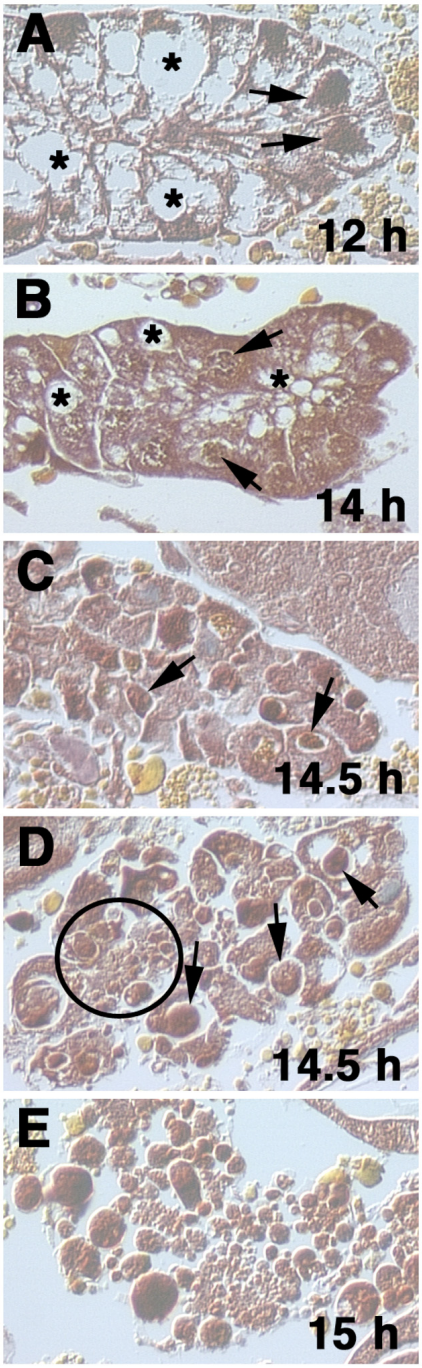

Figure 5. Salivary gland cells fragment as they die. (A) Twelve-hour salivary glands have large vacuoles (asterisks) and nuclei (arrows). (B) Vacuoles (asterisks) are smaller in salivary glands of 14-hour animals, and nuclei (arrows) begin to separate from the cytoplasm. (C-E) Salivary glands rapidly degenerate 14.5 hours to 15 hours after puparium formation. (C, D) Nuclei (arrows) and cytoplasm of salivary glands separate 14.5 hours after puparium formation, and fragments of cytoplasm (enclosed in circle) are present that appear to be similar to cell fragmentation that occurs during apoptosis. (E) By 15 hours after puparium formation, fragments of cellular debris are scattered throughout the area that was occupied by salivary glands. All images are at the same magnification.

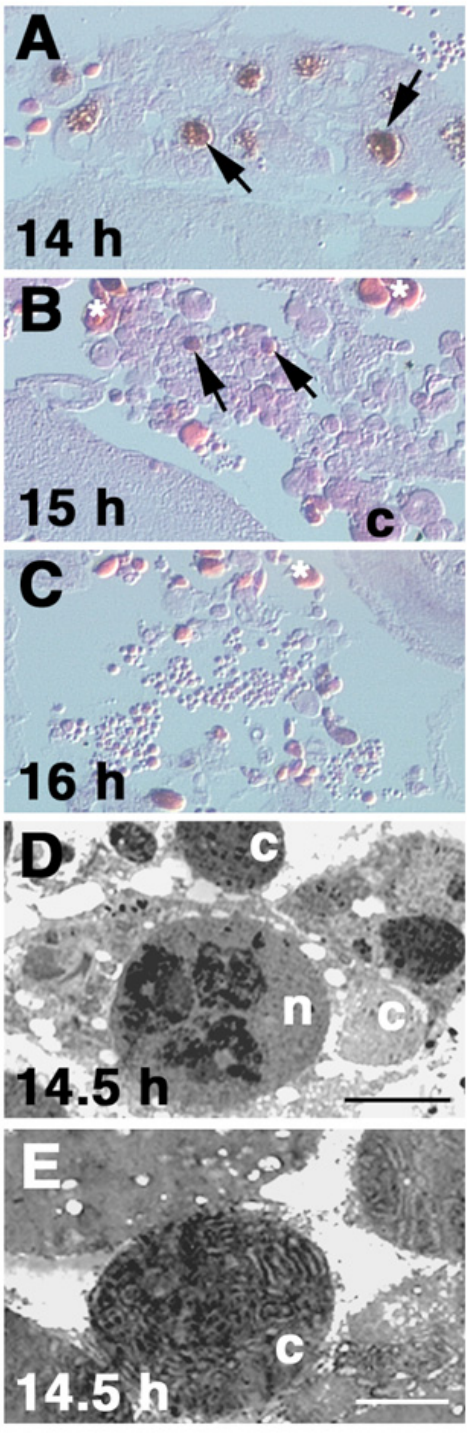

Figure 6. Salivary glands appear to degrade without the assistance of phagocytes. (A) At 14 hours after puparium formation, salivary glands possess TUNEL-positive nuclei (arrows). (B) TUNEL-positive nuclei (arrows) are surrounded by TUNEL-negative structures that are presumably fragments of salivary gland cytoplasm 15 hours after puparium, as well as by a small number of unidentified cells (asterisks). (C) At 16 hours after puparium formation, few if any TUNEL-positive structures are present in the location where salivary glands reside prior to destruction, and unidentified cells (asterisks) are present. (D) Transmission electron micrograph of salivary glands 14.5 hours after puparium formation shows the separation of the nucleus (n) from the cytoplasm (c). (E) Membranous structures reminiscent of smooth endoplasmic reticulum are present in some of the balls of cytoplasm (c). Images in A-C are the same magnification. Scale bar in D 10 μm, E 1μm.

Changes in protein levels and localization are associated with increased caspase activity during autophagic cell death.

Salivary glands undergo dynamic morphological changes during autophagic cell death (Lee and Baehrecke, 2001; Figures 1, 2). These changes in cell shape and organization may be controlled by the modification of structural protein organization and/or by the activity of proteases including caspases. Since structural proteins have been implicated as substrates for caspases (Cryns and Yuan, 1998), we examined changes in the localization and abundance of structural proteins during cell death. Wild-type Canton S animals were staged either 8, 10, 12, or 14 hours after puparium formation, salivary glands were dissected, fixed and stained with antibodies against α -Tubulin, α -Spectrin, nuclear Lamin DmO or Croquemort, and rhodamine phalloidin was used to label filamentous Actin (Figure 7, n = many cells from 20 animals/stage/stain). The localization of both α -Tubulin and filamentous Actin changes from a network spread across the cytoplasm of salivary gland cells 8 hours after puparium formation to a less evenly distributed and somewhat clustered localization in the case of filamentous Actin 10 hours after puparium formation (Figure 7). By 12 hours after puparium formation, α -Tubulin is difficult to detect, and filamentous Actin is extremely clustered in the cytoplasm and spread along the cortical region of the cell. By 14 hours after puparium formation, α -Tubulin is absent and filamentous Actin is difficult to detect. Although α -Spectrin remains present and associated with the cortex, its levels also begin to decrease between 12 and 14 hours following puparium formation in dying salivary glands. Nuclear Lamins are also present 8 hours after puparium formation, and decrease in abundance in 10- to 12-hour salivary glands. This change initially appears as spots

associated with the chromosomes, and Lamins are difficult to detect by 14 hours after puparium formation. At the stage when nuclear Lamins are nearly absent in salivary glands, Croquemort is initially detected in the cytoplasm, making this protein an excellent marker for late stage cytoplasmic changes.

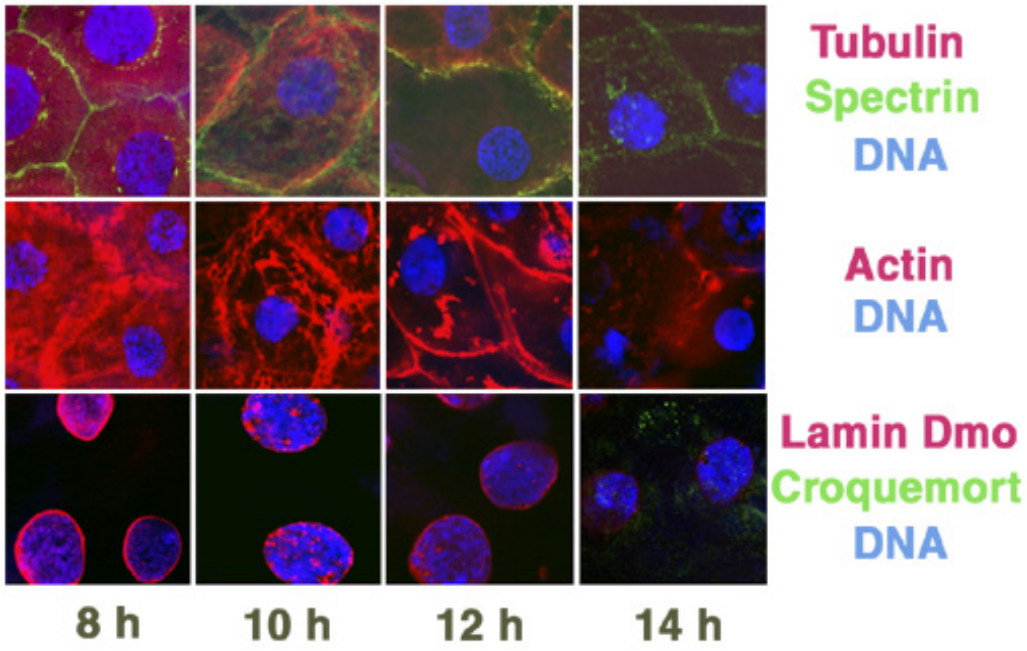

Figure 7. Structural proteins exhibit dynamic changes during salivary gland autophagic cell death. Salivary glands of staged wild-type Canton S animals were stained with antibodies against α -Tubulin (red) and α - Spectrin (green) in the top panels, rhodamine phalloidin to visualize filamentous Actin (red) in the middle panels, antibodies against nuclear Lamin DmO (red) and Croquemort (green) in the lower panels, and the nuclei are labeled with TOTO-3 (blue) in all images. The α -Tubulin network which is present in a uniform pattern in the cytosol in early stages starts to disappear by 12 hours after puparium formation, and is no longer detectable 14 hours after puparium formation. α - Spectrin is present along the cortex at 8, 10 and 12 hours after puparium formation and is nearly absent at 14 hours. Filamentous Actin changes from a cytoplasmic network at 8 hours to aggregates within the cytoplasm and along the cortical region 10 and 12 hours after puparium formation, and is difficult to detect by 14 hours after puparium formation. Nuclear Lamin DmO is expressed in a uniform pattern along the nuclear envelope in 8-hour salivary gland cells, becomes more punctate and is less abundant in 10- and 12-

hour salivary glands, and is nearly absent in salivary glands 14 hours after puparium formation. Croquemort is not detectable at early stages of salivary gland cell death, but appears in the cytoplasm at 14 hours after puparium formation making it a good marker for late stage changes during salivary gland autophagic cell death.

Nuclear Lamins have been implicated as caspase substrates (McCall and Steller, 1998; Rao et al., 1996). Therefore, we examined if changes in nuclear Lamin DmO levels and localization are associated with the expression of active Caspases and cleavage of nuclear Lamins (Figure 8, n = many cells from 22 animals/stage/stain). Active Caspase-3/Drice protein level increases in the cytoplasm as nuclear Lamin DmO decreases in abundance 10 to12 hours after puparium formation, and this is the time when the cleaved form of nuclear Lamin appears in the cytoplasm. By 14 hours after puparium formation, the levels of Lamin DmO are low or absent, and active Caspase-3/Drice and cleaved Lamins are abundant in the cytoplasm (Figure 8, n = many cells from 46 animals/stage/stain).

The association of protein changes with increases in active Caspase levels suggests that proteolysis by Caspases occurs during salivary gland autophagic cell death. It is possible that changes in structural protein localization in the absence of proteolysis are also important for proper cell degradation to occur. Protein was extracted from salivary glands of wild-type animals that were staged 8, 10, 12 and 14 hours after puparium formation and equal amounts of protein/stage were separated by electrophoresis and analyzed by Western/immuno blot to assess quantitative changes in proteins. Western blots were incubated with antibodies against Lamin and Actin (Figure 9). Full length 76 kD Lamin is cleaved to 45 kD 10 hours after puparium formation, which is consistent with the expected size based on the location of the caspase cleavage site in Lamin, and the timing of changes in immuno-localization of this protein (Figure 7). This 45 kD cleavage product is also present 12 and 14 hours after puparium

formation. In contrast, the full length 42 kD Actin protein is present in equal quantity until 12 hours after puparium formation and is absent by 14 hours with no detectable cleavage product. The difference in the timing of the degradation of nuclear Lamins and Actin is intriguing, and suggests the possibility that the changes in filamentous Actin localization observed 10 hours after puparium formation (Figure 7) are not due to proteolysis of Actin by caspases, but may be caused by reorganization of Actin followed by proteolysis 14 hours after puparium formation.

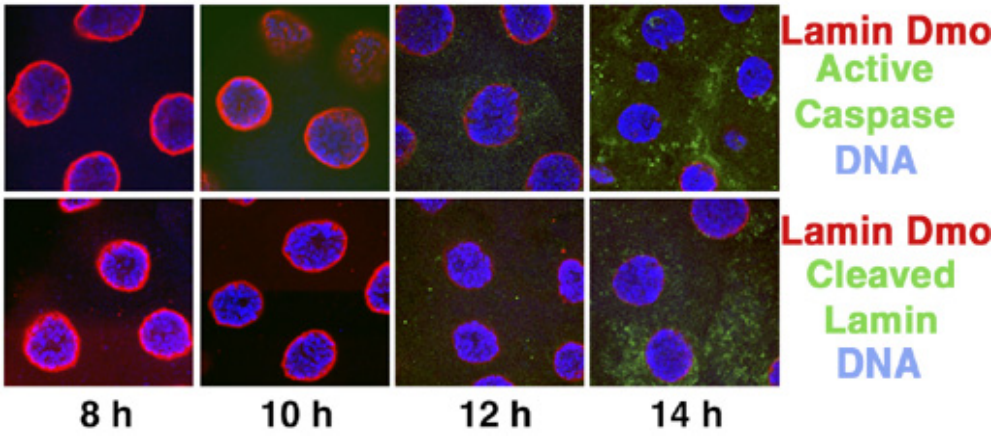

Figure 8. Changes in nuclear Lamins are associated with increased levels of active caspase. Salivary glands from wild-type Canton S were dissected and stained with antibodies against nuclear Lamin DmO (red) and active Caspase-3/Drice (green) in the top panels and nuclear Lamin DmO (red) and cleaved nuclear Lamin (green) in the bottom panels. Nuclear Lamin DmO is present in 8 and 10 hours after puparium formation and decreases by 12 hours after puparium formation. At this stage, active Caspase-3/Drice and cleaved nuclear Lamin are present in the cytoplasm, and increase by 14 hours after puparium formation.

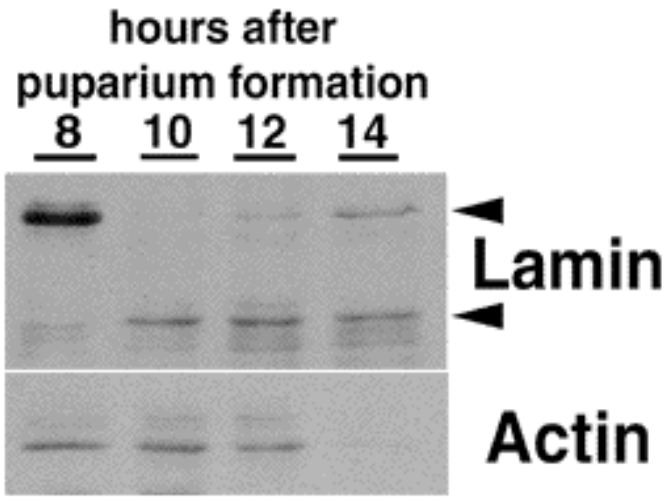

Figure 9. Changes in the localization of Lamins coincide with their degradation, while Actin changes localization prior to degradation. Western blot of wild-type Canton S salivary gland protein extracts show that full length 76 kD Lamin is cleaved to 45 kD (the expected size following caspase cleavage) starting 10 hours after puparium formation. In contrast, full length Actin persists through 12 hours, and is not detected in extracts of salivary glands 14 hours after puparium formation.

Mutations in steroid-regulated genes impact protein changes and caspase activation during autophagic cell death.

Animals with mutations in the ecdysone regulated genes *ßFTZ-F1, E93, BR-C* and *E74A* have salivary glands that persist past the time when wild-type salivary glands are destroyed (Broadus et al., 1999; Lee and Baehrecke, 2001; Restifo and White, 1992). Each of these mutants appears to be arrested at different stages of cell destruction (Lee and Baehrecke, 2001), enabling the examination of how *ßFTZ-F1, E93, BR-C* and *E74A* impact protein changes and Caspase activation during autophagic cell death. Salivary glands were dissected from mutants aged to 24 hours after puparium formation (8 hours after salivary glands are destroyed in wild-type animals) and stained with antibodies against either α -Tubulin, α -Spectrin, nuclear Lamin DmO or Croquemort, and rhodamine phalloidin was used to label filamentous Actin (Figure 10, n = many cells from 20 animals/genotype/stain). *ßFTZ-F1* mutant salivary glands are arrested prior to the onset of most changes in these proteins (see Figure 7 for comparison with wild-type), although filamentous Actin is in clumps in the cytoplasm indicating that some protein changes progress to slightly later stages. *E93* mutant salivary gland cells possess α -Tubulin and α -Spectrin protein levels and localization that are similar to that observed in 10- to 12-hour salivary gland cells. However, filamentous Actin localization has changed to a late stage that is similar to 12 to14 hour wild-type, and decreased levels of Lamin DmO and the presence of Croquemort protein indicates that several protein changes have occurred that are normally associated with cell death. *BR-C* mutant salivary gland cells possess abnormal structural protein changes that we never observe in wild-type cells. For example, α -Tubulin and α -Spectrin staining do not overlap and α -Spectrin is present in

a wider area than expected. This is interesting, as α -Spectrin remains present in the cortical region of the cell in *BR-C* mutants even though these cells appear to lack plasma membranes (Lee and Baehrecke, 2001). In addition, filamentous Actin appears speckled in the cytoplasm of *BR-C* mutants. *E74A* mutant salivary gland cells progress to a late stage in cell death, as filamentous Actin and nuclear Lamin staining are weak, and Croquemort is present similar to 14 hour wild-type cells. The only exceptions are that α -Tubulin and α -Spectrin are both present, and that there are fragments of α -Spectrin staining in the cytoplasm, which are consistent with the apparent presence of membrane fragments in *E74A* mutant salivary glands (Lee and Baehrecke, 2001).

The differences in the distribution of proteins in *ßFTZ-F1*, *E93*, *BR-C* and *E74A* salivary glands may indicate that differences in Caspase activation occur in these mutants. Therefore, we examined the distribution of active Caspase-3/Drice, nuclear Lamin DmO and cleaved nuclear in *ßFTZ-F1*, *E93*, *BR-C* and *E74A* mutants (Figure 11, n = many cells from 10 animals/genotype/stain). Active Caspase and cleavage of Lamin are not detected the salivary glands of *ßFTZ-F1* mutant animals. *E93* mutant salivary glands possess low levels of active Caspase and cleaved Lamin, and retain substantial amounts of Lamin DmO. In *BR-C* mutant salivary glands, Lamin DmO is localized in spots, low levels of active Caspase associated with the nucleus, and cleaved Lamin was not detected. *E74A* mutants progress to a late stage with little Lamin DmO staining, and high levels of active Caspase-3/Drice and cleaved Lamin being present in the cytoplasm. These results indicate that the differences in the cell morphology of *ßFTZ-F1*, *E93*, *BR-C* and *E74A* mutant salivary glands may be caused by the amount of Caspase activity in these mutants.

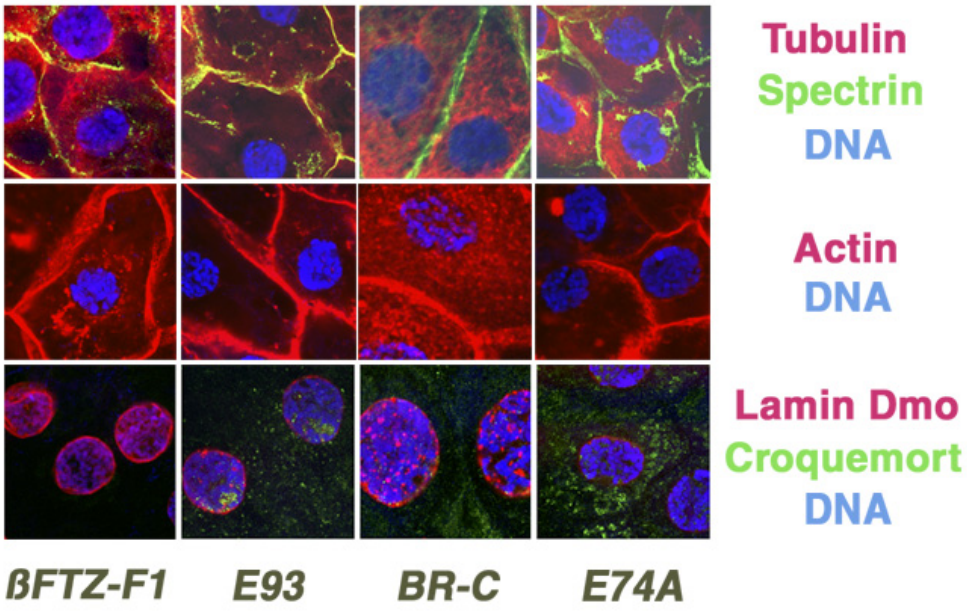

Figure 10. Animals with mutations in *ßFTZ-F1*, *E93*, *BR-C*, and *E74A* have altered levels and localization of structural proteins. Salivary glands were dissected from mutants 24 hours after puparium formation, and analyzed for the levels and localization of α -Tubulin (red) and α -Spectrin (green) in the top panels, filamentous Actin (red) in the middle panels, and nuclear Lamin DmO (red) and Croquemort (green) in lower panels. The α -Tubulin network is present in the salivary glands of all of these mutants, but it appears to be slightly lower in the cytoplasm of *E93* mutants. α -Tubulin appears to be absent near the cortex in *BR-C* and *E74A* mutant animals given the lack of overlap with α -Spectrin staining. α -Spectrin is present along the in *ßFTZ-F1*, *E93*, and *BR-C*, and in fragments in the cytoplasm of *E74A* mutant salivary glands. Filamentous Actin is aggregated in clumps in the cytosol and is expressed along the cortical region of salivary gland cells in *ßFTZ-F1*, *E93*, *BR-C*, and *E74A* mutant animals, although differences clearly exist in the localization of this protein in the different mutants. Nuclear Lamin DmO is present and evenly expressed in association with the nuclear membrane in *ßFTZ-F1* mutant salivary gland cells, is expressed at a lower level with punctate spots in *E93*

and *BR-C* salivary glands, and is difficult to detect in *E74A* mutant salivary gland cells. Croquemort is not detectable in *ßFTZ-F1* mutant salivary glands, is expressed at a lower level in *E93* and *BR-C* salivary glands, and is highly expressed in *E74A* mutant salivary gland cells.

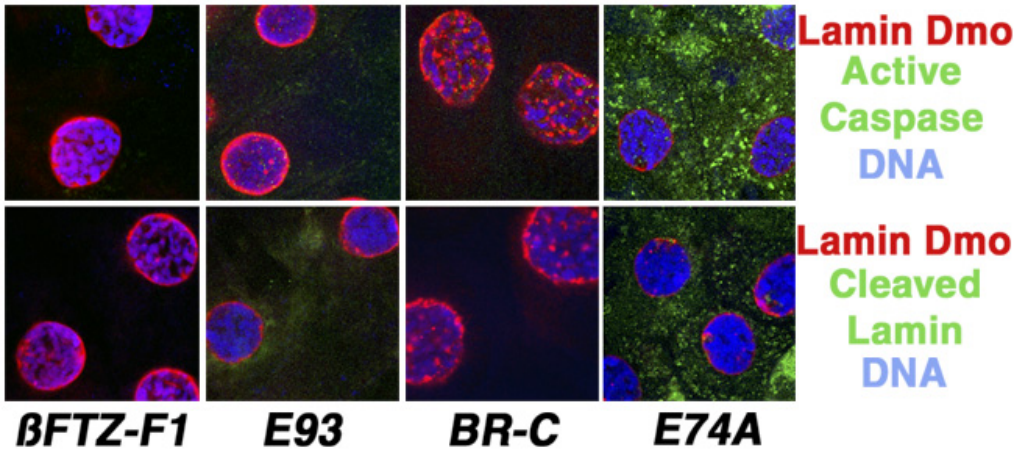

Figure 11. Mutations in *ßFTZ-F1*, *E93*, *BR-C*, and *E74A* impact caspase activation during autophagic cell death. Salivary glands were dissected from mutants 24 hours after puparium formation, and either analyzed for abundance and localization of nuclear Lamin DmO (red) and active Caspase-3/Drice (green) in the top panels, or nuclear Lamin DmO (red) and cleaved nuclear Lamin (green) in the bottom panels. Active Caspase-3/Drice and cleaved nuclear Lamins are absent in *ßFTZ-F1* salivary glands, are present at extremely low levels in *E93* and *BR-C* salivary gland cells, and are expressed at elevated levels in *E74A* mutant salivary gland cells.

Inhibition of caspases alters protein changes that occur during autophagic cell death.

Expression of the caspase inhibitor p35 is sufficient to prevent salivary gland destruction and DNA fragmentation, although inhibition of caspases does not prevent changes in vacuolar structures in these cells (Lee and Baehrecke, 2001). Since transcription of the initiator caspase *dronc* immediately precedes salivary gland cell death (Lee et al., 2000), we tested if expressing a dominant-negative form of Dronc is sufficient to prevent salivary gland cell death. In animals that express a dominant negative Dronc C318A transgene under the control of a heat-inducible promoter, 22% of the pupae had persistent salivary glands 24 hours after puparium formation (n = 383), while no salivary gland cells persisted in control animals containing the same transgene that were not heat-shocked. Similar analyses using the salivary gland-specific fkh-GAL4 driver resulted in 10% of the animals having persistent salivary glands (n = 122). As in studies of p35, expression of dominant negative Dronc is sufficient to prevent DNA fragmentation in persistent salivary glands (Figure 12A, n = 8), even though DNA is fragmented in midguts. In addition, expression of dominant negative Dronc does not prevent vacuolar changes in the cytoplasm of persistent salivary glands (Figure 12A).

To determine which proteins changes are regulated by caspases during salivary gland autophagic cell death, p35 and dominant negative Dronc were expressed in salivary glands prior to cell death changes and analyzed 24 hours after puparium formation (Figure 12B, n = many cells from 8 animals/transgene/stain). When p35 is expressed, α -Tubulin and α -Spectrin are localized in a pattern that is similar to that of 8-hour salivary gland cells (see Figure 7 to compare to wild-type cells), indicating that caspases are

involved in regulating changes in these proteins. Similarly, nuclear Lamin DmO levels and localization appear similar to that in 8-hour salivary glands. The cytoplasm of these cells has clearly progressed to a later stage, however, as Croquemort is expressed (we never observe high levels of both Lamin DmO and Croquemort in wild-type cells). While expression of p35 blocks several protein changes, filamentous Actin localization is similar to later stages in dying salivary glands, suggesting that the changes in Actin structure may not be dependent on caspase function. This is consistent with the differences in the timing of changes in nuclear Lamins and filamentous Actin based on quantitative western blot studies (Figure 9). Salivary glands that survive following the expression of dominant negative Dronc exhibit limited changes in α -Tubulin, α -Spectrin, and nuclear Lamin DmO (Figure 12B). Croquemort expression is observed, however, indicating that changes in the cytoplasm have occurred. Expression of dominant-negative Dronc was not sufficient to prevent changes in filamentous Actin, consistent with the possibility that some changes in proteins during autophagic cell death of salivary glands are not regulated by Caspases.

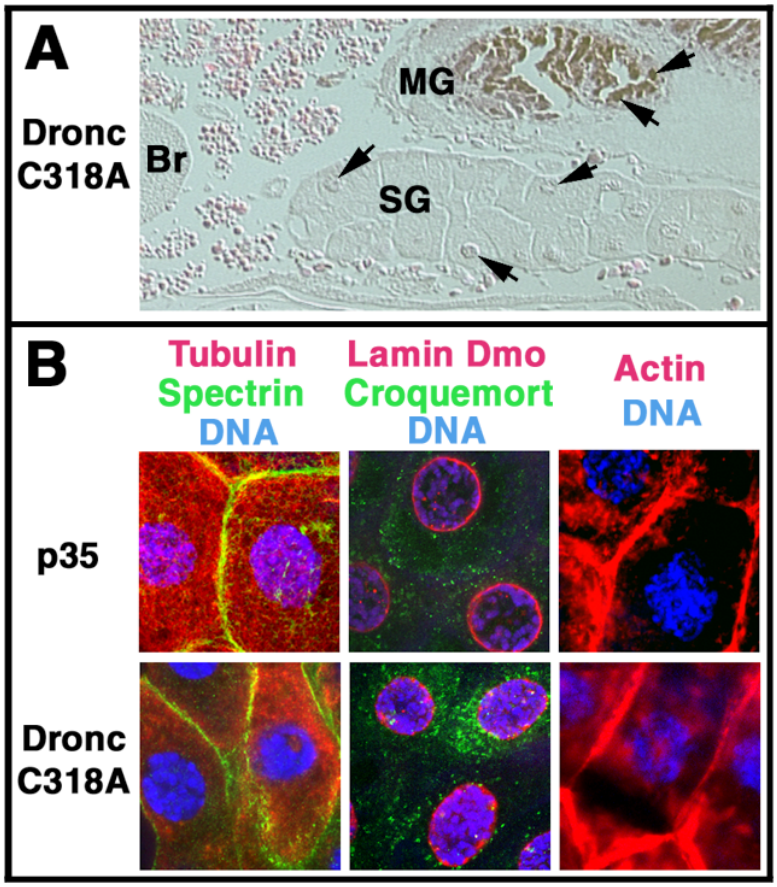

Figure 12. Inhibition of Caspases prevents protein changes and salivary gland cell death. (A) Animals staged 24 hours after puparium formation that express the dominant negative form of Dronc C318A possess persistent salivary glands (SG) that lack vacuoles, but have nuclei with intact DNA (arrows) even though the DNA of the larval midgut (MG) is fragmented (dark stain, arrows). The brain (Br) is indicated to assist with orientation. (B) Expression of p35 and dominant negative Dronc C318A prevent changes in the expression of α -Tubulin (red) and α -Spectrin (green) in the left panels, and nuclear Lamin DmO (red) in the middle panels. In contrast, expression of p35 and dominant negative Dronc C318A did not prevent the increase in abundance of Croquemort (green in the middle panels) in the cytoplasm even though nuclear Lamin DmO (red) is expressed in the same cell, indicating that some cytoplasmic changes are

not regulated by Caspases. Similarly, filamentous Actin (red in the right panels) changes proceed and resemble 12 hour wild-type salivary gland cells even though expression of p35 and dominant negative Dronc C318A prevents the death of these cells.

2.4 Discussion.

Apoptosis and autophagic cell death are the two most common morphological forms of physiological cell death that occur in developing animals (Baehrecke, 2002; Clarke, 1990). While substantial details are known about the mechanisms that regulate apoptosis (Hengartner, 2000; Martin, 2002; Shi, 2002), far less is known about autophagic cell death. The distinct morphology of apoptotic and autophagic cells led to the identification of unique features in very different cell types (Schwartz et al., 1993). Here we show that the mechanisms that regulate these different forms of cell death may not be as unique as their morphologies imply. While *Drosophila* salivary glands appear to die without the assistance of phagocytes, Caspases function in their autophagic cell death. The accumulation of active Caspases in salivary glands depends on the function of steroid-regulated transcription factors, and correlates with decreased levels of caspase substrates including nuclear Lamins. Since inhibition of Caspase activity is sufficient to prevent cleavage of Caspase substrates and destruction of salivary glands, this study indicates that Caspases are not only important for apoptosis, but also play a central role in autophagic programmed cell death.

Apoptosis and autophagic cell death share some morphological characteristics.

Studies of dying salivary glands indicate that autophagic cell death has similarities to and differences from apoptosis. Several markers of apoptosis including nuclear staining by acridine orange and DNA fragmentation appear 2 hours following the rise in steroid hormone that triggers salivary gland cell death (Jiang et al., 1997). The cytoplasm and membranes of salivary gland cells bleb and fragment as these cells

degrade (Figures 5 and 6), and these are characteristics that are common to apoptotic cells (Kerr et al., 1972). These common morphologies raise the questions of what distinguishes apoptosis from autophagic cell death and what common and different regulatory mechanisms mediate these forms of cell killing. The mechanisms of cell degradation and removal appear to provide the clearest distinction between apoptosis and autophagic cell death. In salivary glands, dynamic changes in vacuole structure immediately precede their demise, and such changes have not been reported in apoptotic cells (Kerr et al., 1972; Schweichel and Merker, 1973). Within one hour of salivary gland DNA degradation, large vacuoles appear to break into smaller vacuoles, and this occurs within 2 hours of complete tissue destruction (Lee and Baehrecke, 2001; Figure 1). As these large vacuoles fragment, smaller but distinct vacuoles accumulate near the plasma membrane, and autophagic vacuoles containing components of the cytoplasm including mitochondria are formed. Salivary gland cells then begin to fragment, and TUNEL-positive nuclei and components of the cytoplasm then disperse within the haemocoel with little or no appearance of phagocytes (Figure 6). Although we can not exclude a role for phagocytes in autophagic cell death, it is clear that salivary gland cells proceed to late stages of degradation without the assistance of phagocytes. It has been suggested that phagocytes may play a secondary role in the removal of cellular debris towards the end autophagic cell death (Schweichel and Merker, 1973), and our results are consistent with this possible conclusion. The presence of autophagic vacuoles in degrading salivary glands further indicates that autophagic cells utilize their own lysosomes for degradation, while apoptotic cells depend on phagocytes for the bulk degradation of long-lived cellular proteins. Therefore, salivary glands appear to possess

the combined machinery of an apoptotic cell and a phagocyte, as they utilize Caspases and are able to internalize and degrade their organelles within their own lysosomes.

Maintenance of the Actin cytoskeleton may be necessary for autophagic cell death.

Dying cells exhibit dynamic changes in cell shape (Kerr et al., 1972; Schweichel and Merker, 1973). The changes in cell shape and organization that occur during autophagic cell death of salivary glands are likely controlled by the modification of structural protein organization. Indeed, dynamic changes in the abundance and localization of filamentous Actin, α -Tubulin, α Spectrin, and nuclear Lamins immediately precede the death of salivary glands (Figure 6). At least two possible explanations exist for how such changes in protein expression are regulated in dying cells. One model is that proteases including Caspases cleave structural proteins (Cryns and Yuan, 1998), and that this results in the changes in cell shape that are typical of apoptosis including blebbing and fragmentation. Alternatively, the same changes in cell shape could be regulated by changes in the assembly of cytoskeletal proteins such as filamentous Actin through signaling that is mediated by small GTPases (Coleman and Olson, 2002).

Proteolysis and changes in the assembly of the cytoskeleton both appear to be involved in the regulation of changes that occur during autophagic cell death of salivary glands. While Caspases play an important role in autophagic cell death of salivary glands, several lines of evidence suggest that some changes in the structure of the cytoskeleton may occur in a caspase-independent manner. First, while changes in filamentous Actin localization occur in synchrony with changes in proteins such as

nuclear Lamins that are cleaved by Caspases (Figure 7), changes in Actin protein levels are delayed by 4 hours (Figure 9). Second, mutations in steroid-signaling genes such as *ßFTZ-F1* that prevent expression of active Caspase 3 and cleavage of nuclear Lamins do not prevent changes in filamentous Actin localization (Figure 10). Third, while inhibition of Caspases by expression of either p35 or a dominant negative form of DRONC is sufficient to prevent changes in nuclear Lamins and α -Tubulin, these inhibitors are not sufficient to block changes in filamentous Actin (Figure 12). These data are further supported by the observation that numerous small GTPases increase their expression immediately prior to salivary gland cell death (Lee et al., 2003). Although previous studies have suggested that changes in the Actin cytoskeleton are required for autophagic cell death (Bursch et al., 2000; Jochova et al., 1997), the failure to distinguish between cytoskeleton proteolysis and rearrangement has made it difficult to interpret the potential significance of maintenance of the cytoskeleton during cell death.

Several possibilities exist to explain why the cytoskeleton is maintained during cell death. The cytoskeleton is utilized to restrict the sub-cellular location and activity of pro-apoptotic regulators of the Bcl-2 family and activation of apoptosis (Puthalakath et al., 1999; Puthalakath et al., 2001). While this mechanism is certainly possible, this seems unlikely during salivary gland autophagic cell death since the Actin cytoskeleton is maintained after caspase-dependent cleavage of substrates including nuclear Lamins (Figures 7-9, 12). Alternatively, the Actin cytoskeleton could be maintained as a substrate to localize proteins, membranes and vacuoles within the cell. Intracellular trafficking plays an important role in autophagy, as membrane-bound cytoplasmic components (autophagic vacuoles) are transported to the lysosome for degradation

(Baehrecke, 2003; Klionsky and Emr, 2000; Ohsumi, 2001). Since we observe autophagic vacuoles at stages after caspase activation and cleavage of substrates such as nuclear Lamins (Lee and Baehrecke, 2001; Figures 7-9), it is possible that the Actin cytoskeleton is maintained to enable transport of vacuoles to lysosomes. While this is an appealing model, little is known about the role of the cytoskeleton in autophagic cell death, and empirical studies are needed to determine how cargo is transported in these dying cells, and what other possible roles the cytoskeleton may play in the regulation of autophagic cell death.

Caspases are required for autophagic cell death.

Studies of salivary glands indicate that Caspases play an important role in their autophagic cell death. The caspase-encoding genes *dronc* and *drice* increase in transcription following the rise in steroid that triggers salivary gland autophagic cell death (Lee et al., 2003; Lee et al., 2002a; Lee et al., 2000). This increase in caspase transcription corresponds to the increase in active Caspase protein levels and cleavage of substrates such as nuclear Lamins in dying salivary glands (Figures 8, 9). Mutations in the steroid-regulated *ßFTZ-F1*, *E93*, and *BR-C* genes that prevent salivary gland cell death exhibit little or no active Caspase-3/Drice expression, and have altered α -Tubulin, α -Spectrin, nuclear Lamin expression in salivary glands (Figures 10, 11). Although *E74A* mutants prevent salivary gland cell death, they have elevated Caspase-3/Drice levels and degraded nuclear Lamins (Figure 11). While these data are consistent with the partially degraded morphology of *E74A* mutant salivary glands (Lee and Baehrecke, 2001), it remains unclear what factor(s) *E74A* may regulate that are required for normal

cell death. Our data indicate, however, that *ßFTZ-F1*, *E93*, and *BR-C* play a critical role in determining Caspase levels in dying salivary gland cells, and this is supported by the impact of these genes on transcription of dronc (Lee et al., 2002a). Significantly, inhibition of Caspases by expression of either p35 or dominant negative Dronc is sufficient to prevent DNA fragmentation, changes in nuclear Lamins and α -Tubulin, and death of salivary glands (Jiang et al., 1997; Lee and Baehrecke, 2001; Figure 12). Combined, compelling evidence points to the importance of Caspases during autophagic cell death of *Drosophila* salivary glands. The morphologies of dying cells indicate that apoptosis and autophagy are distinct. However, the difference between these cells becomes less apparent when one considers characteristics that were previously considered to be specific to apoptosis. Clearly, markers such as DNA fragmentation, expression and function of Caspases, and cleavage of Caspase substrates can exist in cells that possess the morphology of autophagic cell death. Since expression of dominant negative Dronc is sufficient to block caspase-dependent changes in salivary glands, our studies also indicate that the mechanism for Caspase activation during autophagic cell death is similar to apoptosis during development of *Drosophila*; the initiator caspase Dronc regulates the activation of the executioner caspase Drice and cleavage of cell substrates (Yu et al., 2002). It is surprising how little is known about the activity of Caspases in developing animals, as these important proteases have been a subject of substantial investigation. Recent studies indicate that Caspases do not only function during autophagic and apoptotic cell death, but that they are also used to degrade proteins during the differentiation of sperm in *Drosophila* (Arama et al., 2003; Huh et al, 2004). Successful development of sperm must require spatially restricted activity of Caspases

with in the cell, and the same may be true for dying cells. Studies of salivary glands indicate that the distinction between apoptosis and autophagic cell death may be more subtle than their morphology suggests, and raise the question of what makes these cells look so different. Restriction of Caspase activity within compartments of the dying cell may provide one possible explanation, but it is also possible that other mechanisms of proteolysis occur during autophagic cell death. This possibility is supported by the large increase in transcription of non-caspase proteases just before cell death of salivary glands (Lee et al., 2003), and the fact that unlike apoptotic cells that require phagocyte lysosomes, salivary gland cells appear to degrade much of themselves through autophagy. Future studies should provide important insights into the similarities and differences in the mechanisms that regulate apoptosis and autophagic programmed cell death.

2.5 Materials and Methods.

Salivary gland histology.

Wild-type Canton S *Drosophila* were maintained at 25°C and aged to different stages following puparium formation. For paraffin sections and light microscopy, whole pupae were fixed, embedded, sectioned, and either stained with Gill's Hematoxylin and Pollack Trichrome or analyzed using the TUNEL method as previously described (Lee and Baehrecke, 2001) and examined using a Zeiss Axiophot II microscope. For examination of thin sections by electron microscopy, whole pupae were fixed for 4 hours in 4% paraformaldehyde, 8 hours in 3% glutaraldehyde/0.2% tannic acid in 0.1 M Mops buffer (pH 7.0) at room temperature and for 16 hours in 3% glutaraldehyde/1%

paraformaldehyde in 0.1 Mops buffer (pH 7.0) at 4oC, post fixed in 1% osmium tetroxide for 1 hour, embedded in Spurr's resin, sectioned and analyzed using a Zeiss EM 10 transmission electron microscope.

Antibody staining.

Antibodies against α -Spectrin (Dubreuil et al., 1987), Lamin Dm0 ADL84 (Stuurman et al., 1995), α -Tubulin 3A5 (Piperno and Fuller, 1985), Croquemort (Franc et al., 1996), and active Drice (Yoo et al., 2002) were obtained from Drs. D. Branton, P. A. Fisher, M.T. Fuller, N. C. Franc, and B. A. Hay respectively. Antibodies against cleaved Caspase-3 (Asp175) and cleaved Lamin (Asp230) were obtained from Cell Signaling Technology (Beverly, MA), and rhodamine Phalloidin, TOTO-3 and secondary antibodies were purchased from Molecular Probes (Eugene, OR). Wild-type Canton S, and *ßFTZ-F1* (*ßFTZ-F1*^{17}/*ßFTZ-F1*^{19}), *BR-C* (*rbp*^{5}/*Y*), *E74A* (*E74A*$^{p[neo]}$/*Df(3L)st-81k19*), and *E93* (*E93*^{1}/*Df(3R)93F*$_{x2}$) mutant salivary glands were dissected from animals staged relative to puparium formation at 25^{o}C, fixed in 4% paraformaldehyde/heptane for 20 minutes at room temperature, blocked in phosphate buffered saline containing 1% BSA and 0.1% Triton-X (PBSBT), and incubated with primary antibodies for 16 hours at 4^{o}C. Salivary glands were washed for 2 hours in PBSBT, incubated with appropriate secondary antibodies for two hours at room temperature, washed for another 2 hours in PBSBT at room temperature, incubated in 0.5 µl TOTO-3 in 1 ml PBSBT for ten minutes at room temperature, and washed in PBSBT for an additional hour at room temperature. For rhodamine Phalloidin staining of filamentous Actin, salivary glands were fixed in 16% paraformaldehyde, incubated in 1% Triton-X in PBS and incubated in

5 µl of rhodamine Phalloidin in 100 µl PBS for 20 minutes at room temperature as previously described (Frydman and Spradling, 2001). Salivary glands were mounted in Vectashield (Vector Laboratories) and examined using a Zeiss Axiovert 100 M confocal microscope.

Expression of p35 and dominant negative Dronc in salivary glands.

To express p35 in salivary glands, *y, w*; *UAS-p35*/*UAS-p35* males were crossed to *y,w, fkh-GAL4*/*y,w, fkh-GAL4* virgin females. Progeny of this cross were aged to 24 hours after puparium formation and stained for expression of nuclear Lamin Dm0, Croquemort, α -Tubulin, α -Spectrin and filamentous Actin as described above. To examine the impact of expressing dominant negative Dronc in salivary glands, transgenic males containing either dominant negative *UAS-Dronc C318A* (Meier et al., 2000) or *UAS-Dronc C318G* (Quinn et al., 2000) were crossed to virgin females of either the salivary gland GAL4 promoter strain *y,w, fkh-GAL4*/*y,w, fkh-GAL4* or the heat-inducible promoter strain *y,w, hs-GAL4*/*y,w, hs-GAL4*. Controls consisted of the dominant negative Dronc transgenic strains that were not crossed to a GAL4 driver strain. Since the dominant negative Dronc C318A strain had a higher level of persistent salivary glands in preliminary studies, all data that are reported were derived from this strain. Progeny derived from the *fkh-GAL4* and *UAS-Dronc C318A* cross were aged to 24 hours after puparium formation and analyzed for salivary gland persistence. Progeny from derived from the *hs-GAL4* and *UAS-Dronc C318A* cross were heat-shocked for 30 minutes at 37^{o}C at 11, 13 and 16 hours after puparium formation, and analyzed for salivary gland persistence. Persistent salivary glands were stained for expression of nuclear Lamin

Dm0, Croquemort, α -Tubulin, α -Spectrin and filamentous Actin as described above.

Protein extraction and western/immuno blot analysis.

Wild-type Canton S salivary glands were dissected from animals staged 8, 10, 12, and 14 hours after puparium formation, homogenized in 0.1% glycerol, 2% SDS, 0.125% 1M Tris (pH 6.8), 0.05% ß-mercaptoethanol, and 0.05% Bromo-phenol blue, and boiled for 5 minutes at 100^{o}C. Equal amounts of total protein extracts were separated by electrophoresis on 12% acrylamide gels and either transferred to 0.45 µm Immobilon-P membranes (Millipore), or duplicate gels of identical extracts were assessed for equal loading and integrity by Coomasie blue staining (Bio-Rad). Membranes were blocked in 10% non-fat milk in PBS with 1% Tween 20 for 1 hour at 37^{o}C, incubated in primary antibody for 16 hours at 4^{o}C, washed in PBS containing 1% Tween 20 at room temperature, incubated with the appropriate HRP conjugated secondary antibody for 1 hour at 37^{o}C, washed and developed using ECL detection reagents 1 and 2 (Amersham) at 25^{o}C, and exposed to film.

Chapter 3.

Proteomic analysis of steroid-triggered autophagic programmed cell death in *Drosophila melanogaster*.

3.1 Abstract.

A pulse of the steroid ecdysone 12 hours after puparium formation triggers salivary gland autophagic cell death. While caspases play an important role in salivary gland cell death, evidence suggests that other proteins contribute to this process. A shotgun proteome analysis has been used to identify proteins that are expressed during salivary gland autophagic cell death. A total of 5,313 proteins were identified from two salivary gland stages. Several interesting categories of proteins were identified including components and regulators of the autophagy, ubiquitin, cell polarity, growth regulation, cell proliferation and cell cycle processes.

3.2 Introduction.

Two prominent physiological forms of cell killing, apoptotic and autophagic programmed cell death, assist in the maintenance of homeostasis during development of higher eukaryotes (Clarke, 1990; Schweichel and Merker, 1973; Baehrecke, 2002). Most research on the regulation of programmed cell death has focused on apoptosis. Apoptosis usually occurs in isolated dying cells and is followed by subsequent removal of the dying cells by a phagocyte (Clarke, 1990; Schweichel and Merker, 1973). In contrast, autophagic programmed cell death usually occurs when groups of cells or an entire tissue die. These autophagic cells use their own lysosomal machinery to degrade their organelles and cytoplasm by internalizing components of their cytoplasm into autophagic

vacuoles as cargo for destruction (Clarke, 1990; Baehrecke, 2002). Although defects in autophagy have been implicated in human disorders such as cancer and neurodenergation (Yuan et al, 2003; Baehrecke, 2003), the molecular mechanisms governing this type of cell death are not well understood.

Drosophila larval salivary glands have provided valuable insights into our understanding of autophagic programmed cell death. Studies of *Drosophila* have shown that cells undergoing apoptotic and autophagic programmed cell death utilize some similar genes despite the differences in their cell morphology (Lee and Baehrecke, 2001; Martin and Baehrecke, 2004; Chapter 2). Salivary gland histolysis is triggered by an increase in titer of the steroid hormone ecdysone, which occurs 10 to 12 hours after puparium formation. Ecdysone acts through its heterodimeric receptor, encoded by *EcR* and *usp*, in combination with the competence factor *ßFTZ-F1*, to activate the ecdysone regulated early genes *E93*, *BR-C* and *E74A* (Broadus et al., 1999; Woodard et al., 1994). These genes in turn activate a subset of late genes including *rpr*, *hid*, *ark*, *dronc*, and *drice* that are known to function in apoptosis as either caspase proteases or caspase regulators (Hay et al., 1995; Goyal et al., 2000; Wang et al., 1999; Kanuka et al., 1999; Rodriguez et al., 2002; Rodriguez et al., 1999; Zhou et al., 1999). Salivary glands fail to die in animals with mutations in *ßFTZ-F1*, *E93*, *BR-C* and *E74A*, and exhibit altered transcription of the secondary response cell death genes *rpr*, *hid*, *ark*, *dronc*, and *drice* during autophagic cell death (Broadus et al., 1999; Jiang et al., 2000; Lee et al., 2003; Lee et al., 2002b; Lee et al., 2000; Restifo and White, 1992).

Caspases are required for cell death, but evidence indicates that caspase-independent events are important for salivary gland cell death. For example, inhibition of

caspases prevents DNA fragmentation but fails to prevent changes in salivary gland vacuoles (Lee and Baehrecke, 2001). While changes in the levels of proteins including nuclear Lamin and α -Tubulin are regulated by caspase cleavage, filamentous Actin reorganizes in a caspase-independent manner prior to salivary gland degradation (Martin and Baehrecke, 2004; Chapter 2). These studies indicate that caspases are only part of the mechanism that is used during salivary gland death, and suggest that other possible mechanisms may be involved in regulating changes in cell shape, organization, and degradation during autophagic cell death.

Genomic approaches including DNA microarrays and proteomics have been widely used to gain a comprehensive understanding of molecular changes in the cell (Wiseman and Singer, 2002; Liu et al, 2002). DNA microarrays enable the identification of genome-wide changes in RNA levels, and this approach resulted in the identification of 932 genes transcripts that changed 5-fold or higher in dying salivary glands (Lee et al, 2003). Cell death is often regulated post-transcriptionally, however, and it is important to understand changes in proteins as cells die. Many investigators use 2-dimensional isoelectric focusing and SDS-PAGE followed by mass spectrometry (MS) to identify proteins (O'Farrell, 1975; Yates, 1998). This approach has the liability of requiring large milligrams quantities of protein and limited ability to identify low abundance proteins (Cooper and Lee, 2004). Recent advances in microfluids separation have improved the capability to identify proteins from complex mixtures (Chen et al, 2003). Here we utilized a shotgun proteomic technique to examine the presence of proteins before and after the start of steroid-triggered salivary gland autophagic cell death. This resulted in the identification of several groups of proteins that may be important for salivary gland

destruction including proteins involved in cell and protein degradation, cell remodeling, growth control, and cell cycle.

3.3 Results.

Ten to twelve hours after puparium formation, a rise in the ecdysone titer triggers the larval salivary glands to undergo autophagic programmed cell death. At this time, proteins such as caspases are induced to participate in the destruction of the salivary gland. Therefore, we wanted to identify additional proteins that are expressed in salivary glands before and following the rise in ecdysone that triggers cell death. Soluble proteins were extracted from salivary glands dissected from wild-type animals that were aged 6 hours (before salivary gland histolysis) and 13 hours (one hour after the start of salivary gland histolysis) after puparium formation. Two independent samples of Trypsin digested protein from each time point were separated by capillary isoelectric focusing, and twelve different fractions were separated further by capillary reverse phase liquid chromatography. These fractions were analyzed using a ThermoFinigan LCQ ion trap mass spectrometer. Three MS/MS scans were performed and raw data files were processed and submitted for database searching using MASCOT (Matrix Science). Separation of proteins and initial MS data analyses were performed by Dr. Jenny Chen and Brian Balgley.

Proteins were identified as peptide sequences that were fully cleaved by trypsin. The number of unique peptide sequences (upep) that were identified in each protein, and the total number of peptide sequences (tpep) that were identified in each protein were determined. These values can be used to identify proteins that are present

within a sample, but they cannot be use to accurately determine the abundance of a protein. In order to use the values obtained for upeps and tpeps, a control for each peptide sequence identified by MS/MS will be needed since each peptide is ionized differently. Since the number of peptides used to identify proteins is so enormous, obtaining a control for each peptide is impossible. It is also not possible to compare the intensity of scans obtained for similar peptides in each timepoint since scans of peptides followed by scans of whole proteins interrupt peptide peaks. The criteria for identification of the protein were written into the algorithms of the MASCOT program that was used to search specific databases of *Drosophila melanogaster*. The MASCOT program has a 95% threshold, so that proteins were identified with 95% confidence. A total of 3,557 proteins were identified in the 6 hour time point with greater than 95% confidence, and 1,033 proteins were identified by 2 or more unique peptide sequences (Appendix 1). In contrast, 3,476 proteins were identified in the 13 hour time point with greater than 95% confidence, and 955 proteins were identified by 2 or more unique peptide sequences (Appendix 2). The total number of proteins identified in both samples was 5,313 with 1,721 proteins common to both 6-hour and 13-hour time points.

A total of 3,557 proteins were identified in the 6 hour time point with greater than 95% confidence, and 1,033 proteins were identified by 2 or more unique peptide sequences (Appendix I). In contrast, 3,476 proteins were identified in the 13 hour time point with greater than 95% confidence, and 955 proteins were identified by 2 or more unique peptide sequences (Appendix II). The total number of proteins identified in both samples was 5,313 with 1,721 proteins common to both 6-hour and 13-hour time points.

The results of the proteome analyses were validated using western blot and immuno-histochemical staining. Soluble protein extracts were obtained from wild-type Canton S salivary glands staged 6 and 13 hours after puparium formation, electrophoresed on 12% acrylamide gels and transferred to membranes. Each membrane was incubated with antibodies against Bruce, Cactus, Highwire, and Kelch (Figure 13). For immuno-histochemical staining, salivary glands were obtained from wild-type Canton S animals staged to 6 and 13 hours after puparium formation, fixed in 4% paraformaldehyde and incubated with antibodies against Bruce, the Insulin receptor (DInR), Highwire (Hiw), Choline acetyltransferase (Cha), Cactus (Cact), Osa, Kelch (Kel), Quail (Qua), Crumbs (Crb), and Discs large (Dlg) (Figure 14). Although we were limited by antibody availability, we were able to validate the presence of several proteins that were not previously identified in salivary glands. The localization of these proteins in salivary gland cells is similar to their localization in other cells. Immunohistochemistry stains of Bruce have not been published, but localization in the cytoplasm is logical for a ubiquitin conjugating enzyme. DInR is typically located on the plasma membrane, but it is present in the cytoplasm of salivary gland cells. One possible explanation is that the cleavage product of DInR was identified by the antibody, and this product is present in the cytoplasm of salivary glands. Western blot analyses using the same DInR antibody identified a 60 Kd band that could be the catalytic subunit of DInR, but we have not been able to repeat these results. Hiw is located in the cytoplasm of neurons and is also present in the cytoplasm of salivary gland cells (Wan et al., 2000). Cha is associated with synaptic vesicles and it is located in a punctate cytoplasmic pattern in salivary glands suggesting it could be associated with vacuoles or lysosomes that are

formed at that stage (Takagawa and Salvaterra, 1996; Bowman et al, 1999). Cact is localized in the cytoplasm of follicle cells in ovaries and is also seen in the cytoplasm of salivary gland cells (Whalen and Steward, 1993). Osa is located in the nuclei of third instar salivary gland cells similar of its localization just prior to cell death (Collins et al, 1999). Kelch and Quail are associated with Actin are a component of intracellular bridges in egg chambers, and are required for Actin bundle assembly during oogeneisis (Xue and Cooley, 1993; Mahajan-Miklos and Cooley, 1994). Therefore it is reasonable that Kelch and Quail are in the cytoplasm since Actin is also localized in the cytoplasm of salivary gland cells (Martin and Baehrecke, 2004). Crb is localized near the cortex of the epithelial cells similar to its location in salivary gland cells (Tepass and Knust, 1993). Dlg is also localized to the plasma membrane or cell junctions, and it is localized to the plasma membrane of salivary gland cells (Parnas et al, 2001).

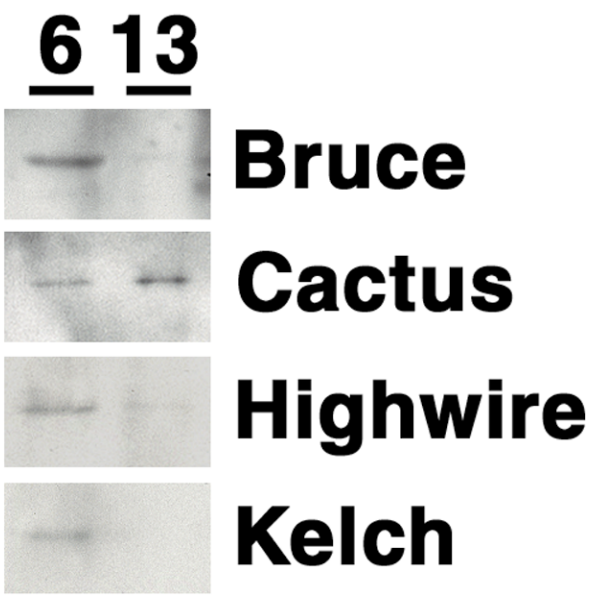

Figure 13. Verification of proteome results using western blot analyses. Western blots of wild-type Canton S salivary glands protein extracts show the presence of Cactus, Highwire in salivary glands at both 6 hours and 13 hours after puparium formation. Bruce and Kelch are seen only detected 6 hours after puparium formation. The results are consistent with the results obtained by the proteome analyses.

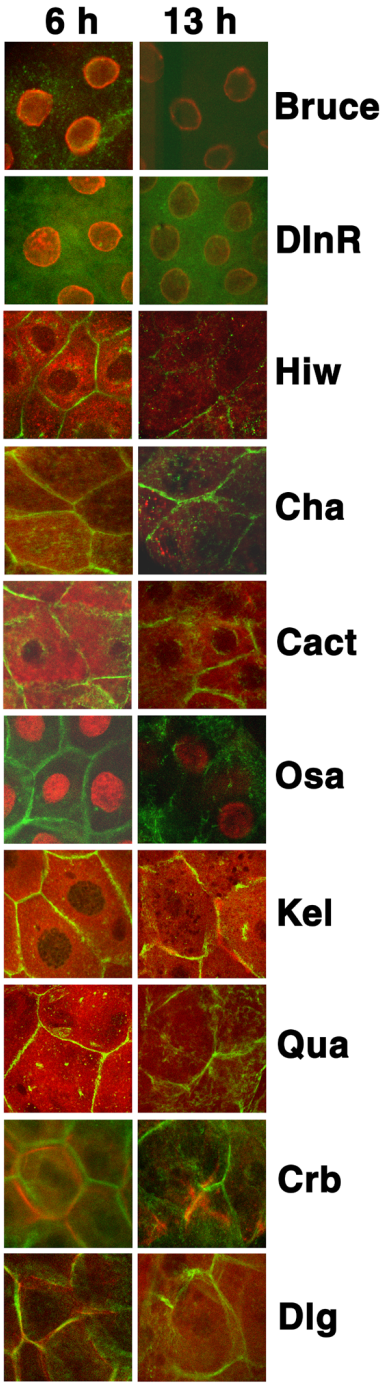

Figure 14. Verification of proteome results by immunohistochemistry. In the first two panels, salivary glands of stage wild-type Canton S animals were stained with antibodies against Bruce and DInR (green) and nuclear Lamin (red). Salivary glands of staged wild-type Canton S animals in the other panels were stained with antibodies against Highwire (Hiw), Choline acetyltransferase (Cha), Cactus (Cact), Osa, Kelch (Kel), Quail (Qua), Crumbs (Crb), and Discs large (Dlg) (red) and spectrin (green).

Several interesting categories of proteins were identified in dying salivary gland cells. Proteins that are involved in the regulation of transcription including the ecdysone-regulated genes, transcription co-repressors, and transcription co-activators are shown in Table 2. The ecdysone regulated proteins EIP93F (E93) and the nuclear hormone receptors E75B, EcR and Usp were all detected using this approach, and this is consistent with DNA microarray studies (Lee et al., 2003). Salivary glands also contained numerous other proteins that regulate transcription including Cactus, Sox14, and the Trap proteins Trap100, Trap170 and Trap220. Little is known about the transcription co-activators and co-repressors that are involved in programmed cell death, and the identification of several proteins in these categories provides a starting point for investigating their function in autophagic programmed cell death.

Table 2. Transcription

				6hr		13hr	
Category	**Name**	**Fbgn #**	**Notes**	**upep**	**tpep**	**upep**	**tpep**
Ecdysone-Regulated	Eip75B*	FBgn0000568	Nuclear receptor	2	2	3	3
	Eip93F*	FBgn0013948	Nuclear receptor	3	3	1	1
	Hr39*	FBgn0010229	Hormone receptor	1	1		
	Hr78*	FBgn0015239	Hormone receptor	2	2	1	3
	Usp*	FBgn0003964	Ecdysone receptor	1	1	1	1
	EcR*	FBgn0000546	Ecdysone receptor	2	2		
Transcription Reg.	Cact*	FBgn0000250	Antifungal response			2	2
	Bun*	FBgn0010460	RNA Pol II trans. factor	1	1		
	Trap220*	FBgn0037109	RNA Pol II trans. Med.	8	8	4	6
	Sox14*	FBgn0005612	Trans. factor activity			1	1
	Tou*	Fbgn0033636	Chromatin binding	8	13	4	23
	Hsf*	FBgn0001222	Heat shock factor			1	1
	Trap80*	FBgn0038578	RNA Pol II trans. Med.	1	1		
	Trap100*	FBgn0035851	RNA Pol II trans. Med.	1	2	1	1
	Trap170*	FBgn0035145	RNA Pol II trans. Med.	2	2	2	2

* denotes that protein was identified in microarray data set (Clough et al., unpublished).

Table 2. Transcription (continued)

				6hr		13hr	
Category	**Name**	**Fbgn #**	**Notes**	**upep**	**tpep**	**upep**	**tpep**
Trans. co-activators	Bon	FBgn0023097	Trans. co-activator	3	3	1	1
	Hcf*	FBgn0039904	Trans. co-activator	3	3	1	1
	Nej*	FBgn0015624	Synaptic vesicle trans.	2	4	3	3
	Tai	FBgn0041092	Border cell migration	4	6	2	6
	Brm*	FBgn0000212	Trans. co-activator			1	1
Trans. co-repressors	CtBP*	FBgn0020496	Trans. co-repressor	1	6	2	7
	Gug	FBgn0010825	Leg morphogenesis	2	4	2	2
	H*	FBgn0001169	(-) reg. of N signaling	1	1	2	3
	Hira	FBgn0022786	Trans. co-repressor	1	1		
	Per	FBgn0003068	Mating behavior	3	3		
	Bin1	FBgn0024491	Trans. co-repressor			2	2
	Smr*	FBgn0024308	Trans. co-repressor	4	27		

* denotes that protein was identified in microarray data set (Clough et al., unpublished).

Components of the salivary gland rapidly degrade during autophagic programmed cell death (Martin and Baehrecke, 2004; Chapter 2). Many categories of proteins may contribute to this process including those involved in apoptosis, autophagy, ubiquitination and lysosome biogenesis. Several proteins that function during apoptosis were detected including the Bcl-2 family member Debcl, the caspase activator Ark, and the caspases Dream and Dronc (Table 3). Other proteins of interest are also present including Rep1, which plays a role in DNA fragmentation, and the apoptosis activators Rep2 and MESR4. Even though active caspases play an important role in cell destruction during salivary gland death, it is interesting that non-caspase proteases such as Mmp1 and Nep1, both of which possess metalloendopeptidase activity, and the di- and tri-peptidyl peptidases Dip-C and tppII are present. The ubiquitin pathway serves an important role in the degradation of short-lived proteins including caspase regulators. Several proteins involved in ubiquitination such as the activating enzyme Uba1, ubiquitin conjugating enzymes Bruce and UbcD2, and the ubiquitin protein ligases including Archipelago (Ago), Lack, Nedd4 as well as a ubiquitin specific protease Ubp64E are also present. Autophagy requires lysosomes, but models of this process assume that the lysosome is present in the cell waiting for the autophagic vacuole to deliver its cargo (Klionsky and Emr; 2000). Therefore, it is intriguing that several proteins involved in lysosome biogenesis and organization such as NPC1, which is present in the lysosome membrane, Ect3 that causes an increase in ß-galactisidase activity and Beached1, which is involved in intracellular protein and lysosome transport were identified. Salivary gland cell death involves the internalization of cell components into autophagic vacuoles. Even though the mechanism by which autophagy is regulated is not fully understood, the presence of

known autophagy proteins provides an opportunity to investigate the function of this process in programmed cell death (Table 3). Significantly, proteins encoded by CG1241(Atg2-like), CG5489 (Atg7-like), CG3615 (Atg9-like) and CG12821 (Atg10-like), and the activator of autophagy Tor are all present one hour after the start of salivary gland autophagy.

Table 3. Cell and Protein Degradation

				6hr		13hr	
Category	**Name**	**Fbgn #**	**Notes**	**upep**	**tpep**	**upep**	**tpep**
Apoptosis	Debcl	FBgn0029131	Proapop. bcl-2 member	2	2	1	1
	Iap2*****	FBgn0015247	Inhibitor of apoptosis	1	2	1	2
	Thread*****	FBgn0003691	Anti-apoptosis			1	1
	Rep1*****	FBgn0024732	DNA fragmentation	1	1	2	2
	Ark*	FBgn0024252	Caspase activation			1	1
	Dream*****	FBgn0033051	Caspase			1	3
	Dronc*	FBgn0026404	Caspase			1	1
	Rep2	FBgn0028408	Induction of apoptosis	1	2	2	2
	MESR4*****	FBgn0034240	Apoptosis, reg. of cell cycle	1	1	2	2
Non-Caspase Protease/ Inhibit.	Mmp1*****	FBgn0035049	Metalloendopeptidase	1	1	1	1
	Nep1	FBgn0029843	Metallopeptidase activity			1	1
	Nep2*****	FBgn0027570	Metallopeptidase activity	2	2		
	Nep3	FBgn0031081	Metallopeptidase activity	2	2		
	Dip-C	FBgn0000455	Dipeptidyl peptidase activity			2	2
	TppII*****	FBgn0020370	Tripeptidyl peptidase activity	1	1	1	1
	Rpn6*****	FBgn0028689	Endopeptidase activity	1	1		

* denotes that protein was identified in microarray data set (Clough et al., unpublished).

Table 3. Cell and Protein Degradation (continued)

				6hr		13hr	
Category	**Name**	**Fbgn #**	**Notes**	**upep**	**tpep**	**upep**	**tpep**
Ubiquitin	Uba1*****	FBgn0023143	Ubiquitin Act. enzyme	1	1		
	Bruce*****	FBgn0037808	Ubiquitin Conjug. enzyme	5	5		
	UbcD2*****	FBgn0015320	Ubiquitin Conjug. enzyme	2	2		
	Uev1A*	FBgn0035601	Ubiquitin Conjug. enzyme	1	1		
	Ago	FBgn0041171	Ubiquitin protein ligase	2	2	1	2
	Ari-1*****	FBgn0017418	Ubiquitin protein ligase	1	1		
	Cul-4*****	FBgn0033260	Ubiquitin protein ligase	1	2	1	2
	HERC2*****	FBgn0031107	Ubiquitin protein ligase	2	2	3	3
	Hyd*****	FBgn0002431	Ubiquitin protein ligase	2	2	3	3
	Lack	FBgn0029006	Ubiquitin protein ligase	2	2	2	2
	Neur*****	FBgn0002932	Ubiquitin protein ligase	2	3		
	Slmb*****	FBgn0023423	Ubiquitin protein ligase	1	1		
	Ubp64E*****	FBgn0016756	Ubiquitin specific protease	1	1	1	2
	Nedd4*****	FBgn0036736	Ubiquitin protein ligase			1	1

* denotes that protein was identified in microarray data set (Clough et al., unpublished).

Table 3. Cell and Protein Degradation (continued)

				6hr		13hr	
Category	**Name**	**Fbgn #**	**Notes**	**upep**	**tpep**	**upep**	**tpep**
Lysosome Biogen./Organ.	Dip-B	FBgn0000454	Leucyl aminopeptidase	1	1	1	1
	Cm*	FBgn0000330	Lysosome organ./Biogenesis	1	3		
	Or	FBgn0003008	Lysosome organ./Biogenesis	1	1	1	1
	Rb	FBgn0003210	Lysosome organ./Biogenesis	1	1	1	1
	NPC1*	FBgn0024320	Lysosome membrane protein			1	1
	Ect3*	FBgn0037977	Beta-galactosidase activity			1	1
	Beached 1	FBgn0043362	Intracell. protein/lysosome trans.			2	2
	G	FBgn0001087	Eye pigment biosynthesis			1	1
Autophagy	CG1241*	FBgn0035373	Atg-2 like			3	3
	Aut1*	FBgn0036813	Atg-3 like	1	1		
	CG5429*	FBgn0039144	Atg-6 like	1	1		
	CG5489*	FBgn0034366	Atg-7 like			1	1
	CG3615*	FBgn0034110	Atg-9 like	1	3	2	4
	CG12821	FBgn0040780	Atg-10 like			1	1
	CG8678*	FBgn0032935	Atg-18 like	1	1		
	Tor	FBgn0021796	Target of rapamycin	2	2	1	1

* denotes that protein was identified in microarray data set (Clough et al., unpublished).

While the morphological changes that occur during salivary gland cell death could be caused by the cleavage of proteins by active caspases, the reorganization of the cytoskeleton and other categories of proteins could play an important role in autophagic cell death. For example, changes in the cytoplasmic structures including vacuoles and the Actin cytoskeleton are independent of caspase activation (Lee and Baehrecke, 2001; Chapter 2). Therefore, it is intriguing that we have identified a number of proteins that participate in changes in cell organization including GTPases, Arfs and Arps, Formin Homology Proteins (FHP), and Motors (Table 4). For example, the GTPases Rab9, Rab10, and Rab11 are involved in intracellular protein transport and receptor mediated endocytosis (Pereira and Seabra, 2001; Satoh et al, 1997; Dollar et al, 2002), the ARFs and ARPs Garz and Gap69C function in intracellular protein and vesicle-mediated transport (Battersby et al, 2003; Frolov and Alatortsev, 2001; Kraut et al, 2001), and the FHPs Capu and Dia are involved in Actin cytoskeleton organization (Kellar et al, 2003; Afshar et al, 2000). We also identified proteins involved in cytoskeleton biogenesis and reorganization (Table 4). A large number of motor proteins are also present in salivary glands 13 hours after puparium formation including several kinesins and dyneins (Table 4). Motor proteins have been implicated in the generation of lysosomes, the movement of cargo within a cell, and regulation of apoptosis (Day et al, 2004; Yamaguchi et al, 2003; Rodriguez-Crespo et al, 2001; Puthalakath et al, 1999). Epithelial cell death, such as dying salivary gland cells, involves the separation from a basement membrane and likely changes in cell junctions and loss of cell polarity. However, the relationship between loss of cell contact and polarity and their association with cell death are not well understood. Salivary glands contain several cell polarity proteins such as Lethal giant

larvae (Lgl), Discs large (Dlg) and Scribble (Scrib) (Table 4). Changes in these proteins may be important for salivary gland autophagic death to occur.

Table 4. Cell organization

				6hr		13hr	
Category	**Name**	**Fbgn #**	**Notes**	**upep**	**tpep**	**upep**	**tpep**
GTPases	Rep*	FBgn0026378	Rab escort protein	1	1		
	Rab3-GEF*	FBgn0030613	Nucleotide exchange fac.	3	3	4	9
	RabX6	FBgn0035155	GTPase activity	1	1	1	1
	Rab 9	FBgn0032782	GTPase activity	2	4	1	10
	Rab10*	FBgn0015789	GTPase activity	1	1		
	Rab27	FBgn0025382	GTPase activity	1	2	1	2
	Rab30	FBgn0031882	GTPase activity	2	2	1	1
	RhoGAP88C*	FBgn0038226	Rho GTPase activator	2	3	1	1
	RhoGAPp190	FBgn0026375	Rho GTPase activator	4	6	2	8
	Pbl*	FBgn0003041	Nucleotide exchange fac.	1	1	1	1
	RhoGEF2*	FBgn0023172	Nucleotide exchange fac.	2	2	1	1
	RhoGEF4	FBgn0035761	Nucleotide exchange fac.	1	1	1	1
	Sif	FBgn0019652	Nucleotide exchange fac.	2	3	2	2
	Trio	FBgn0024277	Nucleotide exchange fac.	5	5	1	1
	Sra-1*	FBgn0038320	Rho interactor activity	2	2	1	1
	Rab11*	FBgn0015790	GTPase activity			1	1
	Rab23	FBgn0037364	GTPase activity			1	1
	Rab26	FBgn0037072	GTPase activity			1	1
	Rab39*	FBgn0029959	GTPase activity			1	1
	RhoGEF3	FBgn0035128	GTPase activity			2	2
	Cip4*	FBgn0035533	Rho interactor activity			1	1

* denotes that protein was identified in microarray data set (Clough et al., unpublished).

Table 4. Cell organization (continued)

				6hr		13hr	
Category	**Name**	**Fbgn #**	**Notes**	**upep**	**tpep**	**upep**	**tpep**
ARFs and ARPs	CenG1A	FBgn0028509	ARF GTPase act.	1	1	1	1
	Gap69C*	FBgn0020655	ARF GTPase act.	1	1		
	Garz*	FBgn0033714	GTPase activity	1	1	1	3
	Arp14D*	FBgn0011742	Constituent of cytoskeleton	1	1		
	Arp53D	FBgn0011743	Constituent of cytoskeleton	1	1		
FHP	Capu*	FBgn0000256	Pole plasma RNA localization	2	2		
	Dia*	FBgn0011202	Spermatogenesis	3	7	2	2
	Formin2	FBgn0052384	Actin binding	3	3	2	2
	CG14622	FBgn0025641	Actin binding	1	1	2	2
	Formin3	FBgn0052030	Actin binding	2	2	1	1
	CG32138	FBgn0052138	Actin binding			2	2
Cytoskeleton Biogen.	Cora*	FBgn0010434	Cytoskeleton Organ./Biogen.	2	2		
	Hem*	FBgn0011771	Axonogenesis	2	2	1	1
	Psn*	FBgn0019947	Cytoskeleton Organ./Biogen.	1	1		
	RhoGAP93B*	FBgn0038853	Cytoskeleton Organ./Biogen.	2	3	2	2
	Fidipidine	FBgn0025519	Cytoskeleton Organ./Biogen.	1	1	1	1
	Bap55	FBgn0025716	Cytoskeleton Organ./Biogen.			1	2
	Fau	FBgn0020439	Cytoskeleton Organ./Biogen.			1	1
	Mst89B	FBgn0020399	Cytoskeleton Organ./Biogen.			1	1
	NinaC	FBgn0002938	Protein serine/threonine kinase			1	1
	Vhl	FBgn0041174	Tracheal system development			1	1
	Chc*	FBgn0003319	Sperm individualization			1	1

* denotes that protein was identified in microarray data set (Clough et al., unpublished).

Table 4. Cell organization (continued)

				6hr		13hr	
Category	**Name**	**Fbgn #**	**Notes**	**upep**	**tpep**	**upep**	**tpep**
Motors	Cana	FBgn0040233	Kinesin motor			3	3
	Crinkled*	FBgn0000317	Myosin ATPase	3	3	1	1
	Dhc16F*	FBgn0013809	Dynein motor	2	6	4	5
	Dhc36C	FBgn0013810	Dynein motor	4	5	2	2
	Dhc36D	FBgn0032657	Dynein motor			1	1
	Dhc62B	FBgn0013811	Dynein motor	6	7	7	8
	Dhc64C	FBgn0010349	Dynein motor			2	3
	Dhc93AB*	FBgn0013812	Dynein motor	3	5	5	8
	Dhc98D	FBgn0013813	Dynein motor	1	1	3	3
	Dlic2*	FBgn0030276	Dynein ATPase	1	1		
	Kap*	FBgn0030287	Kinesin motor	2	2		
	Khc*	FBgn0001308	Kinesin heavy chain	1	1	2	4
	Klp10A*	FBgn0030268	Kinesin motor	1	3		
	Klp31E	FBgn0032243	Kinesin motor	1	1	2	2
	Klp3A*	FBgn0011606	Kinesin like protein	1	1	1	1
	Klp61F*	FBgn0004378	Kinesin like protein	1	1	2	2
	Myo28B1	FBgn0040299	Actin binding	2	2	1	1
	Myo61F*	FBgn0010246	Myosin ATPase	1	1	2	2
	Sdic	FBgn0025801	Dynein ATPase activity	1	1		
	Zipper*	FBgn0005634	Myosin ATPase	3	3	1	1
	Klp59D	FBgn0034827	Kinesin motor			1	1
	Klp68D*	FBgn0004381	Kinesin motor			2	2
	Myo31DF*	FBgn0011673	Myosin ATPase			1	1

* denotes that protein was identified in microarray data set (Clough et al., unpublished).

Table 4. Cell organization (continued)

				6hr		13hr	
Category	**Name**	**Fbgn #**	**Notes**	**upep**	**tpep**	**upep**	**tpep**
Cell Polarity	Bazooka*	FBgn0000163	Protein kinase C binding	2	2	1	1
	Crumbs*	FBgn0000368	Establish./Main. of cell polarity	2	3	3	3
	Dlg1	FBgn0001624	Establish./Main. of cell polarity	1	1	2	3
	Dystroglycan	FBgn0034072	Establish./Main. of cell polarity	2	3	1	1
	Stardust	FBgn0003349	Establish./Main. of cell polarity	2	3	1	1
	L(2)gl	FBgn0002121	Establish./Main. of Foll. Epi. polarity	3	3		
	Scrib	FBgn0026178	Cell proliferation			1	1
	Dachsous*	FBgn0000497	Calcium dependent cell adhesion			4	4
	Dishevelled*	FBgn0000499	Establish./Main. of cell polarity	2	2		
	Shark*	FBgn0015295	Protein-tyrosine kinase	2	2		

* denotes that protein was identified in microarray data set (Clough et al., unpublished).

An intricate relationship between cell proliferation and cell death must exist for growth and development of an organism. Although salivary gland cells stop dividing early in development, they continue to endo-replicate DNA (Smith and Orr-Weaver, 1991). It is interesting that several cell cycle and proliferation proteins were identified from salivary glands (Table 5). Further, it will be important to determine if these factors are essential for cell growth and death. It is intriguing that Loki and Scar, which are involved in DNA damage cell cycle checkpoint and cell cycle dependent Actin reorganization are present during salivary gland cell death (Abdu et al, 2002; Zallen et al, 2002). One key pathway in the regulation of cell growth is the Insulin Receptor (InR) pathway. Some components of this pathway are also present in the proteome during salivary gland autophagy including InR, Ilp3 and Ilp4. Other proteins that participate in growth control and also interact in the InR pathway are also present during salivary gland cell death such as the PI3 kinases PI3K59F, PI3K68D and PI3K93E as well as the phosolipid phosphatase PTEN. An understanding of the relationship between cell proliferation and cell death has emerged through studies of Hippo, Warts and Salvador (Sav) (Justice et al., 1995; Xu et al., 1995; Kango-Singh et al., 2002; Tapon et al., 2002; Pantalacci et al., 2003; Udan et al., 2003; Harvey et al., 2003; Wu et al., 2003). Cell proliferation proteins such as Cyclin D and Dachsous are present during salivary gland autophagy and studying these proteins may lead to a greater understanding of the relationship between cell death and proliferation.

Table 5. Growth Regulation/Control and Cell Cycle

				6hr		13hr	
Category	**Name**	**Fbgn #**	**Notes**	**upep**	**tpep**	**upep**	**tpep**
Cell Cycle	Atu*	FBgn0019637	DNA replication, cell cycle	2	3		
	Btsz	FBgn0010940	Cell cycle and proliferation	4	7	2	2
	C11.1	FBgn0040236	Vesicle mediated transport	1	1	1	1
	Grp*	FBgn0011598	Cell cycle checkpoint	1	1		
	L(3)j2D3	FBgn0011335	Cell cycle and communication	2	2		
	Ptr	FBgn0003159	Cell cycle and proliferation	1	1	2	2
	Rev7*	FBgn0037345	Chromosome segre./mitosis	1	1		
	YT-521B*	FBgn0027616	DNA metabolism and replication	1	3		
	Sced	FBgn0013732	Actin filament reorganization	1	1	2	4
	Dtr	FBgn0023090	Cell communication/reg. of cell cycle			1	1
	Lok	FBgn0019686	Cell cycle checkpoint			1	1
	SCAR	FBgn0041781	Cytoskeletal regulator activity			1	1
Ins. Receptor/IR activity	InR*	FBgn0013984	Insulin receptor	3	3	4	4
	Ilp3	FBgn0044050	Insulin receptor binding	2	3	1	8
	Chico	FBgn0024248	IRS-homolog	1	1		
	Ilp4	FBgn0044049	Insulin receptor binding			1	1

* denotes that protein was identified in microarray data set (Clough et al., unpublished).

Table 5. Growth Regulation/Control and Cell Cycle (continued)

				6hr		13hr	
Category	**Name**	**Fbgn #**	**Notes**	**upep**	**tpep**	**upep**	**tpep**
Regulation of growth	Shot*	FBgn0013733	Actin binding, microtubule binding	10	16	8	11
	E2f	FBgn0011766	RNA Pol II Trans. factor	1	1		
	Wnt5*	FBgn0010194	Receptor binding/signal transducer act.	2	3	9	7
	Wts	FBgn0011739	Protein serine/threonine kinase act.			2	2
	PI3K59F	FBgn0015277	Protein targeting			2	3
	PI3K68D*	FBgn0015278	Protein targeting			1	1
	PI3K92E*	FBgn0015279	Defense response			1	1
	PTEN*	FBgn0026379	IR signal.	1	1		
	TSC1	FBgn0026317	Response to nutrients	1	2	2	3
	Gigas*	FBgn0005198	Intracellular Protein Trans.	2	2		
Cell Proliferation	Ft	FBgn0001075	Cell adhesion receptor	3	3		
	Gukh	FBgn0026239	Cell proliferation	1	1		
	Hop*	FBgn0004864	Janus kinase activity	1	1	2	3
	SelD*	FBgn0020615	Imaginal disc develop.	1	1		
	CycD*	FBgn0010315	Cyclin depend. protein kinase			4	4
	Dom	FBgn0020306	Gene silencing			2	2
	Ds*	FBgn0000497	Calcium depend. cell adhesion			1	1
	Mod*	FBgn0002780	Spermatid development			2	4

* denotes that protein was identified in microarray data set (Clough et al., unpublished).

3.4 Discussion.

Important advances have been made in understanding the mechanism of autophagic programmed cell death in dying larval salivary glands of *Drosophila*. It is not surprising that we have identified a number of transcription factors, as these are known to participate in salivary gland autophagic programmed cell death (Jiang et al., 1997; Lee et al., 2000; Lee et al., 2002; Jiang et al., 2000; Lee et al., 2003). These studies indicate that caspase activation is important for salivary gland autophagic cell death to occur. The data obtained from these proteome analyses support this conclusion as we identified several components of the apoptotic machinery. Blocking caspases does not prevent changes in cytoplasmic vacuoles and some structural proteins (Lee and Baehrecke, 2001; Chapter 2), indicating that proteins involved in cytoskeleton biogenesis and reorganization may also be involved in cell death. Indeed, numerous such proteins were identified.

Most studies of dying cells assume that caspases are the only critical regulators of cell death. While this may be true during apoptosis, careful evaluation of apoptotic cells for other possible degradation mechanisms is limited. Dying salivary glands have an autophagic morphology, and this has prompted broader investigations of possible degradation mechanisms. Shotgun proteomics has enabled us to identify non-caspase proteases, components of the ubiquitin pathway, proteins involved in lysosome biogenesis, and proteins that are similar to the yeast autophagy proteins. Lysosomes are membrane bound organelles containing a variety of acid hydrolases (Luzio et al, 2003). Cell components can be targeted for degradation by either ubiquitin-mediated destruction by the 26S proteosome or by transfer to the lysosome by a number of pathways including

autophagy (Luzio et al, 2003). Yeast autophagy proteins have been shown to act in two related ubiquitin-like pathways that are required for yeast autophagy. In yeast, ATG12 and ATG8 encode proteins with functional similarity to ubiquitin. These proteins are activated by an E1-like protein ATG7, which initiates the conjugation of ATG12 and ATG8 to the E2-like proteins ATG10 and ATG3 respectively. ATG12 is then conjugated to E3-like protein ATG5, whereas ATG8 is tethered to phosphatidylethanolamine, which is associated with the forming autophagic vacuole isolation membrane. Future studies of the function of autophagy proteins in cell death will test if this process can be used in both cell survival and cell death.

Recently, studies in *Drosophila* have revealed that insulin-like molecules (DILPs) control growth and metabolism via signaling through a single insulin receptor InR. The signaling molecules regulated by this receptor are highly conserved between flies and mammals (Goberdhan and Wilson, 2003). InR signaling also plays a role in the regulation of nutrients in the fly. Flies with a reduction of the InR show similar phenotypes to those with calorie restrictions including decrease in the proliferation rate of stem cells and their progeny (Drummond-Barbosa and Spradling, 2001). There is no known role for InR activity during autophagy, but it is possible that there may be an indirect role through TOR. In yeast, loss of TOR activity leads to the induction of autophagy, whereas during mammalian development mTOR negatively regulates protein synthesis and positively regulates autophagy (Dennis et al., 1999; Kunz et al., 1993; Barbet et al., 1996; Noda and Ohsumi, 1998; Cardenas et al., 1999; Hardwick et al., 1999). During Drosophila development, dTOR is needed for normal growth and cells

lacking dTOR are reduced in size and proliferative capacity (Zhang et al., 2000). Future studies of dTOR could reveal its function during salivary gland autophagy.

While growth control is widely studied in proliferating cells, less is known about this process and its association with cell death. The identification of several proteins involved in cell proliferation and growth control suggest the possibility that they may be involved in regulating death of salivary glands. This is not surprising, as others have linked growth control to cell death through studies of Hippo, Sav and Warts (Justice et al., 1995; Xu et al., 1995; Kango-Snigh et al., 2002; Tapon et al., 2002; Pantalacci et al., 2003; Udan et al., 2003; Harvey et al., 2003; Wu et al., 2003). These genes act in a similar pathway to aid in the regulation of cell proliferation and cell death. Reduction in protein levels of Hippo, Sav and Warts leads to altered levels of Cyclin E and DIAP1 (Harvey et al., 2003; Wu et al., 2003). Functional studies of these factors in autophagic cell death could provide novel insights into the relationship between cell proliferation and growth and cell death.

One of the challenges of performing reverse genetic screens such as high-throughput proteomics is the sorting through the enormous amounts of data and selecting the best genes to study. One approach for this data set is to first examine proteins that are only present 13 hours after puparium formation. These proteins could be important for salivary gland cell death by temporal association. Similar DNA microarray analyses of salivary glands undergoing cell death were performed and identified a number a genes that are upregulated 5-fold or greater during that time. We could select proteins that are present only 13 hours after puparium formation and are also up-regulated in the DNA microarray data set. We can further narrow this set of genes by placing proteins into

different groups (Tables 2-5), and then select protein for analysis based on the identification of several components of a pathway. Alternatively, we could also study proteins that are only present 13 hours after puparium formation and are not present in the microarray data as this may provide useful information about proteins that are regulated post-transcription. This may be a very small set of proteins as many of the proteins in the proteome were also identified by DNA microarray analyses.

3.5 Materials and Methods.

Protein extraction.

Soluble protein extracts were obtained from wild-type Canton S salivary glands that were dissected from animals staged 6 and 13 hours after puparium formation. Salivary glands were homogenized in 40mM Tris buffer, and incubated for 5 minutes at 100^{o}C. Proteins were denatured, reduced and alkylated in 20mM Tris buffer containing 8M urea, 0.1M dithiothreitol and 0.1M iodoacetamide. Denatured, reduced and akylated proteins were reconstituted in a solution of 10mM Tris, 0.4M urea and 10mM DTT using regenerated cellulose membrane filters (Millipore) with a 5,000 molecular weight cut off. Trypsin (1:50, w/w, Promega modified sequencing grade, Madison, WI) was added and the mixture was incubated at 37^{o}C for overnight.

Proteomics.

Independent samples of Trypsin-digested proteins from each timepoint were separated by capillary isoelectric focusing and twelve different fractions were separated further by capillary reverse phase liquid chromatography. These fractions were analyzed

using a ThermoFinigan LCQ ion trap mass spectrophotometer (MS). Three MS/MS scans were performed on the top 3 ions from the preceding MS scan. The raw data files were processed through Distiller (Matrix Science) and the resulting data files were submitted for database search using MASCOT (Matrix Science). The database that was searched was a non-redundant compilation of the Swiss-plot and TREMBL *Drosophila melanogaster* data sets available from EBI (This work was conducted by Dr. Jenny Chen and Brian Balgley).

Western/immuno blot analysis.

Wild-type Canton S salivary glands were dissected from animals staged 6 and 13 hours after puparium formation, homogenized in 0.1% glycerol, 2% SDS, 0.125% 1M Tris (pH 6.8), 0.05% ß-mercaptoethanol, and 0.05% Bromo-phenol blue, and incubated for 5 minutes at 100^{o}C. Equal amounts of total protein extracts were separated by electrophoresis on 12% acrylamide gels and either transferred to 0.45 µm Immobilon-P membranes (Millipore), or duplicate gels of identical extracts were assessed for equal loading and integrity by Coomasie blue staining (Bio-Rad). Membranes were blocked in 10% non-fat milk in PBS with 1% Tween 20 for 1 hour at 37^{o}C, incubated in primary antibody for 16 hours at 4^{o}C, washed in PBS containing 1% Tween 20 at room temperature, incubated with the appropriate HRP conjugated secondary antibody for 1 hour at 37^{o}C, washed and developed using ECL detection reagents 1 and 2 (Amersham) at 25^{o}C, and exposed to film.

Immunohistochemistry.

Antibodies against Cactus, Highwire, Discs large, Cha, Crumbs, Kelch, Quail, and Osa were obtained from the Hybridoma Bank (University of Iowa). Antibody against Bruce was obtained from Bruce Hay and antibody against DInR was obtained from Dr. L. Pick and Dr. R. Fernandez. Wild-type Canton S salivary glands were dissected from animals staged 6 hours and 13 hours after puparium formation at 25^{o}C, fixed in 4% paraformaldehyde/heptane for 20 minutes at room temperature, blocked in phosphate buffered saline containing 1% BSA and 0.1% Triton-X (PBSBT), and incubated with primary antibodies for 16 hours at 4^{o}C. Salivary glands were washed for 2 hours in PBSBT, incubated with appropriate secondary antibodies for two hours at room temperature and washed for another 2 hours in PBSBT at room temperature. Salivary glands were mounted in Vectashield (Vector Laboratories) and examined using a Zeiss Axiovert 100 M confocal microscope.

Chapter 4.

The *Drosophila* LC8 homolog, *ctp* functions in autophagic programmed cell death of salivary glands.

4.1 Abstract.

Salivary gland cells undergo many morphological changes during autophagic cell death. The cleavage of some structural proteins, such as nuclear Lamin by active caspases, contributes to some of the changes that occur during this process. However, some structural protein changes and changes in the cytoplasm are caspase independent, indicating that other genes are involved in the destruction of salivary gland cells. Here we show that *cutup* (*ctp*), a light chain of a dynein motor, plays a role in salivary gland cell death. Animals with mutations in *ctp* have salivary glands that persist past the time when they are normally destroyed even though caspases are activated. These data suggest that *ctp* is involved in the transportation of cargo and organization of the cytoplasm during salivary gland autophagic cell death.

4.2 Introduction.

Two prominent forms of programmed cell death, apoptosis and autophagic cell death, play an important role in homeostasis of animals by eliminating unwanted cells and tissues, sculpting developing structures, removing abnormal cells and controlling cell numbers (Jacobson et al., 1997; Thompson, 1995). Studies of apoptosis have led to tremendous progress in understanding the mechanisms of programmed cell death. By contrast, not much is known about the mechanism and cell components that are necessary to drive autophagic cell death, even though autophagy has been implicated in human

diseases such as neurodenergative brain disorders and cancer (Baehrecke, 2003; Yuan et al, 2003).

Studies of *Drosophila* larval salivary gland histolysis have resulted in a clearer understanding of the mechanisms that control the cellular changes observed during autophagic programmed cell death. During *Drosophila* metamorphosis, the steroid hormone ecdysone triggers the elimination of unwanted cells and tissues. Ten to twelve hours after puparium formation, a pulse of ecdysone triggers salivary gland autophagic cell death that is complete by 16 hours after puparium formation. Ecdysone is bound by its heterodimer receptor encoded by *EcR* and *usp*, and acts in combination with the competence factor *ßFTZ-F1* to activate transcription of the primary response genes *E93*, *BR-C* and *E74A* (Broadus et al., 1999; Woodard et al., 1994). These genes regulate the transcription of apoptosis genes including *rpr*, *hid*, *Ark/Dark/DApaf1/Hac-1*, *dronc*, *drice* and *crq* immediately following the start of ecdysone-triggered salivary gland cell death. Animals with mutations in the ecdysone regulated genes *ßFTZ-F1*, *E93*, *BR-C* and *E74A* have salivary glands that persist past the time when salivary glands are normally destroyed (Broadus et al., 1999; Jiang et al., 2000; Lee et al., 2003; Lee et al., 2002b; Lee et al., 2000; Restifo and White, 1992).

Even though dying salivary gland cells contain autophagic vacuoles, they also appear to use apoptosis genes including caspases. Expression of the caspase inhibitor p35 blocks salivary gland cell death, DNA fragmentation and cleavage of proteins such as α-Spectrin, α-Tubulin and nuclear Lamin (Lee and Baehrecke, 2001; Chapter 2). However, expression of p35 does not prevent changes in the cytoplasm including alterations in vacuoles and filamentous Actin from occurring, and this indicates that

reorganization of Actin may be needed for salivary gland autophagic cell death (Lee and Baehrecke, 2001; Chapter 2). Therefore, it is important to identify and study genes that encode proteins that may also play a role in the regulation of such changes during salivary gland autophagy.

Cells organize their cytoplasm by moving different organelles and macromolecular complexes along microtubules and Actin filaments. These movements are powered by numerous motor proteins including Kinesins, Myosins and Dyneins (Karcher et al., 2002). Dyneins are large molecular motor complexes that generate force towards the minus end of microtubules and are involved in a number of different processes including mitosis, maintenance of the Golgi apparatus and trafficking of membranous vesicles and other intracellular particles (King, 2000). Cytoplasmic Dyneins consist of two heavy chains, as well as several intermediate, light intermediate and light chains, which can associate with various cargoes (Karcher et al., 2002). Light chains of Dynein motors are divided into three families including the Tctex1 light chain family, the roadblock/LC7 light chain family and the LC8 light chain family (King, 2000). The LC8 light chains are located on the outer arm of the Dynein motor and are highly conserved in mammals, nematodes, flies and plants (King, 2000; Wilson et al., 2001). The LC8 homolog in flies *cutup* (*ctp*) functions in axon guidance during CNS development in pupae, and animals with mutations in *ctp* display disruption in sensory axon projections (Phillis et al., 1996). Here we present data that *ctp* is needed for autophagic cell death. Animals with mutations in *ctp* have larval salivary glands that persist past the time when they are normally destroyed, and these salivary glands display

a delayed activation of caspases. Studies of *ctp* indicate that dynein motors play a role in autophagic programmed cell death.

4.3 Results.

Identification of *ctp* as a gene that functions in autophagic cell death.

A collection of 1,475 stocks containing a single lethal P-element insertion with a *lacZ* reporter were screened to identify genes that are expressed 13 hours after puparium formation (screen conducted by Dr. Claudio Simon). Mutant lines that exhibited such a *lacZ* expression pattern were then screened to identify mutant animals with defects in salivary gland histolysis 24 hours after puparium formation. This resulted in the identification of the P-element line *l(1)G0371* as a gene that is required for salivary gland cell death. Homozygous mutant animals head-evert at 15 hours after puparium formation and die during pupal development, indicating that the cell death phenotype was not caused by a defect in ecdysone levels. The location of the P-element was verified by sequencing DNA flanking the P-element insertion site, and it is located 124 bp 3-prime of the end of the first exon in the gene *ctp* (Figure 15).

The P-element was excised to obtain precise and imprecise excision alleles. Of the 24 lines that were obtained 9 lines were viable, and 15 lines were lethal. These lines were tested for removal of the P-element via sequencing with primers that were designed against the 5' and 3' end of the P-element. Fourteen of the lethal excisions lines were discarded due to the presence of P-element ends. The remaining lethal line showed removal of the P-element along with neighboring sequence, but was lethal before puparium formation. Hence, we were unable to use it to test for defects in salivary gland

autophagic cell death. Two of the viable excision lines, ctp^{ex6} and ctp^{ex14} were evaluated for removal of the P-element and were identical in sequence to the wild-type sequence of *ctp*, indicating the P-element insertion was removed without deletion of flanking genomic DNA. Therefore, mutant animals for the P-element insertion $ctp^{(G0371)}$ and animals with a precise excision ctp^{ex14} ($ctp^{(rev)}$, control) were used to determine the role of *ctp* in salivary gland autophagic cell death.

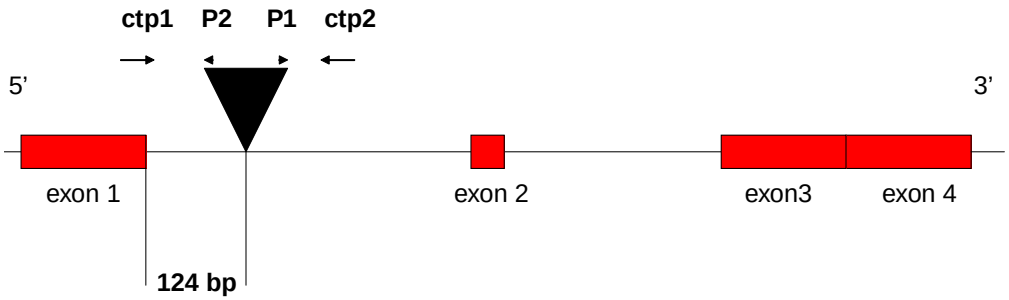

Figure 15. Location of P-element in *ctp*$^{(G0371)}$. P-element (black triangle) was mapped to its location using primers designed against the ends of the P-element and flanking DNA sequence. The P-element is located 124 bp upstream of the 3' end of the first exon (first red rectangle). The primers used were P1 - AAG TGT ATA CTT CGG TAA GC (arrowhead), P2 – AAA TGC GTC GTT TAG AGC AG (arrowhead), ctp1 – TCA GCA CGT CCA CAT CCA C (arrow), and ctp2 – GCT AAA TCG AAT GCA CCC GA (arrow).

Dynein light chain is required for salivary gland autophagic programmed cell death.

To determine if *ctp* is required for salivary gland autophagic cell death, wild-type Canton S, $ctp^{(rev)}$ and $ctp^{(G0371)}$ mutant animals were aged 12 hours after head eversion, embedded in paraffin, sectioned and stained (Figure 16). Wild-type animals lack salivary glands 12 hours after head eversion (Figure 16 A). Animals with the P-element insertion $ctp^{(G0371)}$ have salivary glands present 12 hours after head eversion (Figures 16 B-C, I, n = 47). Eighty-five percent of $ctp^{(G0371)}$ animals have intact salivary glands with cells containing large vacuoles (Figure 16 B, F). The remaining 15% of the $ctp^{(G0371)}$ mutant animals have large remnants of individual salivary gland cells (Figure 16 C, G). On closer examination, these cells also contain large vacuoles and nuclei (Figure 16 G). This phenotype is never seen in dying salivary glands of wild-type Canton S animals (Chapter 2). The morphology of the salivary glands of these *ctp* mutant animals was compared to animals mutant for another strong loss-of-function *ctp* allele, ctp^{e73} (Phillis et al, 1996). Animals mutant for ctp^{e73} also have salivary glands present 12 hours after head eversion (Figure 16 D, I, n = 37). The cells of ctp^{e73} salivary glands have nuclei and large vacuoles, and resemble wild-type salivary glands 12 hours after puparium formation (Figure 5 A, Chapter 2). Animals from the precise excision line ctp^{rev} do not have salivary glands 12 hours after head eversion (Figure 16 E, n=25), and this is similar to what is seen in wild-type Canton S animals. These results indicate that *ctp* functions in salivary gland cell death.

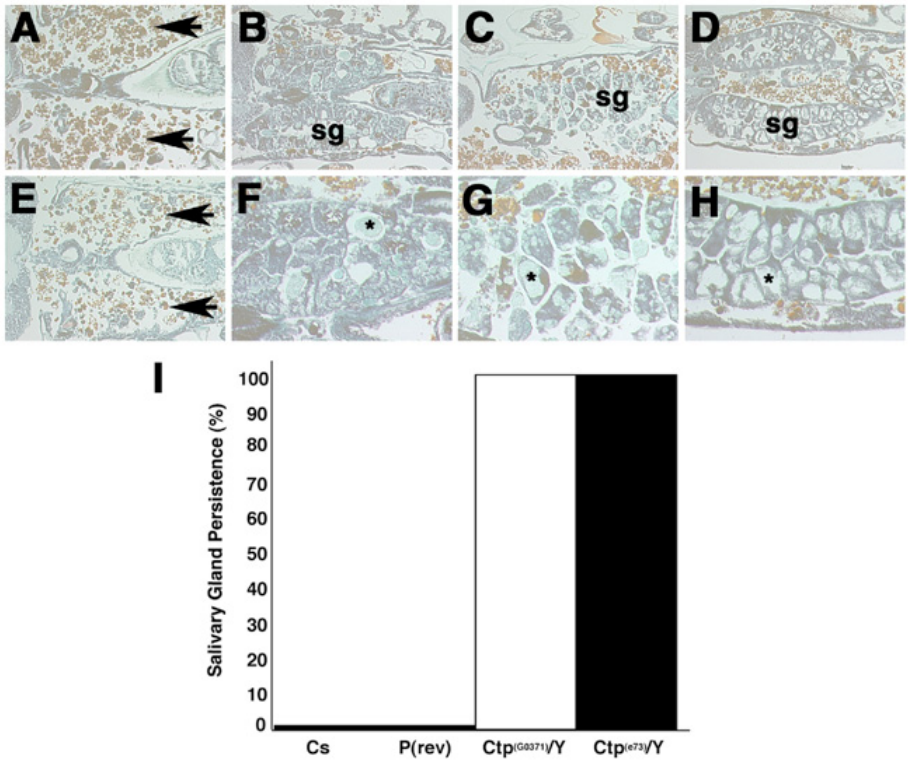

Figure 16. Animals with mutations in *ctp* have persistent salivary glands. (A) Wild-type animals lack salivary glands 12 hours after head eversion. (B) 85% of $ctp^{(G0371)}/Y$ animals have intact salivary glands 12 hours after head eversion. (C) 15% of $ctp^{(G0371)}/Y$ animals have salivary glands that have initiated degradation but have abnormal morphology. (D) Animals lacking $ctp^{(e73)}$ have persistent salivary glands. (E) Precise excision of the *ctp (G0371)* P-element, $ctp^{(rev)}$ leads to loss of the persistent salivary gland phenotype. (F,G) Salivary glands of $ctp^{(G0371)}$ have large vacuoles (asterisk). (H) Salivary glands of $ctp^{(e73)}$ have large vacuoles (asterisks). (I) Quantification of the percent persistent salivary glands in different genotypes 12 hours after head eversion.

Caspase activation is delayed in salivary glands of *ctp* mutants.

ctp encodes the light chain of a Dynein motor that is extremely similar to LC8 in mammals (Phillis et al., 1996) . At least two possible hypotheses could explain why *ctp* mutants exhibit defects in salivary gland cell death. A motor may be used to transport cellular material for localized destruction. Alternatively, destruction may be prevented by tethering a regulator of cell death, and this possibility has been suggested as a mechanism for the regulation of caspase activation (Puthalakath et al, 1999). During salivary gland autophagic death, active caspases cleave structural proteins and also regulate DNA fragmentation (Lee and Baehrecke, 2001; Chapter 2). Since *ctp* mutants have intact salivary glands, we wanted to test if DNA is fragmented in these cells as a marker of caspase activation. $ctp^{(rev)}$ and $ctp^{(G0371)}$ mutant animals were staged relative to head eversion, embedded in paraffin, sectioned and the TUNEL assay was performed to detect fragmentation of DNA (Figure 17). $ctp^{(rev)}$ animals have fragmented DNA as indicated by TUNEL positive nuclei 2 hours after head eversion (Figure 17 A, n=21). By 3-4 hours after head eversion, $ctp^{(rev)}$ salivary glands are largely degraded (Figure 17 B,C, n=15). This is similar to what is observed during salivary gland autophagic cell death in wild-type Canton S animals (Chapter 2). By contrast, TUNEL-positive nuclei are never observed in $ctp^{(G0371)}$ mutant animals 4 hours after head eversion (Figure 17 D, n=14). However, TUNEL-positive nuclei are observed 8 and 12 hours after head eversion in salivary glands of $ctp^{(G0371)}$ mutants (Figure 17 E, F, n=31). These results indicate that DNA fragmentation, and possibly caspase activation is delayed in *ctp* mutant salivary glands.

To directly test if caspase activation is delayed in *ctp* mutants, salivary glands from $ctp^{(rev)}$ and $ctp^{(G0371)}$ mutant animals were staged relative to head eversion, dissected and stained with antibodies against active caspase-3/Drice and nuclear Lamin. In $ctp^{(rev)}$ salivary glands, active caspase-3/Drice is not present in salivary glands 4 hours before head eversion (Figure 18 A, n=16), and is abundant 2 hours after head eversion (Figure 18 B, n=14); this is similar to the timing of caspase activation in dying wild-type Canton S salivary glands (Chapter 2). Active caspase-3/Drice is not detected 4 hours after head eversion in $ctp^{(G0371)}$ mutants (Figure 18 C, n=32) and is observed 8 hours after these mutants have undergone head eversion (Figure 18 D, n=25), indicating that caspase activation is delayed. Nuclear Lamin also seems to be very disorganized as compared to the pattern in controls (Figure 18 B, D).

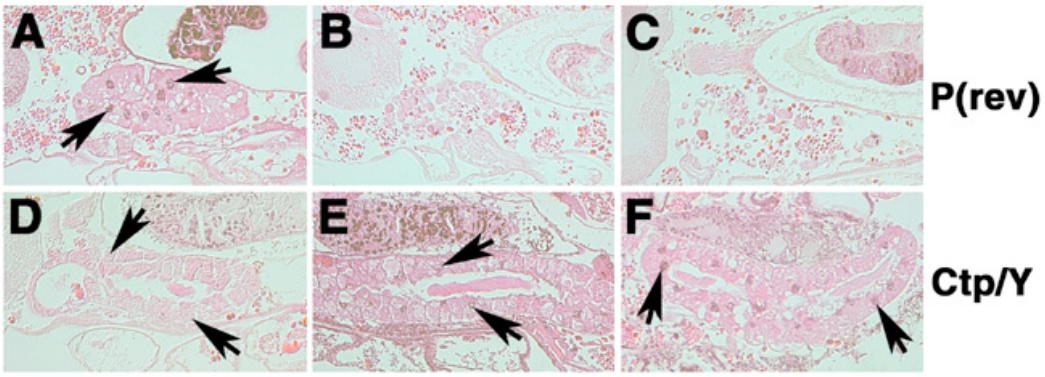

Figure 17. DNA fragmentation is delayed in salivary glands of *ctp* mutant animals. (A) Salivary gland nuclei of $ctp^{(rev)}$ control possess fragmented DNA (arrows) 2 hours head eversion. (B) Salivary glands of $ctp^{(rev)}$ are partly degraded 3 hours after head eversion. (C) Salivary glands of $ctp^{(rev)}$ are degraded 4 hours after head eversion. (D) Salivary glands of $ctp^{(G0371)}$ mutant animals have no DNA degradation (arrows) 4 hours after head eversion. (E,F) Salivary glands of $ctp^{(G0371)}$ mutants have fragmented DNA (arrows) 8 and 12 hours after head eversion.

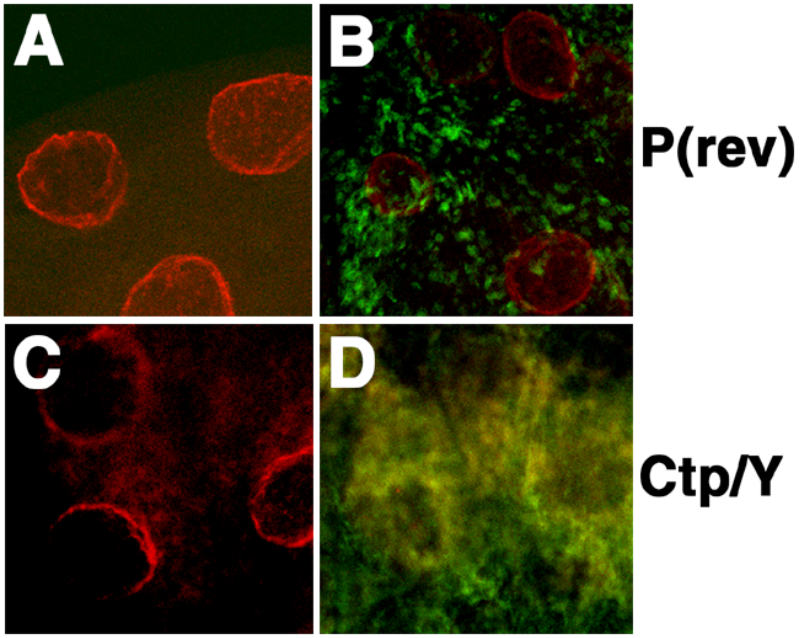

Figure 18. Animals with mutations in *ctp* have delayed caspase-3 activation. (A) Salivary glands of P(rev) control animals 4 hours before head eversion possess intact nuclear Lamin (red) and no active caspase 3 (green). (B) Salivary glands of P(rev) control animals 2 hours after head eversion possess low levels of nuclear Lamin (red) and elevated active caspase 3 (green). (C) Salivary glands of $ctp^{(G0371)}$ have Lamin staining (red) and no active caspase 3 (green) 4 hours after head eversion. (D) $ctp^{(G0371)}$ mutant salivary glands have elevated caspase 3 (green) and disorganized Lamin (red) staining 8 hours after head eversion.

4.4 Discussion.

Mutations in *ctp* prevent salivary gland autophagic cell death.

Salivary gland autophagic programmed cell death is dependent on a number of different genes and therefore biological processes for degradation. Although active caspases play a very important role in the degradation of salivary glands, evidence from previous studies show that other processes, such as cytoskeleton reorganization and lysosome biogenesis may also be needed. Studies of *ctp*, a light chain that is associated with dynein motors, lend further evidence to the possible importance of the organization of the cell during salivary gland autophagic death. *ctp* was also identified in a similar genetic screen for defects in salivary gland cell death (A. Basirullah and C. Thummel, personal communication)and this further indicates the importance of this gene. Furthermore, animals with mutations in two different P-element alleles of *ctp* both displayed defects in salivary gland autophagic death.

Dynein light chain functions during autophagic cell death.

ctp encodes a Dynein light chain with high sequence homology to the mammalian LC8 family (Wilson et al., 2001). The LC8 protein was identified as an integral component of the outer arm of dynein in *Chlamydomonas*. Loss of LC8 in these animals results in disruption of retrograde intraflagellar transport in such a way that rafts of transported material accumulate in large clusters at the distal tips of the flagella (Pazour et al., 1998). In *Drosophila*, partial loss-of- function of LC8 homologs lead to morphogenetic defects in bristle and wing development, female sterility, and alterations in axon guidance (Dick et al., 1996; Phillis et al., 1996).

Mutations in *ctp* could affect salivary gland autophagic cell death in several ways. It could disrupt the orientation of the cytoskeleton within the salivary glands. Light chains are associated with Dynein motors which use microtubules as their network for transport (Karcher et al., 2002). Microtubule arrangement in the cells may require the function of microtubule-based motor proteins. For example, during CNS development when a growth cone selects a particular direction of growth, the microtubule array changes from a scattered to a bundled arrangement, and disruption in Dynein function could disrupt the formation of the bundle (Tanaka and Sabry, 1995). It is quite possible that disruption of the Dynein motor due to loss of proper *ctp* function could lead to disorganization of the microtubule network and hence its transport system. Immunohistochemistry staining of Tubulin in *ctp* mutant salivary glands could help to determine if this is the case in these animals. Dynein heavy chains have also been implicated in Tubulin-based transport. Analyses of dynein heavy chain (*dhc*) alleles with *ctp* alleles showed no change in salivary gland persistence. Furthermore, homozygous *dhc* mutants did not have salivary gland defects. Further analyses will be performed to test for interactions of *ctp* with alternative dynein heavy chains.

Mutations in *ctp* could also affect the transport or localization of protein complexes needed for salivary gland autophagic cell death. An association of dynein light chain with cell death was discovered when it was observed that the mammalian light chain LC8 associates with the pro-apoptotic Bcl-2 family member Bim (Puthalakath et al., 1999; Rodriguez-Crespo et al., 2001). In healthy cells, LC8 binds to Bim and sequesters it to the dynein motor complex, but upon stimulation by a death signal LC8 releases its hold on Bim, allowing Bim to assist in the death of the cell through the

activation of caspases. Even though caspase activation did occur in *ctp* mutants, it was delayed. Intriguingly, the pro-apoptotic Bcl-2 homolog, Debcl is present in salivary glands one hour after the start of salivary gland cell death (Chapter 3, Table 3). It is not clear is Debcl plays a role in caspase activation, however, it would be interesting to determine if Ctp could interact with Debcl. This could be pursued by doing either yeast two-hybrid screens or co-immunoprecipitation experiments. The LC8 light chain has also been shown to associate with Myosin V, which is an actin-based motor (Benashski et al., 1997). Myosin V is involved in the transport of membranous cargo such as vacuoles and secretary vesicles. During salivary gland cell death, Actin aggregates in the cortical region of cells (Chapter 2, Figure 7). At that time, lysosomes are present in the same region and it is possibility that these lysosomes could be involved in degradation of cytoplasmic contents during cell death (Lee et al., 2001; Cranford and Baehrecke, unpublished). It is possible that *ctp* could be associated with Myosin and disruption of *ctp* function disrupts the transport of vesicles or the formation of vacuoles needed for salivary gland autophagic cell death. Further evaluation of these *ctp* mutant salivary glands by Transmission Electron Microscopy (TEM) will be needed to determine the effects of *ctp* on vacuole formation.

Cytoplasmic dyneins have been implicated in maintaining the position of organelles such as nuclei within a cell (Eshel et al., 1993, Li et al., 1993). The location of organelles within a cell during development is very important and alterations in the localization of the nucleus could lead to abnormal development (Fischer, 2000). For example, nuclear position is important in the Drosophila oocyte since the position of the nucleus determines both A-P and D-V axes of the embryo through the gurken gene

(Fischer, 2000; van Eeden and St. Johnston, 1999). There is some evidence for the importance of the dynein motor in nuclear positioning that was obtained through studies of animals mutated for the *DLis-1* gene. Animals with this mutation show mislocalization of the nucleus and a lack of localization of the Dynein heavy chain (Swan et al., 1999; Fischer, 2000). Animals with mutations in *ctp* also appear to display defects in the location of the nuclei. Normally, the nuclei of dying salivary gland cells are located in the center of the cell. In *ctp* mutant animals, the nuclei are located at the cortex of cells, and most of the time along the lumen/apical side of the salivary gland. Molecules or proteins that need to enter the nucleus for the activation of genes required for salivary gland cell death are unable to do so, since the nucleus is not in its proper position. Immunohistochemical-labeling of *ctp* within salivary glands will help determine if its protein associates with the nuclei during salivary gland autophagic cell death and TEM studies will determine if other abnormal morphology exists in these mutant cells.

4.5 Materials and Methods.

Mapping of P-element and P-element excision.

Fourteen hundred and seventy-five lines containing a lethal P-element insertion with a *lacZ* reporter gene were obtained from the Bloomington stock collection and screened for genes that were expressed 13 hours after puparium formation. P-element insertion lines that showed *lacZ* expression at that time were screened for salivary gland persistence, and this led to the identification of the P-element line*l(1)G0371* (screen was conducted by Dr. Claudio Simon). Excision alleles were generated by crossing

l(1)G0371 to Δ2-3 transposase according to standard methods (Robertson et al., 1988). All stocks were maintained over the *FM7C* balancer chromosome.

Salivary gland histology.

Wild-type Canton S, *ctp* (*ctp*$^{(G0371)}$ *and ctp*^{e73}) and the precise excision line *ctp*$^{(rev)}$ animals were maintained at 25^{o}C and aged to different stages following puparium formation. The alleles for *ctp* were balanced over the *FM7, Actin-GFP* for genotyping the hemizygous progeny. For paraffin sections and light microscopy, whole pupae were fixed, embedded, sectioned, and either stained with Gill's Hematoxylin and Pollack Trichrome or analyzed using the TUNEL method as previously described (Lee and Baehrecke, 2001) and examined using a Zeiss Axiophot II microscope.

Antibody staining.

Antibodies against Lamin Dm0 ADL84 (Stuurman et al., 1995), and cleaved Caspase-3 (Asp175) were obtained from P. A. Fisher, and Cell Signaling Technology (Beverly, MA) respectively. *ctp*$^{(rev)}$ and *ctp*$^{(G0371)}$ mutant salivary glands were dissected from animals staged relative to puparium formation at 25^{o}C, fixed in 4% paraformaldehyde/heptane for 20 minutes at room temperature, blocked in phosphate buffered saline containing 1% BSA and 0.1% Triton-X (PBSBT), and incubated with primary antibodies for 16 hours at 4^{o}C. Salivary glands were washed for 2 hours in PBSBT, incubated with appropriate secondary antibodies for two hours at room temperature, washed for another 2 hours in PBSBT at room temperature, incubated in 0.5 µl TOTO-3 in 1 ml PBSBT for ten minutes at room temperature, and washed in PBSBT for an additional hour at room temperature. Salivary glands were mounted in Vectashield

(Vector Laboratories) and examined using a Zeiss Axiovert 100 M confocal microscope.

Chapter 5.

Summary and Future Work.

5.1 Conclusions.

Programmed cell death is an integral part of eukaryotic development. A wealth of knowledge exists about the mechanisms that regulate apoptosis. By contrast, our understanding of the mechanisms that regulate autophagic programmed cell death remains sparse, even though this process has been implicated in many human disorders, such as neurodegeneration and cancer (Baehrecke, 2003; Yuan et al, 2003). Therefore, it is imperative to pursue research on autophagic cell death that will lead to a better understanding of its mechanisms.

Most of the knowledge of autophagic cell death is based on studies of dying larval salivary glands during*Drosophila melanogaster* development. The steroid ecdysone triggers salivary gland destruction which begins 12 hours after puparium formation and is complete by 16 hours after puparium formation (Jiang et al., 1997). Ecdysone acts through its heterodimeric nuclear receptor complex, *EcR* and *usp*, with the nuclear receptor *βFTZ-F1* serving as a competence factor to activate the ecdysone regulated genes *E93*, *BR-C* and *E74A* (Burtis et al., 1990; DiBello et al., 1991; Seagraves and Hogness, 1990; Broadus et al., 1999; Woodard et al., 1994; Lee et al., 2000; Yao et al, 1993). These genes in turn activated a set of late genes including the apoptosis regulators *rpr, hid, ark, dronc*, and *drice*, and these genes play a more direct role in salivary gland cell death (Jiang et al., 1997; Lee et al., 2000; Lee et al., 2002; Jiang et al., 2000). During this time, significant changes in the morphology of salivary gland cells occur. Before the start of death, salivary gland cells are cube-like in shape, and contain large eosin-positive

vacuoles. Following the rise in ecdysone, these large vacuoles fragment and smaller vacuoles appear within the cytoplasm. Some of these vacuoles are clearly autophagic as they contain organelles such as mitochondria (Lee and Baehrecke, 2001). These cells seem to degrade themselves, as phagocytes are not seen during this process (Chapter 2).

Changes in salivary gland morphology during death were thought to be the result of active caspases. Indeed, active caspases are responsible for some the morphological changes, as caspase substrates such as nuclear Lamin, α-Tubulin and α-Spectrin are cleaved (Chapter 2). However, changes in filamentous Actin occur in the absence of caspase activity, and Actin is not degraded until late stages of salivary gland cell death (Chapter 2). This suggests that cytoskeleton organization is important for salivary gland cell death and that proteins other than caspases may be involved in autophagic cell death.

We identified a large number of proteins that are present in the salivary gland during cell death. These proteins are involved in a numerous processes including transcription, cell and protein degradation, cell organization, cell growth control and the cell cycle, suggesting complex possibilities for the mechanisms that regulate autophagic cell death (Chapter 3). A forward genetic screen led to the identification of a gene that provides support for the idea that genes other than caspases are important for salivary gland cell death. Mutations in *ctp* a light chain of the dynein motor, prevent salivary gland histolysis. Dynein motors have been implicated in microtubule organization, lysosome biogenesis, cargo trafficking, nuclei positioning, and regulation of apoptosis. *ctp* has significant sequence homology with LC8 and this light chain associates with the actin-based motor, Myosin V, which is involved in the transport of vacuoles and secretory vesicles. Further studies of this gene may provide a better understanding of the role of

motors in salivary gland cell death. Based on this research, a new model for salivary gland autophagy is proposed (Figure 19).

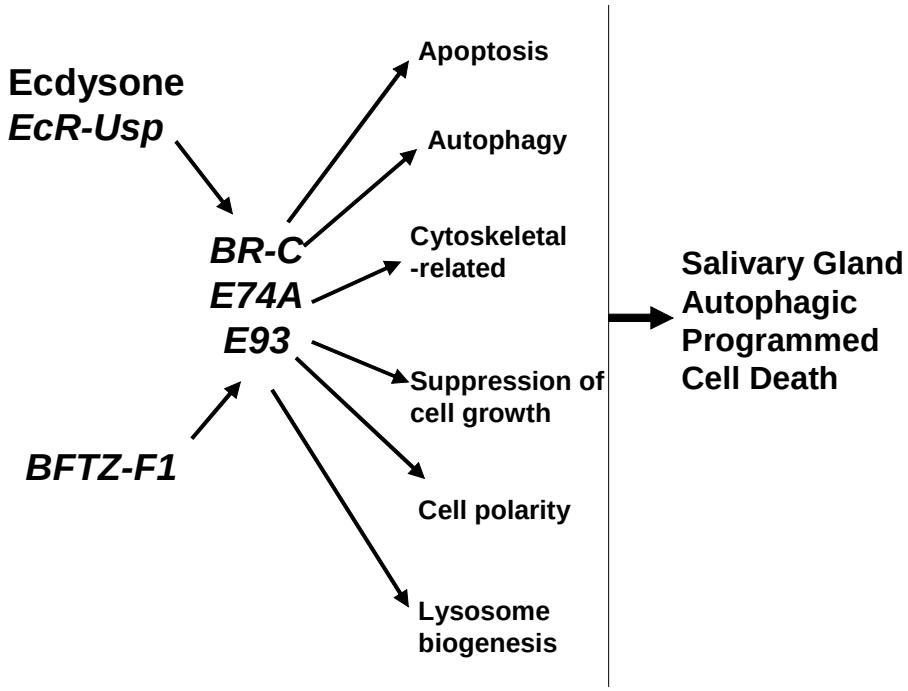

Figure 19. Model of steroid-regulation of salivary gland autophagy. Several genes that are involved in many different biological processes may help drive the process of cell death to completion including genes involved in apoptosis, autophagy, cytoskeleton organization, suppression cell growth, cell polarity and lysosome biogenesis.

5.2 Reorganization of the cytoplasm, cytoskeleton and associated proteins during autophagic cell death.

Previous studies reported that cytoplasmic changes in vacuole structure occur in a caspase-independent manner in dying salivary glands (Lee and Baehrecke, 2001). The results from chapter 2 also suggest that changes in filamentous Actin organization during salivary gland autophagic death are caspase-independent. Other studies of cytoskeleton changes during autophagic cell death also support this conclusion. Bursch et al. (2000) showed that polymerization of G-Actin to F-Actin takes place during autophagic cell death of MCF-7 breast cancer cells. In addition, Cytokeratin is redistributed but not degraded during cell death of MCF-7 cells. This suggests that some parts of the cytoskeleton are needed to drive the process of autophagic cell death. Although the data to support this hypothesis are limited, many pieces of evidence support this conclusion. During salivary gland cell death, the aggregation of Actin at the cortical region of the cell occurs around the same time as autophagic vacuoles and lysosomes increase (Chapter 2; Lee and Baehrecke, 2001). It is possible that the cytoskeleton is needed to provide a structure for lysosomal transport or the movement of cargo within a cell during autophagy.

Several proteins involved in cytoskeleton reorganization were idenitified from the proteomics work (Chapter 3, Table 4). We identified a number of Formin Homology Proteins (FHP), which play a role in cytoskeleton reorganization (Waller and Alberts, 2003). We could study the importance of these proteins in salivary gland cell death by knocking down or knocking out the function of these genes with either loss-of-function mutants or RNAi. We also identified a number of proteins involved in cytoskeleton

biogenesis and numerous motor proteins. Studies were performed on a component of motor proteins *ctp*, which encodes a light chain of a dynein motor and also has a sequence homology to the mammalian LC8 protein (Wilson et al., 2001; Chapter 4). Dynein motors are believed to be involved in microtubule organization or bundling and organelle localization, and disruption of the Dynein motor disrupts microtubule and cytoplasm organization (Tanaka and Sabry, 1995; Eshel et al., 1993, Li et al., 1993 Eshel et al., 1993, Li et al., 1993). Animals with mutations in *ctp* display features of disorganization of the cytoplasm such as mislocalization of the nuclei. Further experiments on *ctp* will help determine if cytoskeleton organization is important for salivary gland autophagic cell death. We could determine if *ctp* is localized to the nuclei of salivary gland cells by performing immunohistochemistry or immunogold-labeling followed by TEM. Antibody staining of other cytoskeleton components such as filamentous Actin and α-Tubulin could also help determine if the cytoskeleton is disorganized. We could also perform co-immunoprecipitation experiments to determine to Ctp interacts with any proteins involved in cytoskeleton organization.

5.3 Autophagy and cell death.

Autophagy is conserved in organisms that are as diverse as yeast and mammals (Baehrecke, 2003). Autophagy occurs in yeast cells during nutrient-deprivation and ensures the survival of these cells. In mammals, autophagy has also been implicated in the survival of cancer cells by either optimizing nutrient use for cell survival, or by degrading organelles such as depolarized mitochondria that may lead to cell demise (Alva et al., 2004).

Recent studies suggest the possibility that autophagy is needed for cell death to occur under some circumstances. Mice lacking one Beclin 1 (Atg 6) allele suffer a higher incidence of spontaneous tumors including lymphoma and hepatocellular carcinoma (Yue et al., 2003; Qu et al., 2003). These animals also exhibit a decrease in the formation of autophagic vacuoles, indicating that autophagy plays an important role in the regulation of tumor development in animals. Embryonic stem cells deficient in both Beclin 1 alleles exhibit defects in embryoid body formation due to a reduction in cell clearance, and these cells are capable of dying by apoptosis (Yue et al., 2003; Qu et al., 2003). A recent study showed that autophagy is activated when the apoptotic pathway is defective, and this leads to cell death of fibrosarcoma cells. Significantly, Atg genes are needed to activate this autophagic cell death (Yu et al., 2004). Therefore, the *Drosophila* Atg homologs may be needed for salivary gland autophagic cell death. We identified several Atg homologs in our proteome analyses (Chapter 3, Table 3), and a number of RNAi experiments are currently progress to test their requirement in salivary gland cell death.

We have also identified Tor, which encodes protein kinase (Kozma and Thomas, 2002; Chapter 3, Table 3). Tor induces the formation of autophagic vacuoles under nutrient deprivation conditions. A number of experiments are currently in progress to test the importance of Tor in salivary gland autophagy. Tor is present within the salivary glands at 6 hours after puparium formation. Rapamycin inhibits Tor and prevents its function in cell growth (Kozma and Thomas, 2002). Currently, different doses of rapamycin are being injected into pupae at 6 hours after puparium formation to determine if inhibition of Tor induces early cell death of salivary glands. We are also performing similar experiments on animals with mutations in the*E93* gene. Animals with mutations

in E93 do not display any cytoplasmic changes associated with salivary gland autophagic cell death (Lee and Baehrecke, 2001). If injections of rapamycin into these animals induce the formation of vacuoles normally seen in salivary glands undergoing cell death, it could mean that E93 could be a negative regulator of Tor in either a direct or indirect manner.

5.4 Importance of cell death in growth control.

An intricate relationship between cell proliferation, growth and death is required for proper development of an organism. In some animals, the same signal may be responsible for different and similar populations of cells to initiate proliferation, differentiation, morphogenesis, and programmed cell death. For example, during *Drosophila* metamorphosis, ecdysone can trigger the formation of adult structures while larval tissues undergo cell death (Riddiford, 1993; Baehrecke, 2000). Similarly, thyroid hormone appears to trigger cell proliferation, differentiation, morphogenesis and death in amphibians (Brinkmann, 1994). The balance between cell proliferation and death also plays an important role in the abnormal growth of typical of cancer. Oncogenes and growth factors such as Myc, Ras and Epidermal growth factor can induce transformation, proliferation, apoptosis and growth arrest (Green and Evan, 2002; Sewing et al., 1997; Kerkhoff and Rapp, 1998). It is still unclear how the same signal could be the cause of several different responses, and it is important to understand the mechanisms underlying signaling during normal and abnormal growth.

One model suggests that cell death acts as a safeguard to prevent abnormal proliferation of cells that could otherwise lead to neoplastic growth typical of cancer.

Studies of the *salvador* (*sav*), *warts/lats*, and *hippo* (*hpo*) genes in the developing *Drosophila* eye support this concept. It is believed that these genes act in the same pathway to regulate cell growth, proliferation and death. Loss of the tumor suppressor gene *sav* leads to an increase in cell proliferation and a decrease in apoptosis which is associated with elevated levels of Cyclin E and *Drosophila* inhibitor of apoptosis (DIAP1) (Tapon et al., 2002). Loss of *warts/lats* also results in similar phenotypes (Justice et al., 1995). Most recently it was shown that *hpo*, a member of the Ste-20 family protein kinases functions in the regulation of cell number and organ size. The eyes of animals mutant for *hpo* contain slightly larger ommatidial facets and more interommadital cells than those of wild-type animals (Wu et al., 2003; Harvey et al., 2003). In addition, *hpo* may be needed to promote cell death, as loss of *hpo* leads to elevated levels of DIAP1. The mammalian homolog of *hpo* MST2 is a Map4Kinase which regulates several biological functions including cellular growth, proliferation, differentiation and cell death through a series of kinase signaling cascades (Wu et al., 2003; Harvey et al., 2003). Ectopic expression of MST2 in *Drosophila hpo* mutants rescues the phenotypes mentioned above indicating that this system is conserved (Wu et al., 2003; Harvey et al., 2003; Graves et al., 1998). Another gene that acts in a similar manner is *archipelago* (*ago*) which was identified in a screen for genes that restrict cell numbers and tissue growth during development (Moberg et al., 2001). Mutations in *ago* lead to an increase in cell proliferation and elevated levels of Cyclin E. In addition, co-expression of *ago* with the caspase inhibitor p35 leads to a greater number of cells indicating a role of ago in mediating the balance between cell proliferation and cell death. The human *ago* ortholog, hCdc4, is mutated in several cancer cell lines (Moberg et al.,

2001). Micro RNAs (miRNAs) also play a role in maintaining the coordination of the rates of cell proliferation and cell death. The miRNA *bantam*, balances cell proliferation and death through transcriptional regulation of the cell death gene *hid*. Over-expression of *bantam* in *Drosophila* eyes that ectopically express *hid* leads to a rescue of an eye ablation phenotype (Brennecke et al., 2003).

We have identified a number of proteins that are involved in cell proliferation, cell cycle and growth control (Chapter 3, Table 5). A number of proteins from this group stand out, including proteins involved in the Insulin receptor pathway, and Wts, several PI3 Kinases and TSC1. Studies of TSC1 and its interaction with the autophagy protein Tor could be intriguing and may help us to understand how cell growth and salivary gland autophagic cell death occurs. TSC1 encodes a tumor suppressor gene that acts downstream of the Insulin receptor, although the precise mechanism by which this occurs is unknown (Goberdhan and Wilson, 2003). TSC1 negatively regulates Tor and prevents cell growth and proliferation (Kozma and Thomas, 2002). Even though salivary glands do not undergo proliferation, the production and growth of organelles and other cytoplasm components may occur (Smith and Orr-Weaver, 1991), and when these cells undergo cell death this process is likely terminated. We could test the importance of TSC1 in salivary gland cell death by analysis of loss-of-function mutants and performing RNAi experiments. We could also look for interactions of TSC1 and Tor in the salivary glands by performing co-immunoprecipitation experiments.

We have presented data indicating that caspases function to cleave cell substrates during autophagic cell death of *Drosophila* salivary glands (Chapter 2). Although caspases function in the death of these cells, our data also suggest that other processes are

needed to properly destroy salivary glands. High-throughput proteomic studies resulted in the identification of several categories of proteins that may be needed for autophagic cell death (Chapter 3). Among these proteins, a large group of motors were identified and genetic analyses of Dynein light chain indicated that motors are required for the death of salivary glands (Chapter 4). Future genetic and biochemical studies of the proteins involved in the regulation of cell organization, autophagy, growth control and others should clarify their involvement in autophagic cell death.

Appendix 1. List of proteins identified in salivary glands 6 hours after puparium formation

Flybase ID#	upep	tpep
FBgn0000014	1	3
FBgn0000024	1	2
FBgn0000042	5	8
FBgn0000043	5	8
FBgn0000044	5	8
FBgn0000045	3	6
FBgn0000052	1	1
FBgn0000053	1	1
FBgn0000083	1	1
FBgn0000117	1	3
FBgn0000142	1	1
FBgn0000163	2	2
FBgn0000166	1	1
FBgn0000181	1	1
FBgn0000183	1	1
FBgn0000210	1	1
FBgn0000229	1	1
FBgn0000242	1	1
FBgn0000256	2	2
FBgn0000286	2	4
FBgn0000299	3	3
FBgn0000307	1	1
FBgn0000317	3	3
FBgn0000319	2	4
FBgn0000330	1	3
FBgn0000340	1	1
FBgn0000368	2	3
FBgn0000376	1	1
FBgn0000382	3	3
FBgn0000412	1	1
FBgn0000416	1	1
FBgn0000448	1	1
FBgn0000463	2	2
FBgn0000489	1	3
FBgn0000490	1	1
FBgn0000499	2	2
FBgn0000524	2	2
FBgn0000546	2	2
FBgn0000556	3	11
FBgn0000557	2	7
FBgn0000559	3	4
FBgn0000564	1	2
FBgn0000567	3	4
FBgn0000568	2	2
FBgn0000579	2	2
FBgn0000617	2	2
FBgn0000629	2	2

FBgn0000639	2	3
FBgn0000640	1	1
FBgn0000721	2	3
FBgn0000723	1	1
FBgn0000810	3	4
FBgn0000986	2	2
FBgn0001078	1	1
FBgn0001091	3	3
FBgn0001092	2	2
FBgn0001104	1	1
FBgn0001108	2	2
FBgn0001112	2	2
FBgn0001142	2	2
FBgn0001149	2	3
FBgn0001169	1	1
FBgn0001202	1	1
FBgn0001215	2	2
FBgn0001219	5	15
FBgn0001220	1	1
FBgn0001224	1	3
FBgn0001233	1	1
FBgn0001250	1	1
FBgn0001301	6	6
FBgn0001308	1	1
FBgn0001309	5	7
FBgn0001316	1	2
FBgn0001991	1	1
FBgn0002306	1	1
FBgn0002413	1	5
FBgn0002431	2	2
FBgn0002441	2	2
FBgn0002526	9	10
FBgn0002528	4	12
FBgn0002564	1	1
FBgn0002579	1	1
FBgn0002593	1	2
FBgn0002643	2	3
FBgn0002645	2	3
FBgn0002716	1	1
FBgn0002777	2	2
FBgn0002778	1	1
FBgn0002783	3	4
FBgn0002868	1	1
FBgn0002905	2	2
FBgn0002921	1	1
FBgn0002926	3	3
FBgn0002932	2	3
FBgn0003016	1	1
FBgn0003041	1	1
FBgn0003044	1	3

FBgn0003048	9	11
FBgn0003057	1	1
FBgn0003067	1	1
FBgn0003075	1	1
FBgn0003138	1	1
FBgn0003139	1	1
FBgn0003150	1	1
FBgn0003175	1	1
FBgn0003177	2	2
FBgn0003187	1	1
FBgn0003189	1	1
FBgn0003204	1	1
FBgn0003206	1	2
FBgn0003218	1	1
FBgn0003261	1	1
FBgn0003274	1	1
FBgn0003277	1	1
FBgn0003301	2	3
FBgn0003334	1	1
FBgn0003346	2	2
FBgn0003366	2	2
FBgn0003373	1	1
FBgn0003374	1	1
FBgn0003377	1	1
FBgn0003378	1	5
FBgn0003391	1	1
FBgn0003396	4	7
FBgn0003444	1	1
FBgn0003450	1	1
FBgn0003460	1	1
FBgn0003464	4	7
FBgn0003471	1	1
FBgn0003495	1	1
FBgn0003502	2	2
FBgn0003507	3	4
FBgn0003514	1	1
FBgn0003520	1	1
FBgn0003575	4	4
FBgn0003656	4	4
FBgn0003716	1	1
FBgn0003717	1	1
FBgn0003721	1	1
FBgn0003862	4	4
FBgn0003887	1	3
FBgn0003891	1	1
FBgn0003963	1	1
FBgn0003964	1	1
FBgn0004002	4	7
FBgn0004103	1	2
FBgn0004107	1	1

FBgn0004167	1	1
FBgn0004177	1	1
FBgn0004236	1	2
FBgn0004243	4	4
FBgn0004362	1	1
FBgn0004364	1	1
FBgn0004368	1	1
FBgn0004378	1	1
FBgn0004390	1	1
FBgn0004395	1	1
FBgn0004396	2	2
FBgn0004397	1	1
FBgn0004419	2	2
FBgn0004432	1	6
FBgn0004507	1	1
FBgn0004509	1	1
FBgn0004551	1	4
FBgn0004556	1	1
FBgn0004568	1	1
FBgn0004584	1	1
FBgn0004586	1	1
FBgn0004587	1	4
FBgn0004592	1	1
FBgn0004593	1	2
FBgn0004595	1	2
FBgn0004607	1	1
FBgn0004643	1	1
FBgn0004648	1	1
FBgn0004649	2	2
FBgn0004654	1	1
FBgn0004655	3	6
FBgn0004656	3	4
FBgn0004657	3	4
FBgn0004687	2	3
FBgn0004834	2	4
FBgn0004842	1	1
FBgn0004858	3	3
FBgn0004864	1	1
FBgn0004868	1	2
FBgn0004879	1	1
FBgn0004880	1	1
FBgn0004885	1	1
FBgn0004888	2	2
FBgn0004893	4	7
FBgn0004915	1	1
FBgn0005198	2	2
FBgn0005386	5	5
FBgn0005585	4	6
FBgn0005624	3	5
FBgn0005634	3	3

FBgn0005636	2	2
FBgn0005638	1	1
FBgn0005642	1	1
FBgn0005674	2	2
FBgn0005695	2	2
FBgn0005771	2	2
FBgn0008635	1	1
FBgn0010051	2	2
FBgn0010083	2	2
FBgn0010173	1	1
FBgn0010194	2	3
FBgn0010217	2	2
FBgn0010229	1	1
FBgn0010246	1	1
FBgn0010252	1	1
FBgn0010288	1	2
FBgn0010309	2	2
FBgn0010313	2	2
FBgn0010316	3	5
FBgn0010355	1	1
FBgn0010356	1	1
FBgn0010380	1	1
FBgn0010391	1	1
FBgn0010412	1	1
FBgn0010413	1	1
FBgn0010417	1	1
FBgn0010434	2	2
FBgn0010435	1	1
FBgn0010441	1	3
FBgn0010460	1	1
FBgn0010621	1	2
FBgn0010747	2	2
FBgn0010851	1	2
FBgn0011202	3	7
FBgn0011230	4	4
FBgn0011285	1	1
FBgn0011571	4	9
FBgn0011573	1	1
FBgn0011591	1	1
FBgn0011598	1	1
FBgn0011603	2	2
FBgn0011606	1	1
FBgn0011666	1	1
FBgn0011693	2	2
FBgn0011712	1	1
FBgn0011737	1	1
FBgn0011742	1	1
FBgn0011747	1	3
FBgn0011771	2	2
FBgn0011824	1	1

FBgn0011826	1	1
FBgn0011829	1	2
FBgn0011836	1	1
FBgn0012049	1	1
FBgn0013263	3	3
FBgn0013269	1	1
FBgn0013548	1	1
FBgn0013576	1	1
FBgn0013726	1	1
FBgn0013733	10	16
FBgn0013765	1	1
FBgn0013773	1	2
FBgn0013809	2	6
FBgn0013812	3	5
FBgn0013948	3	3
FBgn0013953	1	1
FBgn0013955	1	1
FBgn0013969	1	1
FBgn0013974	1	1
FBgn0013984	3	3
FBgn0013988	8	8
FBgn0013997	1	1
FBgn0013998	1	1
FBgn0014002	11	22
FBgn0014018	1	1
FBgn0014027	2	4
FBgn0014073	1	1
FBgn0014075	2	2
FBgn0014133	6	9
FBgn0014141	2	2
FBgn0014184	2	2
FBgn0014362	1	1
FBgn0014388	1	1
FBgn0014396	1	1
FBgn0014861	1	1
FBgn0015010	1	1
FBgn0015019	2	2
FBgn0015025	1	1
FBgn0015033	1	1
FBgn0015221	1	1
FBgn0015234	3	3
FBgn0015239	2	2
FBgn0015240	1	1
FBgn0015247	1	2
FBgn0015295	2	2
FBgn0015320	2	2
FBgn0015513	2	3
FBgn0015520	1	1
FBgn0015542	1	1
FBgn0015575	2	2

FBgn0015589	2	2
FBgn0015602	1	1
FBgn0015615	2	2
FBgn0015623	1	1
FBgn0015624	2	4
FBgn0015714	1	1
FBgn0015773	2	2
FBgn0015789	1	1
FBgn0015808	1	1
FBgn0015816	1	1
FBgn0015829	1	1
FBgn0015838	2	10
FBgn0015907	2	5
FBgn0015933	2	2
FBgn0015954	1	1
FBgn0016059	2	2
FBgn0016076	1	1
FBgn0016078	1	1
FBgn0016119	1	1
FBgn0016120	1	1
FBgn0016132	1	1
FBgn0016685	1	3
FBgn0016693	2	2
FBgn0016724	3	6
FBgn0016756	1	1
FBgn0016762	1	1
FBgn0016794	1	1
FBgn0016917	1	1
FBgn0016930	1	3
FBgn0016977	7	8
FBgn0017418	1	1
FBgn0017549	1	1
FBgn0017550	1	1
FBgn0017561	3	3
FBgn0017565	1	3
FBgn0017566	2	2
FBgn0017577	1	1
FBgn0017581	2	3
FBgn0019637	2	3
FBgn0019890	4	5
FBgn0019925	1	1
FBgn0019947	1	1
FBgn0019990	1	1
FBgn0020235	1	1
FBgn0020269	2	2
FBgn0020278	1	1
FBgn0020294	1	1
FBgn0020299	1	2
FBgn0020370	1	1
FBgn0020378	1	1

FBgn0020381	1	1
FBgn0020385	2	9
FBgn0020388	2	2
FBgn0020389	1	1
FBgn0020412	1	2
FBgn0020443	1	1
FBgn0020493	1	1
FBgn0020496	1	6
FBgn0020506	1	1
FBgn0020510	1	1
FBgn0020513	1	1
FBgn0020611	1	1
FBgn0020615	1	1
FBgn0020616	1	1
FBgn0020647	1	1
FBgn0020655	1	1
FBgn0021979	1	1
FBgn0022343	1	2
FBgn0022361	4	11
FBgn0022710	4	5
FBgn0022720	1	1
FBgn0022764	1	3
FBgn0022787	2	2
FBgn0023023	1	1
FBgn0023081	1	1
FBgn0023129	1	1
FBgn0023130	1	1
FBgn0023143	1	1
FBgn0023167	3	3
FBgn0023172	2	2
FBgn0023215	1	1
FBgn0023216	1	1
FBgn0023395	1	1
FBgn0023395	1	1
FBgn0023417	1	5
FBgn0023423	1	1
FBgn0023479	2	2
FBgn0023506	1	1
FBgn0023511	1	1
FBgn0023515	1	1
FBgn0023529	1	1
FBgn0023530	1	2
FBgn0023546	1	1
FBgn0024150	3	6
FBgn0024230	1	1
FBgn0024249	1	1
FBgn0024251	1	1
FBgn0024285	1	1
FBgn0024291	1	2
FBgn0024308	4	27

FBgn0024732	1	1
FBgn0024754	1	1
FBgn0024814	1	1
FBgn0024913	1	3
FBgn0024923	1	1
FBgn0024947	1	1
FBgn0024996	2	2
FBgn0025117	1	2
FBgn0025335	1	1
FBgn0025381	1	1
FBgn0025454	2	2
FBgn0025455	1	1
FBgn0025458	2	2
FBgn0025558	1	1
FBgn0025616	1	2
FBgn0025617	1	1
FBgn0025638	1	1
FBgn0025639	1	1
FBgn0025725	1	2
FBgn0025742	1	1
FBgn0025743	2	3
FBgn0025802	1	1
FBgn0025803	2	5
FBgn0025830	1	1
FBgn0025937	2	2
FBgn0026059	3	3
FBgn0026077	1	1
FBgn0026084	1	2
FBgn0026090	1	1
FBgn0026190	1	1
FBgn0026319	1	1
FBgn0026378	1	1
FBgn0026379	1	1
FBgn0026380	1	1
FBgn0026417	1	2
FBgn0026428	3	3
FBgn0026620	1	2
FBgn0026630	2	3
FBgn0026761	1	1
FBgn0026787	1	1
FBgn0026869	1	1
FBgn0027049	1	1
FBgn0027055	1	1
FBgn0027363	1	1
FBgn0027495	1	1
FBgn0027497	1	1
FBgn0027508	2	2
FBgn0027512	1	1
FBgn0027515	1	1
FBgn0027518	1	1

FBgn0027524	1	1
FBgn0027527	1	14
FBgn0027532	1	1
FBgn0027534	2	2
FBgn0027546	1	1
FBgn0027553	1	1
FBgn0027556	2	2
FBgn0027567	1	1
FBgn0027570	2	2
FBgn0027572	1	1
FBgn0027579	1	1
FBgn0027580	1	1
FBgn0027581	5	8
FBgn0027587	1	1
FBgn0027593	1	1
FBgn0027594	2	3
FBgn0027598	3	3
FBgn0027601	1	1
FBgn0027607	2	2
FBgn0027616	1	3
FBgn0027621	1	1
FBgn0027655	1	1
FBgn0027660	3	3
FBgn0027793	1	2
FBgn0027836	1	1
FBgn0027844	1	1
FBgn0027889	1	1
FBgn0028382	2	2
FBgn0028397	2	2
FBgn0028399	2	3
FBgn0028467	2	4
FBgn0028469	1	1
FBgn0028476	2	2
FBgn0028479	1	1
FBgn0028484	1	1
FBgn0028486	1	1
FBgn0028490	2	10
FBgn0028496	1	1
FBgn0028519	1	1
FBgn0028560	1	1
FBgn0028563	1	1
FBgn0028582	2	2
FBgn0028675	1	1
FBgn0028679	1	1
FBgn0028689	1	1
FBgn0028692	2	2
FBgn0028695	1	1
FBgn0028717	1	1
FBgn0028848	1	1
FBgn0028876	1	2

FBgn0028939	6	6
FBgn0028949	1	1
FBgn0028968	1	1
FBgn0028969	2	2
FBgn0029167	4	4
FBgn0029523	1	1
FBgn0029537	1	1
FBgn0029658	1	1
FBgn0029688	2	2
FBgn0029716	1	4
FBgn0029721	1	1
FBgn0029737	1	1
FBgn0029738	3	5
FBgn0029764	2	3
FBgn0029766	1	1
FBgn0029798	1	1
FBgn0029854	1	1
FBgn0029865	1	1
FBgn0029873	1	1
FBgn0029876	1	1
FBgn0029878	1	1
FBgn0029889	3	3
FBgn0029893	2	5
FBgn0029896	1	1
FBgn0029913	1	1
FBgn0029930	1	1
FBgn0029944	1	1
FBgn0029961	3	3
FBgn0029969	2	4
FBgn0029970	1	1
FBgn0029983	1	1
FBgn0029992	2	2
FBgn0030035	2	2
FBgn0030038	2	5
FBgn0030048	1	1
FBgn0030052	1	3
FBgn0030089	1	3
FBgn0030093	1	1
FBgn0030112	1	1
FBgn0030114	2	2
FBgn0030130	7	10
FBgn0030184	1	3
FBgn0030189	1	1
FBgn0030194	1	1
FBgn0030205	5	5
FBgn0030223	1	1
FBgn0030243	4	6
FBgn0030246	1	1
FBgn0030263	1	1
FBgn0030268	1	3

FBgn0030274	1	1
FBgn0030276	1	1
FBgn0030286	2	2
FBgn0030287	2	2
FBgn0030289	1	1
FBgn0030299	1	1
FBgn0030320	2	2
FBgn0030326	1	1
FBgn0030336	1	1
FBgn0030343	3	3
FBgn0030344	1	1
FBgn0030345	1	1
FBgn0030346	1	1
FBgn0030350	1	1
FBgn0030351	3	9
FBgn0030357	2	2
FBgn0030362	1	1
FBgn0030364	1	2
FBgn0030365	1	1
FBgn0030390	1	1
FBgn0030396	1	2
FBgn0030433	1	5
FBgn0030437	1	1
FBgn0030443	1	1
FBgn0030457	1	4
FBgn0030469	1	2
FBgn0030471	1	1
FBgn0030479	2	15
FBgn0030481	1	1
FBgn0030494	1	1
FBgn0030501	1	1
FBgn0030504	2	2
FBgn0030505	1	1
FBgn0030510	1	2
FBgn0030530	1	1
FBgn0030554	1	1
FBgn0030555	1	1
FBgn0030556	1	1
FBgn0030558	1	1
FBgn0030582	2	2
FBgn0030596	1	1
FBgn0030608	2	6
FBgn0030613	3	3
FBgn0030631	1	1
FBgn0030646	1	1
FBgn0030648	1	1
FBgn0030653	1	1
FBgn0030659	1	1
FBgn0030666	1	1
FBgn0030672	1	1

FBgn0030674	4	12
FBgn0030716	2	2
FBgn0030726	2	2
FBgn0030731	1	1
FBgn0030735	2	2
FBgn0030755	1	1
FBgn0030808	1	1
FBgn0030809	2	2
FBgn0030812	2	9
FBgn0030820	1	1
FBgn0030830	3	7
FBgn0030832	2	3
FBgn0030838	1	1
FBgn0030845	1	1
FBgn0030858	1	2
FBgn0030887	1	1
FBgn0030891	2	6
FBgn0030926	1	1
FBgn0030927	3	3
FBgn0030930	1	4
FBgn0030941	1	2
FBgn0030955	1	1
FBgn0030959	1	1
FBgn0030961	2	4
FBgn0030967	2	2
FBgn0030973	1	1
FBgn0030974	2	5
FBgn0030996	1	2
FBgn0031001	1	1
FBgn0031011	1	1
FBgn0031016	4	5
FBgn0031021	2	2
FBgn0031038	1	1
FBgn0031046	3	5
FBgn0031047	1	1
FBgn0031051	2	2
FBgn0031079	3	3
FBgn0031094	1	1
FBgn0031098	1	2
FBgn0031107	2	2
FBgn0031114	1	2
FBgn0031118	3	3
FBgn0031143	1	1
FBgn0031161	1	1
FBgn0031186	1	1
FBgn0031187	1	1
FBgn0031190	1	1
FBgn0031227	1	4
FBgn0031228	1	1
FBgn0031240	1	1

FBgn0031250	1	1
FBgn0031266	2	2
FBgn0031291	4	17
FBgn0031309	1	2
FBgn0031320	2	2
FBgn0031327	2	2
FBgn0031358	1	1
FBgn0031360	1	1
FBgn0031362	2	2
FBgn0031374	5	8
FBgn0031389	1	1
FBgn0031408	1	1
FBgn0031417	1	1
FBgn0031432	1	1
FBgn0031453	1	1
FBgn0031457	1	1
FBgn0031474	1	1
FBgn0031490	1	1
FBgn0031497	1	3
FBgn0031500	1	1
FBgn0031505	1	1
FBgn0031515	1	2
FBgn0031518	1	1
FBgn0031536	1	1
FBgn0031538	1	1
FBgn0031548	1	2
FBgn0031571	3	3
FBgn0031589	3	3
FBgn0031599	1	1
FBgn0031600	1	1
FBgn0031603	1	1
FBgn0031629	1	1
FBgn0031653	1	1
FBgn0031674	1	1
FBgn0031681	2	2
FBgn0031711	1	1
FBgn0031741	1	1
FBgn0031747	1	1
FBgn0031762	2	2
FBgn0031768	2	2
FBgn0031771	1	1
FBgn0031773	1	1
FBgn0031799	2	2
FBgn0031812	1	1
FBgn0031871	1	1
FBgn0031872	1	1
FBgn0031879	7	7
FBgn0031883	1	6
FBgn0031885	1	1
FBgn0031894	1	1

FBgn0031896	1	1
FBgn0031897	1	1
FBgn0031899	5	8
FBgn0031905	1	1
FBgn0031912	1	1
FBgn0031939	1	1
FBgn0031950	1	2
FBgn0031972	1	1
FBgn0031985	1	2
FBgn0031993	2	2
FBgn0031999	1	1
FBgn0032001	2	2
FBgn0032006	2	2
FBgn0032013	1	1
FBgn0032018	2	2
FBgn0032061	3	4
FBgn0032072	1	1
FBgn0032089	1	1
FBgn0032114	1	1
FBgn0032120	1	1
FBgn0032129	2	2
FBgn0032132	1	1
FBgn0032136	3	3
FBgn0032157	1	1
FBgn0032172	2	4
FBgn0032178	1	2
FBgn0032180	2	4
FBgn0032190	1	1
FBgn0032194	1	1
FBgn0032196	1	1
FBgn0032204	2	2
FBgn0032208	2	2
FBgn0032210	2	2
FBgn0032215	1	1
FBgn0032246	2	2
FBgn0032249	1	1
FBgn0032308	1	1
FBgn0032330	1	1
FBgn0032340	3	4
FBgn0032342	1	1
FBgn0032348	1	3
FBgn0032363	3	4
FBgn0032376	1	1
FBgn0032395	2	2
FBgn0032401	1	1
FBgn0032409	1	1
FBgn0032415	1	1
FBgn0032416	1	1
FBgn0032430	1	1
FBgn0032444	1	1

FBgn0032455	1	1
FBgn0032467	1	1
FBgn0032475	2	2
FBgn0032477	1	1
FBgn0032481	1	1
FBgn0032482	1	1
FBgn0032484	1	1
FBgn0032485	1	1
FBgn0032497	1	1
FBgn0032511	1	1
FBgn0032514	1	1
FBgn0032517	1	1
FBgn0032518	1	1
FBgn0032524	1	1
FBgn0032586	1	1
FBgn0032587	2	3
FBgn0032597	2	2
FBgn0032638	1	1
FBgn0032642	1	1
FBgn0032655	1	1
FBgn0032681	1	1
FBgn0032683	1	1
FBgn0032686	2	2
FBgn0032689	1	1
FBgn0032713	1	1
FBgn0032717	1	1
FBgn0032771	1	1
FBgn0032814	1	1
FBgn0032821	2	2
FBgn0032832	1	1
FBgn0032838	1	1
FBgn0032847	1	1
FBgn0032853	1	1
FBgn0032863	1	1
FBgn0032865	1	1
FBgn0032935	1	1
FBgn0032938	2	2
FBgn0032969	1	1
FBgn0032979	1	1
FBgn0032986	1	1
FBgn0033028	1	1
FBgn0033032	1	1
FBgn0033035	1	1
FBgn0033050	1	1
FBgn0033055	1	1
FBgn0033092	1	1
FBgn0033102	2	2
FBgn0033108	2	3
FBgn0033129	1	1
FBgn0033134	1	1

FBgn0033160	1	1
FBgn0033179	1	1
FBgn0033187	1	2
FBgn0033192	2	2
FBgn0033205	1	1
FBgn0033240	1	1
FBgn0033260	1	2
FBgn0033265	1	1
FBgn0033289	2	2
FBgn0033313	2	2
FBgn0033320	1	1
FBgn0033321	1	1
FBgn0033383	1	1
FBgn0033402	1	2
FBgn0033413	1	1
FBgn0033424	1	1
FBgn0033454	2	5
FBgn0033468	1	1
FBgn0033475	1	6
FBgn0033476	1	1
FBgn0033486	1	2
FBgn0033491	1	1
FBgn0033504	2	2
FBgn0033534	2	5
FBgn0033556	1	1
FBgn0033583	2	13
FBgn0033609	2	2
FBgn0033616	1	1
FBgn0033630	1	2
FBgn0033631	1	1
FBgn0033636	8	13
FBgn0033639	1	1
FBgn0033653	2	2
FBgn0033657	1	1
FBgn0033663	1	2
FBgn0033688	1	1
FBgn0033698	1	1
FBgn0033707	1	1
FBgn0033714	1	1
FBgn0033717	1	1
FBgn0033728	1	2
FBgn0033735	1	2
FBgn0033738	1	1
FBgn0033750	1	2
FBgn0033751	1	1
FBgn0033755	1	1
FBgn0033757	1	1
FBgn0033785	1	1
FBgn0033789	1	1
FBgn0033802	1	1

FBgn0033814	1	1
FBgn0033815	1	1
FBgn0033835	1	3
FBgn0033837	1	1
FBgn0033842	1	1
FBgn0033846	1	1
FBgn0033885	1	1
FBgn0033905	1	1
FBgn0033926	1	6
FBgn0033934	1	1
FBgn0033935	1	1
FBgn0033958	1	1
FBgn0033964	1	1
FBgn0033995	1	7
FBgn0034035	2	2
FBgn0034057	1	1
FBgn0034058	1	1
FBgn0034079	3	7
FBgn0034083	2	2
FBgn0034089	1	1
FBgn0034093	1	1
FBgn0034094	1	1
FBgn0034103	1	2
FBgn0034110	1	3
FBgn0034112	1	1
FBgn0034114	2	3
FBgn0034117	1	2
FBgn0034118	1	2
FBgn0034134	1	1
FBgn0034138	1	1
FBgn0034141	1	1
FBgn0034158	1	1
FBgn0034160	1	1
FBgn0034165	1	1
FBgn0034184	1	1
FBgn0034221	1	1
FBgn0034240	1	1
FBgn0034243	1	1
FBgn0034262	1	1
FBgn0034274	1	1
FBgn0034282	1	1
FBgn0034308	1	1
FBgn0034314	1	1
FBgn0034345	1	1
FBgn0034367	1	1
FBgn0034372	1	2
FBgn0034378	1	1
FBgn0034380	2	2
FBgn0034381	1	1
FBgn0034394	2	8

FBgn0034400	1	1
FBgn0034410	1	1
FBgn0034417	1	1
FBgn0034421	1	1
FBgn0034422	1	1
FBgn0034432	2	2
FBgn0034441	1	2
FBgn0034474	1	2
FBgn0034477	1	1
FBgn0034520	1	1
FBgn0034528	1	1
FBgn0034529	1	1
FBgn0034590	1	2
FBgn0034598	4	6
FBgn0034612	2	4
FBgn0034618	1	1
FBgn0034638	2	4
FBgn0034644	1	2
FBgn0034669	1	1
FBgn0034685	1	1
FBgn0034691	1	1
FBgn0034695	1	1
FBgn0034708	1	1
FBgn0034709	1	1
FBgn0034750	2	4
FBgn0034753	1	1
FBgn0034756	1	1
FBgn0034760	1	3
FBgn0034775	1	1
FBgn0034786	1	1
FBgn0034792	4	4
FBgn0034797	1	1
FBgn0034802	2	7
FBgn0034804	1	1
FBgn0034821	2	3
FBgn0034851	2	2
FBgn0034853	2	2
FBgn0034860	1	1
FBgn0034873	1	1
FBgn0034877	1	1
FBgn0034878	1	1
FBgn0034921	2	2
FBgn0034926	2	3
FBgn0034967	1	6
FBgn0034971	1	1
FBgn0034975	1	2
FBgn0034987	2	4
FBgn0034989	1	1
FBgn0034990	1	1
FBgn0034997	2	2

FBgn0035016	1	1
FBgn0035026	1	1
FBgn0035049	1	1
FBgn0035082	1	1
FBgn0035107	1	1
FBgn0035111	1	1
FBgn0035113	1	1
FBgn0035142	2	4
FBgn0035145	2	2
FBgn0035153	2	2
FBgn0035175	1	1
FBgn0035202	1	1
FBgn0035204	1	1
FBgn0035205	2	4
FBgn0035211	1	1
FBgn0035233	1	1
FBgn0035237	2	2
FBgn0035244	1	1
FBgn0035253	3	3
FBgn0035265	3	4
FBgn0035268	4	4
FBgn0035296	2	2
FBgn0035297	1	2
FBgn0035324	1	1
FBgn0035338	3	4
FBgn0035348	1	6
FBgn0035357	1	2
FBgn0035371	1	1
FBgn0035372	1	1
FBgn0035376	2	6
FBgn0035382	1	1
FBgn0035388	1	1
FBgn0035400	1	1
FBgn0035425	1	1
FBgn0035429	3	3
FBgn0035438	2	2
FBgn0035448	2	2
FBgn0035478	3	4
FBgn0035490	1	1
FBgn0035504	2	3
FBgn0035518	4	4
FBgn0035523	1	1
FBgn0035532	1	1
FBgn0035540	1	1
FBgn0035568	2	2
FBgn0035574	4	5
FBgn0035589	1	1
FBgn0035601	1	1
FBgn0035617	2	2
FBgn0035637	1	1

FBgn0035673	1	1
FBgn0035693	1	4
FBgn0035704	1	16
FBgn0035713	2	2
FBgn0035766	1	1
FBgn0035785	2	2
FBgn0035787	1	1
FBgn0035812	1	1
FBgn0035823	1	1
FBgn0035838	1	1
FBgn0035851	1	2
FBgn0035866	1	1
FBgn0035879	1	1
FBgn0035887	1	1
FBgn0035891	1	1
FBgn0035909	1	1
FBgn0035910	2	2
FBgn0035938	3	3
FBgn0035946	1	1
FBgn0035947	1	1
FBgn0035951	1	4
FBgn0035960	1	1
FBgn0035976	2	2
FBgn0035981	1	1
FBgn0035985	1	1
FBgn0035989	1	1
FBgn0036004	1	1
FBgn0036043	2	2
FBgn0036044	1	1
FBgn0036057	1	1
FBgn0036059	1	1
FBgn0036060	1	1
FBgn0036066	2	2
FBgn0036117	1	1
FBgn0036127	2	2
FBgn0036143	1	1
FBgn0036148	3	3
FBgn0036149	2	2
FBgn0036152	1	1
FBgn0036172	1	1
FBgn0036180	1	1
FBgn0036205	1	1
FBgn0036220	1	1
FBgn0036226	1	5
FBgn0036248	1	2
FBgn0036258	1	1
FBgn0036261	1	1
FBgn0036268	1	5
FBgn0036271	1	1
FBgn0036278	2	2

FBgn0036279	2	2
FBgn0036288	1	1
FBgn0036302	1	1
FBgn0036316	1	1
FBgn0036321	2	2
FBgn0036326	1	1
FBgn0036329	1	2
FBgn0036333	1	1
FBgn0036341	1	2
FBgn0036360	2	2
FBgn0036363	1	1
FBgn0036365	1	1
FBgn0036375	1	1
FBgn0036376	1	1
FBgn0036377	2	2
FBgn0036389	1	1
FBgn0036428	1	1
FBgn0036449	1	1
FBgn0036451	2	2
FBgn0036471	1	1
FBgn0036472	3	3
FBgn0036484	2	2
FBgn0036488	1	2
FBgn0036489	2	2
FBgn0036505	1	1
FBgn0036511	7	14
FBgn0036516	1	1
FBgn0036518	3	6
FBgn0036548	3	3
FBgn0036549	1	1
FBgn0036558	1	1
FBgn0036566	3	5
FBgn0036571	1	1
FBgn0036623	1	1
FBgn0036627	2	3
FBgn0036648	1	1
FBgn0036655	1	1
FBgn0036663	4	5
FBgn0036678	1	1
FBgn0036680	3	4
FBgn0036682	1	1
FBgn0036684	1	1
FBgn0036686	1	1
FBgn0036690	1	1
FBgn0036702	2	2
FBgn0036710	1	1
FBgn0036718	1	2
FBgn0036732	1	1
FBgn0036737	1	1
FBgn0036746	1	1

FBgn0036759	2	2
FBgn0036761	1	1
FBgn0036768	1	1
FBgn0036789	1	1
FBgn0036805	1	1
FBgn0036806	1	1
FBgn0036813	1	1
FBgn0036814	2	2
FBgn0036828	2	3
FBgn0036848	1	1
FBgn0036855	1	1
FBgn0036856	1	2
FBgn0036896	1	2
FBgn0036910	1	1
FBgn0036913	2	2
FBgn0036930	2	2
FBgn0036958	2	2
FBgn0036967	1	1
FBgn0036974	1	1
FBgn0037001	1	1
FBgn0037003	1	1
FBgn0037018	3	3
FBgn0037021	2	2
FBgn0037066	1	1
FBgn0037074	1	1
FBgn0037084	1	1
FBgn0037093	1	1
FBgn0037098	1	1
FBgn0037109	8	8
FBgn0037116	1	2
FBgn0037120	2	2
FBgn0037137	1	1
FBgn0037146	1	1
FBgn0037151	1	1
FBgn0037182	1	1
FBgn0037186	1	1
FBgn0037199	1	2
FBgn0037213	1	1
FBgn0037215	1	1
FBgn0037236	2	2
FBgn0037239	1	1
FBgn0037240	1	1
FBgn0037256	4	4
FBgn0037277	2	18
FBgn0037285	1	1
FBgn0037290	1	1
FBgn0037303	1	1
FBgn0037307	1	1
FBgn0037308	1	2
FBgn0037344	3	3

FBgn0037345	1	1
FBgn0037347	1	1
FBgn0037363	1	1
FBgn0037415	1	2
FBgn0037420	1	1
FBgn0037443	1	1
FBgn0037444	1	1
FBgn0037447	1	1
FBgn0037448	2	2
FBgn0037461	2	2
FBgn0037468	1	1
FBgn0037493	1	1
FBgn0037515	1	1
FBgn0037531	2	2
FBgn0037533	1	1
FBgn0037541	1	1
FBgn0037548	2	9
FBgn0037549	1	1
FBgn0037607	2	2
FBgn0037621	1	1
FBgn0037623	2	2
FBgn0037650	1	4
FBgn0037653	1	1
FBgn0037655	1	1
FBgn0037657	1	1
FBgn0037660	1	1
FBgn0037678	2	2
FBgn0037687	1	1
FBgn0037701	3	3
FBgn0037716	1	1
FBgn0037720	2	2
FBgn0037721	1	1
FBgn0037731	1	1
FBgn0037733	2	2
FBgn0037734	1	1
FBgn0037744	2	2
FBgn0037757	1	2
FBgn0037758	1	4
FBgn0037759	1	1
FBgn0037777	1	1
FBgn0037800	1	1
FBgn0037804	1	1
FBgn0037808	5	5
FBgn0037872	1	1
FBgn0037874	3	3
FBgn0037897	2	2
FBgn0037901	1	1
FBgn0037924	1	1
FBgn0037934	1	1
FBgn0037944	1	1

FBgn0037954	2	2
FBgn0037963	1	1
FBgn0037967	1	2
FBgn0037975	1	1
FBgn0037978	2	2
FBgn0037981	1	1
FBgn0037992	1	1
FBgn0038001	1	1
FBgn0038005	1	1
FBgn0038037	1	4
FBgn0038041	1	1
FBgn0038053	1	1
FBgn0038056	2	2
FBgn0038058	1	1
FBgn0038074	1	1
FBgn0038088	1	1
FBgn0038098	1	1
FBgn0038130	1	1
FBgn0038146	1	1
FBgn0038149	1	2
FBgn0038157	1	1
FBgn0038171	1	1
FBgn0038180	1	1
FBgn0038186	1	1
FBgn0038201	1	1
FBgn0038220	1	1
FBgn0038226	2	3
FBgn0038237	1	1
FBgn0038244	1	1
FBgn0038251	1	1
FBgn0038259	2	2
FBgn0038263	1	1
FBgn0038279	2	3
FBgn0038286	1	1
FBgn0038289	1	1
FBgn0038293	1	1
FBgn0038301	1	2
FBgn0038316	1	1
FBgn0038320	2	2
FBgn0038337	1	1
FBgn0038341	1	1
FBgn0038344	1	1
FBgn0038363	1	1
FBgn0038364	1	1
FBgn0038376	1	1
FBgn0038400	1	1
FBgn0038416	1	1
FBgn0038473	1	1
FBgn0038482	1	2
FBgn0038488	1	1

FBgn0038504	1	1
FBgn0038505	1	1
FBgn0038524	1	1
FBgn0038550	1	2
FBgn0038556	6	7
FBgn0038574	2	2
FBgn0038578	1	1
FBgn0038583	1	1
FBgn0038587	1	1
FBgn0038639	1	1
FBgn0038651	1	1
FBgn0038652	1	1
FBgn0038655	1	1
FBgn0038674	1	1
FBgn0038679	2	11
FBgn0038704	2	2
FBgn0038708	1	1
FBgn0038715	2	2
FBgn0038745	1	1
FBgn0038747	1	1
FBgn0038752	2	2
FBgn0038760	1	1
FBgn0038803	1	1
FBgn0038826	1	1
FBgn0038853	2	3
FBgn0038854	2	2
FBgn0038859	1	1
FBgn0038862	1	1
FBgn0038873	1	1
FBgn0038876	1	1
FBgn0038889	1	2
FBgn0038901	1	3
FBgn0038912	1	1
FBgn0038927	2	2
FBgn0038951	1	1
FBgn0039000	1	1
FBgn0039018	2	2
FBgn0039023	1	1
FBgn0039026	2	2
FBgn0039050	1	1
FBgn0039069	1	1
FBgn0039084	1	1
FBgn0039085	1	1
FBgn0039101	1	1
FBgn0039110	1	1
FBgn0039117	1	1
FBgn0039122	2	2
FBgn0039126	1	1
FBgn0039130	1	1
FBgn0039132	1	2

FBgn0039139	1	1
FBgn0039144	1	1
FBgn0039164	1	1
FBgn0039169	1	1
FBgn0039179	1	2
FBgn0039182	2	3
FBgn0039187	2	2
FBgn0039189	2	2
FBgn0039195	1	1
FBgn0039203	1	6
FBgn0039213	2	4
FBgn0039223	1	1
FBgn0039224	1	1
FBgn0039234	3	3
FBgn0039240	3	3
FBgn0039241	1	1
FBgn0039261	1	2
FBgn0039265	1	1
FBgn0039297	1	1
FBgn0039303	1	1
FBgn0039325	1	1
FBgn0039335	1	1
FBgn0039338	2	2
FBgn0039347	2	2
FBgn0039349	1	1
FBgn0039381	1	1
FBgn0039402	1	2
FBgn0039427	1	3
FBgn0039433	4	9
FBgn0039447	1	1
FBgn0039488	1	1
FBgn0039492	1	1
FBgn0039494	1	1
FBgn0039523	1	1
FBgn0039528	2	3
FBgn0039543	1	1
FBgn0039559	1	1
FBgn0039560	1	1
FBgn0039590	4	5
FBgn0039623	1	1
FBgn0039626	1	2
FBgn0039637	1	1
FBgn0039638	1	1
FBgn0039672	2	2
FBgn0039674	1	1
FBgn0039680	2	2
FBgn0039691	1	1
FBgn0039714	1	1
FBgn0039715	1	1
FBgn0039732	1	1

FBgn0039733	1	1
FBgn0039741	1	1
FBgn0039776	1	1
FBgn0039844	2	2
FBgn0039846	2	2
FBgn0039863	1	3
FBgn0039877	1	1
FBgn0039889	1	1
FBgn0039890	2	3
FBgn0039904	3	3
FBgn0039907	5	13
FBgn0039919	1	1
FBgn0039936	1	1
FBgn0040615	1	1
FBgn0040637	4	24
FBgn0040650	1	1
FBgn0040793	1	1
FBgn0040813	1	1
FBgn0040878	1	1
FBgn0040955	2	2
FBgn0040968	2	5
FBgn0040992	1	1
FBgn0040995	2	4
FBgn0000011	3	6
FBgn0000017	5	26
FBgn0000037	2	3
FBgn0000046	5	8
FBgn0000047	3	6
FBgn0000055	1	1
FBgn0000061	1	1
FBgn0000079	1	1
FBgn0000092	1	1
FBgn0000095	1	1
FBgn0000108	1	1
FBgn0000114	2	2
FBgn0000119	4	4
FBgn0000140	2	6
FBgn0000153	1	1
FBgn0000158	1	1
FBgn0000171	1	1
FBgn0000180	1	1
FBgn0000221	1	1
FBgn0000241	1	1
FBgn0000287	1	1
FBgn0000289	1	1
FBgn0000303	1	1
FBgn0000313	1	1
FBgn0000326	2	2
FBgn0000355	1	1
FBgn0000394	1	3

FBgn0000395	1	1
FBgn0000410	1	1
FBgn0000414	4	4
FBgn0000427	2	2
FBgn0000447	1	1
FBgn0000451	1	1
FBgn0000454	1	1
FBgn0000462	1	1
FBgn0000464	1	1
FBgn0000479	3	11
FBgn0000527	1	1
FBgn0000533	1	1
FBgn0000535	1	1
FBgn0000541	1	3
FBgn0000547	1	1
FBgn0000560	1	1
FBgn0000581	1	1
FBgn0000625	1	1
FBgn0000630	2	2
FBgn0000715	1	2
FBgn0000928	1	1
FBgn0001075	3	3
FBgn0001083	1	1
FBgn0001086	1	1
FBgn0001090	1	1
FBgn0001128	2	2
FBgn0001167	1	1
FBgn0001187	1	1
FBgn0001203	1	1
FBgn0001204	1	1
FBgn0001206	1	1
FBgn0001216	3	13
FBgn0001218	6	31
FBgn0001248	1	1
FBgn0001253	4	9
FBgn0001269	1	4
FBgn0001296	1	1
FBgn0001320	1	1
FBgn0001321	1	1
FBgn0001323	3	17
FBgn0001324	2	2
FBgn0001325	2	2
FBgn0001341	1	1
FBgn0001402	4	6
FBgn0001624	1	1
FBgn0001972	1	1
FBgn0001978	2	2
FBgn0001990	1	3
FBgn0002021	1	1
FBgn0002121	3	3

FBgn0002440	2	11
FBgn0002522	1	1
FBgn0002531	1	1
FBgn0002576	1	1
FBgn0002638	1	1
FBgn0002673	3	16
FBgn0002707	2	2
FBgn0002715	1	1
FBgn0002719	2	2
FBgn0002774	1	1
FBgn0002865	1	1
FBgn0002872	1	1
FBgn0002873	1	1
FBgn0002878	1	1
FBgn0002906	1	1
FBgn0002920	2	3
FBgn0002931	1	1
FBgn0002939	1	1
FBgn0002989	1	1
FBgn0002997	1	1
FBgn0003008	1	1
FBgn0003011	1	1
FBgn0003013	1	1
FBgn0003023	1	1
FBgn0003028	2	2
FBgn0003037	1	1
FBgn0003042	1	1
FBgn0003053	1	1
FBgn0003062	3	12
FBgn0003068	3	3
FBgn0003089	1	1
FBgn0003090	2	2
FBgn0003093	1	1
FBgn0003117	1	1
FBgn0003118	1	1
FBgn0003137	3	5
FBgn0003149	1	1
FBgn0003159	1	1
FBgn0003210	1	1
FBgn0003217	3	55
FBgn0003249	1	2
FBgn0003255	1	1
FBgn0003256	1	1
FBgn0003276	2	3
FBgn0003278	2	2
FBgn0003285	1	1
FBgn0003308	2	2
FBgn0003321	1	1
FBgn0003326	2	2
FBgn0003349	2	3

FBgn0003358	2	2
FBgn0003380	1	2
FBgn0003383	1	1
FBgn0003386	1	2
FBgn0003415	1	1
FBgn0003425	1	1
FBgn0003429	1	1
FBgn0003432	5	6
FBgn0003459	2	2
FBgn0003470	1	1
FBgn0003482	1	1
FBgn0003483	3	7
FBgn0003510	1	1
FBgn0003511	1	1
FBgn0003654	1	5
FBgn0003715	2	2
FBgn0003719	1	3
FBgn0003732	1	1
FBgn0003744	2	2
FBgn0003749	3	3
FBgn0003861	2	3
FBgn0003866	3	4
FBgn0003870	1	3
FBgn0003889	1	3
FBgn0003892	1	1
FBgn0003969	2	2
FBgn0003975	1	1
FBgn0003977	1	1
FBgn0004009	1	1
FBgn0004028	1	1
FBgn0004045	2	2
FBgn0004049	1	1
FBgn0004101	1	1
FBgn0004102	3	4
FBgn0004110	1	13
FBgn0004174	1	1
FBgn0004175	1	8
FBgn0004197	3	3
FBgn0004366	1	2
FBgn0004370	1	1
FBgn0004373	1	1
FBgn0004377	2	2
FBgn0004387	2	2
FBgn0004391	2	2
FBgn0004428	1	1
FBgn0004446	3	3
FBgn0004449	3	4
FBgn0004493	1	1
FBgn0004512	1	1
FBgn0004513	1	1

FBgn0004571	1	1
FBgn0004572	1	1
FBgn0004575	2	2
FBgn0004606	2	2
FBgn0004623	1	1
FBgn0004647	7	7
FBgn0004650	1	1
FBgn0004784	2	2
FBgn0004795	1	1
FBgn0004832	1	1
FBgn0004852	3	3
FBgn0004861	1	1
FBgn0004870	2	2
FBgn0004873	4	4
FBgn0004875	1	1
FBgn0005322	2	3
FBgn0005390	1	2
FBgn0005536	3	5
FBgn0005558	1	1
FBgn0005592	2	2
FBgn0005596	1	1
FBgn0005614	1	1
FBgn0005619	3	3
FBgn0005626	1	1
FBgn0005629	1	1
FBgn0005630	3	8
FBgn0005660	1	1
FBgn0005666	1	2
FBgn0005677	3	3
FBgn0005779	1	1
FBgn0008646	2	6
FBgn0010019	2	2
FBgn0010044	1	1
FBgn0010052	1	1
FBgn0010070	4	4
FBgn0010100	1	1
FBgn0010114	2	2
FBgn0010197	2	2
FBgn0010241	3	3
FBgn0010247	1	1
FBgn0010256	3	4
FBgn0010258	3	6
FBgn0010295	1	1
FBgn0010328	2	2
FBgn0010347	1	1
FBgn0010382	2	2
FBgn0010395	2	4
FBgn0010398	1	1
FBgn0010399	1	1
FBgn0010482	1	1

FBgn0010488	2	5
FBgn0010575	3	5
FBgn0010590	1	1
FBgn0010591	2	2
FBgn0010611	2	2
FBgn0010620	1	1
FBgn0010633	2	2
FBgn0010768	1	1
FBgn0010786	2	2
FBgn0010803	1	8
FBgn0010825	2	4
FBgn0010830	2	2
FBgn0010905	1	3
FBgn0010909	2	2
FBgn0010926	1	1
FBgn0010940	4	7
FBgn0011232	1	1
FBgn0011259	1	1
FBgn0011276	1	1
FBgn0011286	3	7
FBgn0011295	1	1
FBgn0011335	2	2
FBgn0011425	1	1
FBgn0011481	1	1
FBgn0011576	1	1
FBgn0011589	1	1
FBgn0011596	1	1
FBgn0011604	1	1
FBgn0011659	1	1
FBgn0011660	1	1
FBgn0011676	1	1
FBgn0011743	1	1
FBgn0011766	1	1
FBgn0011818	1	1
FBgn0012344	1	1
FBgn0013275	4	11
FBgn0013276	4	11
FBgn0013278	5	13
FBgn0013308	1	1
FBgn0013334	1	1
FBgn0013467	2	3
FBgn0013531	1	2
FBgn0013563	1	1
FBgn0013591	1	1
FBgn0013684	1	1
FBgn0013725	1	1
FBgn0013732	1	1
FBgn0013756	2	2
FBgn0013763	2	2
FBgn0013764	1	1

FBgn0013810	4	5
FBgn0013811	6	7
FBgn0013813	1	1
FBgn0013949	1	1
FBgn0014179	1	1
FBgn0014343	2	3
FBgn0014417	1	1
FBgn0014455	1	1
FBgn0014859	1	1
FBgn0014870	2	4
FBgn0015001	1	1
FBgn0015008	1	1
FBgn0015034	1	1
FBgn0015035	1	1
FBgn0015037	1	1
FBgn0015038	1	1
FBgn0015040	1	1
FBgn0015075	1	1
FBgn0015245	2	2
FBgn0015269	1	1
FBgn0015270	1	1
FBgn0015316	1	1
FBgn0015336	2	2
FBgn0015350	1	1
FBgn0015390	5	6
FBgn0015391	1	1
FBgn0015393	1	1
FBgn0015396	1	1
FBgn0015399	1	1
FBgn0015477	2	16
FBgn0015541	1	2
FBgn0015553	1	1
FBgn0015561	1	1
FBgn0015569	3	4
FBgn0015570	1	1
FBgn0015577	1	2
FBgn0015585	1	1
FBgn0015600	2	3
FBgn0015609	3	5
FBgn0015663	2	3
FBgn0015778	1	1
FBgn0015803	1	1
FBgn0015905	2	2
FBgn0015930	1	1
FBgn0016047	4	7
FBgn0016075	3	3
FBgn0016754	1	1
FBgn0016797	2	4
FBgn0016920	3	3
FBgn0017590	1	1

FBgn0019652	2	3
FBgn0019664	1	1
FBgn0019809	1	1
FBgn0019839	1	1
FBgn0019928	1	1
FBgn0019938	1	1
FBgn0019960	1	4
FBgn0019982	1	1
FBgn0019985	1	1
FBgn0020238	1	1
FBgn0020250	1	2
FBgn0020279	2	3
FBgn0020371	2	6
FBgn0020377	1	1
FBgn0020379	1	1
FBgn0020391	1	1
FBgn0020392	1	1
FBgn0020429	1	1
FBgn0020517	1	1
FBgn0020756	1	1
FBgn0020912	1	1
FBgn0021760	3	3
FBgn0021761	1	1
FBgn0021768	1	1
FBgn0021776	1	1
FBgn0021796	2	2
FBgn0021847	2	2
FBgn0021873	3	4
FBgn0021875	1	1
FBgn0022201	1	1
FBgn0022700	1	1
FBgn0022708	1	1
FBgn0022724	1	1
FBgn0022786	1	1
FBgn0022985	2	3
FBgn0023097	3	3
FBgn0023174	1	1
FBgn0023179	2	2
FBgn0023184	1	2
FBgn0023441	2	3
FBgn0023458	5	7
FBgn0023489	1	1
FBgn0023507	2	2
FBgn0023518	3	3
FBgn0023527	1	1
FBgn0023536	1	1
FBgn0023542	2	7
FBgn0023548	1	1
FBgn0024182	1	1
FBgn0024183	1	1

FBgn0024187	1	1
FBgn0024242	2	2
FBgn0024248	1	1
FBgn0024273	1	2
FBgn0024277	5	5
FBgn0024314	2	2
FBgn0024321	2	2
FBgn0024329	3	3
FBgn0024330	1	1
FBgn0024365	1	1
FBgn0024555	1	1
FBgn0024836	1	1
FBgn0024897	1	1
FBgn0024944	1	1
FBgn0024963	1	1
FBgn0024992	1	5
FBgn0024993	2	2
FBgn0025109	1	1
FBgn0025111	2	2
FBgn0025140	1	1
FBgn0025376	1	1
FBgn0025382	1	2
FBgn0025383	1	6
FBgn0025388	2	3
FBgn0025390	2	2
FBgn0025391	1	1
FBgn0025519	1	1
FBgn0025525	1	1
FBgn0025573	1	1
FBgn0025592	1	1
FBgn0025618	2	2
FBgn0025623	2	2
FBgn0025625	3	3
FBgn0025641	1	1
FBgn0025643	2	3
FBgn0025676	1	1
FBgn0025678	1	1
FBgn0025686	1	2
FBgn0025692	2	2
FBgn0025712	1	1
FBgn0025720	2	3
FBgn0025726	3	4
FBgn0025801	1	1
FBgn0025866	2	2
FBgn0025874	1	1
FBgn0026060	1	1
FBgn0026064	1	1
FBgn0026083	4	8
FBgn0026087	1	1
FBgn0026145	2	2

FBgn0026160	3	5
FBgn0026188	2	3
FBgn0026193	2	2
FBgn0026196	2	3
FBgn0026206	2	3
FBgn0026207	1	1
FBgn0026239	1	1
FBgn0026255	1	1
FBgn0026257	1	1
FBgn0026309	1	1
FBgn0026317	1	2
FBgn0026371	1	1
FBgn0026375	4	6
FBgn0026385	1	1
FBgn0026388	1	1
FBgn0026392	1	1
FBgn0026393	1	3
FBgn0026399	1	1
FBgn0026411	1	1
FBgn0026427	2	2
FBgn0026432	1	1
FBgn0026438	1	1
FBgn0026562	1	2
FBgn0026573	1	1
FBgn0026575	1	1
FBgn0026576	1	1
FBgn0026577	2	2
FBgn0026582	1	1
FBgn0026611	1	1
FBgn0026718	1	1
FBgn0026722	2	12
FBgn0026729	1	1
FBgn0026875	2	3
FBgn0027079	2	2
FBgn0027080	1	1
FBgn0027082	1	1
FBgn0027084	1	2
FBgn0027086	1	1
FBgn0027088	1	1
FBgn0027091	1	1
FBgn0027093	2	2
FBgn0027107	2	2
FBgn0027342	2	2
FBgn0027348	2	2
FBgn0027490	1	1
FBgn0027498	1	1
FBgn0027499	1	1
FBgn0027500	1	1
FBgn0027503	2	2
FBgn0027514	1	1

FBgn0027521	1	1
FBgn0027522	1	1
FBgn0027537	1	1
FBgn0027563	1	1
FBgn0027571	4	6
FBgn0027575	2	2
FBgn0027578	1	1
FBgn0027588	1	1
FBgn0027600	1	1
FBgn0027602	2	2
FBgn0027654	1	1
FBgn0027658	1	1
FBgn0027783	1	1
FBgn0027794	1	1
FBgn0027903	1	1
FBgn0027951	1	1
FBgn0028369	1	1
FBgn0028370	1	1
FBgn0028371	3	3
FBgn0028383	1	1
FBgn0028386	2	3
FBgn0028387	1	1
FBgn0028408	1	2
FBgn0028412	1	1
FBgn0028420	2	3
FBgn0028422	1	1
FBgn0028427	1	1
FBgn0028428	1	4
FBgn0028431	3	6
FBgn0028435	2	6
FBgn0028474	4	4
FBgn0028481	1	2
FBgn0028482	1	1
FBgn0028485	1	1
FBgn0028494	1	3
FBgn0028509	1	1
FBgn0028532	1	1
FBgn0028545	1	2
FBgn0028554	2	2
FBgn0028562	1	1
FBgn0028577	1	1
FBgn0028622	1	1
FBgn0028642	2	2
FBgn0028644	1	2
FBgn0028646	2	2
FBgn0028704	1	1
FBgn0028707	1	1
FBgn0028737	2	2
FBgn0028833	2	4
FBgn0028852	1	1

FBgn0028859	1	1
FBgn0028862	1	1
FBgn0028863	4	5
FBgn0028878	2	2
FBgn0028881	1	1
FBgn0028883	1	1
FBgn0028888	1	1
FBgn0028891	1	1
FBgn0028893	1	1
FBgn0028901	1	1
FBgn0028903	1	1
FBgn0028906	1	1
FBgn0028918	2	2
FBgn0028924	1	1
FBgn0028925	1	1
FBgn0028938	1	1
FBgn0028953	1	1
FBgn0028962	1	1
FBgn0028963	1	2
FBgn0028970	2	4
FBgn0028979	2	2
FBgn0028980	1	1
FBgn0028987	1	1
FBgn0028999	1	1
FBgn0029006	2	2
FBgn0029082	3	4
FBgn0029084	3	3
FBgn0029090	2	2
FBgn0029095	1	3
FBgn0029105	1	1
FBgn0029118	1	1
FBgn0029131	2	2
FBgn0029137	1	1
FBgn0029147	1	1
FBgn0029157	1	1
FBgn0029176	1	1
FBgn0029503	2	3
FBgn0029512	1	1
FBgn0029608	1	1
FBgn0029642	1	1
FBgn0029643	1	1
FBgn0029649	1	1
FBgn0029660	1	1
FBgn0029662	1	1
FBgn0029686	1	1
FBgn0029710	1	1
FBgn0029717	1	1
FBgn0029719	1	1
FBgn0029723	1	2
FBgn0029725	2	7

FBgn0029750	2	2
FBgn0029753	1	1
FBgn0029762	1	1
FBgn0029769	1	3
FBgn0029772	1	1
FBgn0029782	1	1
FBgn0029791	2	2
FBgn0029795	1	1
FBgn0029808	1	7
FBgn0029812	1	1
FBgn0029814	1	1
FBgn0029823	1	1
FBgn0029826	1	1
FBgn0029837	1	2
FBgn0029846	1	1
FBgn0029850	1	1
FBgn0029851	1	1
FBgn0029864	2	2
FBgn0029871	1	1
FBgn0029872	1	1
FBgn0029874	2	3
FBgn0029879	1	1
FBgn0029881	1	1
FBgn0029885	1	1
FBgn0029895	1	1
FBgn0029899	2	2
FBgn0029901	2	6
FBgn0029904	1	1
FBgn0029920	1	2
FBgn0029922	1	2
FBgn0029931	1	1
FBgn0029955	2	2
FBgn0029968	1	1
FBgn0029985	2	2
FBgn0029989	1	4
FBgn0029999	2	8
FBgn0030000	1	1
FBgn0030026	1	1
FBgn0030030	1	1
FBgn0030033	2	3
FBgn0030062	1	1
FBgn0030067	1	1
FBgn0030076	1	1
FBgn0030082	1	1
FBgn0030086	2	2
FBgn0030097	1	1
FBgn0030102	1	1
FBgn0030106	1	1
FBgn0030144	2	2
FBgn0030171	1	1

FBgn0030172	1	1
FBgn0030182	1	1
FBgn0030186	3	6
FBgn0030193	2	2
FBgn0030195	1	1
FBgn0030196	1	1
FBgn0030216	2	4
FBgn0030219	3	6
FBgn0030242	1	1
FBgn0030248	4	4
FBgn0030249	2	2
FBgn0030254	1	4
FBgn0030257	1	1
FBgn0030264	1	1
FBgn0030266	3	4
FBgn0030293	1	5
FBgn0030302	1	1
FBgn0030339	1	1
FBgn0030340	1	1
FBgn0030349	2	2
FBgn0030353	4	7
FBgn0030355	1	1
FBgn0030361	1	1
FBgn0030376	3	3
FBgn0030387	3	10
FBgn0030388	1	2
FBgn0030397	2	4
FBgn0030412	2	10
FBgn0030417	1	1
FBgn0030420	1	1
FBgn0030429	1	1
FBgn0030444	3	5
FBgn0030474	1	1
FBgn0030476	1	3
FBgn0030502	2	43
FBgn0030511	1	6
FBgn0030528	1	1
FBgn0030538	1	1
FBgn0030543	1	1
FBgn0030553	1	1
FBgn0030565	4	4
FBgn0030566	2	2
FBgn0030571	1	15
FBgn0030574	1	1
FBgn0030586	1	1
FBgn0030588	1	1
FBgn0030597	1	3
FBgn0030598	1	1
FBgn0030600	3	5
FBgn0030607	2	3

FBgn0030618	1	1
FBgn0030619	1	1
FBgn0030636	3	4
FBgn0030643	1	1
FBgn0030647	1	3
FBgn0030664	1	1
FBgn0030665	3	3
FBgn0030675	1	1
FBgn0030680	1	1
FBgn0030681	2	2
FBgn0030684	1	1
FBgn0030685	1	1
FBgn0030687	1	1
FBgn0030697	1	1
FBgn0030706	4	4
FBgn0030715	1	1
FBgn0030725	2	2
FBgn0030747	1	1
FBgn0030759	1	1
FBgn0030769	1	1
FBgn0030770	1	1
FBgn0030773	1	1
FBgn0030780	1	1
FBgn0030827	1	1
FBgn0030836	1	1
FBgn0030841	1	1
FBgn0030842	2	2
FBgn0030864	1	1
FBgn0030868	1	1
FBgn0030871	1	1
FBgn0030874	1	1
FBgn0030889	1	1
FBgn0030893	3	3
FBgn0030904	1	1
FBgn0030913	2	2
FBgn0030914	2	2
FBgn0030915	1	1
FBgn0030942	2	2
FBgn0030954	2	3
FBgn0030965	1	1
FBgn0030994	1	1
FBgn0030997	3	3
FBgn0030998	1	2
FBgn0031000	1	1
FBgn0031022	2	2
FBgn0031023	1	1
FBgn0031048	1	1
FBgn0031060	1	1
FBgn0031064	1	1
FBgn0031071	3	4

FBgn0031077	1	1
FBgn0031078	4	6
FBgn0031081	2	2
FBgn0031083	2	2
FBgn0031088	1	2
FBgn0031100	2	2
FBgn0031111	1	1
FBgn0031122	1	1
FBgn0031124	1	1
FBgn0031148	1	1
FBgn0031150	1	4
FBgn0031168	1	1
FBgn0031169	2	3
FBgn0031170	1	1
FBgn0031181	2	2
FBgn0031192	1	1
FBgn0031194	2	2
FBgn0031195	3	12
FBgn0031196	1	1
FBgn0031226	2	2
FBgn0031238	1	2
FBgn0031239	1	1
FBgn0031243	1	1
FBgn0031248	1	1
FBgn0031255	1	1
FBgn0031257	1	1
FBgn0031262	1	1
FBgn0031265	2	2
FBgn0031293	1	1
FBgn0031294	1	1
FBgn0031311	2	3
FBgn0031325	1	1
FBgn0031347	1	1
FBgn0031349	3	4
FBgn0031390	1	1
FBgn0031392	2	2
FBgn0031398	1	1
FBgn0031407	1	2
FBgn0031416	4	8
FBgn0031424	1	1
FBgn0031441	2	5
FBgn0031443	1	1
FBgn0031444	1	1
FBgn0031461	1	1
FBgn0031467	1	1
FBgn0031468	1	1
FBgn0031472	1	1
FBgn0031473	2	2
FBgn0031485	1	1
FBgn0031517	1	2

FBgn0031519	2	2
FBgn0031523	1	1
FBgn0031527	1	1
FBgn0031540	1	1
FBgn0031545	4	6
FBgn0031549	1	1
FBgn0031556	1	1
FBgn0031568	1	1
FBgn0031592	1	2
FBgn0031602	1	1
FBgn0031606	1	1
FBgn0031609	1	1
FBgn0031611	1	1
FBgn0031619	1	1
FBgn0031623	1	1
FBgn0031638	1	1
FBgn0031639	1	1
FBgn0031650	1	1
FBgn0031654	1	1
FBgn0031655	1	1
FBgn0031695	1	1
FBgn0031702	1	6
FBgn0031706	1	1
FBgn0031722	1	1
FBgn0031725	1	1
FBgn0031737	1	3
FBgn0031757	1	1
FBgn0031763	1	1
FBgn0031765	1	2
FBgn0031774	1	3
FBgn0031775	1	1
FBgn0031809	1	1
FBgn0031821	1	1
FBgn0031837	1	1
FBgn0031838	1	1
FBgn0031848	1	1
FBgn0031850	1	1
FBgn0031857	3	3
FBgn0031858	1	1
FBgn0031859	2	2
FBgn0031860	1	2
FBgn0031866	3	3
FBgn0031880	1	1
FBgn0031882	2	2
FBgn0031888	1	1
FBgn0031902	2	2
FBgn0031903	1	1
FBgn0031908	1	1
FBgn0031918	2	2
FBgn0031929	1	1

FBgn0031935	1	1
FBgn0031947	1	1
FBgn0031954	1	1
FBgn0031970	1	1
FBgn0031981	1	1
FBgn0031988	1	1
FBgn0032008	1	1
FBgn0032019	1	1
FBgn0032021	1	2
FBgn0032025	1	3
FBgn0032040	1	1
FBgn0032058	1	1
FBgn0032065	1	1
FBgn0032066	1	1
FBgn0032073	1	1
FBgn0032083	1	1
FBgn0032116	1	1
FBgn0032119	2	2
FBgn0032124	1	1
FBgn0032161	1	1
FBgn0032162	1	1
FBgn0032187	1	1
FBgn0032195	1	1
FBgn0032198	1	2
FBgn0032221	1	1
FBgn0032223	1	1
FBgn0032224	2	3
FBgn0032229	1	1
FBgn0032243	1	1
FBgn0032250	1	2
FBgn0032252	2	2
FBgn0032256	1	1
FBgn0032262	1	1
FBgn0032268	2	6
FBgn0032269	1	1
FBgn0032271	1	3
FBgn0032276	2	2
FBgn0032283	1	1
FBgn0032285	2	3
FBgn0032286	1	1
FBgn0032293	1	1
FBgn0032294	1	2
FBgn0032296	1	1
FBgn0032301	1	1
FBgn0032317	1	1
FBgn0032321	1	1
FBgn0032343	1	2
FBgn0032346	1	1
FBgn0032359	1	1
FBgn0032369	1	1

FBgn0032371	1	1
FBgn0032378	2	17
FBgn0032414	2	2
FBgn0032434	1	1
FBgn0032437	1	1
FBgn0032442	2	2
FBgn0032448	1	3
FBgn0032454	2	3
FBgn0032488	2	2
FBgn0032492	1	1
FBgn0032502	1	1
FBgn0032513	1	2
FBgn0032523	1	1
FBgn0032528	1	1
FBgn0032563	1	1
FBgn0032598	2	3
FBgn0032607	1	1
FBgn0032619	3	6
FBgn0032621	1	1
FBgn0032624	1	1
FBgn0032625	1	2
FBgn0032632	1	1
FBgn0032644	1	1
FBgn0032645	3	6
FBgn0032646	2	2
FBgn0032650	2	2
FBgn0032660	1	1
FBgn0032661	1	5
FBgn0032685	1	1
FBgn0032723	1	1
FBgn0032741	3	3
FBgn0032742	1	4
FBgn0032750	1	1
FBgn0032752	1	1
FBgn0032761	1	1
FBgn0032772	1	1
FBgn0032774	2	3
FBgn0032782	2	4
FBgn0032797	1	2
FBgn0032800	2	2
FBgn0032805	1	1
FBgn0032811	1	1
FBgn0032818	1	1
FBgn0032819	1	1
FBgn0032825	1	1
FBgn0032826	1	14
FBgn0032836	1	1
FBgn0032850	1	1
FBgn0032856	2	2
FBgn0032864	1	1

FBgn0032879	1	1
FBgn0032891	1	1
FBgn0032911	1	3
FBgn0032912	1	1
FBgn0032915	1	1
FBgn0032919	1	1
FBgn0032925	1	1
FBgn0032945	3	5
FBgn0032957	1	1
FBgn0032966	1	1
FBgn0032976	2	3
FBgn0032982	1	1
FBgn0033039	1	1
FBgn0033043	1	1
FBgn0033048	1	1
FBgn0033052	1	1
FBgn0033059	1	1
FBgn0033061	2	2
FBgn0033063	1	1
FBgn0033072	1	1
FBgn0033073	5	31
FBgn0033113	2	4
FBgn0033149	1	1
FBgn0033153	1	1
FBgn0033159	2	3
FBgn0033169	2	2
FBgn0033174	1	1
FBgn0033183	1	1
FBgn0033185	1	2
FBgn0033190	1	1
FBgn0033194	3	4
FBgn0033196	1	1
FBgn0033204	1	1
FBgn0033210	2	2
FBgn0033212	2	2
FBgn0033226	1	1
FBgn0033246	1	1
FBgn0033247	1	1
FBgn0033252	2	2
FBgn0033264	2	2
FBgn0033271	1	1
FBgn0033274	1	1
FBgn0033282	2	4
FBgn0033286	1	1
FBgn0033309	1	1
FBgn0033323	1	1
FBgn0033337	1	1
FBgn0033342	1	1
FBgn0033354	2	2
FBgn0033358	1	1

FBgn0033360	1	1
FBgn0033362	1	1
FBgn0033367	2	2
FBgn0033371	2	2
FBgn0033379	1	1
FBgn0033382	1	5
FBgn0033405	2	2
FBgn0033417	1	1
FBgn0033427	1	1
FBgn0033447	1	1
FBgn0033464	1	1
FBgn0033484	3	3
FBgn0033494	1	1
FBgn0033509	1	1
FBgn0033510	3	6
FBgn0033524	1	1
FBgn0033541	1	1
FBgn0033557	1	2
FBgn0033580	1	1
FBgn0033582	1	1
FBgn0033590	3	46
FBgn0033603	2	2
FBgn0033615	1	1
FBgn0033618	3	4
FBgn0033633	1	1
FBgn0033644	2	2
FBgn0033648	2	3
FBgn0033650	1	1
FBgn0033652	1	2
FBgn0033661	2	16
FBgn0033667	2	2
FBgn0033668	2	2
FBgn0033676	2	2
FBgn0033702	1	2
FBgn0033704	2	2
FBgn0033709	1	3
FBgn0033713	1	1
FBgn0033718	1	3
FBgn0033720	2	2
FBgn0033732	1	1
FBgn0033741	1	1
FBgn0033744	1	1
FBgn0033754	1	1
FBgn0033766	1	4
FBgn0033767	1	1
FBgn0033775	1	1
FBgn0033791	1	1
FBgn0033831	1	1
FBgn0033834	1	1
FBgn0033850	1	1

FBgn0033860	1	1
FBgn0033864	2	3
FBgn0033868	1	1
FBgn0033879	1	2
FBgn0033881	1	1
FBgn0033890	1	1
FBgn0033891	1	1
FBgn0033897	2	2
FBgn0033898	2	4
FBgn0033900	1	1
FBgn0033913	1	1
FBgn0033914	4	6
FBgn0033939	2	2
FBgn0033948	1	1
FBgn0033974	1	1
FBgn0033975	3	6
FBgn0033978	1	2
FBgn0033979	1	1
FBgn0033987	2	2
FBgn0033990	1	1
FBgn0033992	2	2
FBgn0033998	2	3
FBgn0033999	1	1
FBgn0034011	1	1
FBgn0034013	2	3
FBgn0034020	2	8
FBgn0034022	1	1
FBgn0034060	1	2
FBgn0034071	2	2
FBgn0034072	2	3
FBgn0034073	1	1
FBgn0034095	2	2
FBgn0034106	1	1
FBgn0034109	1	1
FBgn0034121	3	3
FBgn0034122	1	1
FBgn0034133	1	1
FBgn0034137	1	1
FBgn0034145	1	1
FBgn0034147	1	1
FBgn0034161	1	1
FBgn0034170	1	2
FBgn0034191	1	1
FBgn0034195	2	8
FBgn0034216	1	3
FBgn0034229	2	2
FBgn0034238	1	1
FBgn0034249	1	1
FBgn0034251	1	2
FBgn0034253	2	2

FBgn0034275	1	1
FBgn0034289	1	1
FBgn0034300	1	1
FBgn0034304	1	1
FBgn0034317	1	1
FBgn0034323	1	2
FBgn0034326	1	1
FBgn0034331	1	1
FBgn0034360	1	1
FBgn0034374	1	1
FBgn0034376	1	1
FBgn0034412	5	14
FBgn0034423	1	1
FBgn0034433	1	1
FBgn0034436	1	1
FBgn0034437	2	3
FBgn0034440	1	1
FBgn0034467	1	1
FBgn0034489	1	1
FBgn0034496	1	1
FBgn0034498	1	1
FBgn0034499	1	1
FBgn0034506	1	1
FBgn0034510	1	1
FBgn0034519	1	1
FBgn0034530	1	1
FBgn0034542	1	1
FBgn0034553	3	4
FBgn0034560	1	1
FBgn0034567	1	1
FBgn0034568	2	3
FBgn0034580	1	1
FBgn0034586	1	1
FBgn0034587	1	1
FBgn0034588	1	1
FBgn0034589	1	1
FBgn0034595	1	1
FBgn0034603	1	1
FBgn0034606	4	4
FBgn0034617	1	1
FBgn0034622	1	1
FBgn0034641	1	1
FBgn0034656	3	3
FBgn0034660	1	1
FBgn0034662	4	4
FBgn0034663	1	1
FBgn0034664	1	1
FBgn0034680	5	6
FBgn0034690	1	2
FBgn0034692	2	2

FBgn0034693	1	1
FBgn0034715	1	1
FBgn0034730	1	2
FBgn0034733	1	1
FBgn0034734	1	1
FBgn0034735	1	1
FBgn0034738	3	4
FBgn0034745	2	2
FBgn0034778	2	2
FBgn0034810	1	1
FBgn0034814	1	1
FBgn0034829	1	1
FBgn0034841	1	1
FBgn0034842	1	1
FBgn0034858	1	1
FBgn0034859	1	1
FBgn0034867	1	1
FBgn0034885	1	1
FBgn0034886	1	1
FBgn0034939	1	1
FBgn0034972	3	3
FBgn0034979	1	1
FBgn0034994	1	3
FBgn0034996	1	1
FBgn0034998	2	2
FBgn0035001	3	3
FBgn0035006	1	1
FBgn0035008	1	1
FBgn0035010	1	1
FBgn0035048	2	2
FBgn0035053	1	1
FBgn0035079	1	1
FBgn0035086	1	1
FBgn0035087	1	1
FBgn0035099	3	4
FBgn0035100	1	1
FBgn0035106	1	1
FBgn0035110	1	1
FBgn0035125	1	2
FBgn0035126	1	16
FBgn0035143	1	1
FBgn0035150	2	2
FBgn0035151	1	1
FBgn0035155	1	1
FBgn0035167	1	1
FBgn0035169	1	1
FBgn0035171	3	5
FBgn0035190	3	4
FBgn0035191	1	1
FBgn0035210	1	2

FBgn0035218	1	1
FBgn0035227	1	1
FBgn0035229	3	3
FBgn0035232	1	1
FBgn0035241	1	1
FBgn0035260	2	2
FBgn0035262	1	1
FBgn0035267	1	1
FBgn0035278	1	1
FBgn0035282	1	1
FBgn0035293	1	1
FBgn0035295	1	1
FBgn0035298	1	1
FBgn0035316	1	1
FBgn0035330	1	1
FBgn0035344	1	1
FBgn0035356	1	1
FBgn0035364	1	1
FBgn0035365	2	2
FBgn0035366	1	2
FBgn0035367	2	3
FBgn0035381	1	2
FBgn0035392	1	1
FBgn0035398	1	2
FBgn0035399	1	1
FBgn0035411	1	1
FBgn0035416	1	1
FBgn0035424	1	5
FBgn0035428	1	1
FBgn0035451	1	1
FBgn0035473	1	1
FBgn0035477	4	5
FBgn0035481	1	1
FBgn0035488	1	1
FBgn0035501	1	1
FBgn0035505	1	1
FBgn0035507	2	2
FBgn0035522	2	2
FBgn0035530	3	4
FBgn0035536	1	1
FBgn0035538	1	1
FBgn0035555	1	1
FBgn0035557	1	1
FBgn0035575	1	1
FBgn0035577	3	3
FBgn0035581	1	1
FBgn0035586	2	3
FBgn0035591	2	3
FBgn0035606	2	2
FBgn0035612	1	1

FBgn0035619	1	1
FBgn0035623	1	1
FBgn0035625	2	2
FBgn0035626	1	1
FBgn0035638	1	1
FBgn0035641	1	2
FBgn0035642	1	1
FBgn0035655	1	6
FBgn0035671	1	2
FBgn0035676	1	1
FBgn0035677	1	1
FBgn0035685	2	2
FBgn0035687	1	1
FBgn0035691	1	1
FBgn0035695	1	1
FBgn0035697	1	1
FBgn0035707	1	1
FBgn0035708	1	1
FBgn0035711	1	1
FBgn0035720	3	7
FBgn0035727	1	1
FBgn0035730	1	1
FBgn0035761	1	1
FBgn0035784	1	2
FBgn0035790	1	1
FBgn0035795	1	4
FBgn0035797	2	2
FBgn0035798	4	6
FBgn0035802	1	1
FBgn0035813	1	1
FBgn0035832	1	1
FBgn0035842	1	1
FBgn0035844	1	1
FBgn0035852	1	1
FBgn0035864	1	1
FBgn0035872	1	1
FBgn0035873	1	1
FBgn0035880	1	2
FBgn0035886	1	5
FBgn0035888	2	2
FBgn0035898	4	4
FBgn0035901	3	7
FBgn0035902	1	1
FBgn0035903	2	3
FBgn0035911	1	1
FBgn0035915	2	2
FBgn0035928	1	2
FBgn0035930	2	2
FBgn0035941	1	1
FBgn0035988	1	1

FBgn0036008	1	1
FBgn0036009	1	1
FBgn0036018	1	1
FBgn0036022	1	1
FBgn0036031	1	1
FBgn0036038	1	1
FBgn0036075	1	1
FBgn0036082	1	1
FBgn0036093	1	1
FBgn0036099	1	1
FBgn0036102	1	2
FBgn0036104	2	6
FBgn0036112	1	1
FBgn0036122	1	1
FBgn0036125	1	1
FBgn0036133	1	1
FBgn0036134	1	1
FBgn0036135	2	2
FBgn0036139	1	2
FBgn0036144	1	1
FBgn0036162	1	1
FBgn0036173	2	2
FBgn0036183	1	1
FBgn0036186	1	1
FBgn0036192	1	1
FBgn0036195	2	2
FBgn0036206	1	1
FBgn0036222	1	1
FBgn0036223	2	4
FBgn0036227	1	4
FBgn0036234	1	1
FBgn0036235	1	1
FBgn0036240	1	1
FBgn0036249	1	1
FBgn0036260	1	1
FBgn0036287	2	2
FBgn0036295	1	1
FBgn0036301	1	1
FBgn0036328	2	2
FBgn0036330	1	1
FBgn0036340	2	2
FBgn0036346	1	1
FBgn0036348	1	2
FBgn0036359	1	1
FBgn0036368	2	3
FBgn0036374	2	2
FBgn0036380	1	5
FBgn0036384	1	1
FBgn0036391	1	1
FBgn0036398	2	2

FBgn0036411	1	1
FBgn0036414	2	2
FBgn0036423	1	1
FBgn0036425	1	1
FBgn0036446	1	1
FBgn0036456	1	1
FBgn0036459	1	3
FBgn0036463	1	1
FBgn0036482	2	2
FBgn0036491	1	1
FBgn0036492	1	1
FBgn0036494	1	1
FBgn0036497	1	1
FBgn0036504	1	1
FBgn0036513	1	1
FBgn0036524	1	2
FBgn0036541	2	5
FBgn0036544	2	3
FBgn0036560	1	1
FBgn0036567	1	1
FBgn0036574	1	1
FBgn0036576	1	1
FBgn0036583	1	1
FBgn0036587	1	1
FBgn0036621	1	2
FBgn0036640	1	1
FBgn0036665	1	1
FBgn0036669	1	1
FBgn0036672	1	2
FBgn0036683	1	1
FBgn0036688	1	1
FBgn0036698	2	2
FBgn0036715	2	5
FBgn0036725	1	1
FBgn0036729	1	1
FBgn0036742	1	2
FBgn0036747	3	3
FBgn0036757	1	1
FBgn0036763	1	1
FBgn0036764	2	2
FBgn0036767	1	1
FBgn0036791	1	1
FBgn0036810	1	1
FBgn0036835	1	1
FBgn0036843	1	1
FBgn0036847	2	2
FBgn0036858	1	1
FBgn0036876	2	2
FBgn0036878	1	2
FBgn0036880	1	1

FBgn0036882	1	1
FBgn0036886	1	1
FBgn0036890	3	7
FBgn0036892	1	1
FBgn0036899	1	1
FBgn0036916	1	1
FBgn0036925	2	2
FBgn0036934	1	1
FBgn0036935	3	4
FBgn0036936	1	1
FBgn0036941	1	1
FBgn0036943	1	2
FBgn0036944	1	1
FBgn0036951	1	1
FBgn0036952	1	1
FBgn0036953	2	2
FBgn0036954	2	2
FBgn0036955	2	2
FBgn0036969	1	1
FBgn0036985	1	1
FBgn0036995	1	1
FBgn0037008	1	1
FBgn0037014	1	1
FBgn0037025	2	2
FBgn0037030	1	1
FBgn0037035	1	1
FBgn0037040	2	2
FBgn0037085	1	1
FBgn0037104	2	2
FBgn0037105	1	1
FBgn0037113	1	2
FBgn0037115	2	2
FBgn0037117	1	1
FBgn0037130	2	2
FBgn0037142	2	2
FBgn0037173	1	1
FBgn0037202	1	1
FBgn0037207	1	1
FBgn0037232	1	1
FBgn0037255	1	1
FBgn0037263	1	2
FBgn0037273	1	1
FBgn0037274	4	16
FBgn0037294	1	1
FBgn0037296	2	4
FBgn0037316	1	1
FBgn0037320	1	1
FBgn0037326	1	1
FBgn0037336	1	1
FBgn0037379	2	2

FBgn0037388	1	1
FBgn0037394	1	1
FBgn0037395	1	1
FBgn0037397	2	2
FBgn0037410	2	4
FBgn0037413	2	2
FBgn0037416	1	1
FBgn0037417	1	1
FBgn0037419	2	3
FBgn0037421	1	1
FBgn0037427	1	3
FBgn0037430	1	1
FBgn0037445	1	1
FBgn0037449	1	1
FBgn0037453	1	1
FBgn0037460	1	1
FBgn0037464	1	1
FBgn0037471	1	1
FBgn0037485	1	1
FBgn0037486	1	1
FBgn0037487	2	2
FBgn0037489	1	1
FBgn0037506	1	1
FBgn0037554	1	1
FBgn0037561	1	1
FBgn0037565	2	2
FBgn0037568	1	1
FBgn0037572	2	2
FBgn0037625	2	2
FBgn0037632	2	3
FBgn0037640	3	3
FBgn0037645	1	1
FBgn0037659	1	1
FBgn0037674	1	1
FBgn0037683	1	1
FBgn0037696	1	1
FBgn0037697	1	1
FBgn0037698	1	1
FBgn0037703	2	2
FBgn0037705	1	4
FBgn0037707	1	2
FBgn0037709	1	1
FBgn0037711	1	1
FBgn0037712	2	4
FBgn0037723	1	1
FBgn0037726	2	3
FBgn0037727	1	1
FBgn0037742	3	3
FBgn0037753	1	1
FBgn0037778	1	1

FBgn0037806	2	2
FBgn0037819	1	1
FBgn0037831	1	1
FBgn0037832	2	2
FBgn0037839	1	1
FBgn0037840	2	2
FBgn0037844	1	2
FBgn0037849	1	1
FBgn0037852	1	1
FBgn0037856	1	1
FBgn0037857	1	1
FBgn0037894	1	1
FBgn0037896	1	1
FBgn0037915	1	3
FBgn0037949	2	2
FBgn0037970	1	1
FBgn0037985	1	3
FBgn0037986	2	11
FBgn0037993	2	2
FBgn0037999	1	1
FBgn0038016	3	30
FBgn0038035	1	1
FBgn0038049	1	1
FBgn0038057	1	1
FBgn0038064	1	1
FBgn0038067	1	1
FBgn0038070	1	1
FBgn0038072	1	1
FBgn0038073	3	3
FBgn0038076	1	1
FBgn0038082	1	1
FBgn0038095	1	1
FBgn0038108	1	1
FBgn0038118	1	1
FBgn0038119	1	1
FBgn0038120	1	1
FBgn0038133	1	1
FBgn0038134	1	1
FBgn0038139	2	3
FBgn0038163	1	1
FBgn0038173	1	2
FBgn0038189	1	1
FBgn0038191	2	2
FBgn0038208	2	2
FBgn0038217	2	2
FBgn0038227	3	4
FBgn0038247	1	1
FBgn0038254	2	2
FBgn0038262	1	1
FBgn0038270	1	2

FBgn0038295	1	1
FBgn0038296	1	1
FBgn0038308	1	1
FBgn0038310	1	1
FBgn0038318	1	1
FBgn0038342	1	1
FBgn0038349	3	3
FBgn0038351	1	1
FBgn0038357	1	1
FBgn0038380	2	4
FBgn0038385	2	2
FBgn0038390	1	1
FBgn0038396	1	1
FBgn0038410	1	1
FBgn0038422	1	1
FBgn0038423	1	2
FBgn0038427	1	1
FBgn0038441	1	2
FBgn0038448	2	8
FBgn0038452	1	2
FBgn0038454	1	1
FBgn0038472	1	1
FBgn0038476	3	3
FBgn0038477	1	1
FBgn0038494	1	4
FBgn0038498	1	1
FBgn0038516	3	3
FBgn0038523	1	2
FBgn0038530	1	1
FBgn0038538	1	1
FBgn0038541	1	2
FBgn0038544	3	5
FBgn0038554	1	1
FBgn0038567	1	1
FBgn0038575	2	3
FBgn0038576	1	1
FBgn0038597	2	2
FBgn0038606	1	1
FBgn0038607	3	4
FBgn0038621	2	3
FBgn0038629	1	1
FBgn0038633	1	1
FBgn0038638	2	2
FBgn0038644	1	1
FBgn0038676	1	1
FBgn0038678	1	1
FBgn0038683	1	1
FBgn0038693	2	3
FBgn0038700	1	1
FBgn0038730	1	1

FBgn0038733	2	5
FBgn0038734	1	1
FBgn0038744	2	2
FBgn0038753	1	1
FBgn0038761	1	1
FBgn0038762	3	3
FBgn0038776	1	1
FBgn0038799	1	1
FBgn0038814	2	2
FBgn0038816	3	4
FBgn0038827	1	1
FBgn0038832	1	1
FBgn0038837	1	1
FBgn0038852	1	1
FBgn0038867	2	2
FBgn0038897	2	2
FBgn0038915	1	1
FBgn0038919	1	1
FBgn0038930	1	8
FBgn0038948	3	13
FBgn0038968	1	1
FBgn0038985	1	1
FBgn0038993	1	1
FBgn0039016	1	1
FBgn0039038	1	1
FBgn0039060	1	1
FBgn0039063	2	2
FBgn0039064	1	1
FBgn0039065	1	1
FBgn0039071	1	1
FBgn0039075	2	2
FBgn0039078	3	5
FBgn0039080	1	1
FBgn0039087	1	2
FBgn0039093	2	2
FBgn0039127	1	2
FBgn0039145	1	1
FBgn0039152	3	5
FBgn0039155	1	1
FBgn0039186	2	2
FBgn0039193	1	1
FBgn0039214	2	2
FBgn0039225	1	1
FBgn0039227	1	1
FBgn0039235	1	1
FBgn0039237	1	1
FBgn0039244	2	2
FBgn0039268	1	2
FBgn0039274	1	1
FBgn0039277	1	1

FBgn0039280	1	1
FBgn0039282	2	2
FBgn0039286	2	2
FBgn0039288	1	1
FBgn0039299	1	1
FBgn0039301	1	1
FBgn0039302	1	1
FBgn0039307	1	1
FBgn0039312	1	1
FBgn0039319	3	6
FBgn0039329	1	1
FBgn0039348	1	1
FBgn0039358	1	1
FBgn0039368	1	1
FBgn0039378	1	1
FBgn0039387	2	2
FBgn0039398	1	1
FBgn0039400	1	1
FBgn0039407	1	1
FBgn0039411	2	5
FBgn0039415	1	1
FBgn0039419	2	2
FBgn0039421	1	1
FBgn0039431	1	1
FBgn0039448	1	4
FBgn0039470	1	1
FBgn0039471	2	2
FBgn0039472	1	1
FBgn0039478	1	1
FBgn0039484	5	15
FBgn0039490	2	13
FBgn0039510	4	7
FBgn0039513	2	2
FBgn0039519	2	2
FBgn0039527	3	3
FBgn0039529	1	1
FBgn0039530	1	1
FBgn0039544	1	1
FBgn0039556	1	1
FBgn0039558	1	1
FBgn0039561	1	1
FBgn0039570	1	1
FBgn0039584	2	3
FBgn0039585	1	1
FBgn0039599	1	2
FBgn0039617	1	1
FBgn0039620	2	6
FBgn0039629	1	1
FBgn0039630	1	1
FBgn0039633	3	3

FBgn0039654	3	3
FBgn0039665	1	1
FBgn0039668	1	1
FBgn0039673	2	2
FBgn0039688	1	1
FBgn0039690	1	2
FBgn0039694	1	2
FBgn0039711	1	2
FBgn0039718	1	1
FBgn0039726	1	1
FBgn0039734	1	2
FBgn0039736	2	3
FBgn0039742	1	1
FBgn0039760	1	1
FBgn0039766	1	1
FBgn0039768	1	1
FBgn0039770	1	1
FBgn0039788	1	1
FBgn0039804	1	1
FBgn0039827	1	1
FBgn0039831	1	1
FBgn0039833	1	2
FBgn0039841	2	2
FBgn0039850	1	6
FBgn0039859	1	1
FBgn0039905	1	1
FBgn0039908	1	1
FBgn0039911	2	2
FBgn0039912	1	1
FBgn0039938	2	3
FBgn0039969	2	6
FBgn0039972	2	5
FBgn0040037	1	1
FBgn0040064	1	1
FBgn0040066	1	1
FBgn0040068	1	1
FBgn0040080	1	1
FBgn0040107	1	1
FBgn0040108	1	1
FBgn0040208	2	2
FBgn0040232	1	1
FBgn0040235	1	1
FBgn0040236	1	1
FBgn0040253	1	1
FBgn0040268	4	7
FBgn0040273	1	2
FBgn0040281	1	1
FBgn0040284	3	27
FBgn0040286	1	1
FBgn0040290	2	8

FBgn0040295	1	1
FBgn0040297	1	1
FBgn0040299	2	2
FBgn0040333	1	1
FBgn0040335	3	19
FBgn0040341	1	2
FBgn0040342	1	1
FBgn0040344	2	2
FBgn0040350	2	2
FBgn0040355	1	1
FBgn0040369	1	2
FBgn0040372	2	4
FBgn0040379	1	1
FBgn0040384	1	1
FBgn0040385	1	1
FBgn0040387	1	1
FBgn0040390	1	1
FBgn0040394	3	4
FBgn0040395	1	1
FBgn0040398	1	1
FBgn0040483	1	1
FBgn0040493	1	1
FBgn0040499	2	3
FBgn0040505	1	1
FBgn0040507	1	1
FBgn0040508	1	1
FBgn0040528	1	6
FBgn0040574	1	1
FBgn0040585	1	1
FBgn0040647	1	7
FBgn0040670	1	1
FBgn0040696	1	1
FBgn0040697	1	1
FBgn0040752	2	2
FBgn0040847	1	1
FBgn0040883	1	2
FBgn0040917	2	8
FBgn0040932	1	1
FBgn0040998	2	2
FBgn0041092	4	6
FBgn0041096	4	4
FBgn0041109	1	1
FBgn0041150	1	1
FBgn0041156	1	3
FBgn0041161	1	1
FBgn0041171	2	2
FBgn0041180	2	2
FBgn0041184	1	1
FBgn0041188	1	2
FBgn0041194	2	2

FBgn0041203	2	3
FBgn0041240	1	1
FBgn0041244	2	2
FBgn0041245	1	1
FBgn0041342	3	6
FBgn0041582	2	2
FBgn0041604	2	2
FBgn0041605	1	2
FBgn0041707	1	1
FBgn0041723	4	5
FBgn0042083	1	1
FBgn0042132	1	1
FBgn0042134	1	1
FBgn0042137	2	2
FBgn0042178	1	1
FBgn0042182	2	3
FBgn0042188	1	1
FBgn0042627	2	2
FBgn0042650	3	4
FBgn0042710	1	1
FBgn0043005	1	1
FBgn0043455	1	1
FBgn0043458	1	1
FBgn0043470	1	1
FBgn0043471	1	1
FBgn0043575	1	1
FBgn0043791	1	1
FBgn0043799	1	6
FBgn0043884	1	1
FBgn0043903	1	1
FBgn0043904	1	1
FBgn0044050	2	3
FBgn0044323	1	1
FBgn0044812	1	1
FBgn0044824	1	1
FBgn0045063	3	3
FBgn0045497	1	1
FBgn0045501	1	1
FBgn0045828	1	2
FBgn0045843	1	1
FBgn0045852	4	13
FBgn0046214	1	1
FBgn0046222	4	10
FBgn0046227	1	2
FBgn0046302	1	1
FBgn0046687	1	1
FBgn0046776	1	1
FBgn0046873	1	1
FBgn0046874	3	3
FBgn0046875	1	1

FBgn0046885	1	5
FBgn0046886	1	5
FBgn0046887	1	8
FBgn0047305	1	6
FBgn0047330	1	1
FBgn0050011	1	1
FBgn0050015	2	2
FBgn0050017	1	1
FBgn0050018	1	2
FBgn0050019	4	4
FBgn0050022	1	2
FBgn0050035	1	1
FBgn0050042	2	4
FBgn0050053	1	1
FBgn0050055	1	1
FBgn0050069	4	4
FBgn0050073	2	3
FBgn0050076	1	1
FBgn0050083	1	9
FBgn0050089	4	5
FBgn0050090	1	1
FBgn0050098	1	2
FBgn0050099	1	1
FBgn0050115	3	3
FBgn0050118	1	1
FBgn0050122	4	10
FBgn0050125	2	2
FBgn0050149	1	1
FBgn0050157	1	1
FBgn0050158	3	5
FBgn0050183	1	1
FBgn0050188	1	1
FBgn0050194	1	1
FBgn0050203	2	4
FBgn0050268	1	1
FBgn0050269	1	1
FBgn0050273	1	1
FBgn0050275	1	1
FBgn0050277	1	1
FBgn0050287	1	1
FBgn0050295	2	2
FBgn0050327	1	1
FBgn0050342	1	1
FBgn0050345	2	2
FBgn0050356	1	1
FBgn0050357	1	1
FBgn0050360	2	2
FBgn0050361	1	1
FBgn0050362	1	1
FBgn0050365	1	2

FBgn0050377	1	1
FBgn0050378	1	2
FBgn0050387	1	2
FBgn0050390	1	3
FBgn0050394	2	2
FBgn0050410	1	1
FBgn0050421	1	1
FBgn0050422	1	1
FBgn0050430	1	1
FBgn0050436	1	1
FBgn0050447	1	1
FBgn0050456	1	2
FBgn0050459	1	1
FBgn0050460	2	2
FBgn0050462	1	1
FBgn0050463	1	1
FBgn0050464	1	1
FBgn0050466	1	1
FBgn0050472	1	1
FBgn0050491	1	1
FBgn0050495	1	1
FBgn0051004	1	1
FBgn0051005	1	1
FBgn0051008	1	2
FBgn0051021	1	1
FBgn0051025	1	1
FBgn0051037	1	1
FBgn0051038	1	1
FBgn0051046	1	2
FBgn0051048	2	2
FBgn0051057	1	1
FBgn0051064	1	1
FBgn0051068	1	1
FBgn0051072	3	6
FBgn0051085	1	2
FBgn0051088	1	1
FBgn0051092	1	1
FBgn0051097	1	2
FBgn0051098	2	2
FBgn0051099	2	3
FBgn0051106	1	1
FBgn0051108	1	1
FBgn0051114	1	1
FBgn0051115	1	1
FBgn0051116	1	1
FBgn0051121	1	1
FBgn0051132	1	1
FBgn0051140	2	2
FBgn0051145	1	2
FBgn0051146	2	3

FBgn0051149	2	2
FBgn0051150	1	1
FBgn0051158	2	3
FBgn0051160	1	1
FBgn0051161	2	5
FBgn0051163	1	1
FBgn0051164	1	1
FBgn0051177	3	3
FBgn0051187	3	3
FBgn0051190	2	2
FBgn0051198	1	2
FBgn0051202	1	1
FBgn0051209	4	4
FBgn0051211	3	3
FBgn0051219	1	1
FBgn0051222	3	4
FBgn0051229	2	2
FBgn0051235	1	1
FBgn0051245	1	1
FBgn0051270	1	1
FBgn0051274	1	1
FBgn0051294	1	1
FBgn0051296	1	2
FBgn0051302	3	4
FBgn0051304	1	1
FBgn0051308	1	1
FBgn0051314	1	1
FBgn0051330	1	1
FBgn0051342	1	1
FBgn0051348	1	1
FBgn0051361	1	1
FBgn0051365	2	3
FBgn0051373	1	1
FBgn0051374	1	1
FBgn0051385	1	1
FBgn0051386	1	1
FBgn0051389	1	5
FBgn0051406	1	1
FBgn0051407	2	2
FBgn0051415	1	1
FBgn0051423	1	1
FBgn0051431	2	3
FBgn0051454	1	2
FBgn0051469	1	2
FBgn0051475	1	1
FBgn0051484	1	1
FBgn0051488	1	1
FBgn0051492	2	2
FBgn0051510	1	1
FBgn0051531	1	1

FBgn0051536	1	1
FBgn0051537	1	2
FBgn0051554	1	1
FBgn0051619	1	3
FBgn0051624	1	1
FBgn0051634	1	1
FBgn0051635	2	2
FBgn0051640	3	5
FBgn0051642	1	1
FBgn0051646	1	1
FBgn0051649	1	1
FBgn0051673	1	1
FBgn0051676	1	1
FBgn0051678	2	2
FBgn0051687	2	3
FBgn0051688	3	4
FBgn0051703	1	1
FBgn0051723	1	1
FBgn0051729	1	1
FBgn0051755	1	2
FBgn0051772	1	1
FBgn0051773	1	1
FBgn0051774	1	2
FBgn0051779	1	1
FBgn0051782	1	1
FBgn0051784	1	1
FBgn0051792	1	1
FBgn0051793	3	3
FBgn0051802	1	1
FBgn0051812	1	1
FBgn0051840	1	1
FBgn0051857	1	1
FBgn0051864	1	1
FBgn0051900	1	1
FBgn0051901	1	1
FBgn0051921	1	1
FBgn0051924	1	1
FBgn0051925	1	1
FBgn0051935	1	1
FBgn0051938	1	1
FBgn0051948	2	3
FBgn0051973	3	3
FBgn0051989	1	1
FBgn0051998	1	1
FBgn0052013	1	1
FBgn0052029	1	1
FBgn0052030	2	2
FBgn0052046	1	1
FBgn0052060	1	1
FBgn0052064	3	9

FBgn0052067	4	6
FBgn0052082	1	17
FBgn0052087	1	2
FBgn0052092	2	2
FBgn0052094	1	1
FBgn0052095	1	1
FBgn0052103	1	1
FBgn0052104	2	3
FBgn0052112	1	1
FBgn0052113	2	2
FBgn0052115	1	1
FBgn0052130	1	1
FBgn0052137	1	2
FBgn0052140	1	1
FBgn0052155	1	1
FBgn0052158	1	1
FBgn0052175	1	1
FBgn0052182	1	1
FBgn0052183	2	3
FBgn0052191	1	1
FBgn0052195	2	2
FBgn0052206	2	2
FBgn0052210	1	1
FBgn0052226	2	2
FBgn0052227	1	1
FBgn0052242	1	1
FBgn0052249	1	2
FBgn0052260	1	2
FBgn0052264	3	3
FBgn0052269	2	4
FBgn0052271	1	1
FBgn0052283	1	1
FBgn0052296	1	1
FBgn0052304	2	2
FBgn0052306	2	3
FBgn0052316	1	1
FBgn0052332	1	1
FBgn0052333	2	2
FBgn0052352	1	1
FBgn0052354	1	3
FBgn0052369	1	1
FBgn0052373	2	2
FBgn0052377	2	3
FBgn0052380	1	1
FBgn0052384	3	3
FBgn0052387	1	1
FBgn0052392	1	1
FBgn0052397	2	2
FBgn0052406	1	1
FBgn0052432	2	2

FBgn0052434	2	2
FBgn0052437	1	1
FBgn0052439	1	1
FBgn0052445	1	1
FBgn0052457	1	1
FBgn0052461	1	1
FBgn0052476	1	1
FBgn0052484	1	1
FBgn0052486	3	3
FBgn0052487	2	4
FBgn0052495	1	1
FBgn0052504	1	2
FBgn0052506	1	1
FBgn0052521	1	1
FBgn0052529	3	4
FBgn0052532	1	1
FBgn0052533	1	1
FBgn0052541	1	2
FBgn0052542	2	2
FBgn0052543	3	3
FBgn0052547	2	2
FBgn0052552	1	1
FBgn0052557	1	1
FBgn0052560	5	7
FBgn0052572	4	4
FBgn0052580	4	12
FBgn0052587	1	1
FBgn0052604	1	1
FBgn0052605	1	1
FBgn0052627	3	4
FBgn0052628	4	4
FBgn0052639	1	1
FBgn0052648	5	6
FBgn0052649	1	1
FBgn0052651	1	1
FBgn0052654	2	2
FBgn0052668	1	1
FBgn0052669	1	2
FBgn0052676	2	5
FBgn0052677	1	1
FBgn0052683	2	2
FBgn0052685	2	2
FBgn0052687	2	2
FBgn0052692	1	1
FBgn0052702	3	3
FBgn0052704	1	1
FBgn0052707	1	1
FBgn0052727	1	1
FBgn0052732	2	2
FBgn0052737	3	3

FBgn0052742	1	1
FBgn0052743	1	1
FBgn0052751	1	1
FBgn0052756	1	1
FBgn0052779	2	2
FBgn0052781	1	1
FBgn0052783	1	1
FBgn0052786	1	1
FBgn0052790	1	1
FBgn0052798	1	4
FBgn0052802	1	3
FBgn0052830	2	2
FBgn0052855	2	2
FBgn0052856	1	1
FBgn0052921	1	1
FBgn0052937	1	1
FBgn0052940	1	1
FBgn0052944	1	1
FBgn0052984	1	1
FBgn0052986	1	1
FBgn0053007	2	3
FBgn0053012	2	2
FBgn0053038	1	2
FBgn0053041	1	1
FBgn0053054	1	1
FBgn0053070	1	1
FBgn0053087	6	13
FBgn0053099	1	1
FBgn0053108	1	1
FBgn0053111	1	1
FBgn0053120	1	1
FBgn0053123	1	1
FBgn0053125	1	1
FBgn0053129	1	1
FBgn0053130	1	1
FBgn0053136	1	1
FBgn0053137	1	1
FBgn0053139	2	2
FBgn0053144	5	5
FBgn0053146	1	4
FBgn0053153	1	1
FBgn0053156	1	1
FBgn0053171	1	1
FBgn0053172	1	1
FBgn0053173	2	5
FBgn0053177	1	1
FBgn0053179	2	2
FBgn0053188	1	1
FBgn0053196	55	74
FBgn0053204	2	2

FBgn0053207	1	1
FBgn0053208	1	1
FBgn0053214	1	1
FBgn0060296	1	1
FBgn0061200	2	2
FBgn0061359	2	2
FBgn0061435	1	1
FBgn0062459	2	2
FBgn0062934	3	7
FBgn0063649	3	3
FBgn0065109	1	2

Appendix 2. List of proteins identified in salivary glands 13 hours after puparium formation

Flybase ID#	upep	tpep
FBgn0000014	1	3
FBgn0000042	3	4
FBgn0000043	3	4
FBgn0000044	4	5
FBgn0000045	2	3
FBgn0000052	1	1
FBgn0000053	1	1
FBgn0000054	1	1
FBgn0000099	1	1
FBgn0000100	1	2
FBgn0000142	1	1
FBgn0000163	1	1
FBgn0000166	2	2
FBgn0000183	1	1
FBgn0000210	1	3
FBgn0000212	1	1
FBgn0000250	2	2
FBgn0000275	1	1
FBgn0000299	1	1
FBgn0000317	1	1
FBgn0000319	2	6
FBgn0000340	1	1
FBgn0000368	3	3
FBgn0000382	2	3
FBgn0000404	1	1
FBgn0000416	2	9
FBgn0000448	1	2
FBgn0000463	2	5
FBgn0000482	2	2
FBgn0000486	1	3
FBgn0000489	1	3
FBgn0000497	4	4
FBgn0000556	4	14
FBgn0000557	3	8
FBgn0000559	2	4
FBgn0000564	2	7
FBgn0000567	1	1
FBgn0000568	3	3
FBgn0000579	1	1
FBgn0000617	4	8
FBgn0000629	1	1
FBgn0000634	1	1
FBgn0000667	1	1
FBgn0000711	1	1
FBgn0000719	1	1
FBgn0000721	1	2
FBgn0000723	2	2

FBgn0001078	1	1
FBgn0001091	2	2
FBgn0001112	2	5
FBgn0001134	1	1
FBgn0001149	3	5
FBgn0001169	2	3
FBgn0001219	2	4
FBgn0001220	2	3
FBgn0001222	1	1
FBgn0001230	1	1
FBgn0001247	2	2
FBgn0001301	1	1
FBgn0001308	2	4
FBgn0001309	4	5
FBgn0001942	1	1
FBgn0001961	1	1
FBgn0001970	1	3
FBgn0001991	1	1
FBgn0001994	2	3
FBgn0002031	1	1
FBgn0002413	3	4
FBgn0002431	3	3
FBgn0002441	3	3
FBgn0002526	5	8
FBgn0002528	3	4
FBgn0002564	1	2
FBgn0002643	1	1
FBgn0002716	3	3
FBgn0002780	1	1
FBgn0002781	1	1
FBgn0002781	1	1
FBgn0002783	4	4
FBgn0002905	2	2
FBgn0002926	3	3
FBgn0002968	1	1
FBgn0003041	1	1
FBgn0003044	1	1
FBgn0003048	5	5
FBgn0003057	1	1
FBgn0003071	2	2
FBgn0003074	1	1
FBgn0003134	2	3
FBgn0003138	2	3
FBgn0003141	1	1
FBgn0003151	1	1
FBgn0003165	2	2
FBgn0003175	2	4
FBgn0003177	5	6
FBgn0003189	2	2
FBgn0003218	2	2

FBgn0003261	1	1
FBgn0003268	3	4
FBgn0003274	3	4
FBgn0003292	1	1
FBgn0003301	2	2
FBgn0003310	1	1
FBgn0003319	1	1
FBgn0003328	1	1
FBgn0003353	1	1
FBgn0003366	2	2
FBgn0003373	3	15
FBgn0003375	3	3
FBgn0003377	2	2
FBgn0003378	2	8
FBgn0003391	1	1
FBgn0003396	2	7
FBgn0003410	1	1
FBgn0003435	1	2
FBgn0003444	2	3
FBgn0003462	1	1
FBgn0003464	3	5
FBgn0003501	1	1
FBgn0003502	1	1
FBgn0003507	3	5
FBgn0003575	2	2
FBgn0003638	2	2
FBgn0003656	1	2
FBgn0003691	1	1
FBgn0003717	1	1
FBgn0003721	1	1
FBgn0003742	1	1
FBgn0003862	1	1
FBgn0003884	1	1
FBgn0003885	1	1
FBgn0003886	1	2
FBgn0003887	2	2
FBgn0003963	1	1
FBgn0003964	1	1
FBgn0004002	5	7
FBgn0004118	1	1
FBgn0004133	2	4
FBgn0004179	1	1
FBgn0004210	1	1
FBgn0004227	1	1
FBgn0004237	1	1
FBgn0004243	2	3
FBgn0004362	1	1
FBgn0004368	1	1
FBgn0004378	2	2
FBgn0004380	2	2

FBgn0004381	2	2
FBgn0004396	3	3
FBgn0004419	1	1
FBgn0004432	1	1
FBgn0004509	1	1
FBgn0004551	1	7
FBgn0004556	1	1
FBgn0004568	1	1
FBgn0004583	1	1
FBgn0004584	1	1
FBgn0004587	1	1
FBgn0004593	1	1
FBgn0004595	3	3
FBgn0004598	2	2
FBgn0004607	2	3
FBgn0004622	1	1
FBgn0004625	1	1
FBgn0004644	1	1
FBgn0004649	3	3
FBgn0004655	2	2
FBgn0004656	3	6
FBgn0004657	1	1
FBgn0004687	2	2
FBgn0004834	1	1
FBgn0004858	3	3
FBgn0004864	2	2
FBgn0004876	1	1
FBgn0004879	1	1
FBgn0004885	1	1
FBgn0004888	1	1
FBgn0004893	1	1
FBgn0004922	1	1
FBgn0004924	1	1
FBgn0005386	4	4
FBgn0005391	1	1
FBgn0005410	2	2
FBgn0005585	2	3
FBgn0005612	1	1
FBgn0005624	3	3
FBgn0005634	1	1
FBgn0005636	1	1
FBgn0005642	1	2
FBgn0005649	1	1
FBgn0005655	2	3
FBgn0005674	2	2
FBgn0005695	1	1
FBgn0008635	2	2
FBgn0008654	1	3
FBgn0010051	3	3
FBgn0010173	1	1

FBgn0010194	1	7
FBgn0010235	1	1
FBgn0010246	2	2
FBgn0010280	1	1
FBgn0010300	2	3
FBgn0010315	1	2
FBgn0010316	2	5
FBgn0010355	2	4
FBgn0010356	1	2
FBgn0010380	2	2
FBgn0010385	1	1
FBgn0010389	1	1
FBgn0010397	1	2
FBgn0010407	1	1
FBgn0010415	1	2
FBgn0010435	1	1
FBgn0010441	1	1
FBgn0010583	1	1
FBgn0010621	2	2
FBgn0010747	1	1
FBgn0010851	3	7
FBgn0011202	2	2
FBgn0011211	1	1
FBgn0011230	4	4
FBgn0011236	1	1
FBgn0011274	1	1
FBgn0011289	1	2
FBgn0011341	1	1
FBgn0011571	4	9
FBgn0011603	1	1
FBgn0011606	1	1
FBgn0011653	2	2
FBgn0011655	1	1
FBgn0011673	1	1
FBgn0011674	1	1
FBgn0011715	1	1
FBgn0011722	1	1
FBgn0011740	1	1
FBgn0011747	2	6
FBgn0011768	1	1
FBgn0011771	1	1
FBgn0011823	1	1
FBgn0011824	1	1
FBgn0011826	1	1
FBgn0011829	1	1
FBgn0011836	1	1
FBgn0012034	1	1
FBgn0012066	1	1
FBgn0013272	1	2
FBgn0013548	2	2

FBgn0013576	1	1
FBgn0013726	1	2
FBgn0013733	8	11
FBgn0013771	1	1
FBgn0013773	2	3
FBgn0013809	4	5
FBgn0013812	5	8
FBgn0013948	1	1
FBgn0013951	1	1
FBgn0013974	2	3
FBgn0013984	4	4
FBgn0013988	3	3
FBgn0014002	7	21
FBgn0014024	1	1
FBgn0014027	2	3
FBgn0014028	2	5
FBgn0014133	4	8
FBgn0014163	1	1
FBgn0014362	1	1
FBgn0014469	1	1
FBgn0015011	2	2
FBgn0015019	1	1
FBgn0015229	1	1
FBgn0015239	1	3
FBgn0015247	1	1
FBgn0015268	1	3
FBgn0015278	1	1
FBgn0015279	1	1
FBgn0015286	1	1
FBgn0015287	1	1
FBgn0015509	1	1
FBgn0015513	1	1
FBgn0015520	1	1
FBgn0015521	1	1
FBgn0015542	1	1
FBgn0015567	1	1
FBgn0015572	1	1
FBgn0015589	3	3
FBgn0015615	1	1
FBgn0015622	2	2
FBgn0015624	3	3
FBgn0015737	1	1
FBgn0015772	2	2
FBgn0015773	2	2
FBgn0015788	1	1
FBgn0015790	1	1
FBgn0015794	1	1
FBgn0015838	1	2
FBgn0015907	2	5
FBgn0015933	1	1

FBgn0015954	2	3
FBgn0016059	1	1
FBgn0016132	1	2
FBgn0016641	1	1
FBgn0016691	1	1
FBgn0016693	1	1
FBgn0016694	1	1
FBgn0016696	1	1
FBgn0016715	1	1
FBgn0016724	1	2
FBgn0016756	1	2
FBgn0016794	1	1
FBgn0016930	3	4
FBgn0016977	4	5
FBgn0017453	1	1
FBgn0017549	1	1
FBgn0017566	1	1
FBgn0019830	1	1
FBgn0019886	1	1
FBgn0019890	1	3
FBgn0019952	1	2
FBgn0019968	2	2
FBgn0019990	1	1
FBgn0020129	1	1
FBgn0020251	1	1
FBgn0020258	1	1
FBgn0020261	1	1
FBgn0020270	1	1
FBgn0020294	1	1
FBgn0020299	2	2
FBgn0020307	1	1
FBgn0020309	1	1
FBgn0020369	2	2
FBgn0020370	1	1
FBgn0020385	3	6
FBgn0020386	1	1
FBgn0020388	1	1
FBgn0020389	1	1
FBgn0020414	1	1
FBgn0020415	1	1
FBgn0020416	1	1
FBgn0020496	2	7
FBgn0020503	1	2
FBgn0020510	1	1
FBgn0020616	1	1
FBgn0020618	1	1
FBgn0020762	1	1
FBgn0020910	1	1
FBgn0021764	2	2
FBgn0021818	1	1

FBgn0022343	2	2
FBgn0022359	1	1
FBgn0022361	2	10
FBgn0022710	3	3
FBgn0022764	2	2
FBgn0022768	4	5
FBgn0022787	1	1
FBgn0022935	1	1
FBgn0022981	1	1
FBgn0022986	1	1
FBgn0023001	1	2
FBgn0023023	1	1
FBgn0023081	1	1
FBgn0023130	1	1
FBgn0023172	1	1
FBgn0023211	1	1
FBgn0023215	2	2
FBgn0023216	1	1
FBgn0023395	1	2
FBgn0023395	1	2
FBgn0023416	3	3
FBgn0023417	1	3
FBgn0023444	1	1
FBgn0023506	1	1
FBgn0023508	1	1
FBgn0023511	1	1
FBgn0023515	1	1
FBgn0023529	1	1
FBgn0024150	4	11
FBgn0024232	4	4
FBgn0024238	1	1
FBgn0024251	2	3
FBgn0024252	1	1
FBgn0024291	1	1
FBgn0024308	2	15
FBgn0024320	1	1
FBgn0024326	1	1
FBgn0024361	1	1
FBgn0024371	1	1
FBgn0024732	2	2
FBgn0024913	1	4
FBgn0024923	1	1
FBgn0024958	1	2
FBgn0024996	1	1
FBgn0025394	1	1
FBgn0025455	2	2
FBgn0025458	1	4
FBgn0025593	1	1
FBgn0025630	1	1
FBgn0025631	1	1

FBgn0025639	2	2
FBgn0025682	1	1
FBgn0025725	1	1
FBgn0025741	2	2
FBgn0025743	1	2
FBgn0025802	1	1
FBgn0025803	3	6
FBgn0025814	1	1
FBgn0025864	1	2
FBgn0025937	1	1
FBgn0026059	2	2
FBgn0026084	1	2
FBgn0026090	1	1
FBgn0026319	1	1
FBgn0026380	1	1
FBgn0026404	1	1
FBgn0026417	1	1
FBgn0026418	1	2
FBgn0026428	1	1
FBgn0026597	2	2
FBgn0026619	2	2
FBgn0026620	2	2
FBgn0026741	2	2
FBgn0026753	1	1
FBgn0026761	1	1
FBgn0026777	1	1
FBgn0026787	1	1
FBgn0026872	1	1
FBgn0027363	1	1
FBgn0027495	2	3
FBgn0027497	1	1
FBgn0027507	1	1
FBgn0027508	2	2
FBgn0027512	4	4
FBgn0027518	1	1
FBgn0027523	1	1
FBgn0027527	2	15
FBgn0027529	1	2
FBgn0027532	1	1
FBgn0027534	1	3
FBgn0027538	1	1
FBgn0027540	2	2
FBgn0027550	1	2
FBgn0027554	1	1
FBgn0027556	1	1
FBgn0027561	1	1
FBgn0027569	1	1
FBgn0027580	1	1
FBgn0027581	5	11
FBgn0027582	2	2

FBgn0027584	2	2
FBgn0027594	2	2
FBgn0027596	1	1
FBgn0027598	3	6
FBgn0027607	1	1
FBgn0027655	1	1
FBgn0027660	1	1
FBgn0027836	1	1
FBgn0027950	1	1
FBgn0028382	1	1
FBgn0028397	1	1
FBgn0028398	1	1
FBgn0028399	2	2
FBgn0028467	2	6
FBgn0028470	2	3
FBgn0028475	2	2
FBgn0028476	1	1
FBgn0028479	1	1
FBgn0028484	2	3
FBgn0028486	1	3
FBgn0028490	2	11
FBgn0028496	1	1
FBgn0028500	2	2
FBgn0028513	1	2
FBgn0028539	1	1
FBgn0028633	1	1
FBgn0028679	1	1
FBgn0028686	1	1
FBgn0028694	1	1
FBgn0028695	2	2
FBgn0028717	3	4
FBgn0028741	2	2
FBgn0028848	2	2
FBgn0028876	1	1
FBgn0028877	1	1
FBgn0028879	1	1
FBgn0028892	2	3
FBgn0028939	1	1
FBgn0028940	1	2
FBgn0028946	1	1
FBgn0028969	1	3
FBgn0029167	7	8
FBgn0029525	1	1
FBgn0029687	2	5
FBgn0029688	2	2
FBgn0029693	2	2
FBgn0029716	2	2
FBgn0029718	1	1
FBgn0029721	1	1
FBgn0029724	1	1

FBgn0029738	1	1
FBgn0029756	1	1
FBgn0029763	1	1
FBgn0029766	2	2
FBgn0029798	2	2
FBgn0029824	1	1
FBgn0029870	1	1
FBgn0029891	1	1
FBgn0029893	2	4
FBgn0029897	1	1
FBgn0029912	1	1
FBgn0029925	1	1
FBgn0029932	1	2
FBgn0029944	1	1
FBgn0029959	1	1
FBgn0029970	1	1
FBgn0029992	1	1
FBgn0030018	1	1
FBgn0030038	4	9
FBgn0030047	1	2
FBgn0030052	1	1
FBgn0030087	3	3
FBgn0030088	1	1
FBgn0030093	1	2
FBgn0030112	1	1
FBgn0030115	1	1
FBgn0030121	1	1
FBgn0030130	5	6
FBgn0030142	1	1
FBgn0030174	1	1
FBgn0030183	1	1
FBgn0030184	1	1
FBgn0030194	1	1
FBgn0030205	7	10
FBgn0030223	1	1
FBgn0030243	2	3
FBgn0030245	1	2
FBgn0030246	1	1
FBgn0030286	1	3
FBgn0030289	1	1
FBgn0030296	2	2
FBgn0030299	2	4
FBgn0030306	1	1
FBgn0030311	2	3
FBgn0030321	1	1
FBgn0030329	1	1
FBgn0030345	1	1
FBgn0030351	2	12
FBgn0030357	1	1
FBgn0030364	1	1

FBgn0030390	3	3
FBgn0030433	1	3
FBgn0030437	2	2
FBgn0030438	1	1
FBgn0030448	1	1
FBgn0030457	1	6
FBgn0030478	1	1
FBgn0030479	1	15
FBgn0030503	2	2
FBgn0030504	1	1
FBgn0030505	1	1
FBgn0030506	1	1
FBgn0030522	1	2
FBgn0030530	1	1
FBgn0030554	1	1
FBgn0030569	1	1
FBgn0030582	1	1
FBgn0030589	1	1
FBgn0030612	1	1
FBgn0030613	4	9
FBgn0030625	1	1
FBgn0030638	1	1
FBgn0030646	1	1
FBgn0030660	1	1
FBgn0030666	1	1
FBgn0030674	7	9
FBgn0030700	1	1
FBgn0030701	1	1
FBgn0030702	1	1
FBgn0030718	1	1
FBgn0030726	2	2
FBgn0030731	1	1
FBgn0030749	1	1
FBgn0030755	1	1
FBgn0030758	2	2
FBgn0030790	1	1
FBgn0030796	1	1
FBgn0030808	1	1
FBgn0030812	4	13
FBgn0030820	1	1
FBgn0030832	1	1
FBgn0030843	1	1
FBgn0030854	1	1
FBgn0030858	2	2
FBgn0030859	1	1
FBgn0030863	2	5
FBgn0030878	1	1
FBgn0030879	1	1
FBgn0030882	1	1
FBgn0030887	1	2

FBgn0030891	3	4
FBgn0030927	1	1
FBgn0030930	1	1
FBgn0030945	1	1
FBgn0030967	2	2
FBgn0030974	2	6
FBgn0030985	1	1
FBgn0030986	2	3
FBgn0030987	1	1
FBgn0030990	1	1
FBgn0030999	1	1
FBgn0031001	1	1
FBgn0031011	1	4
FBgn0031016	2	4
FBgn0031024	1	1
FBgn0031038	2	2
FBgn0031046	3	5
FBgn0031051	3	3
FBgn0031089	3	4
FBgn0031098	3	4
FBgn0031107	3	3
FBgn0031118	2	4
FBgn0031140	1	1
FBgn0031160	2	2
FBgn0031162	1	1
FBgn0031187	1	1
FBgn0031201	2	3
FBgn0031216	1	1
FBgn0031227	2	5
FBgn0031233	1	1
FBgn0031260	1	2
FBgn0031266	1	1
FBgn0031291	6	18
FBgn0031312	1	1
FBgn0031313	1	1
FBgn0031314	1	1
FBgn0031326	1	1
FBgn0031356	1	1
FBgn0031358	3	4
FBgn0031374	4	5
FBgn0031408	1	2
FBgn0031415	1	1
FBgn0031450	1	2
FBgn0031456	1	1
FBgn0031464	2	2
FBgn0031489	1	1
FBgn0031500	1	1
FBgn0031511	1	1
FBgn0031515	1	1
FBgn0031536	2	2

FBgn0031538	1	1
FBgn0031566	1	1
FBgn0031571	4	4
FBgn0031600	1	1
FBgn0031689	1	4
FBgn0031713	2	2
FBgn0031717	1	1
FBgn0031762	1	1
FBgn0031779	1	1
FBgn0031781	1	1
FBgn0031799	1	2
FBgn0031836	2	3
FBgn0031855	1	1
FBgn0031861	1	1
FBgn0031868	1	1
FBgn0031879	3	3
FBgn0031883	1	1
FBgn0031894	2	5
FBgn0031896	1	1
FBgn0031897	1	1
FBgn0031899	1	2
FBgn0031904	1	1
FBgn0031905	1	1
FBgn0031925	1	1
FBgn0031930	1	1
FBgn0031955	1	1
FBgn0031965	1	1
FBgn0031985	1	1
FBgn0031992	1	1
FBgn0031995	1	1
FBgn0031999	2	2
FBgn0032002	1	1
FBgn0032013	1	1
FBgn0032033	1	1
FBgn0032034	1	1
FBgn0032047	3	3
FBgn0032055	2	3
FBgn0032114	1	1
FBgn0032120	1	1
FBgn0032129	1	1
FBgn0032132	1	1
FBgn0032136	3	3
FBgn0032157	1	1
FBgn0032167	1	1
FBgn0032170	1	1
FBgn0032172	1	1
FBgn0032178	1	1
FBgn0032180	3	9
FBgn0032204	1	1
FBgn0032207	1	1

FBgn0032208	1	1
FBgn0032210	1	1
FBgn0032213	2	2
FBgn0032215	1	1
FBgn0032234	1	1
FBgn0032309	2	3
FBgn0032330	1	1
FBgn0032339	1	1
FBgn0032340	1	1
FBgn0032348	1	3
FBgn0032363	1	1
FBgn0032389	1	1
FBgn0032394	1	1
FBgn0032400	1	1
FBgn0032401	1	1
FBgn0032409	2	2
FBgn0032420	2	2
FBgn0032430	1	1
FBgn0032467	2	2
FBgn0032469	2	2
FBgn0032473	1	1
FBgn0032476	2	2
FBgn0032479	1	1
FBgn0032480	2	2
FBgn0032485	1	1
FBgn0032497	1	2
FBgn0032516	2	2
FBgn0032517	1	1
FBgn0032524	1	1
FBgn0032587	1	1
FBgn0032622	1	2
FBgn0032633	1	1
FBgn0032638	1	1
FBgn0032642	2	2
FBgn0032655	1	1
FBgn0032681	1	1
FBgn0032683	1	1
FBgn0032686	1	1
FBgn0032690	1	1
FBgn0032729	1	1
FBgn0032745	1	1
FBgn0032749	1	1
FBgn0032763	1	1
FBgn0032794	2	2
FBgn0032817	1	1
FBgn0032821	2	5
FBgn0032831	1	1
FBgn0032835	1	1
FBgn0032838	1	1
FBgn0032847	1	1

FBgn0032865	1	3
FBgn0032877	1	1
FBgn0032883	1	1
FBgn0032899	1	1
FBgn0032923	1	1
FBgn0032938	3	4
FBgn0033005	1	1
FBgn0033021	1	1
FBgn0033051	1	3
FBgn0033092	2	4
FBgn0033108	1	1
FBgn0033184	1	1
FBgn0033191	3	3
FBgn0033192	2	3
FBgn0033205	1	4
FBgn0033224	1	1
FBgn0033249	1	1
FBgn0033257	1	1
FBgn0033260	1	2
FBgn0033269	1	2
FBgn0033310	1	1
FBgn0033317	1	1
FBgn0033321	1	1
FBgn0033339	2	3
FBgn0033351	1	1
FBgn0033352	1	1
FBgn0033377	2	2
FBgn0033398	2	3
FBgn0033402	1	1
FBgn0033424	1	1
FBgn0033442	1	1
FBgn0033448	1	1
FBgn0033454	2	3
FBgn0033459	1	1
FBgn0033475	2	4
FBgn0033486	2	2
FBgn0033495	1	1
FBgn0033504	2	2
FBgn0033539	1	1
FBgn0033555	1	1
FBgn0033583	2	22
FBgn0033594	1	1
FBgn0033636	4	23
FBgn0033638	1	1
FBgn0033653	1	1
FBgn0033654	1	1
FBgn0033675	1	1
FBgn0033707	1	1
FBgn0033714	1	3
FBgn0033717	1	1

FBgn0033724	1	1
FBgn0033750	1	2
FBgn0033789	1	1
FBgn0033814	1	1
FBgn0033835	1	2
FBgn0033837	1	1
FBgn0033844	1	1
FBgn0033846	2	2
FBgn0033885	1	1
FBgn0033886	1	1
FBgn0033889	1	1
FBgn0033904	1	1
FBgn0033917	1	1
FBgn0033920	1	1
FBgn0033926	1	1
FBgn0033957	1	1
FBgn0033964	1	2
FBgn0033982	1	1
FBgn0033995	3	14
FBgn0034009	1	1
FBgn0034029	1	1
FBgn0034035	1	1
FBgn0034049	1	1
FBgn0034052	1	2
FBgn0034070	3	3
FBgn0034075	1	1
FBgn0034079	2	2
FBgn0034083	3	3
FBgn0034091	1	1
FBgn0034110	2	4
FBgn0034112	1	1
FBgn0034117	1	1
FBgn0034118	1	2
FBgn0034119	1	1
FBgn0034141	2	2
FBgn0034162	2	2
FBgn0034186	1	1
FBgn0034187	1	2
FBgn0034214	1	1
FBgn0034219	1	1
FBgn0034221	1	1
FBgn0034240	2	2
FBgn0034246	1	1
FBgn0034262	2	2
FBgn0034265	2	2
FBgn0034308	1	1
FBgn0034313	1	1
FBgn0034314	2	2
FBgn0034355	1	1
FBgn0034366	1	1

FBgn0034367	1	1
FBgn0034380	1	1
FBgn0034381	1	2
FBgn0034387	1	1
FBgn0034394	4	9
FBgn0034396	1	1
FBgn0034400	1	1
FBgn0034410	1	1
FBgn0034417	1	1
FBgn0034421	2	4
FBgn0034422	1	1
FBgn0034441	1	1
FBgn0034447	1	2
FBgn0034474	1	1
FBgn0034528	1	1
FBgn0034529	1	1
FBgn0034540	1	1
FBgn0034573	1	1
FBgn0034583	1	3
FBgn0034590	2	3
FBgn0034598	3	4
FBgn0034612	2	8
FBgn0034618	1	1
FBgn0034638	2	4
FBgn0034685	1	2
FBgn0034691	2	2
FBgn0034706	1	1
FBgn0034708	1	2
FBgn0034712	1	1
FBgn0034718	1	1
FBgn0034724	1	1
FBgn0034728	1	1
FBgn0034750	1	4
FBgn0034760	1	1
FBgn0034786	1	1
FBgn0034797	1	1
FBgn0034802	3	16
FBgn0034853	1	1
FBgn0034862	2	2
FBgn0034888	1	1
FBgn0034898	1	1
FBgn0034926	1	1
FBgn0034967	2	2
FBgn0034970	1	1
FBgn0034976	1	1
FBgn0034987	4	4
FBgn0034999	1	1
FBgn0035015	1	1
FBgn0035016	1	1
FBgn0035024	1	1

FBgn0035028	1	1
FBgn0035030	1	1
FBgn0035049	1	1
FBgn0035056	1	1
FBgn0035060	1	1
FBgn0035085	2	2
FBgn0035091	1	1
FBgn0035107	1	3
FBgn0035111	2	2
FBgn0035113	1	1
FBgn0035145	2	2
FBgn0035148	1	1
FBgn0035152	2	2
FBgn0035154	1	1
FBgn0035189	1	1
FBgn0035204	1	1
FBgn0035205	1	3
FBgn0035206	2	2
FBgn0035231	1	1
FBgn0035234	2	2
FBgn0035236	2	2
FBgn0035237	3	3
FBgn0035244	1	1
FBgn0035253	2	2
FBgn0035268	1	1
FBgn0035296	1	1
FBgn0035297	1	1
FBgn0035323	2	2
FBgn0035333	2	2
FBgn0035338	2	2
FBgn0035348	1	2
FBgn0035357	1	4
FBgn0035373	3	3
FBgn0035382	1	1
FBgn0035397	1	1
FBgn0035400	1	1
FBgn0035402	1	1
FBgn0035403	1	1
FBgn0035404	1	1
FBgn0035438	1	2
FBgn0035440	1	1
FBgn0035448	1	1
FBgn0035482	1	1
FBgn0035484	1	1
FBgn0035490	1	1
FBgn0035497	1	1
FBgn0035500	1	2
FBgn0035504	2	3
FBgn0035513	1	1
FBgn0035533	1	1

FBgn0035539	1	1
FBgn0035540	1	1
FBgn0035568	1	1
FBgn0035574	2	2
FBgn0035633	3	3
FBgn0035637	2	2
FBgn0035693	1	1
FBgn0035704	1	14
FBgn0035713	1	1
FBgn0035769	1	1
FBgn0035770	1	1
FBgn0035827	1	1
FBgn0035833	3	4
FBgn0035835	1	1
FBgn0035848	1	2
FBgn0035851	1	1
FBgn0035871	1	1
FBgn0035877	1	1
FBgn0035879	1	1
FBgn0035910	2	3
FBgn0035938	2	6
FBgn0035947	1	3
FBgn0035950	1	1
FBgn0035953	1	1
FBgn0035976	1	1
FBgn0035978	1	1
FBgn0035986	1	1
FBgn0035989	1	1
FBgn0036017	1	1
FBgn0036020	1	1
FBgn0036032	1	2
FBgn0036043	1	1
FBgn0036052	1	1
FBgn0036053	1	1
FBgn0036057	2	3
FBgn0036059	1	1
FBgn0036060	1	1
FBgn0036063	1	1
FBgn0036066	1	1
FBgn0036111	1	1
FBgn0036127	2	2
FBgn0036143	1	1
FBgn0036148	1	1
FBgn0036180	1	1
FBgn0036213	1	2
FBgn0036220	1	1
FBgn0036226	1	1
FBgn0036248	1	2
FBgn0036271	1	1
FBgn0036279	2	2

FBgn0036286	2	2
FBgn0036299	1	1
FBgn0036302	2	2
FBgn0036309	1	1
FBgn0036318	1	1
FBgn0036321	1	1
FBgn0036341	2	10
FBgn0036347	1	1
FBgn0036364	1	1
FBgn0036376	1	1
FBgn0036389	2	2
FBgn0036436	1	1
FBgn0036440	3	4
FBgn0036449	1	1
FBgn0036450	1	2
FBgn0036472	1	1
FBgn0036475	1	1
FBgn0036484	1	1
FBgn0036505	1	5
FBgn0036510	1	1
FBgn0036511	7	22
FBgn0036518	4	8
FBgn0036529	1	1
FBgn0036533	1	1
FBgn0036534	1	1
FBgn0036548	2	2
FBgn0036558	2	3
FBgn0036566	2	3
FBgn0036573	1	1
FBgn0036580	1	1
FBgn0036612	2	2
FBgn0036627	1	1
FBgn0036637	1	1
FBgn0036642	1	1
FBgn0036663	2	2
FBgn0036678	1	1
FBgn0036680	1	4
FBgn0036684	3	3
FBgn0036686	1	1
FBgn0036695	1	1
FBgn0036702	1	1
FBgn0036736	1	1
FBgn0036741	2	3
FBgn0036746	2	2
FBgn0036761	1	1
FBgn0036762	1	1
FBgn0036814	2	2
FBgn0036816	1	2
FBgn0036819	1	1
FBgn0036826	1	1

FBgn0036827	1	1
FBgn0036836	1	1
FBgn0036837	2	2
FBgn0036838	1	1
FBgn0036894	1	1
FBgn0036896	1	1
FBgn0036901	2	2
FBgn0036904	1	3
FBgn0036913	2	2
FBgn0036930	2	2
FBgn0036931	1	1
FBgn0036932	2	2
FBgn0036964	1	1
FBgn0036974	1	1
FBgn0036994	1	1
FBgn0037066	1	2
FBgn0037074	1	1
FBgn0037090	1	1
FBgn0037093	1	1
FBgn0037098	2	2
FBgn0037109	4	6
FBgn0037120	1	1
FBgn0037129	1	1
FBgn0037135	1	1
FBgn0037137	2	2
FBgn0037144	1	1
FBgn0037150	1	1
FBgn0037170	1	1
FBgn0037185	1	1
FBgn0037186	1	1
FBgn0037213	2	2
FBgn0037218	2	2
FBgn0037238	1	1
FBgn0037239	1	1
FBgn0037244	2	2
FBgn0037248	1	1
FBgn0037256	2	2
FBgn0037277	3	17
FBgn0037278	1	1
FBgn0037279	1	1
FBgn0037285	1	1
FBgn0037307	1	1
FBgn0037308	1	1
FBgn0037312	2	2
FBgn0037344	1	2
FBgn0037346	1	1
FBgn0037347	1	1
FBgn0037356	1	1
FBgn0037370	1	1
FBgn0037373	1	1

FBgn0037381	1	1
FBgn0037415	1	3
FBgn0037420	2	2
FBgn0037434	1	1
FBgn0037444	1	2
FBgn0037447	1	1
FBgn0037448	1	1
FBgn0037466	1	1
FBgn0037469	1	1
FBgn0037470	1	1
FBgn0037472	1	2
FBgn0037530	1	1
FBgn0037531	2	2
FBgn0037536	1	1
FBgn0037541	3	3
FBgn0037548	1	7
FBgn0037562	1	1
FBgn0037582	2	2
FBgn0037619	1	1
FBgn0037623	1	1
FBgn0037650	1	5
FBgn0037655	2	2
FBgn0037660	2	2
FBgn0037663	2	3
FBgn0037680	1	1
FBgn0037701	1	1
FBgn0037708	1	1
FBgn0037715	1	1
FBgn0037718	1	1
FBgn0037720	1	1
FBgn0037730	1	2
FBgn0037744	1	1
FBgn0037757	1	1
FBgn0037758	3	5
FBgn0037763	1	1
FBgn0037781	1	1
FBgn0037800	1	1
FBgn0037804	1	1
FBgn0037816	1	1
FBgn0037901	1	1
FBgn0037928	1	1
FBgn0037929	1	1
FBgn0037931	1	1
FBgn0037954	2	4
FBgn0037960	1	3
FBgn0037964	1	1
FBgn0037967	1	1
FBgn0037973	1	1
FBgn0037975	1	1
FBgn0037977	1	1

FBgn0037980	1	1
FBgn0037989	1	1
FBgn0038037	1	2
FBgn0038038	1	1
FBgn0038041	1	1
FBgn0038074	1	1
FBgn0038088	2	2
FBgn0038098	1	1
FBgn0038111	2	2
FBgn0038124	1	1
FBgn0038146	1	1
FBgn0038151	1	1
FBgn0038166	1	1
FBgn0038171	2	2
FBgn0038197	1	1
FBgn0038220	1	1
FBgn0038226	1	1
FBgn0038237	1	2
FBgn0038241	1	1
FBgn0038251	2	2
FBgn0038259	1	1
FBgn0038261	1	1
FBgn0038301	1	1
FBgn0038311	2	2
FBgn0038312	1	1
FBgn0038316	1	1
FBgn0038319	1	1
FBgn0038320	1	1
FBgn0038321	1	1
FBgn0038344	2	2
FBgn0038364	1	1
FBgn0038376	1	1
FBgn0038407	1	1
FBgn0038437	2	2
FBgn0038463	1	1
FBgn0038473	1	2
FBgn0038482	1	1
FBgn0038488	1	1
FBgn0038492	1	1
FBgn0038504	1	1
FBgn0038505	1	2
FBgn0038547	1	1
FBgn0038550	1	1
FBgn0038556	4	4
FBgn0038559	1	1
FBgn0038598	1	1
FBgn0038611	1	1
FBgn0038652	1	1
FBgn0038655	1	2
FBgn0038679	4	10

FBgn0038686	1	1
FBgn0038704	1	1
FBgn0038708	1	2
FBgn0038739	1	1
FBgn0038740	1	1
FBgn0038742	1	1
FBgn0038745	2	5
FBgn0038747	1	2
FBgn0038760	2	2
FBgn0038786	2	2
FBgn0038803	1	1
FBgn0038810	1	1
FBgn0038853	1	1
FBgn0038854	2	2
FBgn0038855	1	1
FBgn0038863	1	1
FBgn0038874	1	1
FBgn0038877	1	1
FBgn0038881	3	3
FBgn0038889	1	2
FBgn0038912	1	1
FBgn0038925	1	1
FBgn0038951	1	1
FBgn0039000	1	1
FBgn0039003	2	2
FBgn0039026	1	1
FBgn0039043	1	1
FBgn0039073	1	1
FBgn0039084	2	2
FBgn0039091	1	1
FBgn0039094	1	1
FBgn0039101	1	1
FBgn0039117	1	1
FBgn0039122	1	2
FBgn0039130	1	1
FBgn0039132	1	3
FBgn0039169	1	1
FBgn0039178	1	1
FBgn0039179	1	1
FBgn0039187	1	1
FBgn0039189	1	1
FBgn0039203	1	2
FBgn0039207	1	1
FBgn0039208	1	1
FBgn0039211	1	1
FBgn0039223	1	1
FBgn0039224	1	5
FBgn0039226	1	1
FBgn0039229	1	1
FBgn0039240	1	1

FBgn0039249	2	2
FBgn0039260	1	1
FBgn0039265	1	1
FBgn0039297	1	1
FBgn0039338	2	4
FBgn0039349	2	2
FBgn0039352	1	1
FBgn0039366	1	1
FBgn0039420	1	1
FBgn0039433	1	5
FBgn0039451	3	3
FBgn0039488	1	2
FBgn0039523	2	2
FBgn0039560	1	2
FBgn0039562	1	1
FBgn0039590	1	1
FBgn0039594	2	2
FBgn0039626	1	3
FBgn0039628	1	1
FBgn0039632	2	2
FBgn0039637	1	1
FBgn0039639	1	1
FBgn0039644	1	1
FBgn0039674	1	1
FBgn0039680	2	2
FBgn0039691	1	1
FBgn0039696	2	3
FBgn0039712	1	1
FBgn0039714	2	2
FBgn0039732	1	3
FBgn0039737	1	1
FBgn0039756	1	2
FBgn0039774	1	1
FBgn0039776	1	1
FBgn0039790	1	1
FBgn0039818	3	3
FBgn0039846	1	1
FBgn0039857	1	1
FBgn0039863	2	2
FBgn0039889	1	1
FBgn0039904	1	1
FBgn0039907	3	6
FBgn0039928	1	1
FBgn0040523	1	1
FBgn0040637	4	23
FBgn0040663	1	1
FBgn0040717	1	1
FBgn0040900	1	1
FBgn0040968	1	1
FBgn0040995	1	1

FBgn0000008	2	3
FBgn0000011	3	20
FBgn0000017	8	41
FBgn0000018	1	1
FBgn0000046	4	5
FBgn0000047	4	5
FBgn0000061	1	1
FBgn0000108	1	2
FBgn0000119	1	2
FBgn0000140	1	19
FBgn0000171	1	2
FBgn0000179	1	1
FBgn0000228	1	2
FBgn0000251	1	2
FBgn0000303	1	1
FBgn0000313	1	1
FBgn0000326	1	1
FBgn0000337	1	1
FBgn0000349	1	1
FBgn0000351	1	1
FBgn0000394	2	2
FBgn0000410	1	1
FBgn0000414	5	5
FBgn0000427	1	1
FBgn0000442	1	1
FBgn0000454	1	1
FBgn0000455	2	2
FBgn0000464	4	4
FBgn0000472	1	1
FBgn0000479	4	13
FBgn0000520	1	1
FBgn0000527	1	1
FBgn0000541	1	2
FBgn0000576	1	1
FBgn0000581	2	2
FBgn0000592	1	1
FBgn0000630	3	3
FBgn0000826	1	1
FBgn0000927	1	1
FBgn0001083	1	1
FBgn0001086	2	3
FBgn0001087	1	1
FBgn0001099	1	4
FBgn0001128	1	1
FBgn0001174	1	1
FBgn0001179	1	1
FBgn0001180	2	2
FBgn0001216	2	4
FBgn0001217	1	1
FBgn0001218	2	5

FBgn0001253	4	10
FBgn0001263	1	1
FBgn0001269	2	7
FBgn0001321	1	1
FBgn0001323	5	14
FBgn0001324	1	1
FBgn0001325	1	1
FBgn0001341	1	1
FBgn0001402	2	3
FBgn0001612	1	1
FBgn0001624	2	3
FBgn0001965	1	3
FBgn0001967	1	2
FBgn0001978	3	3
FBgn0001986	1	2
FBgn0001990	1	6
FBgn0002021	2	4
FBgn0002174	1	1
FBgn0002440	2	18
FBgn0002478	1	1
FBgn0002534	1	1
FBgn0002542	1	1
FBgn0002577	2	2
FBgn0002673	2	13
FBgn0002709	1	1
FBgn0002715	1	1
FBgn0002774	2	2
FBgn0002791	1	1
FBgn0002872	1	1
FBgn0002901	1	1
FBgn0002917	1	1
FBgn0002920	2	7
FBgn0002924	1	1
FBgn0002931	1	1
FBgn0002938	1	1
FBgn0002945	1	3
FBgn0002948	2	2
FBgn0002970	1	1
FBgn0002989	2	3
FBgn0003002	1	1
FBgn0003008	1	1
FBgn0003011	1	1
FBgn0003013	1	1
FBgn0003015	1	1
FBgn0003022	1	1
FBgn0003028	1	1
FBgn0003060	1	1
FBgn0003062	3	14
FBgn0003076	1	1
FBgn0003090	2	3

FBgn0003137	3	5
FBgn0003149	1	4
FBgn0003159	2	4
FBgn0003162	1	1
FBgn0003200	1	1
FBgn0003210	1	1
FBgn0003217	5	69
FBgn0003244	1	1
FBgn0003255	2	2
FBgn0003300	1	2
FBgn0003308	1	1
FBgn0003321	1	1
FBgn0003349	1	1
FBgn0003358	1	1
FBgn0003380	1	1
FBgn0003392	1	1
FBgn0003411	1	1
FBgn0003425	2	2
FBgn0003429	1	1
FBgn0003432	4	4
FBgn0003459	2	2
FBgn0003470	2	2
FBgn0003483	1	3
FBgn0003525	1	1
FBgn0003559	1	1
FBgn0003654	1	7
FBgn0003676	1	1
FBgn0003715	1	3
FBgn0003719	2	8
FBgn0003732	1	1
FBgn0003744	1	1
FBgn0003749	2	3
FBgn0003861	1	1
FBgn0003865	1	1
FBgn0003870	1	1
FBgn0003882	1	1
FBgn0003890	1	2
FBgn0003892	1	1
FBgn0004009	1	3
FBgn0004045	1	1
FBgn0004053	1	1
FBgn0004057	1	1
FBgn0004102	1	1
FBgn0004110	1	9
FBgn0004143	2	4
FBgn0004174	1	1
FBgn0004175	1	9
FBgn0004197	1	1
FBgn0004244	1	1
FBgn0004372	1	1

FBgn0004373	2	2
FBgn0004374	1	1
FBgn0004377	1	1
FBgn0004387	1	1
FBgn0004391	2	3
FBgn0004400	1	1
FBgn0004401	1	1
FBgn0004407	1	1
FBgn0004431	2	2
FBgn0004449	1	1
FBgn0004461	1	1
FBgn0004493	1	2
FBgn0004512	1	1
FBgn0004513	1	1
FBgn0004575	3	5
FBgn0004579	2	3
FBgn0004581	1	1
FBgn0004606	1	1
FBgn0004647	8	9
FBgn0004650	1	1
FBgn0004652	1	1
FBgn0004778	1	1
FBgn0004797	1	1
FBgn0004833	1	1
FBgn0004839	2	3
FBgn0004854	1	1
FBgn0004870	3	3
FBgn0004873	1	1
FBgn0004875	1	1
FBgn0004878	1	1
FBgn0004892	1	1
FBgn0004897	1	1
FBgn0005322	3	3
FBgn0005390	1	1
FBgn0005536	1	3
FBgn0005558	2	2
FBgn0005563	1	1
FBgn0005592	1	1
FBgn0005596	1	1
FBgn0005614	2	2
FBgn0005617	2	2
FBgn0005619	1	1
FBgn0005626	1	1
FBgn0005630	3	12
FBgn0005639	1	1
FBgn0005654	1	1
FBgn0005666	3	4
FBgn0008646	4	6
FBgn0010019	2	2
FBgn0010040	1	1

FBgn0010053	1	1
FBgn0010070	1	1
FBgn0010110	5	5
FBgn0010197	2	2
FBgn0010198	1	1
FBgn0010241	1	1
FBgn0010247	1	2
FBgn0010258	1	2
FBgn0010303	1	1
FBgn0010323	1	1
FBgn0010338	1	1
FBgn0010340	1	2
FBgn0010349	2	3
FBgn0010382	1	2
FBgn0010416	1	1
FBgn0010453	1	1
FBgn0010473	1	1
FBgn0010488	1	16
FBgn0010575	3	3
FBgn0010611	1	1
FBgn0010768	1	2
FBgn0010786	1	1
FBgn0010803	2	6
FBgn0010825	2	2
FBgn0010877	1	1
FBgn0010905	1	1
FBgn0010909	1	1
FBgn0010940	2	2
FBgn0011204	1	1
FBgn0011227	1	1
FBgn0011232	2	2
FBgn0011244	1	1
FBgn0011278	1	1
FBgn0011281	1	1
FBgn0011286	4	5
FBgn0011305	2	2
FBgn0011425	1	1
FBgn0011474	2	2
FBgn0011481	2	3
FBgn0011596	1	1
FBgn0011643	1	1
FBgn0011694	1	1
FBgn0011700	2	2
FBgn0011739	2	2
FBgn0011774	1	1
FBgn0011828	1	3
FBgn0012051	1	2
FBgn0013275	1	1
FBgn0013276	1	1
FBgn0013277	1	1

FBgn0013278	1	1
FBgn0013279	1	1
FBgn0013334	1	1
FBgn0013442	1	1
FBgn0013531	1	1
FBgn0013679	1	1
FBgn0013732	1	1
FBgn0013756	1	2
FBgn0013763	2	3
FBgn0013772	1	1
FBgn0013810	2	2
FBgn0013811	7	8
FBgn0013813	3	3
FBgn0013983	1	1
FBgn0013995	1	2
FBgn0014189	1	1
FBgn0014374	1	1
FBgn0014432	2	2
FBgn0014455	1	1
FBgn0014859	1	1
FBgn0014863	1	1
FBgn0014870	1	1
FBgn0014931	1	1
FBgn0015034	1	1
FBgn0015039	1	1
FBgn0015245	2	2
FBgn0015269	2	2
FBgn0015277	2	3
FBgn0015380	1	1
FBgn0015390	2	2
FBgn0015391	2	2
FBgn0015402	2	2
FBgn0015477	2	12
FBgn0015541	1	1
FBgn0015546	1	1
FBgn0015553	1	1
FBgn0015574	1	1
FBgn0015600	3	4
FBgn0015609	2	2
FBgn0015618	1	1
FBgn0015625	2	2
FBgn0015781	1	1
FBgn0015799	1	2
FBgn0015905	1	1
FBgn0016047	2	2
FBgn0016075	3	3
FBgn0016081	3	3
FBgn0016684	1	1
FBgn0016718	3	3
FBgn0016792	3	3

FBgn0016797	2	4
FBgn0017457	1	2
FBgn0017590	2	6
FBgn0019652	2	2
FBgn0019686	1	1
FBgn0019839	1	1
FBgn0019938	1	1
FBgn0019960	1	5
FBgn0020257	1	1
FBgn0020300	1	5
FBgn0020306	2	2
FBgn0020312	1	1
FBgn0020371	1	3
FBgn0020377	3	3
FBgn0020399	1	2
FBgn0020439	2	2
FBgn0020497	1	1
FBgn0020517	1	1
FBgn0020642	1	2
FBgn0020756	3	3
FBgn0020880	1	1
FBgn0020887	1	1
FBgn0020907	1	1
FBgn0021742	1	1
FBgn0021760	1	1
FBgn0021761	1	1
FBgn0021767	1	1
FBgn0021776	1	1
FBgn0021796	1	1
FBgn0021872	1	1
FBgn0021873	2	2
FBgn0021874	1	1
FBgn0021895	2	3
FBgn0021906	1	1
FBgn0021995	1	1
FBgn0022160	1	1
FBgn0022201	2	2
FBgn0022288	1	1
FBgn0022699	1	1
FBgn0022702	1	1
FBgn0022772	1	1
FBgn0022774	1	1
FBgn0022985	1	1
FBgn0022987	2	2
FBgn0023083	2	2
FBgn0023090	1	1
FBgn0023097	1	1
FBgn0023171	1	1
FBgn0023181	1	1
FBgn0023184	1	1

FBgn0023441	1	1
FBgn0023458	6	6
FBgn0023496	1	1
FBgn0023510	2	2
FBgn0023517	1	1
FBgn0023518	1	3
FBgn0023524	1	1
FBgn0023527	1	1
FBgn0023535	1	1
FBgn0023540	1	1
FBgn0023542	1	4
FBgn0024177	1	1
FBgn0024179	1	1
FBgn0024191	1	1
FBgn0024227	1	1
FBgn0024242	3	3
FBgn0024273	1	4
FBgn0024277	1	1
FBgn0024314	2	2
FBgn0024321	2	2
FBgn0024329	1	1
FBgn0024332	1	3
FBgn0024365	1	1
FBgn0024366	1	1
FBgn0024491	2	2
FBgn0024510	1	1
FBgn0024698	1	1
FBgn0024740	1	1
FBgn0024836	3	5
FBgn0024909	1	1
FBgn0024941	1	1
FBgn0024956	1	1
FBgn0024963	1	1
FBgn0024973	1	1
FBgn0024992	1	2
FBgn0025355	1	1
FBgn0025382	1	2
FBgn0025383	1	1
FBgn0025387	1	1
FBgn0025388	3	4
FBgn0025391	1	1
FBgn0025393	1	1
FBgn0025525	2	2
FBgn0025574	1	1
FBgn0025583	1	1
FBgn0025613	1	1
FBgn0025618	1	2
FBgn0025620	1	1
FBgn0025623	3	3
FBgn0025625	1	1

FBgn0025641	2	2
FBgn0025681	1	1
FBgn0025686	1	1
FBgn0025709	1	1
FBgn0025716	1	1
FBgn0025726	4	4
FBgn0025739	1	1
FBgn0025740	1	1
FBgn0025777	1	1
FBgn0025808	1	1
FBgn0026015	1	1
FBgn0026079	1	1
FBgn0026083	5	7
FBgn0026087	1	1
FBgn0026145	1	2
FBgn0026160	3	5
FBgn0026178	1	1
FBgn0026193	2	2
FBgn0026206	2	2
FBgn0026268	1	1
FBgn0026313	1	1
FBgn0026315	1	1
FBgn0026317	2	3
FBgn0026373	1	1
FBgn0026375	2	8
FBgn0026402	1	1
FBgn0026427	3	4
FBgn0026438	1	1
FBgn0026567	1	1
FBgn0026575	1	1
FBgn0026577	1	1
FBgn0026578	1	1
FBgn0026598	1	1
FBgn0026616	1	1
FBgn0026722	3	24
FBgn0026729	1	1
FBgn0026875	3	3
FBgn0026876	1	1
FBgn0027070	1	1
FBgn0027080	1	1
FBgn0027087	2	2
FBgn0027091	1	1
FBgn0027101	1	1
FBgn0027342	1	1
FBgn0027348	1	1
FBgn0027375	2	2
FBgn0027376	1	1
FBgn0027499	1	1
FBgn0027500	2	2
FBgn0027509	1	1

FBgn0027522	2	3
FBgn0027541	2	2
FBgn0027559	1	1
FBgn0027571	3	3
FBgn0027575	2	3
FBgn0027578	2	3
FBgn0027585	1	1
FBgn0027602	1	1
FBgn0027620	1	1
FBgn0027654	2	2
FBgn0027792	1	1
FBgn0027794	1	1
FBgn0027903	1	1
FBgn0027929	1	2
FBgn0028369	1	1
FBgn0028370	1	1
FBgn0028371	2	2
FBgn0028386	2	2
FBgn0028388	1	1
FBgn0028400	2	2
FBgn0028408	2	2
FBgn0028418	1	1
FBgn0028420	1	1
FBgn0028427	1	1
FBgn0028428	2	2
FBgn0028431	5	20
FBgn0028435	1	2
FBgn0028474	2	2
FBgn0028494	1	1
FBgn0028509	1	1
FBgn0028514	1	1
FBgn0028520	1	1
FBgn0028525	1	1
FBgn0028529	1	1
FBgn0028532	1	1
FBgn0028543	1	1
FBgn0028554	1	2
FBgn0028562	1	1
FBgn0028570	1	1
FBgn0028572	2	3
FBgn0028573	1	1
FBgn0028577	1	1
FBgn0028642	1	1
FBgn0028647	2	2
FBgn0028699	1	1
FBgn0028701	2	2
FBgn0028704	3	3
FBgn0028707	1	1
FBgn0028734	1	1
FBgn0028838	1	2

FBgn0028841	1	1
FBgn0028862	1	1
FBgn0028863	3	5
FBgn0028870	1	1
FBgn0028881	1	1
FBgn0028891	2	2
FBgn0028893	1	1
FBgn0028897	1	1
FBgn0028899	2	2
FBgn0028901	2	2
FBgn0028918	1	1
FBgn0028920	1	1
FBgn0028947	1	1
FBgn0028956	1	1
FBgn0028961	1	1
FBgn0028963	2	2
FBgn0028970	1	6
FBgn0028974	3	4
FBgn0028978	2	2
FBgn0028979	1	1
FBgn0028987	1	1
FBgn0028991	2	2
FBgn0028996	1	1
FBgn0028997	2	2
FBgn0029006	2	2
FBgn0029082	2	3
FBgn0029084	1	1
FBgn0029092	1	1
FBgn0029095	1	1
FBgn0029131	1	1
FBgn0029147	1	1
FBgn0029157	1	1
FBgn0029174	1	2
FBgn0029176	2	2
FBgn0029503	1	1
FBgn0029507	2	3
FBgn0029531	1	1
FBgn0029535	1	1
FBgn0029608	1	1
FBgn0029648	1	1
FBgn0029684	1	1
FBgn0029694	1	1
FBgn0029704	1	1
FBgn0029708	1	1
FBgn0029728	1	1
FBgn0029731	2	2
FBgn0029736	1	1
FBgn0029745	1	1
FBgn0029748	2	3
FBgn0029749	1	1

FBgn0029750	1	1
FBgn0029762	1	5
FBgn0029769	1	2
FBgn0029782	1	1
FBgn0029795	2	2
FBgn0029797	3	5
FBgn0029808	2	8
FBgn0029812	2	3
FBgn0029814	2	2
FBgn0029818	1	1
FBgn0029834	1	1
FBgn0029835	2	2
FBgn0029836	1	1
FBgn0029840	4	5
FBgn0029843	1	1
FBgn0029846	2	2
FBgn0029849	2	2
FBgn0029850	1	1
FBgn0029857	1	1
FBgn0029869	1	1
FBgn0029871	2	4
FBgn0029872	2	2
FBgn0029874	1	2
FBgn0029875	1	1
FBgn0029887	1	4
FBgn0029895	1	1
FBgn0029901	3	7
FBgn0029904	1	1
FBgn0029920	1	2
FBgn0029922	1	1
FBgn0029931	1	2
FBgn0029963	2	2
FBgn0029966	1	1
FBgn0029979	3	4
FBgn0029999	2	2
FBgn0030000	1	1
FBgn0030003	1	1
FBgn0030009	1	1
FBgn0030011	1	1
FBgn0030016	1	1
FBgn0030033	1	1
FBgn0030034	1	1
FBgn0030051	2	3
FBgn0030057	1	1
FBgn0030065	1	1
FBgn0030081	1	1
FBgn0030090	1	1
FBgn0030091	1	1
FBgn0030100	2	4
FBgn0030103	1	1

FBgn0030106	1	1
FBgn0030108	1	1
FBgn0030144	2	2
FBgn0030150	2	3
FBgn0030170	1	1
FBgn0030171	1	1
FBgn0030172	1	1
FBgn0030181	1	1
FBgn0030186	3	7
FBgn0030195	2	2
FBgn0030206	1	1
FBgn0030207	1	3
FBgn0030216	4	5
FBgn0030217	1	1
FBgn0030219	3	6
FBgn0030224	1	1
FBgn0030248	3	4
FBgn0030249	2	2
FBgn0030251	1	1
FBgn0030252	1	1
FBgn0030257	1	1
FBgn0030259	1	1
FBgn0030264	1	1
FBgn0030266	1	1
FBgn0030291	1	1
FBgn0030293	3	3
FBgn0030300	1	1
FBgn0030339	1	1
FBgn0030353	3	3
FBgn0030369	1	1
FBgn0030375	2	2
FBgn0030376	3	6
FBgn0030377	2	2
FBgn0030387	2	9
FBgn0030388	4	7
FBgn0030397	1	1
FBgn0030401	3	3
FBgn0030412	3	24
FBgn0030417	2	2
FBgn0030420	1	1
FBgn0030444	1	2
FBgn0030462	1	1
FBgn0030476	2	2
FBgn0030500	1	1
FBgn0030502	3	113
FBgn0030508	2	2
FBgn0030511	1	2
FBgn0030553	1	1
FBgn0030566	2	3
FBgn0030570	1	1

FBgn0030571	1	12
FBgn0030591	1	1
FBgn0030592	1	1
FBgn0030594	1	1
FBgn0030597	3	14
FBgn0030600	4	9
FBgn0030617	1	2
FBgn0030634	1	1
FBgn0030636	2	2
FBgn0030647	2	2
FBgn0030655	1	1
FBgn0030661	1	1
FBgn0030664	1	1
FBgn0030675	1	1
FBgn0030681	1	1
FBgn0030683	2	2
FBgn0030684	1	1
FBgn0030685	1	1
FBgn0030687	1	1
FBgn0030696	1	1
FBgn0030706	2	2
FBgn0030707	1	1
FBgn0030717	1	1
FBgn0030721	1	1
FBgn0030741	1	1
FBgn0030746	3	3
FBgn0030747	1	1
FBgn0030761	1	1
FBgn0030769	1	1
FBgn0030773	1	1
FBgn0030787	2	2
FBgn0030789	1	1
FBgn0030794	1	1
FBgn0030823	1	1
FBgn0030833	1	1
FBgn0030835	2	2
FBgn0030841	1	1
FBgn0030842	5	5
FBgn0030851	1	1
FBgn0030868	1	1
FBgn0030869	2	2
FBgn0030871	1	1
FBgn0030872	1	1
FBgn0030877	1	1
FBgn0030881	1	1
FBgn0030901	1	1
FBgn0030904	1	2
FBgn0030909	1	1
FBgn0030913	1	1
FBgn0030914	1	1

FBgn0030940	1	1
FBgn0030942	1	1
FBgn0030943	1	1
FBgn0030950	1	1
FBgn0030964	1	1
FBgn0030965	2	2
FBgn0030975	1	1
FBgn0030993	1	1
FBgn0030997	3	6
FBgn0031006	2	2
FBgn0031020	1	1
FBgn0031023	2	3
FBgn0031033	2	2
FBgn0031048	1	1
FBgn0031052	1	1
FBgn0031057	3	5
FBgn0031078	1	1
FBgn0031088	1	3
FBgn0031111	1	2
FBgn0031119	2	2
FBgn0031123	1	1
FBgn0031124	1	1
FBgn0031148	1	1
FBgn0031149	1	2
FBgn0031168	1	1
FBgn0031170	1	1
FBgn0031171	1	1
FBgn0031189	1	1
FBgn0031191	2	2
FBgn0031192	3	3
FBgn0031194	1	2
FBgn0031195	2	14
FBgn0031225	1	1
FBgn0031226	1	4
FBgn0031238	1	1
FBgn0031239	2	2
FBgn0031243	1	1
FBgn0031257	1	1
FBgn0031258	1	1
FBgn0031262	1	1
FBgn0031265	2	2
FBgn0031275	1	1
FBgn0031281	1	1
FBgn0031293	1	2
FBgn0031311	1	3
FBgn0031325	1	1
FBgn0031332	1	1
FBgn0031349	2	6
FBgn0031361	1	1
FBgn0031367	1	1

FBgn0031373	1	1
FBgn0031375	2	2
FBgn0031377	3	3
FBgn0031406	1	1
FBgn0031414	2	2
FBgn0031416	4	11
FBgn0031419	1	1
FBgn0031424	2	2
FBgn0031441	1	3
FBgn0031443	1	2
FBgn0031444	2	2
FBgn0031451	1	1
FBgn0031452	1	1
FBgn0031468	1	1
FBgn0031473	2	2
FBgn0031492	2	2
FBgn0031509	1	2
FBgn0031519	1	1
FBgn0031522	1	1
FBgn0031523	2	2
FBgn0031527	1	1
FBgn0031540	1	1
FBgn0031545	1	1
FBgn0031546	1	1
FBgn0031547	1	1
FBgn0031556	1	2
FBgn0031592	2	4
FBgn0031602	2	3
FBgn0031610	1	1
FBgn0031611	2	2
FBgn0031620	2	2
FBgn0031622	1	1
FBgn0031634	1	1
FBgn0031644	1	2
FBgn0031652	1	1
FBgn0031654	1	1
FBgn0031696	1	1
FBgn0031698	2	2
FBgn0031702	1	10
FBgn0031724	1	1
FBgn0031728	2	2
FBgn0031730	1	1
FBgn0031737	1	4
FBgn0031745	1	1
FBgn0031749	1	1
FBgn0031751	1	1
FBgn0031754	1	1
FBgn0031757	1	1
FBgn0031766	1	2
FBgn0031770	1	1

FBgn0031775	1	1
FBgn0031777	1	2
FBgn0031783	1	1
FBgn0031824	2	4
FBgn0031826	1	1
FBgn0031850	1	1
FBgn0031857	1	1
FBgn0031859	2	2
FBgn0031866	1	7
FBgn0031874	1	1
FBgn0031878	2	3
FBgn0031881	1	1
FBgn0031882	1	1
FBgn0031900	1	1
FBgn0031902	2	3
FBgn0031918	1	1
FBgn0031926	1	1
FBgn0031927	2	2
FBgn0031936	1	1
FBgn0031945	1	1
FBgn0031947	2	2
FBgn0031959	1	1
FBgn0031961	1	1
FBgn0031970	1	2
FBgn0031981	2	3
FBgn0032021	1	2
FBgn0032029	1	1
FBgn0032050	2	2
FBgn0032051	1	1
FBgn0032073	1	2
FBgn0032083	1	2
FBgn0032142	1	1
FBgn0032162	1	1
FBgn0032175	1	2
FBgn0032176	1	1
FBgn0032183	1	1
FBgn0032206	2	2
FBgn0032224	1	5
FBgn0032243	2	2
FBgn0032250	1	1
FBgn0032252	1	1
FBgn0032260	1	1
FBgn0032262	1	1
FBgn0032268	1	2
FBgn0032269	1	2
FBgn0032271	1	1
FBgn0032286	2	2
FBgn0032292	1	2
FBgn0032296	1	1
FBgn0032310	1	1

FBgn0032311	1	1
FBgn0032329	1	1
FBgn0032338	1	1
FBgn0032343	1	1
FBgn0032345	1	1
FBgn0032347	1	1
FBgn0032359	1	1
FBgn0032360	1	3
FBgn0032368	1	1
FBgn0032378	3	30
FBgn0032379	1	1
FBgn0032387	1	1
FBgn0032414	1	1
FBgn0032433	1	2
FBgn0032437	2	2
FBgn0032442	1	1
FBgn0032454	2	2
FBgn0032470	1	10
FBgn0032471	1	1
FBgn0032474	1	1
FBgn0032492	2	3
FBgn0032502	1	1
FBgn0032506	2	2
FBgn0032512	1	1
FBgn0032513	2	3
FBgn0032515	1	1
FBgn0032520	2	2
FBgn0032521	1	1
FBgn0032522	1	1
FBgn0032585	2	2
FBgn0032598	1	1
FBgn0032619	2	2
FBgn0032625	1	1
FBgn0032645	1	1
FBgn0032647	1	1
FBgn0032657	1	1
FBgn0032661	1	4
FBgn0032666	1	1
FBgn0032668	1	1
FBgn0032675	2	2
FBgn0032677	1	1
FBgn0032678	1	1
FBgn0032679	1	2
FBgn0032684	1	1
FBgn0032723	1	2
FBgn0032742	1	2
FBgn0032752	1	1
FBgn0032759	1	1
FBgn0032760	1	1
FBgn0032768	1	1

FBgn0032772	1	1
FBgn0032775	3	4
FBgn0032782	1	10
FBgn0032790	1	1
FBgn0032797	2	4
FBgn0032798	2	3
FBgn0032800	1	1
FBgn0032801	1	1
FBgn0032803	1	1
FBgn0032805	1	1
FBgn0032811	1	1
FBgn0032812	1	1
FBgn0032818	1	1
FBgn0032826	3	23
FBgn0032850	2	2
FBgn0032872	1	1
FBgn0032873	1	1
FBgn0032891	1	1
FBgn0032898	1	3
FBgn0032906	1	1
FBgn0032911	3	3
FBgn0032919	1	1
FBgn0032920	1	1
FBgn0032926	1	1
FBgn0032929	2	3
FBgn0032934	1	1
FBgn0032944	1	1
FBgn0032945	2	6
FBgn0032947	1	1
FBgn0032982	1	1
FBgn0032988	1	1
FBgn0033030	1	1
FBgn0033039	1	1
FBgn0033052	2	2
FBgn0033059	3	3
FBgn0033060	1	1
FBgn0033061	1	1
FBgn0033073	2	2
FBgn0033109	1	1
FBgn0033113	1	5
FBgn0033136	1	1
FBgn0033159	1	2
FBgn0033164	1	1
FBgn0033169	1	1
FBgn0033185	1	3
FBgn0033194	2	2
FBgn0033195	1	1
FBgn0033212	2	2
FBgn0033235	2	2
FBgn0033243	1	1

FBgn0033246	3	4
FBgn0033248	1	1
FBgn0033252	3	3
FBgn0033258	1	1
FBgn0033264	2	2
FBgn0033277	1	1
FBgn0033282	1	2
FBgn0033283	1	1
FBgn0033286	1	1
FBgn0033288	2	2
FBgn0033294	1	1
FBgn0033304	1	1
FBgn0033316	1	1
FBgn0033354	1	1
FBgn0033361	1	1
FBgn0033362	1	1
FBgn0033365	2	2
FBgn0033367	1	1
FBgn0033368	1	1
FBgn0033373	1	1
FBgn0033374	1	1
FBgn0033389	1	1
FBgn0033403	1	3
FBgn0033405	1	1
FBgn0033419	1	1
FBgn0033427	1	2
FBgn0033435	2	2
FBgn0033464	2	2
FBgn0033482	2	2
FBgn0033484	2	2
FBgn0033494	1	1
FBgn0033501	1	1
FBgn0033515	1	1
FBgn0033524	3	3
FBgn0033541	1	1
FBgn0033557	1	2
FBgn0033566	1	1
FBgn0033579	1	1
FBgn0033590	2	33
FBgn0033593	2	2
FBgn0033603	2	5
FBgn0033612	1	1
FBgn0033615	1	1
FBgn0033618	4	5
FBgn0033637	1	1
FBgn0033645	1	1
FBgn0033648	1	1
FBgn0033661	2	10
FBgn0033664	1	1
FBgn0033667	1	1

FBgn0033702	1	3
FBgn0033703	1	1
FBgn0033704	3	4
FBgn0033718	1	1
FBgn0033720	1	1
FBgn0033762	1	1
FBgn0033765	3	4
FBgn0033766	1	2
FBgn0033772	1	2
FBgn0033775	1	1
FBgn0033794	1	1
FBgn0033827	1	1
FBgn0033831	1	1
FBgn0033834	1	1
FBgn0033845	1	1
FBgn0033848	1	1
FBgn0033856	1	1
FBgn0033860	1	4
FBgn0033862	2	4
FBgn0033863	1	1
FBgn0033870	1	2
FBgn0033871	1	3
FBgn0033874	1	1
FBgn0033876	1	3
FBgn0033880	1	1
FBgn0033883	1	1
FBgn0033898	3	3
FBgn0033901	1	1
FBgn0033914	1	1
FBgn0033916	2	3
FBgn0033960	1	1
FBgn0033969	1	1
FBgn0033975	5	6
FBgn0033983	2	2
FBgn0033987	1	1
FBgn0033992	1	1
FBgn0033998	1	1
FBgn0034002	1	1
FBgn0034004	1	1
FBgn0034020	4	8
FBgn0034060	1	4
FBgn0034071	2	2
FBgn0034072	1	1
FBgn0034121	1	1
FBgn0034122	1	1
FBgn0034133	1	1
FBgn0034135	1	1
FBgn0034137	1	1
FBgn0034147	2	2
FBgn0034153	1	1

FBgn0034161	3	4
FBgn0034170	1	3
FBgn0034173	1	1
FBgn0034195	2	13
FBgn0034198	1	1
FBgn0034210	2	2
FBgn0034229	1	1
FBgn0034249	1	3
FBgn0034251	2	3
FBgn0034253	1	1
FBgn0034264	1	1
FBgn0034269	1	1
FBgn0034272	1	1
FBgn0034276	1	1
FBgn0034300	1	1
FBgn0034319	2	2
FBgn0034323	1	1
FBgn0034346	1	1
FBgn0034356	1	1
FBgn0034360	1	1
FBgn0034374	2	2
FBgn0034376	1	1
FBgn0034392	1	1
FBgn0034412	2	10
FBgn0034416	1	1
FBgn0034425	1	1
FBgn0034435	2	2
FBgn0034437	2	2
FBgn0034446	2	2
FBgn0034452	1	1
FBgn0034454	1	2
FBgn0034467	1	1
FBgn0034485	1	1
FBgn0034493	2	5
FBgn0034502	1	1
FBgn0034519	1	1
FBgn0034532	1	1
FBgn0034546	1	1
FBgn0034553	1	1
FBgn0034568	1	1
FBgn0034572	1	1
FBgn0034587	1	1
FBgn0034588	1	1
FBgn0034589	3	3
FBgn0034605	1	2
FBgn0034606	2	4
FBgn0034627	2	3
FBgn0034656	1	1
FBgn0034662	4	5
FBgn0034663	1	1

FBgn0034680	1	1
FBgn0034687	1	2
FBgn0034690	1	1
FBgn0034704	1	1
FBgn0034715	1	1
FBgn0034722	1	1
FBgn0034725	1	1
FBgn0034732	1	1
FBgn0034734	1	1
FBgn0034738	2	2
FBgn0034776	1	1
FBgn0034787	1	1
FBgn0034789	1	1
FBgn0034810	1	1
FBgn0034814	1	1
FBgn0034824	1	1
FBgn0034825	1	1
FBgn0034827	1	1
FBgn0034832	1	1
FBgn0034854	1	1
FBgn0034856	1	1
FBgn0034859	2	2
FBgn0034867	1	1
FBgn0034886	2	2
FBgn0034903	1	1
FBgn0034908	1	1
FBgn0034911	2	2
FBgn0034918	1	1
FBgn0034950	1	1
FBgn0034972	2	3
FBgn0034974	1	1
FBgn0034979	4	4
FBgn0034998	3	4
FBgn0035001	2	2
FBgn0035007	1	1
FBgn0035008	1	1
FBgn0035010	1	3
FBgn0035019	1	1
FBgn0035048	2	3
FBgn0035079	1	1
FBgn0035086	1	1
FBgn0035106	4	5
FBgn0035110	1	1
FBgn0035125	1	1
FBgn0035126	1	14
FBgn0035128	2	2
FBgn0035132	1	1
FBgn0035134	1	1
FBgn0035144	1	1
FBgn0035149	1	1

FBgn0035155	1	1
FBgn0035167	1	2
FBgn0035168	1	1
FBgn0035169	1	1
FBgn0035171	1	3
FBgn0035186	1	1
FBgn0035187	1	1
FBgn0035190	2	2
FBgn0035191	2	2
FBgn0035203	1	1
FBgn0035218	1	2
FBgn0035220	1	1
FBgn0035229	1	1
FBgn0035232	2	2
FBgn0035264	1	3
FBgn0035281	1	1
FBgn0035291	1	2
FBgn0035293	1	1
FBgn0035312	1	1
FBgn0035316	1	1
FBgn0035325	1	1
FBgn0035330	2	2
FBgn0035331	1	1
FBgn0035336	2	2
FBgn0035344	1	1
FBgn0035367	3	3
FBgn0035381	1	1
FBgn0035385	1	1
FBgn0035410	1	1
FBgn0035411	2	2
FBgn0035414	1	1
FBgn0035424	1	12
FBgn0035439	1	1
FBgn0035443	2	2
FBgn0035458	1	1
FBgn0035477	2	2
FBgn0035483	1	1
FBgn0035505	2	3
FBgn0035507	1	1
FBgn0035510	1	1
FBgn0035517	1	1
FBgn0035522	1	1
FBgn0035543	1	1
FBgn0035564	1	1
FBgn0035575	1	2
FBgn0035577	2	3
FBgn0035581	3	5
FBgn0035591	1	2
FBgn0035607	2	2
FBgn0035612	1	2

FBgn0035626	1	1
FBgn0035645	1	1
FBgn0035647	1	1
FBgn0035655	2	12
FBgn0035687	1	1
FBgn0035689	2	2
FBgn0035690	1	1
FBgn0035710	1	1
FBgn0035711	1	1
FBgn0035720	5	19
FBgn0035734	1	1
FBgn0035756	1	1
FBgn0035761	1	1
FBgn0035772	1	1
FBgn0035780	1	1
FBgn0035788	1	1
FBgn0035795	1	1
FBgn0035797	1	1
FBgn0035798	1	1
FBgn0035799	2	2
FBgn0035808	3	3
FBgn0035842	1	1
FBgn0035843	1	1
FBgn0035844	1	1
FBgn0035847	1	1
FBgn0035852	1	1
FBgn0035861	1	1
FBgn0035864	1	1
FBgn0035872	1	1
FBgn0035874	1	1
FBgn0035875	1	1
FBgn0035878	1	1
FBgn0035880	1	1
FBgn0035886	1	3
FBgn0035888	1	1
FBgn0035895	1	1
FBgn0035898	2	3
FBgn0035901	3	7
FBgn0035903	1	1
FBgn0035911	1	1
FBgn0035923	1	1
FBgn0035928	1	1
FBgn0035929	2	3
FBgn0035930	1	1
FBgn0035937	1	1
FBgn0035942	1	1
FBgn0035977	1	1
FBgn0035988	1	1
FBgn0036008	1	2
FBgn0036009	1	1

FBgn0036010	1	1
FBgn0036016	2	2
FBgn0036022	1	1
FBgn0036030	1	2
FBgn0036038	2	2
FBgn0036039	1	1
FBgn0036082	1	1
FBgn0036090	1	1
FBgn0036102	1	1
FBgn0036104	4	10
FBgn0036122	2	2
FBgn0036124	1	1
FBgn0036135	1	1
FBgn0036141	1	1
FBgn0036170	1	1
FBgn0036183	1	1
FBgn0036188	1	1
FBgn0036206	2	2
FBgn0036218	1	1
FBgn0036219	1	1
FBgn0036223	1	2
FBgn0036228	1	1
FBgn0036230	1	3
FBgn0036232	1	1
FBgn0036233	2	2
FBgn0036235	2	2
FBgn0036249	1	1
FBgn0036266	2	2
FBgn0036295	4	4
FBgn0036301	2	4
FBgn0036315	3	3
FBgn0036319	2	2
FBgn0036332	1	1
FBgn0036340	2	2
FBgn0036346	1	1
FBgn0036350	1	1
FBgn0036369	2	2
FBgn0036380	1	1
FBgn0036386	2	2
FBgn0036391	3	4
FBgn0036398	5	5
FBgn0036414	1	1
FBgn0036421	1	1
FBgn0036422	1	1
FBgn0036427	1	1
FBgn0036459	1	1
FBgn0036463	3	3
FBgn0036476	1	1
FBgn0036486	2	2
FBgn0036487	1	1

FBgn0036491	1	1
FBgn0036494	3	3
FBgn0036504	1	1
FBgn0036541	1	1
FBgn0036544	1	1
FBgn0036564	2	2
FBgn0036577	1	1
FBgn0036621	1	1
FBgn0036624	1	1
FBgn0036654	1	1
FBgn0036660	1	1
FBgn0036688	3	4
FBgn0036689	1	1
FBgn0036698	2	2
FBgn0036712	1	1
FBgn0036714	3	3
FBgn0036715	1	2
FBgn0036725	1	1
FBgn0036747	2	3
FBgn0036767	1	1
FBgn0036772	1	1
FBgn0036795	1	1
FBgn0036800	1	1
FBgn0036809	1	1
FBgn0036810	1	1
FBgn0036821	1	1
FBgn0036829	1	1
FBgn0036832	2	3
FBgn0036839	1	1
FBgn0036843	1	1
FBgn0036844	1	1
FBgn0036877	1	1
FBgn0036886	1	1
FBgn0036890	3	6
FBgn0036907	1	1
FBgn0036924	1	1
FBgn0036935	3	3
FBgn0036936	1	5
FBgn0036943	2	3
FBgn0036944	1	1
FBgn0036949	1	2
FBgn0036955	2	3
FBgn0036970	1	1
FBgn0036979	1	1
FBgn0036984	1	1
FBgn0036985	3	3
FBgn0036986	1	1
FBgn0036991	1	2
FBgn0037000	1	1
FBgn0037014	1	1

FBgn0037020	1	1
FBgn0037023	1	1
FBgn0037036	1	1
FBgn0037038	1	2
FBgn0037040	2	2
FBgn0037041	1	1
FBgn0037057	1	1
FBgn0037072	1	1
FBgn0037085	1	1
FBgn0037107	1	1
FBgn0037113	1	1
FBgn0037115	1	1
FBgn0037121	1	2
FBgn0037130	3	5
FBgn0037167	1	1
FBgn0037219	1	1
FBgn0037226	1	1
FBgn0037227	1	1
FBgn0037230	1	1
FBgn0037233	1	1
FBgn0037255	1	1
FBgn0037260	2	2
FBgn0037263	1	5
FBgn0037273	1	1
FBgn0037274	3	14
FBgn0037275	1	2
FBgn0037282	1	1
FBgn0037291	1	5
FBgn0037320	1	1
FBgn0037324	1	1
FBgn0037338	2	2
FBgn0037362	1	1
FBgn0037364	1	1
FBgn0037371	2	2
FBgn0037372	1	1
FBgn0037375	1	2
FBgn0037379	1	1
FBgn0037382	1	1
FBgn0037392	1	1
FBgn0037405	1	1
FBgn0037409	1	1
FBgn0037410	1	2
FBgn0037411	1	1
FBgn0037412	1	1
FBgn0037416	1	1
FBgn0037419	3	4
FBgn0037421	1	1
FBgn0037427	1	7
FBgn0037435	2	2
FBgn0037436	1	1

FBgn0037445	1	1
FBgn0037456	1	1
FBgn0037460	1	1
FBgn0037464	1	2
FBgn0037471	3	3
FBgn0037480	2	2
FBgn0037486	1	2
FBgn0037490	2	2
FBgn0037503	1	1
FBgn0037512	1	1
FBgn0037546	1	1
FBgn0037552	1	2
FBgn0037561	1	1
FBgn0037565	2	3
FBgn0037568	1	1
FBgn0037572	1	1
FBgn0037579	1	1
FBgn0037600	1	1
FBgn0037606	1	1
FBgn0037632	4	8
FBgn0037645	1	1
FBgn0037659	1	1
FBgn0037662	1	1
FBgn0037677	1	1
FBgn0037684	1	1
FBgn0037689	1	3
FBgn0037690	1	1
FBgn0037703	1	1
FBgn0037705	2	4
FBgn0037707	3	8
FBgn0037712	1	2
FBgn0037717	1	1
FBgn0037726	2	3
FBgn0037755	1	1
FBgn0037767	1	1
FBgn0037778	1	1
FBgn0037786	2	3
FBgn0037796	1	1
FBgn0037806	2	2
FBgn0037810	1	1
FBgn0037814	2	2
FBgn0037829	2	2
FBgn0037831	1	1
FBgn0037832	1	1
FBgn0037837	1	1
FBgn0037838	1	2
FBgn0037840	2	2
FBgn0037849	3	3
FBgn0037857	1	1
FBgn0037858	1	1

FBgn0037862	1	1
FBgn0037881	1	1
FBgn0037892	1	1
FBgn0037894	1	1
FBgn0037895	1	1
FBgn0037911	1	1
FBgn0037915	1	2
FBgn0037921	1	1
FBgn0037923	1	1
FBgn0037930	1	1
FBgn0037949	2	2
FBgn0037985	1	3
FBgn0037986	1	10
FBgn0037993	2	2
FBgn0037996	1	1
FBgn0038016	1	34
FBgn0038049	1	1
FBgn0038057	1	1
FBgn0038068	1	2
FBgn0038072	1	1
FBgn0038073	1	1
FBgn0038080	1	1
FBgn0038089	1	1
FBgn0038095	1	1
FBgn0038108	3	3
FBgn0038118	1	1
FBgn0038120	1	4
FBgn0038125	1	2
FBgn0038133	1	2
FBgn0038167	1	2
FBgn0038173	1	1
FBgn0038191	2	2
FBgn0038200	2	2
FBgn0038208	1	1
FBgn0038211	1	2
FBgn0038217	1	2
FBgn0038229	1	1
FBgn0038230	2	2
FBgn0038247	2	2
FBgn0038248	1	1
FBgn0038254	1	1
FBgn0038258	1	3
FBgn0038268	2	2
FBgn0038276	2	2
FBgn0038291	1	1
FBgn0038295	1	1
FBgn0038296	1	2
FBgn0038308	3	3
FBgn0038327	2	2
FBgn0038334	1	1

FBgn0038342	1	1
FBgn0038349	1	1
FBgn0038350	2	2
FBgn0038354	1	1
FBgn0038385	2	2
FBgn0038391	1	1
FBgn0038397	2	3
FBgn0038398	1	1
FBgn0038410	1	2
FBgn0038423	2	3
FBgn0038427	1	1
FBgn0038432	3	4
FBgn0038433	1	1
FBgn0038434	2	2
FBgn0038441	1	1
FBgn0038447	1	1
FBgn0038448	2	5
FBgn0038449	1	1
FBgn0038470	1	1
FBgn0038476	1	1
FBgn0038494	1	1
FBgn0038500	1	1
FBgn0038511	1	1
FBgn0038516	1	2
FBgn0038526	1	1
FBgn0038530	2	2
FBgn0038534	1	1
FBgn0038541	1	3
FBgn0038543	2	3
FBgn0038544	1	3
FBgn0038554	2	3
FBgn0038564	1	1
FBgn0038576	1	1
FBgn0038597	1	1
FBgn0038606	1	1
FBgn0038608	1	1
FBgn0038609	1	1
FBgn0038633	3	3
FBgn0038638	2	2
FBgn0038644	1	1
FBgn0038659	1	2
FBgn0038684	1	1
FBgn0038693	5	5
FBgn0038695	2	2
FBgn0038700	1	1
FBgn0038725	1	1
FBgn0038732	1	1
FBgn0038736	1	1
FBgn0038744	3	3
FBgn0038761	1	3

FBgn0038763	1	1
FBgn0038773	1	1
FBgn0038780	1	1
FBgn0038783	1	1
FBgn0038790	2	2
FBgn0038796	2	2
FBgn0038806	1	1
FBgn0038815	1	1
FBgn0038816	3	3
FBgn0038827	1	1
FBgn0038850	1	1
FBgn0038870	1	1
FBgn0038880	1	1
FBgn0038902	1	1
FBgn0038916	1	1
FBgn0038919	1	1
FBgn0038930	1	5
FBgn0038941	1	1
FBgn0038948	3	14
FBgn0038952	1	3
FBgn0038953	1	1
FBgn0038975	3	3
FBgn0038985	1	1
FBgn0039016	1	2
FBgn0039036	1	1
FBgn0039039	1	1
FBgn0039055	1	1
FBgn0039060	1	1
FBgn0039064	3	3
FBgn0039065	2	2
FBgn0039070	1	1
FBgn0039071	1	1
FBgn0039080	1	1
FBgn0039087	1	2
FBgn0039108	1	1
FBgn0039125	2	2
FBgn0039152	3	4
FBgn0039153	1	1
FBgn0039155	1	1
FBgn0039157	1	1
FBgn0039159	1	1
FBgn0039186	6	15
FBgn0039214	1	1
FBgn0039222	1	1
FBgn0039225	1	1
FBgn0039233	1	1
FBgn0039246	1	2
FBgn0039251	1	1
FBgn0039258	1	1
FBgn0039274	1	2

FBgn0039277	1	1
FBgn0039281	1	1
FBgn0039286	1	2
FBgn0039301	1	1
FBgn0039302	4	4
FBgn0039307	1	2
FBgn0039309	1	1
FBgn0039321	1	1
FBgn0039326	1	1
FBgn0039332	1	1
FBgn0039368	1	1
FBgn0039394	2	2
FBgn0039400	2	2
FBgn0039411	1	1
FBgn0039415	1	3
FBgn0039418	1	1
FBgn0039419	1	1
FBgn0039431	2	2
FBgn0039448	1	1
FBgn0039463	2	3
FBgn0039470	1	1
FBgn0039474	1	1
FBgn0039476	1	1
FBgn0039478	1	1
FBgn0039484	4	4
FBgn0039490	2	5
FBgn0039503	1	1
FBgn0039508	1	1
FBgn0039510	2	5
FBgn0039513	2	2
FBgn0039527	2	3
FBgn0039529	1	1
FBgn0039530	6	6
FBgn0039536	3	3
FBgn0039564	1	1
FBgn0039568	1	1
FBgn0039574	2	2
FBgn0039579	1	1
FBgn0039597	1	2
FBgn0039598	1	1
FBgn0039617	1	1
FBgn0039620	1	1
FBgn0039633	1	1
FBgn0039640	1	1
FBgn0039645	1	1
FBgn0039651	1	1
FBgn0039654	2	2
FBgn0039663	1	1
FBgn0039668	1	1
FBgn0039669	1	1

FBgn0039683	1	1
FBgn0039687	1	1
FBgn0039688	2	2
FBgn0039690	1	1
FBgn0039694	1	1
FBgn0039707	1	1
FBgn0039709	1	1
FBgn0039722	1	1
FBgn0039728	1	1
FBgn0039736	1	1
FBgn0039769	1	1
FBgn0039770	1	1
FBgn0039787	1	1
FBgn0039788	1	1
FBgn0039798	1	1
FBgn0039812	1	1
FBgn0039841	4	5
FBgn0039850	2	3
FBgn0039867	1	1
FBgn0039870	1	1
FBgn0039881	1	1
FBgn0039883	2	4
FBgn0039905	2	2
FBgn0039908	1	1
FBgn0039911	1	1
FBgn0039927	1	1
FBgn0039938	3	3
FBgn0039969	1	4
FBgn0039972	1	3
FBgn0040037	1	1
FBgn0040063	1	1
FBgn0040075	1	1
FBgn0040080	2	2
FBgn0040106	2	2
FBgn0040108	1	1
FBgn0040207	2	2
FBgn0040208	1	1
FBgn0040229	2	2
FBgn0040233	3	3
FBgn0040236	1	1
FBgn0040250	1	1
FBgn0040268	2	4
FBgn0040281	3	4
FBgn0040283	1	1
FBgn0040284	3	10
FBgn0040285	1	1
FBgn0040286	1	1
FBgn0040290	2	5
FBgn0040295	2	2
FBgn0040297	2	3

FBgn0040299	1	1
FBgn0040319	1	2
FBgn0040335	2	10
FBgn0040344	4	6
FBgn0040348	1	2
FBgn0040350	1	1
FBgn0040353	1	1
FBgn0040364	1	1
FBgn0040367	1	1
FBgn0040369	1	2
FBgn0040378	1	1
FBgn0040387	3	3
FBgn0040390	2	2
FBgn0040394	1	1
FBgn0040483	1	1
FBgn0040499	1	1
FBgn0040505	1	1
FBgn0040508	3	3
FBgn0040510	1	1
FBgn0040512	1	1
FBgn0040574	1	1
FBgn0040585	1	1
FBgn0040629	1	1
FBgn0040647	1	6
FBgn0040670	1	1
FBgn0040752	1	2
FBgn0040780	1	1
FBgn0040821	1	1
FBgn0040892	1	1
FBgn0040917	5	6
FBgn0040959	1	1
FBgn0040971	1	1
FBgn0040998	1	4
FBgn0041092	2	6
FBgn0041096	2	3
FBgn0041097	1	1
FBgn0041100	1	1
FBgn0041111	5	5
FBgn0041145	2	2
FBgn0041147	1	1
FBgn0041161	2	2
FBgn0041171	1	2
FBgn0041174	1	1
FBgn0041180	2	2
FBgn0041183	1	1
FBgn0041194	3	3
FBgn0041195	1	1
FBgn0041210	1	1
FBgn0041244	1	1
FBgn0041246	1	1

FBgn0041252	1	1
FBgn0041342	2	3
FBgn0041581	1	1
FBgn0041604	1	2
FBgn0041605	1	1
FBgn0041712	1	1
FBgn0041723	3	3
FBgn0041781	1	1
FBgn0042105	1	1
FBgn0042137	1	1
FBgn0042182	1	2
FBgn0042206	1	1
FBgn0042627	4	6
FBgn0042641	1	1
FBgn0042650	3	5
FBgn0042693	1	1
FBgn0042696	1	1
FBgn0042710	1	1
FBgn0042711	2	2
FBgn0043362	2	2
FBgn0043472	3	3
FBgn0043799	1	2
FBgn0043854	1	1
FBgn0043884	4	6
FBgn0043903	1	2
FBgn0044047	1	1
FBgn0044049	1	1
FBgn0044050	1	8
FBgn0045073	1	1
FBgn0045442	1	1
FBgn0045479	2	2
FBgn0045487	1	1
FBgn0045828	1	1
FBgn0045852	2	6
FBgn0045862	1	1
FBgn0046222	4	10
FBgn0046253	1	1
FBgn0046281	1	1
FBgn0046302	2	2
FBgn0046704	1	2
FBgn0046812	1	1
FBgn0046885	1	1
FBgn0046886	1	1
FBgn0046887	1	3
FBgn0047178	1	1
FBgn0050007	1	1
FBgn0050011	1	1
FBgn0050015	1	1
FBgn0050017	1	1
FBgn0050019	2	3

FBgn0050022	1	1
FBgn0050025	1	1
FBgn0050035	1	1
FBgn0050037	2	2
FBgn0050046	1	1
FBgn0050055	2	2
FBgn0050065	1	1
FBgn0050069	2	2
FBgn0050081	1	1
FBgn0050083	1	4
FBgn0050084	1	1
FBgn0050085	2	2
FBgn0050088	1	1
FBgn0050089	2	2
FBgn0050096	1	1
FBgn0050097	1	1
FBgn0050099	1	1
FBgn0050104	1	1
FBgn0050115	1	1
FBgn0050118	3	3
FBgn0050122	4	13
FBgn0050125	1	1
FBgn0050127	2	2
FBgn0050130	1	1
FBgn0050151	1	1
FBgn0050157	3	4
FBgn0050158	2	2
FBgn0050164	1	1
FBgn0050174	1	1
FBgn0050175	1	1
FBgn0050187	1	1
FBgn0050194	1	1
FBgn0050196	2	2
FBgn0050263	1	1
FBgn0050268	2	2
FBgn0050271	1	1
FBgn0050273	1	1
FBgn0050274	1	1
FBgn0050275	1	1
FBgn0050277	1	1
FBgn0050284	1	1
FBgn0050289	1	1
FBgn0050325	1	1
FBgn0050329	1	1
FBgn0050334	1	5
FBgn0050337	1	1
FBgn0050344	1	2
FBgn0050357	2	2
FBgn0050360	3	3
FBgn0050361	1	1

FBgn0050364	1	2
FBgn0050371	1	1
FBgn0050377	1	1
FBgn0050378	1	2
FBgn0050387	3	4
FBgn0050389	1	1
FBgn0050390	1	1
FBgn0050394	1	1
FBgn0050405	2	2
FBgn0050421	1	1
FBgn0050429	1	1
FBgn0050443	1	1
FBgn0050446	1	1
FBgn0050456	1	5
FBgn0050460	1	1
FBgn0050490	1	1
FBgn0050492	2	2
FBgn0051004	1	1
FBgn0051010	1	1
FBgn0051017	1	1
FBgn0051025	2	4
FBgn0051029	2	2
FBgn0051037	1	1
FBgn0051038	2	2
FBgn0051048	3	3
FBgn0051052	1	1
FBgn0051063	1	1
FBgn0051064	1	1
FBgn0051072	1	1
FBgn0051075	1	1
FBgn0051080	1	1
FBgn0051084	1	1
FBgn0051098	1	1
FBgn0051099	1	1
FBgn0051116	1	1
FBgn0051139	1	2
FBgn0051140	1	1
FBgn0051146	1	1
FBgn0051149	1	1
FBgn0051150	1	1
FBgn0051156	2	2
FBgn0051157	1	1
FBgn0051161	1	7
FBgn0051170	1	1
FBgn0051176	1	1
FBgn0051177	1	1
FBgn0051184	1	1
FBgn0051187	2	3
FBgn0051188	4	4
FBgn0051190	3	5

FBgn0051205	1	1
FBgn0051209	2	2
FBgn0051211	1	2
FBgn0051212	1	1
FBgn0051217	1	1
FBgn0051222	3	3
FBgn0051224	1	1
FBgn0051230	1	1
FBgn0051233	1	1
FBgn0051235	1	1
FBgn0051238	1	1
FBgn0051241	2	2
FBgn0051257	1	1
FBgn0051274	1	2
FBgn0051279	1	1
FBgn0051291	1	1
FBgn0051296	1	1
FBgn0051301	1	1
FBgn0051302	2	2
FBgn0051304	2	2
FBgn0051314	1	1
FBgn0051318	1	1
FBgn0051324	1	1
FBgn0051330	2	2
FBgn0051351	1	1
FBgn0051354	1	1
FBgn0051357	1	1
FBgn0051360	1	1
FBgn0051363	1	1
FBgn0051365	1	1
FBgn0051367	1	1
FBgn0051368	1	1
FBgn0051369	1	2
FBgn0051374	1	2
FBgn0051385	1	2
FBgn0051389	1	5
FBgn0051407	2	3
FBgn0051421	1	1
FBgn0051422	1	1
FBgn0051431	1	1
FBgn0051463	1	1
FBgn0051465	1	1
FBgn0051481	1	1
FBgn0051499	1	1
FBgn0051510	1	3
FBgn0051531	1	1
FBgn0051536	1	1
FBgn0051537	1	1
FBgn0051549	1	1
FBgn0051551	3	3

FBgn0051617	1	1
FBgn0051633	1	1
FBgn0051634	1	1
FBgn0051635	2	2
FBgn0051640	1	1
FBgn0051643	1	1
FBgn0051646	1	1
FBgn0051649	2	2
FBgn0051652	1	1
FBgn0051653	1	1
FBgn0051660	2	2
FBgn0051663	1	1
FBgn0051665	1	1
FBgn0051678	2	5
FBgn0051687	1	1
FBgn0051688	2	3
FBgn0051693	1	1
FBgn0051698	1	3
FBgn0051700	2	2
FBgn0051703	1	1
FBgn0051713	1	1
FBgn0051715	1	2
FBgn0051720	2	2
FBgn0051729	1	1
FBgn0051746	1	1
FBgn0051755	1	2
FBgn0051760	1	2
FBgn0051772	2	2
FBgn0051774	1	1
FBgn0051780	1	1
FBgn0051782	1	1
FBgn0051786	2	2
FBgn0051791	1	1
FBgn0051792	1	1
FBgn0051793	1	1
FBgn0051801	1	1
FBgn0051802	1	1
FBgn0051818	1	1
FBgn0051820	2	4
FBgn0051821	1	1
FBgn0051823	1	1
FBgn0051825	1	1
FBgn0051855	1	1
FBgn0051857	1	1
FBgn0051860	1	1
FBgn0051862	1	1
FBgn0051897	1	1
FBgn0051901	1	1
FBgn0051902	2	2
FBgn0051913	1	1

FBgn0051916	4	4
FBgn0051924	1	1
FBgn0051956	1	1
FBgn0051973	2	2
FBgn0051990	1	1
FBgn0051992	1	1
FBgn0051997	1	1
FBgn0051998	3	5
FBgn0051999	1	1
FBgn0052000	1	1
FBgn0052010	2	2
FBgn0052016	1	2
FBgn0052017	1	1
FBgn0052023	1	1
FBgn0052029	1	1
FBgn0052030	1	1
FBgn0052046	2	2
FBgn0052048	1	1
FBgn0052057	1	2
FBgn0052064	2	3
FBgn0052067	2	3
FBgn0052079	2	2
FBgn0052082	3	7
FBgn0052087	1	1
FBgn0052088	2	2
FBgn0052091	1	1
FBgn0052092	1	1
FBgn0052094	1	1
FBgn0052095	1	1
FBgn0052103	1	2
FBgn0052106	1	2
FBgn0052111	1	2
FBgn0052113	1	1
FBgn0052121	1	1
FBgn0052130	1	1
FBgn0052137	1	2
FBgn0052138	2	2
FBgn0052150	1	1
FBgn0052158	2	2
FBgn0052170	1	1
FBgn0052181	1	1
FBgn0052182	1	1
FBgn0052183	1	1
FBgn0052193	1	1
FBgn0052206	5	8
FBgn0052226	1	1
FBgn0052242	1	1
FBgn0052245	1	1
FBgn0052249	1	1
FBgn0052251	1	1

FBgn0052260	1	2
FBgn0052264	1	1
FBgn0052267	1	1
FBgn0052269	1	5
FBgn0052283	1	1
FBgn0052297	1	1
FBgn0052301	1	1
FBgn0052306	4	4
FBgn0052311	1	1
FBgn0052316	1	1
FBgn0052343	1	1
FBgn0052353	1	1
FBgn0052354	1	1
FBgn0052364	1	3
FBgn0052372	1	1
FBgn0052374	1	1
FBgn0052377	1	2
FBgn0052384	2	2
FBgn0052387	1	1
FBgn0052392	1	1
FBgn0052394	1	1
FBgn0052397	1	1
FBgn0052399	1	1
FBgn0052432	1	1
FBgn0052434	2	2
FBgn0052438	1	1
FBgn0052446	2	2
FBgn0052458	2	2
FBgn0052465	1	1
FBgn0052475	1	1
FBgn0052494	1	1
FBgn0052495	1	1
FBgn0052496	1	1
FBgn0052523	2	2
FBgn0052529	3	4
FBgn0052533	1	1
FBgn0052541	3	8
FBgn0052542	3	8
FBgn0052547	1	1
FBgn0052553	1	1
FBgn0052556	2	2
FBgn0052560	2	2
FBgn0052569	1	1
FBgn0052572	1	1
FBgn0052580	3	3
FBgn0052584	1	1
FBgn0052586	1	3
FBgn0052587	1	1
FBgn0052594	1	1
FBgn0052611	2	2

FBgn0052626	1	1
FBgn0052628	2	2
FBgn0052632	1	1
FBgn0052636	1	1
FBgn0052647	1	1
FBgn0052648	5	8
FBgn0052654	2	2
FBgn0052662	1	1
FBgn0052668	3	3
FBgn0052676	3	5
FBgn0052685	2	2
FBgn0052686	1	1
FBgn0052687	1	1
FBgn0052702	5	5
FBgn0052703	1	1
FBgn0052704	1	1
FBgn0052707	1	1
FBgn0052733	1	1
FBgn0052737	3	3
FBgn0052742	1	1
FBgn0052743	3	3
FBgn0052767	2	2
FBgn0052778	2	2
FBgn0052779	1	1
FBgn0052782	2	3
FBgn0052783	1	1
FBgn0052786	1	1
FBgn0052790	1	1
FBgn0052791	2	2
FBgn0052792	1	1
FBgn0052815	1	1
FBgn0052820	1	1
FBgn0052833	1	1
FBgn0052855	2	2
FBgn0052921	1	2
FBgn0052937	2	2
FBgn0052944	1	1
FBgn0052985	1	2
FBgn0052986	1	8
FBgn0053008	1	3
FBgn0053012	1	1
FBgn0053013	1	1
FBgn0053038	1	2
FBgn0053041	1	1
FBgn0053061	1	1
FBgn0053070	1	2
FBgn0053087	10	20
FBgn0053095	1	1
FBgn0053123	1	1
FBgn0053129	1	2

FBgn0053130	1	1
FBgn0053139	3	4
FBgn0053144	1	1
FBgn0053145	1	1
FBgn0053146	2	3
FBgn0053147	1	3
FBgn0053156	2	2
FBgn0053171	1	1
FBgn0053173	2	3
FBgn0053179	2	2
FBgn0053191	1	5
FBgn0053192	1	1
FBgn0053196	52	69
FBgn0053202	1	1
FBgn0053203	1	1
FBgn0053207	1	1
FBgn0053208	2	4
FBgn0060296	2	2
FBgn0061200	1	1
FBgn0061354	1	1
FBgn0061356	1	1
FBgn0061362	1	2
FBgn0061435	1	1
FBgn0061476	3	7
FBgn0063649	1	1
FBgn0063667	1	1
FBgn0063910	1	1
FBgn0063912	1	1
FBgn0064806	1	1
FBgn0066101	2	2

REFERENCES

Abdu, U., Brodsky, M., Schupbach, T. (2002). Activation of a meiotic checkpoint during *Drosophila* oogenesis regulates the translation of Gurken through Chk2/Mnk. Curr Biol *12*, 1645-1651.

Adams, J.M., and Cory, S. (1998). The Bcl-2 protein family: arbiters of cell survival. Science *281*, 1322-1326.

Afshar, K., Stuart, B., Wasserman, S.A. (2000). Functional analysis of the *Drosophila* diaphanous FH protein in early embryonic development. Development *127*, 1887-1897.

Alnemri, E.S., Livingston, D.J., Nicholsom, D.W., Salvesen, G., Thornberry, N.A., Wong, W.W., and Yuan, J. (1996). Human ICE/CED-3 protease nomenclature. Cell *87*, 171.

Alva, A., Gultekin, S. H., Baehrecke, E. H. (2004). Autophagy in human tumors: cell survival or death? Cell Death and Differ, in press.

Arama, E., Agapite, J., Steller, H. (2003). Caspase activity and a specific cytochrome C are required for sperm differentiation in *Drosophila*. Dev Cell. *4*, 687-697.

Aravind, L., Dixit, V.M., Koonin, E.V. (2001) Apoptotic molecular machinery: vastly increased complexity in vertebrates revealed by genome comparisons. Science *291*, 1279-1284.

Baehrecke, E.H. (2002). How death shapes life during development. Nat. Rev. Mol. Cell Biol. *3*, 779-787.

Baehrecke, E.H. (2003). Autophagic programmed cell death in *Drosophila*. Cell Death and Differentiation *10*, 940-945.

Barbet, N.C., Schneider, U., Helliwell, S.B., StansfieldI ., Tuite, M.F., Hall, M.N. (1996). TOR controls translation initiation and early G1 progression in yeast. Mol Biol Cell *7*, 25-42.

Battersby, A., Csiszar, A., Leptin, M., Wilson, R. (2003). Isolation of proteins that interact with the signal transduction molecule Dof and identification of a functional domain conserved between Dof and vertebrate BCAP. J Mol Biol *329*, 479-493.

Benashski, S.E., Harrison, A., Patel-King, R.S., King, S.M. (1997). Dimerization of the highly conserved light chain shared by dynein and myosin V. J Biol Chem *272*, 20929-20935.

Bergmann, A., Tugentman, M., Shilo, B.Z., Steller, H. (2002). Regulation of cell number by MAPK-dependent control of apoptosis: a mechanism for trophic survival signaling. Dev. Cell *2*, 159-170.

Bowman, A.B., Patel-King, R.S., Benashski, S.E., McCaffrey, J.M., Goldstein, L.S.B., King, S.M. (1999). *Drosophila* roadblock and *Chlamydomonas* LC7: a conserved family of dynein-associated proteins involved in axonal transport, flagellar motility and mitosis. J Cell Biol *146*, 165-179.

Brachmann, C.B., Jassim, O.W., Wachsmuth, B.D., Cagan, R.L. (2000). The *Drosophila* Bcl-2 family member *dBorg-1* functions in the apoptotic response to UV-irradiation. Curr Biol *10*, 547-550.

Brennecke, J., Hipfner, D.R., Stark, A., Russell, R.B., Cohen, S.M. (2003). *bantam* encodes a developmentally regulated microRNA that controls cell proliferation and regulates the proapoptotic gene *hid* in *Drosophila*. Cell *113*, 25-36.

Brinkmann, A.O. (1994). Steroid hormone receptors: activators of gene transcription. J Pediatr Endocrinol *7*, 275-282.

Broadus, J., McCabe, J.R., Endrizzi, B., Thummel, C.S., Woodard, C.T. (1999). The *Drosophila BFTZ-F1* orphan nuclear receptor provides competence for stage-specific responses to the steroid hormone ecdysone. Mol Cell *3*, 143-149.

Bursch, W., Hochegger, K., Torok, L., Marian, B., Ellinger, A., Hermann, R.S. (2000). Autophagic and apoptotic types of programmed cell death exhibit different fates of cytoskeletal filaments. J Cell Sci *113*, 1189-1198.

Burtis, K.C., Thummel, C.S., Jones, C.W., Karim, F.D., Hogness, D.S. (1990). The *Drosophila* 74EF early puff contains *E74*, a complex ecdysone-inducible gene that encodes two ets-related proteins. Cell *61*, 85-99.

Cain, K., Bratton, S.B., Cohen, G.M. (2002). The Apaf-1 apoptosome: a large caspase-activating complex. Biochimie *84*, 203-214.

Cardenas, M.E., Cutler, N .S., Lorenz, M.C., Di Como, C.J., Heitman, J. (1999). The TOR signaling cascade regulates gene expression in response to nutrients. Genes Dev *13*, 3271-3279.

Chen, J., Gao, J., Lee, C.S. (2003). Dynamic enhancements of sample loading and analyte concentration in capillary isoelectric focusing for proteome studies. J Proteome Res *2*, 249-254.

Chen, P., Nordstrom, W., Gish, B., Abrams, J.M. (1996). *grim*, a novel cell death gene in *Drosophila*. Genes and Dev *10*, 1773-1782.

Chen, P., Rodriguez, A., Erkskine, R., Thach, T., Abrams, J.M. (1998). *Dredd*, a novel effector of the apoptosis activators *reaper*, *grim* and *hid* in *Drosophila*. Dev Biol *201*, 202-216.

Christich, A., Kauppila, S., Chen, P., Sogame, N., Ho, S.I., Abrams, J.M. (2002). The Damage-Responsive *Drosophila* gene sickle encodes a novel IAP binding protein similar but distinct from *reaper*, *grim* and *hid*. Curr Biol *12*, 137-140.

Clarke, P.G.H. (1990). Developmental cell death: morphological diversity and multiple mechanisms. Anat. Embryol. *181*, 195-213.

Clem, R.J., Sheu, T.T., Richter, B.W., He, W.W., Thornberry, N.A., Duckett, C.S., Hardwick, J.M. (2001). c-IAP1 is cleaved by caspases to produce a proapoptotic C-terminal fragment. J Biol Chem *276*, 7602-7608.

Coleman, M.L., Olson, M.F. (2002). Rho GTPase signalling pathways in the morphological changes associated with apoptosis. Cell Death Differ *9*, 493-504.

Collins, R.T., Furukawa, T., Tanese, N., Treisman, J.E. (1999). Osa associates with the Brahma chromatin remodeling complex and promotes the activation of some target genes. EMBO J *18*, 7029-7040.

Colussi, P.A., Quinn, L.M., Huang, D.C.S., Coombe, M., Read, S.H., Richardson, H., Kumar, S. (2000). Debcl, a proapoptotic Bcl-2 homologue, is a component of the *Drosophila melanogaster* cell death machinery. J Cell Biol*148*, 703- 714.

Cooper, J.W. and Lee, C.S. (2004). Integrated and ultrasensitive gel protein identification. Anal Chem *76*, 2196-2202.

Coucouvanis, E. and Martin, G.R. (1995). Signals for death and survival: a two-step mechanism for cavitation in the vertebrate embryo. Cell *83*, 279-287.

Crossgrove, K., Bayer, C.A., Fristrom, J.W., Guild, G.M. (1996). The *Drosophila Broad-Complex* early gene directly regulates late gene transcription during the ecdysone-induced puffing cascade. Dev Biol *180*, 745-758.

Cryns, V., Yuan, J. (1998). Proteases to die for. Genes Dev *12*, 1551-1570.

Das, B., Schreiber, A.M., Huang, H., Brown, D.D. (2002) Multiple thyroid hormone-induced muscle growth and death programs during metamorphosis in *Xenopus laevis*. Proc Natl Acad Sci. *99*, 12230-12235.

Day, C.L., Puthalakath, H., Skea, G., Strasser, A., Barsukov, I., Lian, L.Y., Huang, D.C., Hinds, M.G. (2004). Localization of dynein light chains 1 and 2 and their pro-apoptotic ligands. Biochem J*377*, 597- 605.

Debnath, J., Mills, K.R., Collins, N.L., Reginato, M.J., Muthuswamy, S.K., Brugge, J.S. (2002). The role of apoptosis in creating and maintaining luminal space within normal and oncogene-expressing mammary acini. Cell *111*, 29-40.

Dennis, P.B., Fumagalli, S., Thomas, G. (1999). Target of rapamycin (TOR): balancing the opposing forces of protein synthesis and degradation. Curr Opin Genet Dev *9*, 49-54.

DiBello, P.R., Withers, D.A., Bayer, C.A., Fristrom, J.W., Guild, G.M. (1991). The *Drosophila Broad-Complex* encodes a family of related proteins containing zinc fingers. Genetics *129*, 385-397.

Dick, T., Ray, K., Salz, H.K., Chia, W. (1996). Cytoplasmic dynein (*ddlc1*) mutations cause morphogenetic defects and apoptotic cell death in *Drosophila* melanogaster. Mol Cell Biol *16*, 1966-1977.

Distelhorst, C.W. (2002). Recent insights into the mechanism of glucocorticosteroid-induced apoptosis. Cell Death Differ *9*, 6-19.

Dollar, G., Struckhoff, E., Michaud, J., Cohen, R.S. (2002). Rab11 polarization of the *Drosophila* oocyte: a novel link between membrane trafficking, microtubule organization, and *oskar* mRNA localization and translation. Development *129*, 517-526.

Dorstyn, L., Read, S., Cakouros, D., Huh, J.R., Hay, B.A., Kumar, S. (2002) The role of cytochrome c in caspase activation in *Drosophila melanogaster*cells. J Cell Biol. *156*, 1089-1098.

Dorstyn, L., Colussi, P.A., Quinn, L.M., Richardson, H., Kumar, S. (1999a). DRONC, an ecdysone-inducible *Drosophila* caspase. Proc Natl Acad Sci USA *96*, 4307-4312.

Dorstyn, L., Read, S.H., Quinn, L.M., Richardson, H., Kumar, S. (1999b). DECAY, a novel *Drosophila* caspase related to mammalian caspase-3 and caspase-7. J Biol Chem *274*, 30778-30783.

Doumanis, J., Quinn, L., Richardson, H., Kumar, S. (2001). STRICA, a novel *Drosophila melanogaster* caspase with an unusual serine/threonine-rich prodomain, interacts with DIAP1 and DIAP2. Cell Death and Differentiation *8*, 387-394.

Drummond-Barbosa, D. and Spradling, A.C. (2001). Stem cells and their progeny respond to nutritional changes during *Drosophila* oogenesis. Dev Biol *231*, 265-278.

Dunn, W.A.J. (1990). Studies on the mechanisms of autophagy: formation of the autophagic vacuole. J. Cell Biol. *110*, 1923-1933.

Ellis, R.E., Yuan, J. and Horvitz, R.H. (1991). Mechanisms and functions of cell death. Annu. Rev. Cell Biol. *7*, 663-698.

Eshel, D.L.A., Urrestarazu, S., Vissers, J.C., Januniaux, J.C., van Vliet-Reedijk et al. (1993). Cytoplasmic Dynein is required for normal nuclear segregation in yeast. Proc Natl Acad Sci USA *90,* 11172-11176.

Evans-Strom, R.B. and Cidlowski, J.A. (1995). Regulation of apoptosis by steroid hormones. J Steroid Biochem Molec Biol *53,* 1-6.

Fadok, V.A., Voelker, D.R., Campbell, P.A., Cohen, J.J., Bratton, D.L., Henson, P.M. (1992). Exposure of phosphatidylserine on the surface of apoptotic lymphocytes triggers specific recognition and removal by macrophages. J Immunol. *148,* 2207-2216.

Fesik, S.W. and Shi, Y. (2001). Structural biology. Controlling the caspases. Science *294,* 1477-1478.

Fischer, J.A. (2000). Molecular motors and developmental asymmetry. Current Opinion in Genetics and Development *10,* 489-496.

Fraser, A.G. and Evan, G.I. (1997). Identification of a *Drosophila melanogaster* ICE/CED-3-related protease, drICE. EMBO J *16,* 1805-1813.

Frolov, M.V. and Alatortsev, V.E. (2001). Molecular analysis of novel *Drosophila* gene, g*ap69C,* encoding a homolog of ADP-ribosylation factor GTPase-activating protein. DNA Cell Biol *20,* 107-113.

Goberdhan, D.C. and Wilson, C. (2003). The functions of insulin signaling: size isn't everything, even in *Drosophila*. Differentiation *71,* 375-397.

Gorski, S.M., Chittaranjan, S., Pleasance, E.D., Freeman, J.D., Anderson, C.L., Varhol, R.J., Coughlin, S.M., Zuyderduyn, S.D., Jones, S.J., Marra, M.A. (2003). A SAGE approach to discovery of genes involved in autophagic cell death. Curr Biol *13,* 358-363.

Goyal, L., McCall, K., Agapite, J., Hartwieg, E., Stellar, H. (2000). Induction of apoptosis by *Drosophila reaper*, *hid* and *grim* through inhibition of IAP function. EMBO J *19,* 589-597.

Graves, J.D., Gotoh, Y., Draves, K.E., Ambrose, D., Han, D.K., Wright, M., Chemoff, K., Clark, E.A. and Krebs, E.G. (1998). Caspase-mediated activation and induction of apoptosis by the mammalian Ste20-like kinase Mst1. EMBO J *17,* 2224-2234.

Green, D.R. and Evan, G.I. (2002). A matter of life and death. Cancer Cell *1,* 19-30.

Green, D.R., and Kroemer, G. (1998). The central executioners of apoptosis: caspases or mitochondria? Trends Cell Biol *8,* 267-271.

Grether, M.E., Abrams, J.M., Apapite, J., White, K., Stellar, H. (1999). The *head involution defective* gene of *Drosophila melanogaster* functions in programmed cell death. Genes and Dev *9*, 1694-1708.

Gross, A., McDonnell, J.M., Korsmeyer, S.J. (1999). BCL-2 family members and the mitochondria in apoptosis. Genes Dev. *13*, 1899-1911.

Harding, T.M., Morano, K.A., Scott, S.V., Klionsky, D.J. (1995). Isolation and characterization of yeast mutants in the cytoplasm to vacuole protein targeting pathway. J Cell Biol *131*, 591-602.

Hardwick, J.S., Kuruvilla, F.G., Tong, J.K., Shamji, A.F., Schreiber, S.L. (1999). Rapamycin-modulated transcription defines the subset of nutrient-sensitive signaling pathways directly controlled by the Tor proteins. Proc Natl Acad Sci U S A *96*, 14866-14870.

Harvey, K.F., Pfleger, C.M., Hariharan, I.K. (2003). The *Drosophila* Mst ortholog, *hippo*, restricts growth and cell proliferation and promotes apoptosis. Cell *114*, 457-467.

Harvey, N.L., Daish, T., Mills, K., Dorstyn, L., Quinn, L.M., Read, S.H., Richardson, H., Kumar, S. (2001). Characterization of the *Drosophila* caspase, DAMM. J Biol Chem *276*, 253432-25350.

Hay, B.A., Wassarman, D.A., Rubin, G.M. (1995). *Drosophila* homologs of baculovirus inhibitor of apoptosis proteins function to block cell death. Cell *83*, 1253-1262.

Hegde, R., Srinivasula, S .M., Zhang, Z., Wassell, R., Mukattash, R., Cilenti, L., DuBois, G., Lazebnik, Y., Zervos, A.S., Fernandes-Alnemri, T., Alnemri, E.S. (2001) Identification of Omi/HtrA2 as a mitochondrial apoptotic serine protease that disrupts inhibitor of apoptosis protein-caspase interaction. J Biol Chem. *277*, 432-438.

Hengartner, M.O., Ellis, R.E. and Horvitz, R.H. (1992). *Caenorhabditis elegans* gene *ced-9* protects cells from programmed cell death. Nature *9*, 494-499.

Hengartner, M.O. (2000). The biochemistry of apoptosis. Nature *407*, 770-776.

Huang, H., Joazeiro, C.A., Bonfoco, E., Kamada, S., Leverson, J.D., Hunter, T. (2000). The inhibitor of apoptosis, cIAP2, functions as a ubiquitin-protein ligase and promotes in vitro monoubiquitination of caspases 3 and 7. J Biol Chem*275*, 26661- 26664.

Huh, J.R., Vernooy, S.Y., Yu, H., Yan, N., Shi, Y., Guo, M., Hay, B.A. (2004). Multiple apoptotic caspase cascades are required in nonapoptotic roles for *Drosophila* spermatid individualization. PLoS Biol *2*, E15.

Ichimura, Y., Kirisako, T., Takao, T., Satomi, Y., Shimonishi, Y., Ishihara, N., Mizushima, N., Tanida, I., Kominami, E., Ohsumi, M., Noda, T., Ohsumi, Y. (2000). A ubiquitin-like system mediates protein lipidation. Nature *408*, 488-492.

Igaki, T., Kanuka, H., Inohara, N., Sawamoto, K., Nunez, G., Okano, H., Miura, M. (2000). Drob-1, a *Drosophila* member of the Bcl-2/CED-9 family that promotes cell death. Proc Natl Acad Sci USA *97*, 662-667.

Jacobson, M.D., Weil, M. and Raff, M.C. (1997). Programmed cell death in animal development. Cell *88*, 347-354.

Jenkinson, E.J., Kingston, R., Smith, C.A., Williams, G.T., Owen, J.J. (1989). Antigen-induced apoptosis in developing T-cells: a mechanism for negative selection of the T-cell receptor repertoire. Eur J Immunol. *19*, 2175-2177.

Jiang, C., Baehrecke, E.H., and Thummel, C.S. (1997). Steroid regulated programmed cell death during *Drosophila* metamorphosis. Development *124*, 4673-4683.

Jiang, C., Lamblin, A.F.J., Stellar, H., Thummel, C.S. (2000). A steroid-triggered transcriptional hierarchy controls salivary gland cell death during *Drosophila* metamorphosis. Mol Cell *5*, 445-455.

Justice, R.W., Zilian, O., Woods, D.F., Noll, M., Bryant, P.J. (1995). The *Drosophila* tumor suppressor gene *warts* encodes a homolog of human myotonic dystrophy kinase and is required for the control of cell shape and proliferation. Genes Dev *9*, 534-546.

Kango-Singh, M., Nolo, R., Tao, C., Verstreken, P., Hiesinger, P.R., Bellen, H.J., Halder, G. (2002). Shar-pei mediates cell proliferation arrest during imaginal disc growth in *Drosophila*. Development *129*, 5719-5730.

Kanuka, H., Sawamoto, K., Inohara, N., Matsuno, K., Okano, H., Miura, M. (1999). Control of the cell death pathway by Dapaf-1, a *Drosophila* Apaf-1/CED-4-related caspase activator. Mol Cell *4*, 757-769.

Kappler, J.W., Roehm, N., Marrack, P. (1987). T cell tolerance by clonal elimination in the thymus. Cell *49*, 273-280.

Karcher, R.L., Deacon, S.W., Gelfand, V.I. (2002). Motor-cargo interactions: the key to transport specificity. Trends in Cell Biol *12*, 21-27

Keller, L.C., Maggie, C.M., Parkhurst, S.M. (2003). *cappuccino* acts as a downstream effector of Rho1 GTPase signaling in early *Drosophila* development. A Dros Res Conf *44*, 222C.

Kerkhoff, E. and Rapp, U.R. (1998). High intensity Raf signals convert mitotic cell cycling into cellular growth. Cancer Res *58*, 1636-1640.

King, S.M. (2000). The dynein microtubule motor. Biochim Biophys Acta *1496*, 60-75.

Kraut, R., Menon, K., Zinn, K. (2001). A gain-of-function screen for genes controlling motor axon guidance and synaptogenesis in *Drosophila*. Curr Biol *11*, 417-430.

Kerr, J.F., Wyllie, A.H., and Currie, A.R. (1972). Apoptosis: a basic biological phenomenon with wide-ranging implications in tissue kinetics. Br. J. Cancer *26*, 239-257.

Klionsky, D.J. and Emr, S.D. (2000). Autophagy as a regulated pathway of cellular degradation. Science *290*, 1717-1721.

Kozma, S.C. and Thomas, G. (2002). Regulation of cell size in growth, development and human disease: PI3K, PKB and S6K. Bioessays *24*, 65-71.

Kunz, J., Schneider, U., Howald, I., Schmidt, A., Hall, M.N. (2000). HEAT repeats mediate plasma membrane localization of Tor2p in yeast. J Biol Chem *275*, 37011-37020.

Laage, R. and Ungermann, C. (2001). The N-terminal domain of the t-SNARE Vam3p coordinates priming and docking in yeast vacuole fusion. Mol Biol Cell *12*, 3375-3385.

Lee, C.Y. and Baehrecke, E.H. (2001). Steroid regulation of autophagic programmed cell death during development. Development *128*, 1443-1455.

Lee, C.Y., Clough, E.A., Yellon, P., Teslovich, T.M., Stephan, D.A., Baehrecke, E.H. (2003). Genome-wide analyses of steroid- and radiation-triggered programmed cell death in *Drosophila*. Curr Biol *13*, 350-357.

Lee, C.Y., Simon, C.R., Woodard, C.T., Baehrecke, E.H. (2002). Genetic mechanism for the stage- and tissue-specific regulation of steroid triggered programmed cell death in *Drosophila*. Dev Biol. *252*, 138-148.

Lee, C.Y., Wendel, D.P., Reid, P., Lam, G., Thummel, C.S., Baehrecke, E.H. (2000). E93 directs steroid-triggered programmed cell death in *Drosophila*. Mol Cell *6*, 433-443.

Leist, M., and Jaattela, M. (2001). Four deaths and a funeral: from caspase to alternative mechanisms. Nat. Rev. Mol. Cell Biol *2*, 1-10.

Li, P., Nijhawan, D., Budihardjo, I., Srinivasula, S.M., Ahmad, M., Alnermi, E.S., Wang, X. (1997). Cytochrome c and dATP-dependent formation of Apaf-1/Caspase-9 complex initiates an apoptotic protease cascade. Cell *91*, 479-489.

Li, Y.Y., Yeh, E., Hays, T., Bloom, K. (1993). Disruption of mitotic spindle orientation in a yeast dynein mutant. Proc Natl Acad Sci USA *90*, 10096-10100.

Liu, H., Lin, D., Yates, J.R. (2002). Multidimensional separations for protein/peptide analysis in the post-genomic era. Biotechniques *32*, 898, 900, 902.

Lockshin, R.A. and Zaker, Z. (1991). Programmed cell death and apoptosis. Apoptosis: The molecular basis of cell death *3*, 47-60.

Loeffler, M. and Kroemer, G. (2000). The mitochondrin in cell death control: certainties and incognita. Exp Cell Res. *256*, 19-26.

Luzio, J.P., Poupon, V., Lindsay, M.R., Mullock, B.M., Piper, R.C., Pryor, P.R. (2003). Membrane dynamics and the biogenesis of the lysosomes. Molecular Membrane Biology *20*, 141-154.

MacDonald, H.R. and Lees, R.K. (1990). Programmed death of autoreactive thymocytes. Nature *343*, 642-644.

Mahajan-Miklos, S. and Cooley, L. (1994). The villin-like protein encoded by the *Drosophila quail* gene is required for actin bundle assembly during oogenesis. Cell *78*, 291-301.

Martin, D.N., Baehrecke, E.H. (2004). Caspases function in autophagic programmed cell death in *Drosophila*. Development *131*, 275-284.

Martins, L.M., Iaccarino, I., Tenev, T., Gschmeissner, S., Totty, N.F., Lemoine, N.R., Savopoulos, J., Gray, C.W., Creasy, C.L., Dingwall, C., Downward, J. (2002). The serine protease Omi/HtrA2 regulates apoptosis by binding XIAP through a reaper-like motif. J Biol Chem. *277*, 439-444.

McCall, K. and Stellar, H. (1998). Requirement for DCP-1 caspase during *Drosophila* oogenesis. Science *279*, 230-234.

Melendez, A., Talloczy, Z., Seaman, M., Eskelinen, E.L., Hall, D.H., Levine, B. (2003). Autophagy genes are essential for dauer development and life-span extension in *C. elegans*. Science *301*, 1387-1391.

Mills, K.R., Reginato, M., Debnath, J., Queenan, B., Brugge, J.S. (2004) Tumor necrosis factor-related apoptosis-inducing ligand (TRAIL) is required for induction of autophagy during lumen formation in vitro. Proc Natl Acad Sci USA *101*, 3438-3443.

Moberg, K.H., Bell, D.W., Wahrer, D.C., Haber, D.A., Hariharan, I.K. (2001). *archipelago* regulates Cyclin E levels in *Drosophila* and is mutated in human cancer cell lines. Nature *413*, 311-316.

Noda, T. and Ohsumi, Y. (1998). Tor, a phosphatidylinositol kinase homologue, controls autophagy in yeast. J Biol Chem *273*, 3963-3966.

O'Farrell, P.H. (1975). High resolution two-dimensional electrophoresis of proteins. J Biol Chem *250*, 4007-4021.

Ohsumi, Y. (2001). Molecular dissection of autophagy: two ubiquitin-like systems. Nat Rev Mol Cell Biol *2*, 211-216.

Oppenheim, R.W., Prevette, D., Tytell, M., and Homma, S. (1990). Naturally occurring and induced neuronal death in the chick embryo in vivo requires protein and RNA synthesis: evidence for the role of cell death genes. Dev. Biol *138*, 104-113.

Pantalacci, S., Tapon, N., Leopold, P. (2003). The Salvador partner Hippo promotes apoptosis and cell-cycle exit in *Drosophila*. Nat Cell Biol *5*, 921-927.

Parnas, D., Haghighi, A.P., Fetter, R.D., Kim, S.W., Goodman, C.S. (2001). Regulation of postsynaptic structure and protein localization by the Rho-type guanine nucleotide exchange factor *dPix*. Neuron *32*, 415-424.

Pazour, G.J., Wilkerson, C.G., Witman, G.B. (1998). A dynein light chain is essential for the retrograde particle movement of intraflagellar transport (IFT). J Cell Biol *141*, 979-992.

Pereira-Leal, J.B. and Seabra, M.C. (2001). Evolution of the Rab family of small GTP-binding proteins. J Mol Biol *313*, 889-901.

Phillis, R., Statton, D., Caruccio, P., Murphey, R.K. (1996). Mutations in the 8 kDa dynein light chain gene disrupt sensory axon projections in the *Drosophila* imaginal CNS. Development *122*, 2955-2963.

Puthalakath, H., Huang, D.C., O'Reilly, L.A., KingS .M., Strasser, A. (1999). The proapoptotic activity of the Bcl-2 family member Bim is regulated by interaction with the dynein motor complex. Mol Cell *3*, 287-296.

Puthalakath, H., Villunger, A., O'Reilly, L.A., Beaumont, J.G., Coultas, L., Cheney, R.E., Huang, D.C., Strasser, A. (2001). Bmf: a proapoptotic BH3-only protein regulated by interaction with the myosin V actin motor complex, activated by anoikis. Science *293*, 1829-1832.

Qu, X., Yu, J., Bhagat, G., Furuya, N., Hibshoosh, H., Troxel, A., RosenJ ., Eskelinen, E.L., Mizushima, N., Ohsumi, Y., Cattoretti, G., Levine, B. (2003). Promotion of tumorigenesis by heterozygous disruption of the beclin 1 autophagy gene. J Clin Invest *112*, 1809-1820.

Rao, L., Perez, D., White, E. (1996). Lamin proteolysis facilitates nuclear events during apoptosis. J Cell Biol *135*, 1441-1455.

Reed, J.C. (1997) Bcl-2 family proteins: regulators of apoptosis and chemoresistance in hematologic malignancies. Semin Hematol. *4*, 9-19.

Restifo, L.L. and White, K. (1992). Mutations in a steroid hormone-regulated gene disrupt the metamorphosis of internal tissues in *Drosophila*: salivary glands, muscle, and gut. Wilhelm Roux's Arch Dev Biol *201*, 221-234.

Riddiford, L.M. (1993). Hormone receptors and the regulation of insect metamorphosis. Receptor *3*, 203-209.

Rodriguez, A., Chen, P., Oliver, H., Abrams, J.M. (2002). Unrestrained caspase-dependent cell death caused by loss of Diap1 function requires the *Drosophila* Apaf-1 homolog, Dark. EMBO J *21*, 2189-2197.

Rodriguez, A., Oliver, H., Zou, H., Chen, P., Wang, X., Abrams, J.M. (1999). Dark is a *Drosophila* homologue of Apaf-1/CED-4 and functions in an evolutionarily conserved death pathway. Nat Cell Biol *1*, 272-279.

Rodriguez-Crespo, I., Yelamos, B., Roncal, F., Albar, J.P., Oritz de Montellano, P.R., Gavilanes, F. (2001). Identification of novel cellular proteins that bind to the LC8 dynein light chain using a pepscan technique. FEBS Lett *503*, 135-141.

Satoh, A.K., Tokunaga, F., Ozaki, K. (1997). Rab proteins of *Drosophila melanogaster* novel members of the Rab-protein family. FEBS Lett *404*, 65-69.

Saunders, J.W. (1966). Death in embryonic systems. Science 154, 6-4-612.
Schwartz, L.M., Smith, S.W., Jones, M.E.E., Osborne, B.A. (1993). Do all programmed cell death occur via apoptosis? Proc Natl Acad Sci USA *90*, 980-984.

Schweichel, J.U., and Merker, H.J. (1973). The morphology of various types of cell death in prenatal tissues. Tetratology *7*, 253-266.

Seagraves, W.A. and Hogness, D.S. (1990). The *E75* ecdysone-inducible gene responsible for the 75B early puff in *Drosophila* encodes two new members of the steroid receptor superfamily. Genes Dev *4*, 204-219.

Sewing, A., Wiseman, B., Lloyd, A.C, Land, H. (1997). High intensity Raf signal causes cell cycle arrest mediated by p21Cip1. Mol Cell Biol *17*, 5588-5597.

Shi, Y. (2001) A structural view of mitochondria-mediated apoptosis. Nat Struct Biol. *8*, 394-401.

Shi, Y. (2002). Mechanisms of caspase activation and inhibition during apoptosis. Mol Cell *9*, 459-470.

Shimizu, S., Narita, M., Tsujimoto, Y. (1999) Bcl-2 family proteins regulate the release of apoptogenic cytochrome c by the mitochondrial channel VDAC. Nature *99*, 483-487.

Smith, A.V. and Orr-Weaver, T.L. (1991). The regulation of the cell cycle during *Drosophila* embryogenesis: the transition to polyteny. Development *112*, 997-1008.

Song, Z., McCall, K., Stellar, H. (1997). DCP-1, a *Drosophila* cell death protease essential for development. Science *275*, 536-540.

Sprick, M.R. and Walczak, H. (2004). The interplay between the Bcl-2 family and death receptor-mediated apoptosis. Biochim Biophys Acta. *1664*, 125-132.

Srinivasula, S.M., Datta, P., Kobayashi, M., Wu, J.W., Fujioka, M., Hegde, R., Zhang, Z., Mukattash, R., Fernandes-Alnemri, T., Shi, Y., et al. (2002). *sickle*, a novel *Drosophila* death gene in the *reaper*/*hid*/*grim* region, encodes an IAP-inhibitory protein. Curr Biol *12*, 125-130.

Suzuki, Y., Imai, Y., Nakayama, H., Takahashi, K., Takio, K., Takahashi, R. (2001). A serine protease, HtrA2, is released from the mitochondria and interacts with XIAP, inducing cell death. Mol Cell. *8*, 613-621.

Suzuki, Y., Nakabayashi, Y., Takahashi, R. (2001). Ubiquitin-protein ligase activity of X-linked inhibitor of apoptosis protein promotes proteasomal degradation of caspase-3 and enhances it anti-apoptotic effect in Fas-induced cell death. Proc Natl Acad Sci USA *98*, 8662-8667.

Swan, A., Nguyen, T., Suter, B. (1999). *Drosophila Lissencephaly-1* functions with Bic-D and dynein in oocyte determination and nuclear positioning. Nat Cell Biol *1*, 444-449.

Takagawa, K. and Salvaterra, P. (1996). Analysis of choline acetyltransferase protein in temperature sensitive mutant flies using newly generated monoclonal antibody. Neurosci Res *24*, 237-243.

Tanaka, E. and Sabry, J. (1995). Making the connection: cytoskeletal rearrangements during growth cone guidance. Cell *83*, 171-176.

Tapon, N., Harvey, K.F., Bell, D.W., Wahrer, D.C., Schiripo, T.A., Haber, D.A., Hariharan, I.K. (2002). *salvador* Promotes both cell cycle exit and apoptosis in *Drosophila* and is mutated in human cancer cell lines. Cell *110*, 467-478.

Tepass, U. and Knust, E. (1993). *crumbs* and *stardust* act in a genetic pathway that controls organization of epithelia in *Drosophila melanogaster*. Dev Biol *159*, 311-326.

Thompson, C.B. (1995). Apoptosis in the pathogenesis and treatment of disease. Science *267*, 1456-1462.

Thumm, M., Egner, R., Koch, B., Schlumpberger, M., Straub, M., Veenhuis, M., Wolf D.H. (1994). Isolation of autophagocytosis mutants of *Saccharomyces cerevisiae*. FEBS Lett *349*, 275-280.

Tsukada, M. and Ohsumi, Y. (1993). Isolation and characterization of autophagy-defective mutants of *Saccharomyces cerevisiae*. FEBS Lett *1-2*, 169-174.

Udan, R.S., Kango-Singh, M., NolǾR ., Tao, C., Halder, G. (2003). Hippo promotes proliferation arrest and apoptosis in the Salvador/Warts pathway. Nat Cell Biol *5*, 914-920.

Urness, L.D. and Thummel, C. S. (1995). Molecular analysis of a steroid-induced regulatory hierarchy: the *Drosophila* E74A protein directly regulates L71-6 transcription. EMBO J *14*, 6239-6246.

Vallee, R.B. and Sheetz, M.P. (1996). Targeting of motor proteins. Science*271*, 1539 - 1544.

Van Eeden, F. and St Johnston, D. (1999). The polarization of the anterior-posterior and dorsal-ventral axes during *Drosophila* oogenesis. Curr Opin Genet Dev *9*, 396-404.

van Loo, G., Saelens, X., van Gurp, M., MacFarlane, M., Martin, S.J., Vandenabeele, P. (2002). The role of mitochondrial factors in apoptosis: a Russian roulette with more than one bullet. Cell Death Differ. *9*, 1031-1042.

Verhagen, A.M., Silke, J., Ekert, P.G., Pakusch, M., Kaufmann, H., Connolly, L.M., Day, C.L., Tikoo, A., Burke, R., Wrobel, C., Moritz, R.L., Simpson, R.J., Vaux, D.L. (2002). HtrA2 promotes cell death through its serine protease activity and its ability to antagonize inhibitor of apoptosis proteins. J Biol Chem. *277*, 445-454.

Vernooy, S.Y., Copeland, J., Ghaboosi, N., Griffin, E.E., Yoo, S.J., Hay, B.A. (2000). Cell death regulation in *Drosophila*: conservation of mechanism and unique insights. J Cell Biol *150*, F69-F75.

Waller, B.J. and Alberts, A.S. (2003). The formins: active scaffolds that remodel cytoskeleton. Trends in Cell Biol *13*, 435-446.

Wan, H.I., DiAntonio, A., Fetter, R.D., Bergstrom, K., Strauss, R., Goodman, C.S. (2000). Highwire regulates synaptic growth in *Drosophila*. Neuron *26*, 313-329.

Wang, S.L., Hawkins, C.J., Yoo, S.J., Muller, H.A.J., Hay, B.A. (1999). The *Drosophila* caspase inhibitor DIAP1 is essential for cell survival and is negatively regulated by HID. Cell *98*, 453-463.

Whalen, A.M. and Steward, R. (1993). Dissociation of the dorsal-cactus complex and phosphorylation of the dorsal protein correlate with the nuclear localization of dorsal. J Cell Biol *123*, 523-534.

White, K., Grether, M.E., Abrams, J.M., Young, L., Farrell, K., Stellar, H. (1994). Genetic control of programmed cell death in *Drosophila*. Science *264*, 677-683.

Wing, J.P., Karres, J.S., Ogdahl, J.L., Zhou, L., Schwartz, L.M., Nambu, J.R. (2002). *Drosophila sickle* is a novel *grim-reaper* cell death activator. Curr Biol *12*, 131-135.

Wiseman, S.B. and Singer T.D. (2002). Applications of DNA and protein microarrays in comparative physiology. Biotechnol Adv *20*, 379-389.

Wilson, M.J., Salata, M.W., Susalka, S.J., Pfister, K.K. (2001). Light chains of mammalian cytoplasmic Dynein: Identification and characterization of a family of LC8 light chains. Cell Mol and Cyto *49*, 229-240.

Woodard, C.T., Baehrecke, E.H., Thummel, C.S. (1994). A molecular mechanism for the stage-specificity of the *Drosophila* prepupal genetic response to ecdysone. Cell *79*, 607-615.

Wu, S., Huang, J., Dong, J., Pan, D. (2003). *hippo* encodes a Ste-20 family protein kinase that restricts cell proliferation and promotes apoptosis in conjunction with *salvador* and *warts*. Cell *114*, 445-456.

Wu, G., Chai, J., Suber, T.L., Wu, J.W., Du, C., Wang, X., Shi, Y. (2000). Structural basis of IAP recognition by Smac/DIABLO. Nature *408*, 1008-1012.

Wu, J.W., Cocina, A.E., Chai, J., Hay, B.A., Shi, Y. (2001). Structural analysis of a functional DIAP1 fragment bound to grim and hid peptides. Mol Cell *8*, 95-104.

Wu, T.Y., Wagner, K.W., Bursulaya, B., Schultz, P.G., Deveraux, Q.L. (2003). Development and characterization of nonpeptidic small molecule inhibitors of the XIAP/caspase-3 interaction. Chem Biol. *10*, 759-767.

Wyllie, A.H. (1980). Glucocoticoid-induced thymocyte apoptosis is associated with endogenous endonuclease activation. Nature *284*, 555-556.

Xu, T., Wang, W., Zhang, S., Stewart, R.A., Yu, W. (1995). Identifying tumor suppressors in genetic mosaics: the *Drosophila lats* gene encodes a putative protein kinase. Development *121*, 1053-1063.

Xue, F. and Cooley, L. (1993). Kelch encodes a component of intercellular bridges in *Drosophila* egg chambers. Cell *72*, 681-693.

Yang, Y., Fang, S., Jensen, J.P., Weissman, A.M., Ashwell, J.D. (2000). Ubiquitin protein ligase activity of IAPs and their degradation in proteasomes in response to apoptotic stimuli. Science *288*, 874-877.

Yamaguchi, T., Okada, T., Takeuchi, K., Tonda, T., Ohtaki, M., Shinoda, S., Masuzawa, T., Ozawa, K., Inaba, T. (2003). Enhancement of thymidine kinase-mediated killing of malignant glioma by BimS, a BH3-only cell death activator. Gene Ther *10*, 375-385.

Yates, J.R. (1998). Mass spectrometry and the age of the proteome. J Mass Spectrom *33*, 1-19.

Yu, L., Alva, A., Su, H., Dutt, P., Freundt, E., Welsh, S., Baehrecke, E. H., Lenardo, M. J. (2004). Regulation of an ATG7-beclin 1 program of autophagic cell death by Caspase-8. Science, in press.

Yu, S.Y., Yoo, S.J., Yang, L., Zapata, C., Srinivasan, A., Hay, B.A., Baker, N.E. (2002). A pathway of signals regulating effector and initiator caspases in the developing *Drosophila* eye. Development *129*, 3269-3278.

Yuan, J., Shaham, S., Ledoux, S., Ellis, H.M., Horvitz, H.R. (1993). The *C. elegans* cell death gene *ced-3* encodes a protein similar to mammalian interleukin-1 beta-convertin enzyme. Cell *75*, 641-652.

Yuan, J., Lipinski, M., Degterev, A. (2003). Diversity in the mechanisms of neuronal cell death. Neuron *40*, 401-413.

Yue, Z., Jin, S., Yang, C., Levine, A.J., Heintz, N. (2003). Beclin 1, an autophagy gene essential for early embryonic development, is a haploinsufficient tumor suppressor. Proc Natl Acad Sci U S A *100*, 15077-15082.

Zallen, J.A., Cohen, Y., Hudson, A.M., Cooley, L., Wieschaus, E., Schejter, E.D. (2002). SCAR is a primary regulator of Arp2/3-dependent morphological events in *Drosophila*. J Cell Biol *156*, 689-701

Zhang, H., Stallock, J.P., Ng, J.C., Reinhard, C., Neufeld, T.P. (2000). Regulation of cellular growth by the *Drosophila* target of rapamycin dTOR. Genes Dev *14*, 2712-2724.

Zhou, L., Song, Z., Tittel, J., Stellar, H. (1999). HAC-1, a *Drosophila* homolog of APAF-1 and CED-4, functions in developmental and radiation-induced apoptosis. Mol Cell *4*, 745-755.

Zou, H., Henzel, W.J., Liu, X., Lutschg, A., Wang, X. (1997). Apaf-1, a human protein homologous to *C.elegans* CED-4, participates in cytochrome c-dependent activation of caspase-3. Cell *90*, 405-413.